Final Report

Cracking and Shear Capacity of High Strength Concrete Girders

Research Project

Sponsored
By

Florida Department of Transportation

WPI 0510612
Contract # C-4269

Kamal S. Tawfiq, Ph.D., P.E.

Department of Civil Engineering
FAMU/FSU College of Engineering
Tallahassee, Florida

January, 1995

Technical Report Documentation Page

1. Report No.	2. Government Accession No.	3. Recipient's Catalog No.
FL/DOT/RMC/612(1)-4269		

4. Title and Subtitle	5. Report Date
Cracking and Shear Capacity of High Strength Concrete Bridge Girders	January 24, 1995
	6. Performing Organization Code

7. Author(s)	8. Performing Organization Report No.
Kamal Tawfiq, Ph.D., P.E.	

9. Performing Organization Name and Address	10. Work Unit No.
FAMU/FSU College of Engineering Department of Civil Engineering 2525 Pottsdamer Street Tallahassee, Fl 32316	11. Contract or Grant No.

12. Sponsored Agency Name and Address	13. Type of Report and Period Covered
State of Florida Department of Transportation Research Center 605 Suzannee Street, M.S. 30 Tallahassee, Fl 32301	Final Report Aug. 1, 1992 to January 4, 1995
	14. Sponsoring Agency Code

15. Supplementary Notes

Prepared in cooperation with the Federal Highway Administration

16. Abstract

In this study, field and laboratory tests were performed to investigate the transfer length as well as the shearing capacity of high strength concrete girders. For this purpose, six (6) full-scale AASHTO type II prestressed girders were prepared with 8,000 psi, 10,000 psi and 12,000 psi concrete strengths and tested under controlled testing conditions. The girders were instrumented with both internal and external gages. The internal gages were used in the field to investigate the transfer length of the girders during the releasing of the prestress strands. From the results of these tests a relationship was developed to predict the transfer length of high strength prestressed girders. It has been found that using high strength concrete reduces the transfer length in pretensioned prestressed girders.

To further investigate the behavior of the prestress strands during load transfer, forty (40) direct pullout tests were performed in the laboratory to examine the bonding characteristics between the prestressing strands and the concrete. The strand sizes ranged from 3/8" to 0.6" and the concrete compressive strength ranged from 6,000 psi to 12,000 psi. Results form these tests showed that small strand diameters experienced higher bond stresses, and high concrete strength can withstand higher hoop stresses that develop after initial bond failure.

In the laboratory, both ends of each AASHTO type II girder were tested to failure. Most of the girders failed after a bond failure between the prestressing strand and concrete. The ultimate shear capacity was then compared with the predicted shear capacity using different approaches. High concrete strength was found not to affect the ultimate strength of girders that failed due to bonding failure.

17. Key Words	18. Distribution Statement
High Strength Concrete, Transfer Length, Cracking, Shear Capacity	No restriction. This document is available to the public through the National Technical Information Service, Springfield Va. 22161

19. Security Classif. (of this report)	20. Securety Classif. (of this page)	21. No. of Pages	22. Price
Unclassified	Unclassified	145 Pages	

Form DOT F 1700.7 (8-72)

DISCLAIMER

The opinions, findings and conclusions expressed in this publication are those of the authors and not necessarily those of the Florida Department of Transportation and the Federal Highway Administration.

Prepared in cooperation with the Florida Department of Transportation and the Federal Highway Administration.

ACKNOWLEDGMENTS

The author would like to express his gratitude and sincere regards are extended to Dr. Mohsen Shahawy from the Florida Department of Transportation for his invaluable suggestions and creative criticism to this undertaking. Thanks to Dr. Moussa Issa and Ms. Brenda Robertson for their constructive review. Also, thanks to John Poulson a graduate student at the department of Civil Engineering for his outstanding efforts in sample preparation, laboratory testing and analysis of results. Including in my acknowledgment is Mr. Adnan Alsaad from the FDOT for his assistance on beam preparation and testing. My appreciation is extended to the Civil Engineering Department at FAMU/FSU College of Engineering for providing us with the needed facilities. Lastly, I acknowledge the support provided to us by the Florida Department of Transportation. Without their support this task would not have been feasible.

TABLE OF CONTENTS

CONVERSION FACTORS i
DISCLAIMER ii
ACKNOWLEDGMENTS iii
LIST OF TABLES vii
LIST OF FIGURES viii
NOTATION xiv
ABSTRACT xviii

CHAPTER 1
INTRODUCTION 1
1.1 High Strength Concrete 1
1.2 Transfer Length Background 1
1.3 Shear Strength Background 2
1.4 Objective 2

CHAPTER 2
LITERATURE REVIEW 4
2.1 Bond Strength of Prestressing Strands and Concrete 4
2.2 Transfer Length and Development Length in Precast Girders 5
2.3 Shearing Capacity of Prestressed Girders 7
2.3.1 1989 AASHTO Code 8
2.3.2 ACI Code 10
2.3.3 1994 AASHTO LRFD Code 11

2.3.4 Strut and Tie Models 12

CHAPTER 3

TESTING PROGRAM 16

3.1 Overview 16

3.2 Pullout Bond Test 16

3.2.1 Overview 16

3.2.2 Testing Materials 17

3.2.3 Sample Preparation 18

3.2.4 Setup and Procedure of Pullout Testing 18

3.3 Transfer Length Tests 19

3.3.1 Testing Materials 19

3.3.2 Specimen Preparation 19

3.3.3 Testing Procedure 19

3.4 Shear Testing 20

3.4.1 Testing Materials 20

3.4.2 Sample Preparation 20

3.4.3 Testing Procedure 21

CHAPTER 4

TESTING RESULTS 35

4.1 Pullout Bond Tests 35

4.1.1 Ungreased Specimens 35

4.1.2 Lightly Greased Specimens 36

4.1.3 Heavy Greased Specimens 37

4.1.4 Summary of Pullout Bond Results 37

4.2 Transfer Length Results 37

4.3 Shear Strength Results 39

4.3.1 North End Tests 39
4.3.2 South End Tests 40

CHAPTER 5
DISCUSSION OF RESULTS 70
5.1 Pullout Bond Tests 70
5.1.1 Adhesion Bond Performance 70
5.1.2 Mechanical Bond Performance 71
5.1.3 Comparison of Pullout Bond Results with Other Studies 72
5.2 Transfer Length Results 72
5.3 Relationship Between Pullout Bond and Transfer Length Bond 74
5.4 Shear Strength Tests 75
5.4.1 Effect of Concrete Strength 75
5.4.2 Effect of Increased Shear Reinforcement 76
5.4.3 Code Prediction Results 77
5.4.4 Strut and Tie Models 78
5.4.5 Development Length 79
5.4.6 Test Girder Behavior 80

CHAPTER 6
CONCLUSIONS 123

REFERENCES 127

LIST OF TABLES

2.1 Bond Stress Results Presented by Brearly and Johnston (1990). 14
2.2 Bond Test Results Presented by Deatherage and Burdette (1991). 14
2.3 Bond Test Results Presented by Cousins, Badeau and Moustafa (1992). 15
2.4 Bond Test Results Presented by Yu (1992). 15

3.1 Pullout Test Specimens 23

4.1 Pullout Test Results 41
4.2 Transfer Length Test Results 42
4.3 Summary of Shear Test Results 43

5.1 Pullout Test Results Showing Average U'_1 Results 84
5.2 Pullout Test Results Showing Average U_t Results 85
5.3 Bond Test Results from Direct Tension Pullout Tests 86
5.4 Bond Test Results Compared with Pretensioned Bond Tests 86
5.5 Summary of Slip Results from Shear Tests 87
5.6 Test Shear and Predicted Shear Values at h/2 88
5.7 Test Shear and Predicted Shear Values at d_v 89
5.8 Test Shear and Strut and Tie Predicted Shear Values 90
5.9 Slope of Moment vs. Deflection Plots 91

LIST OF FIGURES

3.1 Pullout Test Configuration 24
3.2 Embedded Gages Used for Transfer Length Measurements 25
3.3 Flame Cutting of Strands 26
3.4 Cross Section of Test Girders 27
3.5 Web Reinforcement in R Girders 28
3.6 Web Reinforcement in 2R Girders 29
3.7 North End Test Configuration 30
3.8 South End Test Configuration 31
3.9 Gages Used to Measure Strand Slip 32
3.10 Location of External Strain Gages for North End Tests 33
3.11 Location of External Strain Gages for South End Tests 34

4.1 Load VS Slip Plot for Specimen 4-UC-7-B 44
4.2 Load VS Slip Plot for Specimen 4-UC-11-A 44
4.3 Load VS Slip Plot for Specimen 5-UC-7-A 45
4.4 Load VS Slip Plot for Specimen 5-UL-6-C 45
4.5 Load VS Slip Plot for Specimen 5-GCF-10-B 46
4.6 Load VS Slip Plot for Specimen 6-GCH-6-A 46
4.7 Transfer Length Plot for Girder R-8 47
4.8 Transfer Length Plot for Girder 2R-8 47
4.9 Transfer Length Plot for Girder R-10 48
4.10 Transfer Length Plot for Girder R-12 49
4.11 Transfer Length Plot for Girder 2R-12 49

4.12 Strand Slip at Failure for Girder 2R-12-S 50

4.13 Girder 2R-12-S at Failure 51

4.14 Test Shear at Failure and Predicted Shear for Girder R-8-N 52

4.15 Test Shear at Failure and Predicted Shear for Girder R-8-S 52

4.16 Test Shear at Failure and Predicted Shear for Girder R-10-N 53

4.17 Test Shear at Failure and Predicted Shear for Girder R-10-S 53

4.18 Test Shear at Failure and Predicted Shear for Girder R-12-N 54

4.19 Test Shear at Failure and Predicted Shear for Girder R-12-S 54

4.20 Test Shear at Failure and Predicted Shear for Girder 2R-8-N 55

4.21 Test Shear at Failure and Predicted Shear for Girder 2R-8-S 55

4.22 Test Shear at Failure and Predicted Shear for Girder 2R-10-N 56

4.23 Test Shear at Failure and Predicted Shear for Girder 2R-10-S 56

4.24 Test Shear at Failure and Predicted Shear for Girder 2R-12-N 57

4.25 Test Shear at Failure and Predicted Shear for Girder 2R-12-S 57

4.26 Cracking Pattern for Girder R-8-N 58

4.27 Cracking Pattern for Girder R-10-N 59

4.28 Cracking Pattern for Girder R-12-N 60

4.29 Cracking Pattern for Girder 2R-8-N 61

4.30 Cracking Pattern for Girder 2R-10-N 62

4.31 Cracking Pattern for Girder 2R-12-N 63

4.32 Cracking Pattern for Girder R-8-S 64

4.33 Cracking Pattern for Girder R-10-S 65

4.34 Cracking Pattern for Girder R-12-S 66

4.35 Cracking Pattern for Girder 2R-8-S 67

4.36 Cracking Pattern for Girder 2R-10-S 68

4.37 Cracking Pattern for Girder 2R-12-S 69

5.1 Transfer Length Regression Results Using Effective Prestress Force 92

5.2 Transfer Length Regression Results Using Initial Prestress Force 92

5.3 Total Moment vs. Deflection Plot for Girder R-8-N 93

5.4 Total Moment vs. Deflection Plot for Girder R-8-S 93

5.5 Total Moment vs. Deflection Plot for Girder R-10-N 94

5.6 Total Moment vs. Deflection Plot for Girder R-10-S 94

5.7 Total Moment vs. Deflection Plot for Girder R-12-N 95

5.8 Total Moment vs. Deflection Plot for Girder R-12-S 95

5.9 Total Moment vs. Deflection Plot for Girder 2R-8-N 96

5.10 Total Moment vs. Deflection Plot for Girder 2R-8-S 96

5.11 Total Moment vs. Deflection Plot for Girder 2R-10-N 97

5.12 Total Moment vs. Deflection Plot for Girder 2R-10-S 97

5.13 Total Moment vs. Deflection Plot for Girder 2R-12-N 98

5.14 Total Moment vs. Deflection Plot for Girder 2R-12-S 98

5.15 Total Moment vs. Strand Slip Plot for Strands 1-4 for Girder R-8-N 99

5.16 Total Moment vs. Strand Slip Plot for Strands 5-9 for Girder R-8-N 99

5.17 Total Moment vs. Strand Slip Plot for Strands 10-16 for Girder R-8-N 99

5.18 Total Moment vs. Strand Slip Plot for Strands 1-4 for Girder R-10-N 100

5.19 Total Moment vs. Strand Slip Plot for Strands 5-9 for Girder R-10-N 100

5.20 Total Moment vs. Strand Slip Plot for Strands 10-16 for Girder R-10-N 100

5.21 Total Moment vs. Strand Slip Plot for Strands 1-4 for Girder R-12-N 101

5.22 Total Moment vs. Strand Slip Plot for Strands 5-9 for Girder R-12-N 101

5.23 Total Moment vs. Strand Slip Plot for Strands 10-16 for Girder R-12-N 101

5.24 Total Moment vs. Strand Slip Plot for Strands 1-4 for Girder R-8-S 102

5.25 Total Moment vs. Strand Slip Plot for Strands 5-9 for Girder R-8-S 102

5.26 Total Moment vs. Strand Slip Plot for Strands 10-16 for Girder R-8-S 102

5.27 Total Moment vs. Strand Slip Plot for Strands 1-4 for Girder R-10-S 103

5.28 Total Moment vs. Strand Slip Plot for Strands 5-9 for Girder R-10-S 103

5.29 Total Moment vs. Strand Slip Plot for Strands 10-16 for Girder R-10-S 103

5.30 Total Moment vs. Strand Slip Plot for Strands 1-4 for Girder R-12-S 104

5.31 Total Moment VS Strand Slip Plot for Strands 5-9 for Girder R-12-S 104

5.32 Total Moment VS Strand Slip Plot for Strands 10-16 for Girder R-12-S 104

5.33 Total Moment vs. Strand Slip Plot for Strands 1-4 for Girder 2R-8-N 105

5.34 Total Moment vs. Strand Slip Plot for Strands 5-9 for Girder 2R-8-N 105

5.35 Total Moment vs. Strand Slip Plot for Strands 10-16 for Girder 2R-8-N 105

5.36 Total Moment vs. Strand Slip Plot for Strands 1-4 for Girder 2R-10-N 106

5.37 Total Moment vs. Strand Slip Plot for Strands 5-9 for Girder 2R-10-N 106

5.38 Total Moment vs. Strand Slip Plot for Strands 10-16 for Girder 2R-10-N 106

5.39 Total Moment vs. Strand Slip Plot for Strands 1-4 for Girder 2R-12-N 107

5.40 Total Moment vs. Strand Slip Plot for Strands 5-9 for Girder 2R-12-N 107

5.41 Total Moment vs. Strand Slip Plot for Strands 10-16 for Girder 2R-12-N 107

5.42 Total Moment vs. Strand Slip Plot for Strands 1-4 for Girder 2R-8-S 108

5.43 Total Moment vs. Strand Slip Plot for Strands 5-9 for Girder 2R-8-S 108

5.44 Total Moment vs. Strand Slip Plot for Strands 10-16 for Girder 2R-8-S 108

5.45 Total Moment vs. Strand Slip Plot for Strands 1-4 for Girder 2R-10-S 109

5.46 Total Moment vs. Strand Slip Plot for Strands 5-9 for Girder 2R-10-S 109

5.47 Total Moment vs. Strand Slip Plot for Strands 10-16 for Girder 2R-10-S 109

5.48 Total Moment vs. Strand Slip Plot for Strands 1-4 for Girder 2R-12-S 110

5.49 Total Moment vs. Strand Slip Plot for Strands 5-9 for Girder 2R-12-S 110

5.50 Total Moment vs. Strand Slip Plot for Strands 10-16 for Girder 2R-12-S 110

5.51 Moment and Slip vs. Deflection for Girder R-8-N 111

5.52 Moment and Slip vs. Deflection for Girder R-8-S 111

5.53 Moment and Slip vs. Deflection for Girder R-10-N 112

5.54 Moment and Slip vs. Deflection for Girder R-10-S 112

5.55 Moment and Slip vs. Deflection for Girder R-12-N 113

5.56 Moment and Slip vs. Deflection for Girder R-12-S 113

5.57 Moment and Slip vs. Deflection for Girder 2R-8-N 114

5.58 Moment and Slip vs. Deflection for Girder 2R-8-S 114

5.59 Moment and Slip vs. Deflection for Girder 2R-10-N 115

5.60 Moment and Slip vs. Deflection for Girder 2R-10-S 115

5.61 Moment and Slip vs. Deflection for Girder 2R-12-N 116

SI* (MODERN METRIC) CONVERSION FACTORS

APPROXIMATE CONVERSIONS TO SI UNITS

Symbol	When You Know	Multiply By	To Find	Symbol
	LENGTH			
in	inches	25.4	millimeters	mm
ft	feet	0.305	meters	m
yd	yards	0.914	meters	m
mi	miles	1.61	kilometers	km
	AREA			
in^2	square inches	645.2	square millimeters	mm^2
ft^2	square feet	0.093	square meters	m^2
yd^2	square yards	0.836	square meters	m^2
ac	acres	0.405	hectares	ha
mi^2	square miles	2.59	square kilometers	km^2
	VOLUME			
fl oz	fluid ounces	29.57	milliliters	ml
gal	gallons	3.785	liters	l
ft^3	cubic feet	0.028	cubic meters	m^3
yd^3	cubic yards	0.765	cubic meters	m^3
NOTE: Volumes greater than 1000 l shall be shown in m^3.				
	MASS			
oz	ounces	28.35	grams	g
lb	pounds	0.454	kilograms	kg
T	short tons (2000 lb)	0.907	megagrams	Mg
	TEMPERATURE (exact)			
°F	Fahrenheit temperature	5(F-32)/9 or (F-32)/1.8	Celcius temperature	°C
	ILLUMINATION			
fc	foot-candles	10.76	lux	l
fl	foot-Lamberts	3.426	candela/m^2	cd/m^2
	FORCE and PRESSURE or STRESS			
lbf	poundforce	4.45	newtons	N
psi	poundforce per square inch	6.89	kilopascals	kPa

APPROXIMATE CONVERSIONS FROM SI UNITS

Symbol	When You Know	Multiply By	To Find	Symbol
	LENGTH			
mm	millimeters	0.039	inches	in
m	meters	3.28	feet	ft
m	meters	1.09	yards	yd
km	kilometers	0.621	miles	mi
	AREA			
mm^2	square millimeters	0.0016	square inches	in^2
m^2	square meters	10.764	square feet	ft^2
m^2	square meters	1.195	square yards	ac
ha	hectares	2.47	acres	mi^2
km^2	square kilometers	0.386	square miles	
	VOLUME			
ml	milliliters	0.034	fluid ounces	fl oz
l	liters	0.264	gallons	gal
m^3	cubic meters	35.71	cubic feet	ft^3
m^3	cubic meters	1.307	cubic yards	yd^3
	MASS			
g	grams	0.035	ounces	oz
kg	kilograms	2.202	pounds	lb
Mg	megagrams	1.103	short tons (2000 lb)	T
	TEMPERATURE (exact)			
°C	Celcius temperature	1.8C + 32	Fahrenheit temperature	°F
	ILLUMINATION			
lx	lux	0.0929	foot-candles	fc
cd/m^2	candela/m^2	0.2919	foot-Lamberts	fl
	FORCE and PRESSURE or STRESS			
N	newtons	0.225	poundforce	lbf
kPa	kilopascals	0.145	poundforce per square inch	psi

* SI is the symbol for the International System of Units. Appropriate rounding should be made to comply with Section 4 of ASTM E380.

(Revised August 1992)

5.62 Moment and Slip vs. Deflection for Girder 2R-12-S 116

5.63 Total Moment vs. Confining Bar Strain for Girder R-8-N 117

5.64 Total Moment vs. Confining Bar Strain for Girder R-8-S 117

5.65 Total Moment vs. Confining Bar Strain for Girder R-10-N 118

5.66 Total Moment vs. Confining Bar Strain for Girder R-10-S 118

5.67 Total Moment vs. Confining Bar Strain for Girder R-12-N 119

5.68 Total Moment vs. Confining Bar Strain for Girder R-12-S 119

5.69 Total Moment vs. Confining Bar Strain for Girder 2R-8-N 120

5.70 Total Moment vs. Confining Bar Strain for Girder 2R-8-S 120

5.71 Total Moment vs. Confining Bar Strain for Girder 2R-10-N 121

5.72 Total Moment vs. Confining Bar Strain for Girder 2R-10-S 121

5.73 Total Moment vs. Confining Bar Strain for Girder 2R-12-N 122

5.74 Total Moment vs. Confining Bar Strain for Girder 2R-12-S 122

NOTATION

A_{cs} = cross-sectional area of a strut in strut-and-tie model (IN^2)

A_{ps} = area of prestressing steel (IN^2)

A_s = area of non-prestressed tension reinforcement (IN^2)

A^*_s = area of prestressing steel

A_{st} = total area of longitudinal mild steel reinforcement (IN^2)

A_v = area of a transverse reinforcement within a distance s (IN^2)

b' = width of a web of a flanged member

b_v = effective web width (IN)

b_w = web width

d = distance from extreme compressive fiber to centroid of the prestressing force

d_b = nominal diameter of a reinforcing bar, wire or prestressing strand (IN)

d_s = nominal diameter of a prestressing strand (IN)

d_v = effective shear depth (IN)

E_c = modulus of elasticity of concrete (KSI)

E_p = modulus of elasticity of prestressing tendons (KSI)

E_s = modulus of elasticity of reinforcing bars (KSI)

F_ϵ = reduction factor

f'_c = specified compressive strength of concrete at 28 days (KSI)

f'_{ci} = specified compressive strength of concrete at time of initial loading or prestressing (KSI)

f_{cu} = the limiting concrete compressive stress for design by strut-and-tie model (KSI)

f_d = stress due to unfactored dead load, at extreme fiber of section where tensile stress is caused by externally applied loads

f_{pc} = compressive stress in concrete (after allowance for all prestress losses) at centroid of cross section resisting externally applied loads or at junction of web and flange when the centroid lies within the flange (In a composite member, fpc is resultant compressive stress at centroid of composite section or at junction of web and flange when the centroid lies

within the flange, due to both prestress and moments resisted by precast member acting alone)

f_{pe} = compressive stress in concrete due to effective prestress force only (after allowance for all prestress losses) at extreme fiber of section where tensile stress is caused by externally applied loads applied loads (1989 AASHTO)

f_{pe} = effective stress in the prestressing steel after losses (KSI) (1994 LRFD AASHTO)

f_{po} = stress in the prestressing steel when the stress in the surrounding concrete is 0.0 (KSI)

f_{ps} = average stress in prestressing steel at the time for which the nominal resistance of member is required (KSI)

f_{se} = effective steel prestress after losses

f_{si} = initial steel prestress before losses

f_{sy} = yield stress of non-prestressed conventional reinforcement in tension

f_v = stress in transverse web reinforcement

f_y = specified minimum yield strength of reinforcing bars (KSI)

I = moment of inertia about the centroid of the cross section

ℓ_d = development length (IN)

l_e = embedded length

l_t = transfer length

M_{cr} = moment causing flexural cracking at a section due to externally applied loads

M_{max} = maximum factored moment at a section due to externally applied loads

M_u = factored moment at the section (K-IN)

N_u = applied factored axial force taken as positive if compressive (KIP)

P = pullout force

P_1 = pullout force at adhesion bond failure

P_e = effective prestress force

P_n = nominal axial resistance of a strut or tie (KIP)

P_t = pullout force at mechanical bond failure

S_b = lower section modulus

s = spacing of reinforcing bars (IN)

U_1 = bond stress at adhesion bond failure

U'_1 = U_1 divided by the square root of f'_c

U_m = maximum bond stress

U_p = bond stress at free end movement

U_t = bond stress at mechanical bond failure

U'_t = U_t divided by the square root of f'_c

U_{tl} = average bond stress over transfer length

U_s = maximum bond stress

V_c = nominal shear strength provided by concrete

V_{ci} = nominal shear strength provided by concrete when diagonal cracking results from combined shear and moment

V_{cw} = nominal shear strength provided by concrete when diagonal cracking results from excessive principal tensile stress n web

V_d = shear force at section due to unfactored dead load

V_i = factored shear force at section due to externally applied loads occurring simultaneously with M_{max}

V_n = nominal shear resistance of the section considered (KIP)

V_p = component in the direction of the applied shear of the effective prestressing force, positive if resisting the applied shear (KIP)

V_s = nominal shear strength provided by shear reinforcement

V_u = factored shear force at section (KIP)

v = factored shear stress (KSI)

Y_t = distance from centroidal axis of gross section, neglecting reinforcement, to extreme fiber in tension

α = angle of inclination of transverse reinforcement to longitudinal axis (DEG)

β = factor relating effect of longitudinal strain on the shear capacity of concrete, as indicated by the ability of diagonally cracked concrete to transmit tension

ϵ_1 = principal tensile strain in cracked concrete due to factored loads (IN/IN)

ϵ_x = longitudinal strain in web reinforcement on the flexural tension side of the member.

θ = angle of inclination of diagonal compressive stresses (DEG)

θ_s = angle between compression strut and longitudinal axis of the member in a shear truss model of a beam (DEG)

σ_s = the smallest angle between the compressive strut and adjoining tension ties (DEG)

ϕ = resistance factor

CRACKING AND SHEAR CAPACITY OF HIGH-STRENGTH AASHTO TYPE II GIRDERS

ABSTRACT

In this study, field and laboratory tests were performed to investigate the transfer length as well as the shearing capacity of high strength concrete girders. For this purpose, six (6) full-scale AASHTO type II prestressed girders were prepared with 8,000 psi, 10,000 psi and 12,000 psi concrete strengths and tested under controlled conditions. The girders were instrumented with both internal and external gages. The internal gages were used in the field to investigate the transfer length of the girders during the releasing of the prestress strands. From the results of these tests a relationship was developed to predict the transfer length of high strength prestressed girders. It has been found that using high strength concrete reduces the transfer length in pretensioned girders.

To further investigate the behavior of the prestress strands during load transfer, forty (40) direct tension pullout tests were performed in the laboratory to examine the bonding characteristics between the prestressing strands and the concrete. The strand sizes ranged from 3/8" to 0.6" and the concrete compressive strength ranged from 6,000 psi to 12,000 psi. Results form these tests showed that small strand diameters experienced higher bond stresses, and high concrete strength can withstand higher hoop stresses that develop after initial bond failure.

In the laboratory, both ends of each AASHTO type II girder were tested to failure. Most of the girders failed after a bond failure between the prestressing strand and concrete. The ultimate shear capacity was then compared with the predicted shear capacity using different approaches. High concrete strength was found not to appreciably affect the ultimate strength of girders that failed due to bonding failure.

CRACKING AND SHEAR CAPACITY OF HIGH-STRENGTH AASHTO TYPE II GIRDERS

ABSTRACT

In this study, field and laboratory tests were performed to investigate the transfer length as well as the shearing capacity of high strength concrete girders. For this purpose, six (6) full-scale AASHTO type II prestressed girders were prepared with 8,000 psi, 10,000 psi and 12,000 psi concrete strengths and tested under controlled conditions. The girders were instrumented with both internal and external gages. The internal gages were used in the field to investigate the transfer length of the girders during the releasing of the prestress strands. From the results of these tests a relationship was developed to predict the transfer length of high strength prestressed girders. It has been found that using high strength concrete reduces the transfer length in pretensioned girders.

To further investigate the behavior of the prestress strands during load transfer, forty (40) direct tension pullout tests were performed in the laboratory to examine the bonding characteristics between the prestressing strands and the concrete. The strand sizes ranged from 3/8" to 0.6" and the concrete compressive strength ranged from 6,000 psi to 12,000 psi. Results form these tests showed that small strand diameters experienced higher bond stresses, and high concrete strength can withstand higher hoop stresses that develop after initial bond failure.

In the laboratory, both ends of each AASHTO type II girder were tested to failure. Most of the girders failed after a bond failure between the prestressing strand and concrete. The ultimate shear capacity was then compared with the predicted shear capacity using different approaches. High concrete strength was found not to appreciably affect the ultimate strength of girders that failed due to bonding failure.

CHAPTER 1
INTRODUCTION

1.1 High Strength Concrete

Concrete admixtures have been developed in recent years that enable very high strength concrete to be produced at a competitive price. The use of high strength concrete may become more popular in many applications. High strength concrete has different characteristics than normal strength concrete. The behavior of high strength concrete must be investigated to ensure that safe structures are produced using this new material. Few studies have been performed considering the effect of high strength concrete on the transfer and development lengths. The use of existing equations, developed for normal strength concrete, to predict the shear strength of high strength prestressed girders should be examined.

1.2 Transfer Length Background

In manufacturing of pretensioned prestressed concrete girders the reinforcing strands are tensioned before the casting of the concrete. After the concrete has reached approximately 70% of its design compressive strength, the tension in the strands is released. During the release of the strands a compressive stress is transmitted to the lower flange of the girder. The length over which the prestressing force in the strands is transmitted to the girder is the *transfer length*. Bonding forces are the only forces that anchor the strand to the concrete. Under certain loading conditions, when additional tensile forces are carried by the strand, it is possible to have a bond failure that will cause a flexural or shear failure. The additional tensile stresses in the strands, caused by external loads, require an anchorage length beyond the transfer length. The transfer length plus the additional length required to resist the external loads is the *development length*. The development length of a prestressed girder is the distance from the end of the girder where the critical section will fail without a bond failure.

The current ACI and AASHTO codes use equations based on research conducted in the early 1960's to predict the transfer length and development length. Recently, it has been found the current code may be inadequate, and there is a great deal of research being conducted on the transfer length

and development length of prestressed members.

When the critical section of a prestressed girder is within the development length, a bond failure may cause the girder to fail. A simply supported girder will have the maximum shear stresses near the supports. Thus the critical section for shear will most likely be within the development length, and it is therefore possible for a bond failure to occur. The transfer length, development length and shear strength of pretensioned prestressed girders are all affected by the bonding between the strands and concrete.

1.3 Shear Strength Background

The shear strength of prestressed concrete members is an important parameter that will affect the general performance of the member. In most prestressed members the shear force will be most significant near the supports of the member. For simply supported members the locations of the high shear forces will be within the development length. Therefore high shear stresses near the supports may cause bond failures. The response of prestressed members subjected to shear must be understood so that efficient and safe prestressed members can be designed. The design shear strength of prestressed bridge girders is currently determined following the AASHTO code. The 1989 AASHTO code uses a method commonly called the ACI traditional method to determine the shear strength of prestressed members. This method suggests that the shear cracks in the web will be elevated at 45 degrees. The 1994 Load and Resistance Factor Design (LRFD) AASHTO code uses a different methodology that predicts different crack inclinations at various locations along the member. Ideally, a more accurate cracking prediction will enable more accurate shear strength estimates.

1.4 Objective

The main objective of this research was to investigate the cracking and shear capacity of high strength prestressed concrete girders. Inherent in this objective was the investigation of the transfer length and bond strength of prestressed girders. Both full scale transfer length test and small scale bond test were used to examine the bond behavior of prestressing strands and high strength concrete. Then, the girders were tested under loading conditions that produced high shear stresses. The

transfer length test results were used to develop an equation that predicts the transfer length for full scale girders. The static load tests were used to determine which of the current codes best predicts the shear strength of the prestressed girders.

CHAPTER 2
LITERATURE REVIEW

2.1 Bond Strength of Prestressing Strands and Concrete

Hoyer and Friedreich (1939) [1] were among the first researchers to explore the bonding characteristics in prestressed, pretensioned concrete beams. They suggested that when the prestressing force is transmitted to the girder, stresses in the strand are reduced because of the elastic shortening and slip within the transfer length, and the cross-sectional area of the strand would swell in some locations due to Poission's effect. This swelling is presumed to allow a large buildup of frictional forces in the swollen region. This phenomenon has become known as the "Hoyer effect."

In recent years, there have been many published reports that studied the bond between seven wire strand and concrete through pullout tests. These studies have used the average bond stress over the embedded length of the sample for comparison. Some of these studies used seven wire strand that was not tensioned before testing. This testing arrangement is known as the direct tension pullout test. Other testing arrangements use pretensioned seven wire strands.

Strands in the direct tension pullout test do not develop the Hoyer effect; on the contrary, the cross sectional areas of the strands reduce during testing. Tests using pretensioned strands produce the Hoyer effect during testing. Pullout test using pretensioned strands require an apparatus that can secure a tensioned strand during concrete curing. Direct tension specimens are easy to prepare and test under various loading conditions.

Brearly and Johnston (1990) [2] tested fifty-two (52) direct tension pullout tests. These tests were conducted to compare the bond strength between epoxy coated and uncoated strands. They used 5,000 psi concrete and 8" x 8" x 12" samples with an embeddment length of 12". The diameters of the tested strands were 3/8", 1/2" and 0.6". In their tests, they found two distinct bond stresses identified as U_p and U_m. U_p was defined as the average bond stress when free end movement began. The authors defined this movement as a slip exceeding 0.0004". The second bond stress, U_m, was the maximum stress the sample would withstand. *Brearly and Johnston* obtained the ratio of the bond stresses, U_p and U_m, divided by the square root of the compressive strength of the concrete. This ratio was used to compare the results of samples with different compressive strengths. These

terms are assumed to be dimensionless and are noted as U'_p and U'_m. Table 2.1 summarizes the results presented by *Brearly and Johnston* for uncoated strands.

Deatherage and Burdette (1991) [3] conducted a study on the transfer and development lengths of prestressed girders. They performed several direct tension pullout tests as a part of their testing program. The prestressing strands used in the study were: 1/2", 1/2" special (nominal diameter of 0.5224"), 9/16" and 0.6". All of the specimens had a cross sectional area of 6" x 6". Two embedded lengths of 18" and 36" were used in this investigation. The authors presented their pullout results in terms of pullout force rather than bonding stress. The bonding stress for a given test can be easily determined by dividing the pullout force by the nominal surface area. Results form *Deatherage and Burdette* are presented in Table 2.2.

Cousins et al. (1992) [4] tested twenty three (23) specimens to determine the bond characteristics between 3/8", 1/2" and 0.6" diameter prestressed strands and 4,000 psi concrete. To include Hoyer effect, the authors prepared the testing specimens with pretensioned strands. The authors noted that following the bond failure, the resistance remained nearly constant. This resistance was attributed to mechanical interlock, friction and the Hoyer effect. The test results for the uncoated strands are shown in Table 2.3.

Yu (1992) [5] tested seven (7) pretensioned samples to investigate the bond between seven wire strand and concrete. Samples were 6" x 6" x 6" with 1/2" diameter strand and a design concrete strength of 5,000 psi. Yu's results are shown in Table 2.4. He suggested that after the bond failure the specimen can withstand an additional 60 to 70 pounds of load before total failure.

2.2 Transfer Length and Development Length in Precast Girders

Hognestad and Janey (1954) [6] studied the bond between a smooth single wire strand and concrete. They found three factors that contribute to the bond between prestressing strand and concrete. These factors are the following:

1) chemical adhesion between the two media,

2) frictional forces, and

3) mechanical forces.

The authors reasoned that the chemical adhesion is lost when there is a movement or slip

between the two media. They noted that a slip is usually developed during the transfer of the prestressing force from the strands to the beam. Hognestad and Janey suggested that the frictional and mechanical forces are the only bonding forces remaining in the transfer length of a prestressed beam.

In another study, *Janey (1954)* [7] further explored the transfer length in prestressed girders. This study used single wire strands between 0.1" and 0.276" in diameter and concrete strengths of 4,500 psi and 6,000 psi. Janey found that the transfer length becomes moderately greater as the diameter increases. Also, he observed that because transfer length is largely determined by frictional forces, one might not expect a significant difference between the two concrete strengths. His results suggested that the transfer length would increase as the strength of concrete decreases. Janey also suggested that this change in transfer length may be explained by the ability of the higher strength concrete to sustain higher radial pressures exerted by the strand.

Hanson and Kaar's (1959) [8] study on development length has been used by the ACI and AASHTO codes to predict the development length. In their study, they considered the friction and the Hoyer effect to be the major agents affecting the transfer length. They noted that mechanical resistance is probably of a little significance in a single smooth wire, but, may be a significant factor when considering seven wire strand. Hanson and Kaar found that the mechanical interlock can support additional loads in a prestressed beam after a general bond slip, when adhesion and friction have been lost. They concluded that the mechanical bond resistance is an extremely important characteristic of bond performance.

Over and Au (1965) [9] studied the transfer length of 3" x 3" x 80" specimens using seven wire strands. Based on the results obtained from their study they found that:

1) The transfer length increases when larger strands are used,

2) Seven wire strands may develop additional stresses in concrete after they have slipped, and

3) Seven wire strands require less transfer length than equivalent single wire strands.

They also concluded that the mechanical bond is extremely important in the performance of prestressed beams.

Cousins et al. (1986) [10,11] completed an extensive study of the transfer length and development length of prestressed girders. The authors compared the bond characteristics of grit impregnated

epoxy coated strands and uncoated strands. The authors developed an analytical model to predict the transfer length and development length of the various types of strands. The surface condition of the strand was found to have the most significant effect on the transfer length and development length. For the coated strands, as the grit density increased, the bond increased and the transfer length and development length decreased. The bonding of an uncoated strand was significantly less than the bonding of a lightly impregnated epoxy strand.

Shahawy et al. (1992) [12] presented a study of the transfer length in full scale prestressed girders. The variables in that investigation were: the size of the strand, the amount of shielding and the amount of web reinforcement. Their findings showed that larger strands have an increased transfer length. The transfer region for shielded members was measured from the end of the shielding to the point of full transfer of prestressing force. This length was equal to the transfer length of an unshielded member. Thus, the transfer length for a shielded girder was the shielded length plus the transfer length for an equivalent unshielded girder. The authors found that the amount of shear reinforcement did not affect the transfer length.

2.3 Shearing Capacity of Prestressed Girders

The 1989 AASHTO code, ACI code and the 1994 AASHTO LRFD code were reviewed and used as a comparison for the shear test results. Each code divides the ability of a prestressed member to resist shear into a concrete component and a steel component. All of the codes use a truss analogy to predict the steel contribution. The current ACI and AASHTO codes are very similar However, the ACI code offers an equation that may be used as a simplification to more detailed equations used to determine the concrete contribution. The shear section of the AASHTO LRFD code is based on a different theory than the shear sections of the ACI and 1989 AASHTO codes. The AASHTO LRFD code offers a significant departure from the current design codes in the determination of the concrete component. The theory used in the LRFD code also modifies the calculation of the steel component of the shear strength.

The truss analogy was initially developed by Ritter in 1899 to explain the interaction between concrete and reinforcing steel in resisting shearing forces. The truss model assumes that the web reinforcement acts as vertical tension members, diagonal compressive forces are resisted by concrete,

and longitudinal reinforcement acts as tension members to balance the forces. Mörsch refined the truss model in the early 1900's. Mörsch assumed the diagonal compressive stresses, and thus the inclined cracks, to be inclined at 45°. Using this assumption and equilibrium, the shear force carried by vertical stirrups, V_s, is:

$$V_s = \frac{A_v \cdot f_v \cdot d}{s} \qquad 2\text{-}1$$

Mörsch recognized the angle of the stresses was very significant in determining how the stresses would be carried by the member. Mörsch did not see a way to accurately predict the angle of inclination and thus he made the conservative assumption of 45°. If the angle of inclination, θ, was not assumed to be constant, the shear force carried by the stirrups would be:

$$V_s = \frac{A_v \cdot f_v \cdot d \cdot \cot\theta}{s} \qquad 2\text{-}2$$

2.3.1 1989 AASHTO Code

The shear specifications are covered in section 9.20 of the 1989 AASHTO code. The ability of the prestressed member to resist shear forces is divided into two separate components, V_c and V_s. V_c is the shear force that can be resisted by the concrete and V_s is the shear force that can be resisted by the web reinforcement. The code requires that

$$V_u \leq \phi\,(V_c + V_s) \qquad 2\text{-}3$$

where V_s is the shear caused by the factored loads and ϕ is a strength reduction factor.

There are two distinct failure mechanisms that limit the shear strength of the concrete, V_c. The two failure modes are flexure-shear failure and web-shear failure. Flexure-shear failure is caused by an initial flexural crack that extends and produces a shear crack that eventually causes failure. Web-shear failure is caused by a shear crack in the web of the member that develops and causes

and longitudinal reinforcement acts as tension members to balance the forces. Mörsch refined the truss model in the early 1900's. Mörsch assumed the diagonal compressive stresses, and thus the inclined cracks, to be inclined at 45°. Using this assumption and equilibrium, the shear force carried by vertical stirrups, V_s, is:

$$V_s = \frac{A_v \cdot f_v \cdot d}{s} \qquad 2\text{-}1$$

Mörsch recognized the angle of the stresses was very significant in determining how the stresses would be carried by the member. Mörsch did not see a way to accurately predict the angle of inclination and thus he made the conservative assumption of 45°. If the angle of inclination, θ, was not assumed to be constant, the shear force carried by the stirrups would be:

$$V_s = \frac{A_v \cdot f_v \cdot d \cdot \cot\theta}{s} \qquad 2\text{-}2$$

2.3.1 1989 AASHTO Code

The shear specifications are covered in section 9.20 of the 1989 AASHTO code. The ability of the prestressed member to resist shear forces is divided into two separate components, V_c and V_s. V_c is the shear force that can be resisted by the concrete and V_s is the shear force that can be resisted by the web reinforcement. The code requires that

$$V_u \leq \phi\,(V_c + V_s) \qquad 2\text{-}3$$

where V_s is the shear caused by the factored loads and ϕ is a strength reduction factor.

There are two distinct failure mechanisms that limit the shear strength of the concrete, V_c. The two failure modes are flexure-shear failure and web-shear failure. Flexure-shear failure is caused by an initial flexural crack that extends and produces a shear crack that eventually causes failure. Web-shear failure is caused by a shear crack in the web of the member that develops and causes failure. Following the AASHTO code, both the flexure-shear strength (V_{ci}), and the web-shear strength (V_{cw}) are calculated at each desired section. The lower strength at any section is the value

that controls the design. Thus, V_c is taken as the lesser value of V_{ci} and V_{cw}.

The code gives the following equations to compute flexural-shear strength V_{ci}:

$$V_{ci} = 0.6\ b'\ d\ \sqrt{f'_c} + V_d + \frac{V_i\ M_{cr}}{M_{\max}} \qquad 2\text{-}4$$

$$M_{cr} = \frac{I}{Y_t}\ (6\ \sqrt{f'_c} + f_{pe} - f_d) \qquad 2\text{-}5$$

$$V_{ci} > 1.7\ b'\ d\ \sqrt{f'_c} \qquad 2\text{-}6$$

The code gives the following equation to calculate web-shear strength V_{cw}:

$$V_{cw} = b'\ d\ (3.5\ \sqrt{f'_c} + 0.3 f_{pc}) + V_p \qquad 2\text{-}7$$

The code uses the 45° truss analogy and an upper limit for the steel contribution to calculate the shear strength provided by the reinforcement at any location:

$$V_s = \frac{A_v\ f_{sy}\ d}{s} \qquad 2\text{-}8$$

$$V_s < 8\ b'\ d\ \sqrt{f'_c} \qquad 2\text{-}9$$

The calculations were performed using a factor of safety of unity. A factor of safety of one is appropriate for laboratory testing where the test results will be used to verify the analytical model.

2.3.2 ACI Code

The ACI code also divides the ability of a prestressed member to resist shearing forces into a concrete component and a steel component, V_c and V_s respectively. The code gives two methodologies to compute V_c, a simplified method and a more detailed method. The more detailed method is the same method specified in the AASHTO code. The simplified method was used in this research to provide a different comparison for the test results. The simplified equation for V_c is:

$$V_c = (0.6\sqrt{f'_c} + 700\frac{V_u \cdot d}{M}) b_w \cdot d \qquad 2\text{-}10$$

where:

$$2\sqrt{f'_c}\, b_w \cdot d < V_c < 5\sqrt{f'_c}\, b_w \cdot d \qquad 2\text{-}11$$

The ACI code also uses the 45° truss model with an upper limit to compute the steel contribution to resisting the shear forces.

$$V_s = \frac{A_v f_y d}{s} \qquad 2\text{-}12$$

$$V_s < 8\, b_w\, d\sqrt{f'_c} \qquad 2\text{-}13$$

As in the AASHTO Code calculations, the factor of safety was taken as unity.

2.3.3 1994 AASHTO LRFD Code

The AASHTO LRFD code offers a different methodology to design prestressed girders for shear. The LRFD code provisions for shear have been developed from the modified compression field theory, further called the MCFT theory. This theory was based on Wagner's tension field theory that explained the angle of inclination of the principal tensile strains in steel members. The MCFT uses equilibrium conditions to predict the angle of inclination, θ, of the principal stresses. The MCFT also considers the concrete's ability to resist tensile forces between cracks. For low and high values of θ, the web reinforcement and the longitudinal reinforcement will be highly strained, respectively. Knowing θ, more detailed calculations of the shear forces can be performed. Ultimately, the theory should result in more accurate predictions of V_c and V_s. The shearing capacity of prestressed girders is given by the AASHTO LRFD code as:

$$V_n = V_c + V_s + V_p \qquad 2\text{-}14$$

$$V_n = 0.25\, f'_c \cdot b_v \cdot d_v + V_p \qquad 2\text{-}15$$

$$V_c = 0.0316\, \beta \sqrt{f'_c} \cdot b_v \cdot d_v \qquad 2\text{-}16$$

$$V_s = \frac{A_v f_y d_v (\cot\theta + \cot\alpha) \sin\alpha}{s} \qquad 2\text{-}17$$

The AASHTO LRFD code gives additional equations to compute two other factors, v and ϵ_x, which are used to determine θ and using charts or tables provided in the code.

$$v = \frac{V_u - \phi V_p}{\phi \cdot b_v \cdot d_v} \qquad 2\text{-}18$$

$$x = \frac{\frac{M_u}{d_v} + 0.5\ N_u + 0.5\ V_u\ .\ \cot\theta - A_{ps}\ .\ f}{E_s\ .\ A_s + E_p\ .\ A_{ps}} \qquad 2\text{-}19$$

where:

$$f_{po} = f_{pe} + \frac{f_{pc}\ E_p}{E_c} \qquad 2\text{-}20$$

if ϵ_x is negative then ϵ_x is multiplied by a factor F_ϵ

$$F_\epsilon = \frac{E_s\ .\ A_s + E_p\ .\ A_{ps}}{E_c.A_c + E_s\ .\ A_s + E_p\ .\ A_{ps}} \qquad 2\text{-}21$$

2.3.4 Strut and Tie Models

The AASHTO LRFD code discusses the use of strut and tie models in section 5.6.3 of that code. The code states that the use of strut and tie models in prestressed girders is most appropriate for short deep beams or in areas where the distance between the applied load and the support is less than twice the overall height of the member. In their 1991 text, Collins and Mitchell stated that the strut and tie models may best predict girder behavior when the shear span to depth ratio is less than about 2.5.

Strut and tie models offer an alternate means to examine stresses near supports and concentrated loads. In using this method, the geometry of the girder is used to approximate the dimensions of a truss assumed to carry the applied loads. The major components of the truss are the inclined concrete compressive strut, upper longitudinal concrete compressive strut and the lower tension tie. These members of the truss are connected in nodal zones.

After the geometry of the girder and loading arrangement have been determined the strength of the girder can be determined. Because an initial assumption of the geometry is required, a trial and error approach is required in design. The strength of the inclined concrete compressive strut is critical to the resistance of the truss. The code gives the following equations to calculate the nominal resistance of an unreinforced compressive strut:

$$P_n = f_{cu} \cdot A_{cs} \qquad 2\text{-}22$$

The effective area of the strut is determined by the anchorage condition and the width of the web. The equation for the limiting compressive stress is given as:

$$f_{cu} = \frac{f'_c}{0.8 + 170\ \epsilon_1} \leq 0.85 f'_c \qquad 2\text{-}23$$

Where:

$$\epsilon_1 = (\epsilon_s + 0.002)\ \cot^2\sigma_s \qquad 2\text{-}24$$

The code specifies that the tension tie must be anchored to the nodal zone following the anchorage and development requirements of the code. In addition, the code states the tension force must be developed at the inner face of the nodal zone. The LRFD code gives the following equation to determine the nominal resistance of the tension tie

$$P_n = f_y\ A_{st} + A_{ps}\ (f_{pe} + f_y) \qquad 2\text{-}25$$

The required anchorage length for bonded prestressing strands is calculated using the development length equation in chapter 5.11 of the code and is given as:

$$l_d > = (f_{ps} - \frac{2}{3} f_{pe})\ d_b \qquad 2\text{-}26$$

Table 2.1 Bond Test Results After Brearly and Johnson (1990)

D (in.)	# tested	f'_c (psi)	U_p (psi)	U'_p	U_m (psi)	U'_m
3/8"	5	5344	481	6.58	545	7.47
1/2"	8	6130	285	3.67	295	3.81
0.6"	7	6351	262	3.29	265	3.33

Table 2.2 Bond Test Results After Deatherage and Burdette (1991)

Diameter	# tested	f'_c	Strand	U (psi)	U'
1/2"	3	6313	Mill	265	3.32
1/2"	3	5577	Weathered	592	7.92
0.5224"	2	5360	Mill	235	2.99
0.5224"	2	5530	Weathered	584	7.85
9/16"	4	4285	Mill	253	3.91
0.6"	4	4765	Mill	374	5.40

Table 2.3 Bond Test Results After Cousins, Badeau and Moustafa (1992)

Diameter	# tested	f'c (psi)	Us	U's
3/8"	5	3760	1026	16.68
1/2"	3	3490	413	7.00
0.6"	3	3840	553	9.69

Table 2.4 Bond Test Results After Yu (1992)

Diameter	# tested	f_c	U	U'
1/2"	5	5637	464	6.18

CHAPTER 3
TESTING PROGRAM

3.1 Overview

For this study, the testing program was divided into field and laboratory testing. The field testing included experimenting full scale beams for transfer length evaluation. In the laboratory, the beams were further tested to examine the effect of using high strength concrete on the cracking behavior and shear capacity of the beams. In addition, large number of cylindrical pullout samples were tested to investigate the effect of surface condition on the bonding characteristics of the prestress strands. Results from these tests were used to interpret the behavior of the prestress strands during the transfer stage and upon loading. Different phases of the bonding mechanism could be distinguished from the test results. These phases governed the transfer length measurements and the amount of strand slip during shear testing in the beams.

Six (6) full scale AASHTO Type II high strength concrete girders were tested in this study. The concrete strength used for these beams were; 8,000 psi, 10,000 psi and 12,000 psi. Two beams were prepared for each concrete strength. One beam from each set was reinforced with shear reinforcement (C-bars) equal to that required by AASHTO and was designated as R series. The amount of shear reinforcement in the second beam was doubled and was designated as 2R series. The number of prestress strands and the confinement bars (D-bars) in R and 2R series were the same. All the instrumented C and D bars were prepared at FAMU/FSU College of Engineering and transferred to DURASTRESS concrete yard in Leesburg, Florida, for installation. Beam preparation was completed at the yard, and after the transfer length measurements, the beams were cured at the yard and then transported to the Florida Department of Transportation structural laboratory for testing.

3.2 Pullout Bond Test

3.2.1 Overview

Because of its simplicity in both sample preparation and testing procedure, the direct tension pullout test was chosen over a test using pretensioned strands. About forty (40) concrete samples were prepared with different surface conditions and different diameters for the purpose of this test.

It would not have been feasible to prepare this many specimens for a test using pretensioned strands. In addition, the literature review showed that the accuracy of the results, determined by the standard deviation within a particular group, was approximately equal for the two types of testing.

The disadvantage of the direct tension test, however, is that the test does not reproduce the Hoyer effect. Therefore, the pullout bond strengths are expected to be lower than the full scale transfer bond strengths. It is anticipated, however, that the Hoyer effect can be accounted for when developing a relationship between the pullout bond strength and the transfer bond strength.

Previous pullout tests showed that a large sample group is required because of the large standard deviation in the test results. It was desirable to prepare several pullout specimens using the same strand and concrete of each AASHTO girder tested. This allowed comparisons between the pullout and transfer length test results. The direct tension tests performed by Brearly and Johnston show that there are two distinct failure modes U_p and U_m. Approximately half the samples were made using lubricated strands to study the effect of the surface condition on the initial and final bond.

3.2.2 Testing Materials

The pullout specimens were made from six different concrete mixes. Two mixes, produced by Florida Mining in Tallahassee, used the same mix design and had a design strength of 6,000 psi. The remaining mixes were obtained from the DURASTRESS facility and had design strengths of 6,000 psi, 8,000 psi, 10,000 psi, and 12,000 psi.

The prestressing strands were seven wire strands with nominal diameters of 3/8", 7/16", 1/2" and 0.6". The strands had a minimum tensile strength of 270 ksi. Three different types of light lubricant were applied to coat the strands. The three lubricants were WD-40, engine oil, and a light petroleum based oil used as demolding agent by DURASTRESS. In addition to the light lubricants, a very heavy grease was used to eliminate any contact between the strand and the concrete. The purpose of these types of coatings was to produce strands with different surface conditions.

Table 3.1 summarizes the samples tested in this project. The specimens were designated using five symbols. The first number represents the nominal size of the strand in abbreviated decimal form: for example 3, 4, 5 and 6 represent 3/8" (0.375"), 7/16" (0.4375"), 1/2" (0.5") and 0.6", respectively. The second group of letters shows the condition of the strand. The first letter G or U stands for

greased or ungreased, respectively. The second letter represents the surface condition of the strand, clean or lightly rusted. The third letter represents the type of lubricant. The next number represents the compressive strength of the concrete. The final letter is used to distinguish repetitive specimens.

3.2.3 Sample Preparation

All of the samples were prepared using 6" x 12" cylinders. The specimens made at DURASTRESS were rodded following ASTM specifications, then the strands were inserted in the center of the cylinder. The specimens made at the FDOT Structures Laboratory were vibrated before the strand being placed in the cylinder. The top of the strand was supported during curing to keep the strand in the center of the cylinder. The specimens cured for a minimum of 28 days before testing. Before testing, the molds were removed and strain gages were attached to the strand according to the recommended procedure by the manufacturer.

3.2.4 Setup and Procedure of Pullout Testing

The primary components of the testing apparatus were: two fixed steel plates that supported the specimen, a small hydraulic prestressing jack and hand pump that applied the pullout load, a pressure transducer that measured the pressure in the jack, a bushing that protected the strain gage and a dial gage that measured the strand slip. Data was recorded using a computerized data acquisition system. A schematic diagram of the test apparatus is shown in Figure 3.1.

After placing the specimen in the testing apparatus, the griping mechanism on the jack was secured to the strand and the dial gage was placed on the strand. A small amount of load was applied to the strand to secure the griping mechanism and set the cylinder firmly against the fixed plate. This load was then relaxed and zero readings were taken.

The load was then increased steadily using a loading control configuration. Force and displacement readings were concurrently recorded using the data acquisition system. Testing was continued until failure. Failure was noted by a sudden reduction in load and drastic increase in slip.

3.3 Transfer Length Tests

The transfer length specimens consisted of the six (6) full scale AASHTO Type II girders tested at each end for a total of twelve tests. The differences between the girders were the strength of the concrete and the amount of shear reinforcement. In addition, findings *Shahawy et. al.* were used to supplement results obtained from the present study.

3.3.1 Testing Materials

The concrete used to manufacture the girders was made on-site by DURASTRESS, Inc. Three different design strengths of concrete were used: 8,000 psi, 10,000 psi and 12,000 psi. The prestress strands were clean and in good condition when they were placed in the casting bed.

3.3.2 Specimen Preparation

The strands were placed in the casting bed and tensioned to about $0.75f'_s$, or approximately 31,000 lb. per strand (202.5 ksi). The applied load was monitored by a pressure gage attached to the hydraulic jack. The casting bed was 300 feet long and several beams were cast in the same bed.

Embedded gages (PML 60), located at the center of the 16 strands in the lower flange, were used to measure the concrete strain during transfer. Figure 3.2 shows the placement of the embedded gages. Eight gages were installed at each end of each girder. The gages were located every six inches for the first three feet of the beam, then spacing was increased to twelve inches for the following two feet. Each gage was secured to the #3 strand using plastic cable ties. The wire lead for each gage was then led to the top of the girder.

After the embedded gages were secured, the shear reinforcement was tied to the strands, carefully avoiding the gages. Forms were then placed around the strands and the concrete was poured. Several cylinders and the pullout specimens were made with the concrete used to manufacture the girders.

3.3.3 Testing Procedure

The strands were ready to be released when the concrete had reached 70% of its design compressive strength. For some beams, reaching this strength took two to three days. The strands

were then released at each end by flame cutting. The releasing process was divided into four stages of four strands per stage. Figure 3.3 shows the flame cutting of the strands. At each stage, measurements from the embedded gages were recorded using a data acquisition system. This procedure allowed for four complete sets of transfer length data to be recorded for each end of each girder.

3.4 Shear Testing

The shear strength specimens consisted of the same six girders used in the transfer length tests. The girders were tested at each end so there was a total of twelve (12) tests. The load for all of the tests was applied by a single hydraulic jack.

3.4.1 Testing Materials

Before shear testing, 8" x 40" concrete slabs were poured on the test girders. These slabs had the minimum reinforcing steel specified in the AASHTO code. Figure 3.4 shows the cross section of the test girders. Figures 3.5 and 3.6 show the web reinforcement in the R and 2R series girders respectively. The concrete used for the slabs had a design compressive strength of 6,000 psi and was provided by Florida Mining and Materials in Tallahassee, FL.

3.4.2 Sample Preparation

Each girder contained reinforcing bars instrumented with strain gages. Both the web reinforcement, C bars, and the confining reinforcement, D bars, were instrumented before their placement in the girder. The C bars and the D bars were # 4 and #3 deformed bars, respectively. A flat smooth surface was necessary to secure the strain gages to the reinforcing bars. Each instrumented bar was grounded using a rotary grinder to create the surface required for the strain gages. This surface was generally two to three inches long and approximately 3/8" wide. The surfaces were then cleaned and the gages were attached using a quick drying glue. The instrumented location was then coated using materials provided by the manufacturer to insure the operation of the gage after pouring the concrete.

Two different loading configurations were used in the shear tests and were designated as

north and south end tests. After the slab cured the composite girder was placed on the testing frame and instrumented for the north end test. After the north end test was completed, the testing apparatus was configured for the other end. The major features of the north end test were the span length of 40 feet and the distance from the support to the load of 8.5 feet. Figure 3.7 shows the north end test configuration. For the south end the span length was 27.5 feet and the distance between the concentrated load and the support was 7.08 feet. Figure 3.8 shows the south end test configuration.

Displacement gages were placed at the ends of each of the sixteen strands which recorded the movement of the strands relative to the concrete girder. Figure 3.9 shows the gages used to measure end slip. Deflection gages were located at the support, concentrated load and centerline of the girder. A load cell was placed between the hydraulic jack and the girder to measure the applied load.

Twenty-three (23) additional external gages, crack gages, were mounted on the surface of the girder. The crack gages were used to measure strains in three different locations of the girder. A series of gages was placed on the lower flange from the support to a location past the load. Another series of gages was placed directly under the load and readings from these gages were used to locate the neutral axis. Three rosettes were placed on the web of the girder. Figures 3.10 and 3.11 show the location of the external gages for the north and south tests respectively.

3.4.3 Testing Procedure

All of the external and internal gages were connected to a computerized data acquisition system. A total of 64 gages monitored during testing. After balancing the gages initial readings were taken immediately before starting the test.

The concentrated load was applied by a hydraulic jack that was controlled by an electric pump. As the load was increased from zero, readings were taken in increments of ten kips of applied load. The increased loading was held constant after the first crack occurred. The crack was then traced with a black marker and labeled with the maximum applied load that had occurred. After the crack was marked, the load was again increased until additional cracking occurred. The process of increasing the load and marking the cracks was repeated until failure.

Ultimate failure was noted by the inability of the girder to carry additional load. Often the

Table 3.1 Pullout Test Specimens

Specimen	Diameter	Greased or Ungreased	Clean or Light Rust	Lubricant	f'c
3-UC-7-A	3/8"	U	C		7598
3-UC-7-B	3/8"	U	C		7598
3-UC-11-A	3/8"	U	C		11038
3-UC-11-B	3/8"	U	C		11038
4-UC-7-A	7/16"	U	C		7598
4-UC-7-B	7/16"	U	C		7598
4-UC-11-A	7/16"	U	C		11038
4-UC-11-B	7/16"	U	C		11038
5-UC-7-A	1/2"	U	C		7598
5-UC-7-B	1/2"	U	C		7598
5-UC-8-A	1/2"	U	C		8195
5-UC-8-B	1/2"	U	C		8195
5-UC-10-A	1/2"	U	C		9911
5-UC-10-B	1/2"	U	C		9911
5-UC-11-A	1/2"	U	C		11038
5-UL-6-A	1/2"	U	L		6282
5-UL-6-B	1/2"	U	L		6282
5-UL-6-C	1/2"	U	L		6282
5-UL-6-D	1/2"	U	L		6282
5-UL-6-E	1/2"	U	L		6282
6-UC-6-A	0.6"	U	C		6282
6-UC-7-A	0.6"	U	C		7598
6-UC-11-A	0.6"	U	C		11038
3-GCW-7-A	3/8"	G	C	WD-40	7598
4-GCW-7-A	7/16"	G	C	WD-40	7598
4-GCW-11-A	7/16"	G	C	WD-40	11038
5-GCW-7-A	1/2"	G	C	WD-40	7598
5-GCF-8-A	1/2"	G	C	Form Oil	8195
5-GCF-8-B	1/2"	G	C	Form Oil	8195
5-GCF-10-A	1/2"	G	C	Form Oil	9911
5-GCF-10-B	1/2"	G	C	Form Oil	9911
5-GLO-6-A	1/2"	G	L	Oil	6282
5-GLO-6-B	1/2"	G	L	Oil	6282
5-GLO-6-C	1/2"	G	L	Oil	6282
5-GLO-6-D	1/2"	G	L	Oil	6282
6-GCW-11-A	0.6"	G	C	WD-40	11038
6-GCW-11-B	0.6"	G	C	WD-40	11038
6-GCH-6-A	0.6"	G	C	Heavy Grease	6282
6-GCH-6-B	0.6"	G	C	Heavy Grease	6282

SCHEMATIC OF PULLOUT TEST

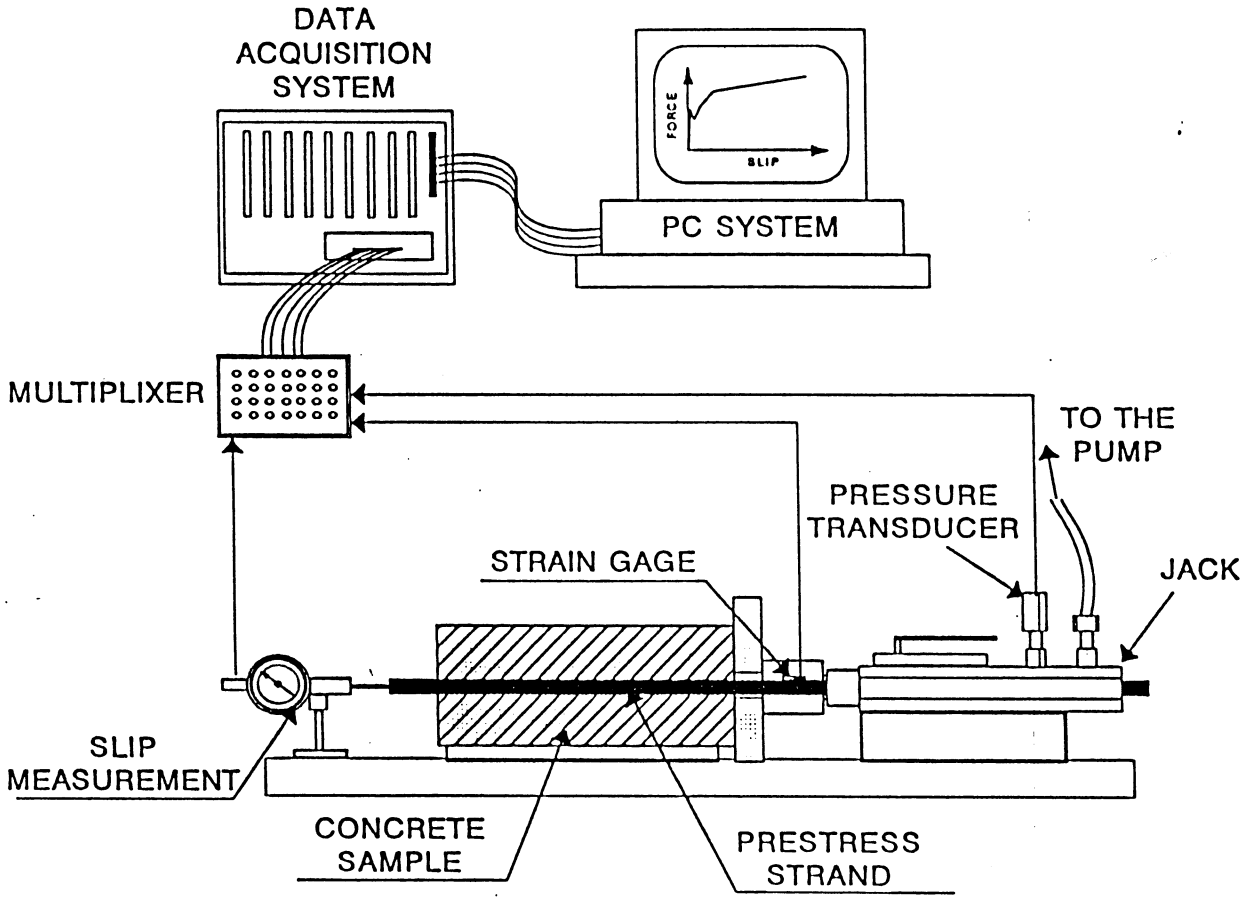

Figure 3.1 Pullout Test Configuration

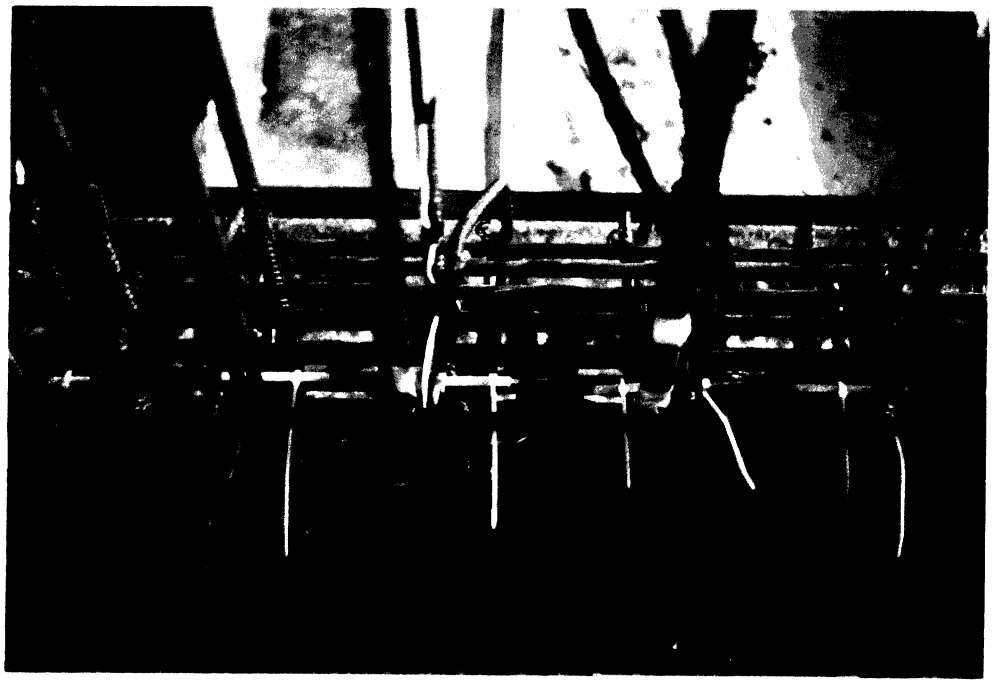

Figure 3.2 Embedded Gages Used for Transfer Length Measurements

Figure 3.3 Flame Cutting of Strands

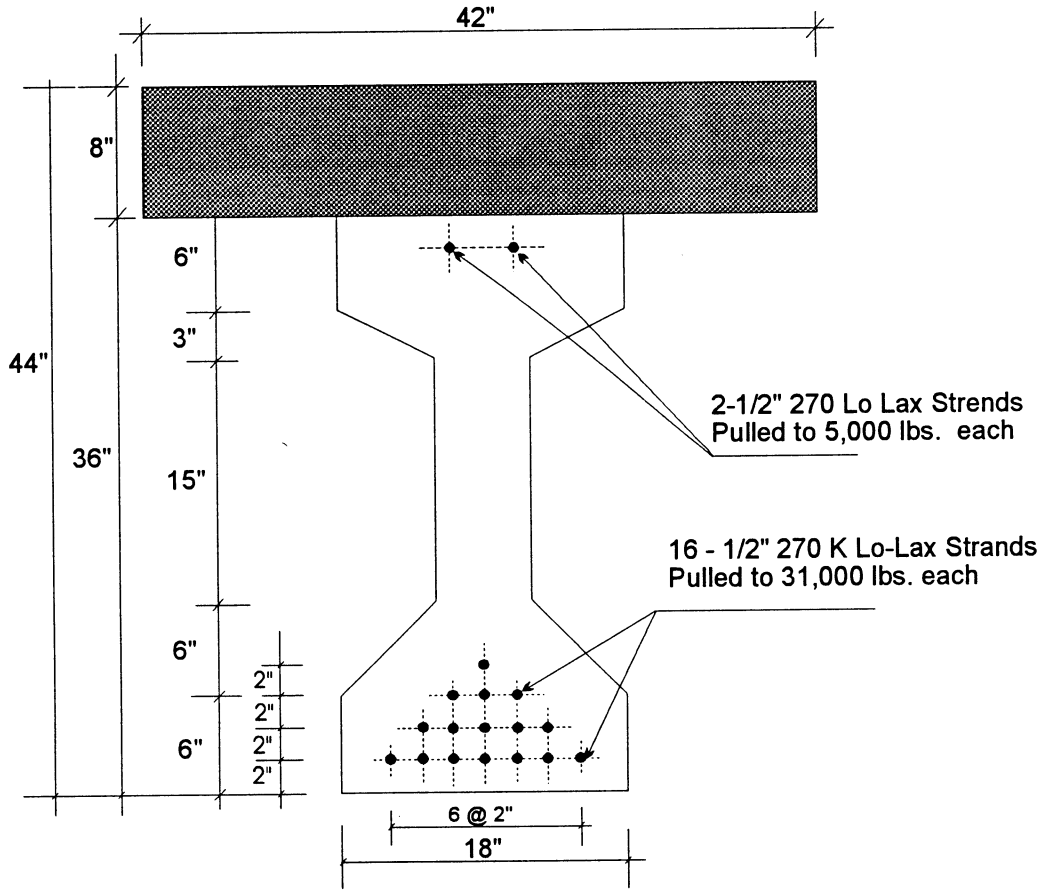

Figure 3.4 Cross-Section of Test Girders

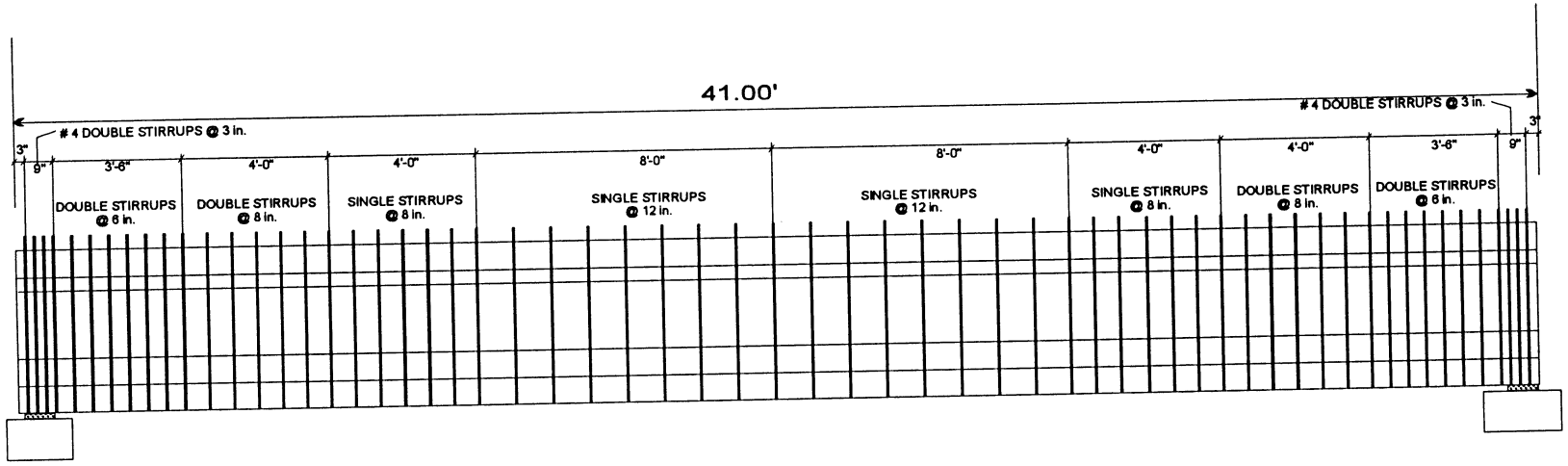

All stirrups are ASTM #4 deformed bars

Figure 3.5 Web Reinforcement in R Girders

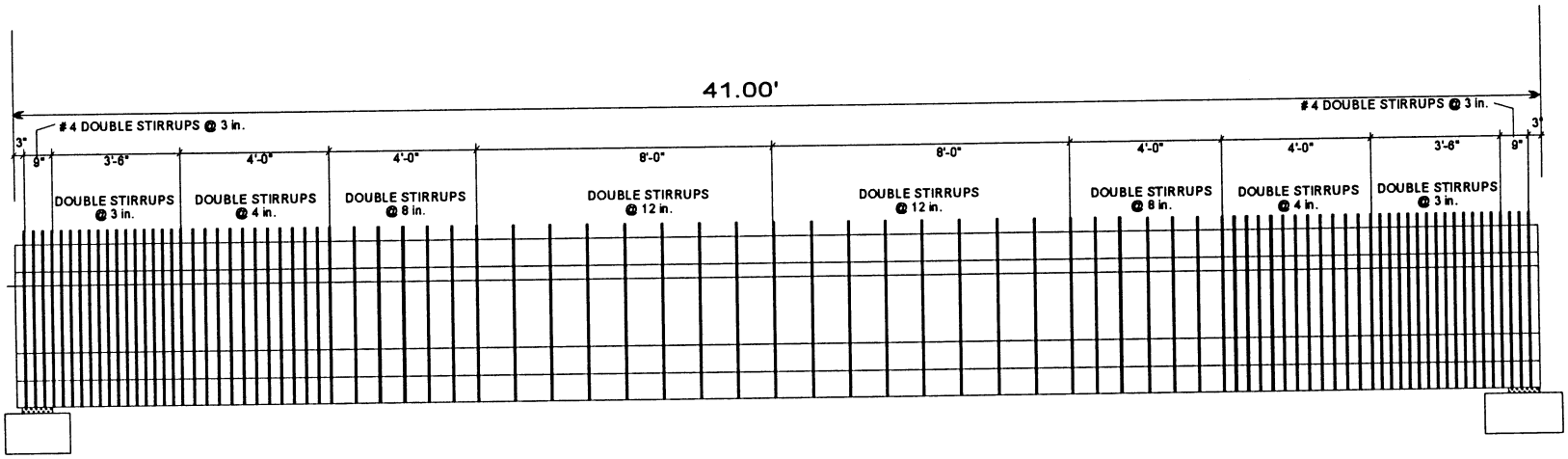

All stirrups are ASTM #4 deformed bars

Figure 3.6 Web Reinforcement in 2R Girders

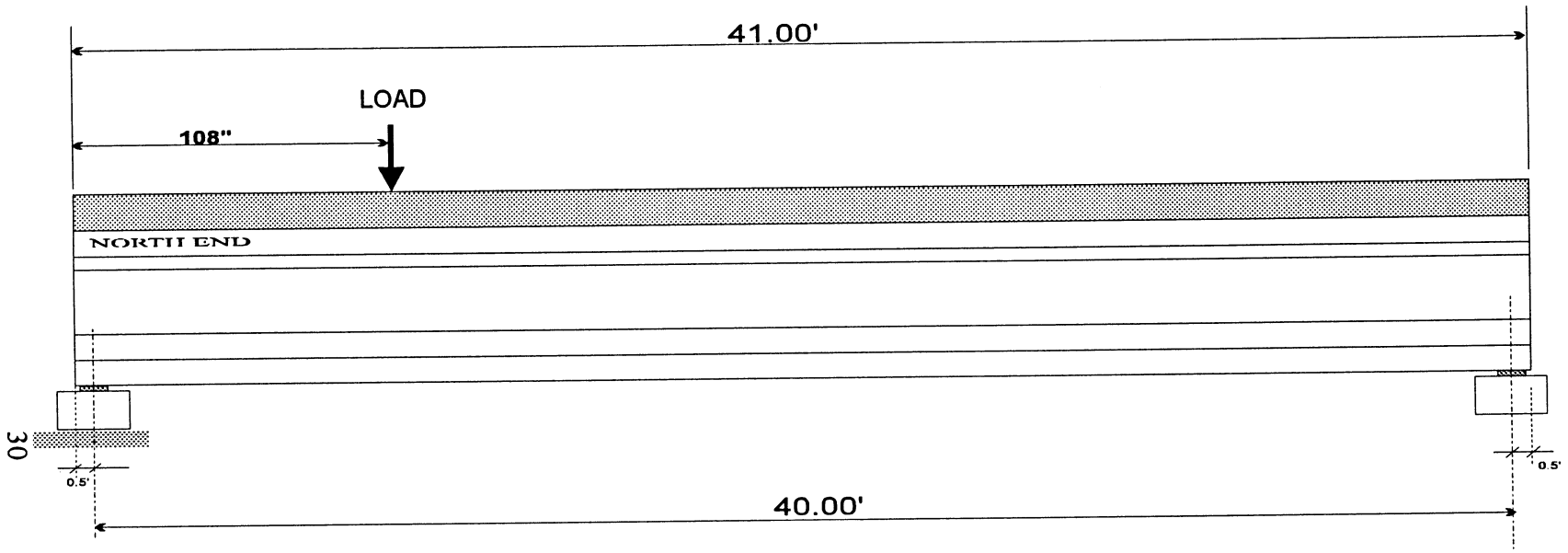

Figure 3.7 North End Test Configuration

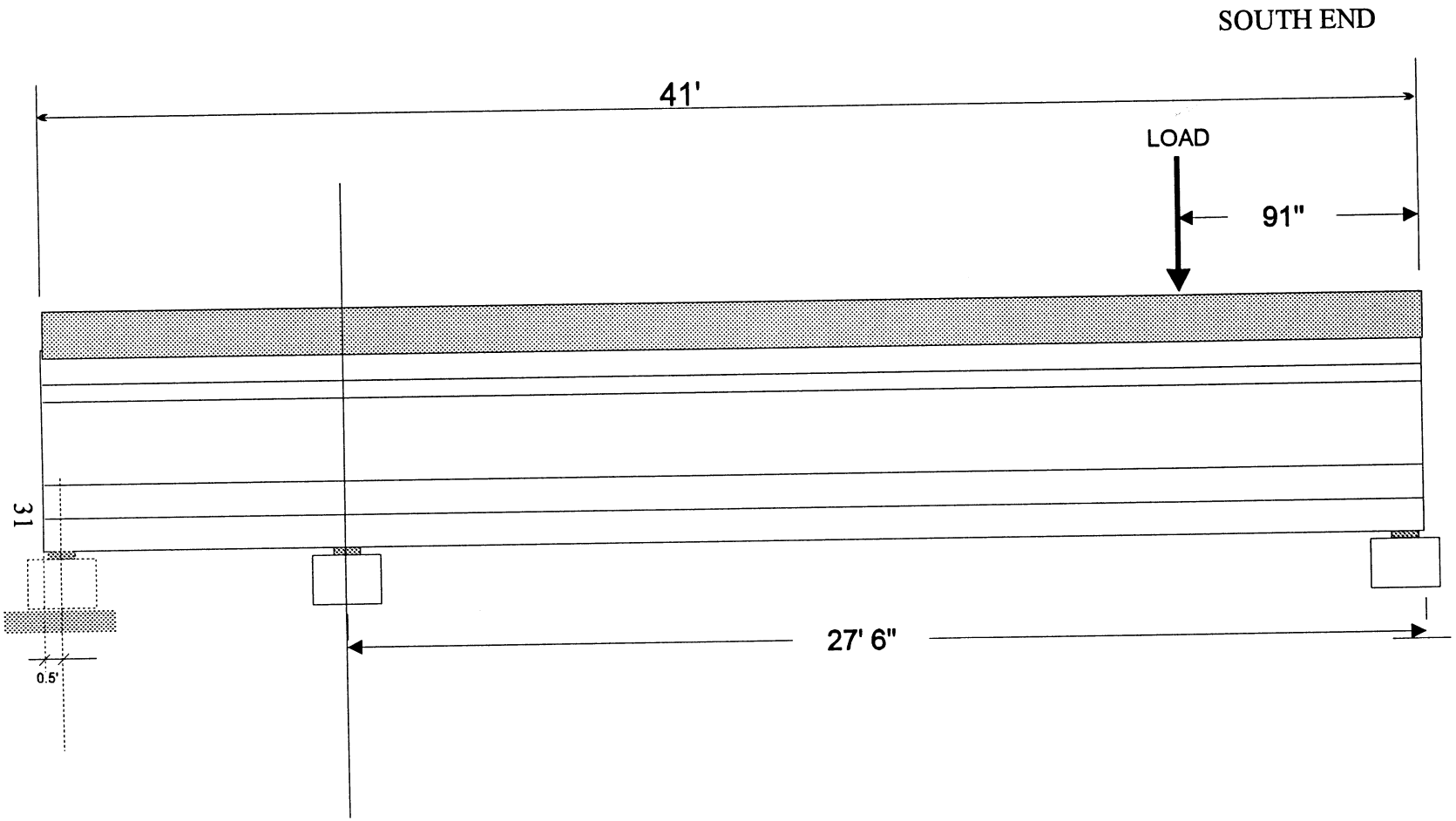

Figure 3.8 South End Test Configuration

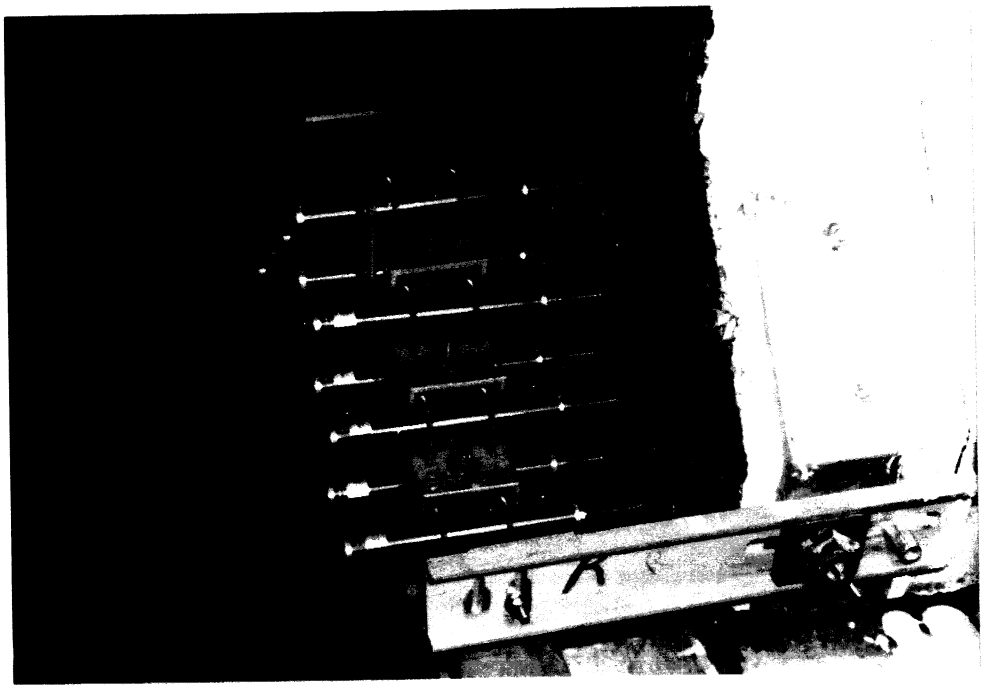

Figure 3.9 Gages Used to Measure Strand Slip

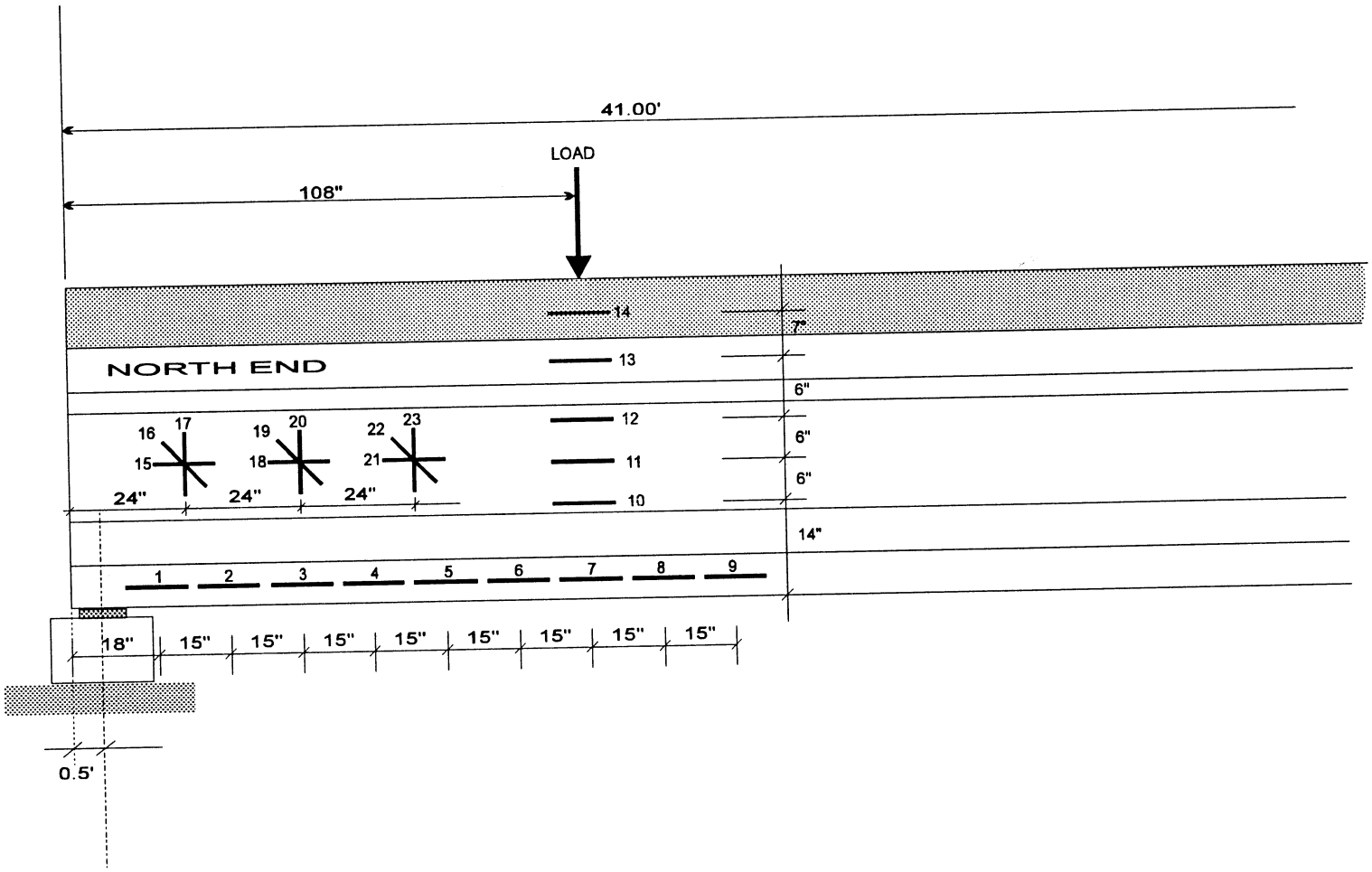

Figure 3.10 Location of External Gages for North End Tests

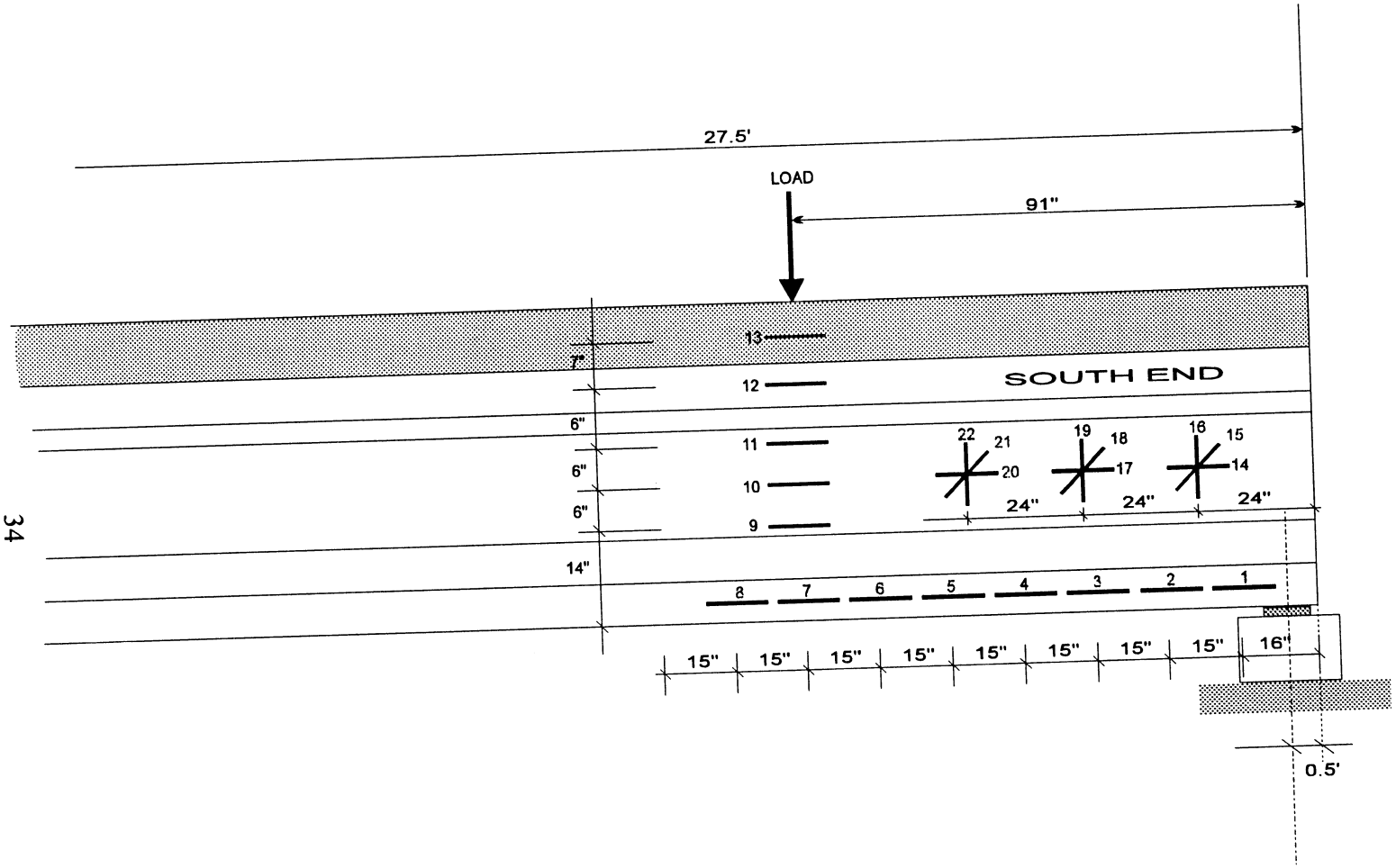

Figure 3.11 Location of External Gages for South End Tests

CHAPTER 4
TESTING RESULTS

4.1 Pullout Bond Tests

The major parameters of interest for the pullout study were the load limits at which the chemical bond, P_l, and the mechanical bond fails, P_t, failed. For each pullout test, a plot of the load vs. slip was obtained and used to measure P_l and P_t.

At any point during testing, the applied load was used to calculate the average bond stress, U. The average bond stress was determined from the total pullout force, P, divided by the nominal surface area. The nominal surface area is the nominal diameter of the strand times π times the embedded length.

$$U = \frac{P}{\pi \cdot d_s \cdot l_e} \qquad 4\text{-}1$$

4.1.1 Ungreased Specimens

Figures 4.1 to 4.4 show plots of the load vs. slip for several pullout tests. Figures 4.1 and 4.2 reflect an increase in the mechanical bond strength when the concrete compressive strength is increased from 7,000 psi to 11,000 psi. Also, Figures 4.3 and 4.4 exhibit increased bond performance with a lightly rusted strand. The plot of the load vs. slip for specimen 5-UL-6-C is shown in Figure 4.4. This plot is typical of the ungreased pullout results. The plot has been divided into three regions to highlight the bonding behavior in each region.

Region 1 starts at the beginning of the test and ends after the adhesion bond failure, P_l. In Figure 4.4 the chemical bond failure occurs at a load, P_l, of about 10,603 lb. For a 1/2" strand, this load implies an average bond stress, U_l, of 563 psi.

The adhesion bond failure is accompanied by a sudden increase in the slip and a decrease in the applied load. This is shown by the negative slope in the beginning of region 2. In Figure 4.4, the load reduced from 10,603 lb. to 9,587 lb., which was equal to a reduction of about 90% of the

CHAPTER 4
TESTING RESULTS

4.1 Pullout Bond Tests

The major parameters of interest for the pullout study were the load limits at which the chemical bond, P_1, and the mechanical bond fails, P_t, failed. For each pullout test, a plot of the load vs. slip was obtained and used to measure P_1 and P_t.

At any point during testing, the applied load was used to calculate the average bond stress, U. The average bond stress was determined from the total pullout force, P, divided by the nominal surface area. The nominal surface area is the nominal diameter of the strand times π times the embedded length.

$$U = \frac{P}{\pi \cdot d_s \cdot l_e} \qquad 4\text{-}1$$

4.1.1 Ungreased Specimens

Figures 4.1 to 4.4 show plots of the load vs. slip for several pullout tests. Figures 4.1 and 4.2 reflect an increase in the mechanical bond strength when the concrete compressive strength is increased from 7,000 psi to 11,000 psi. Also, Figures 4.3 and 4.4 exhibit increased bond performance with a lightly rusted strand. The plot of the load vs. slip for specimen 5-UL-6-C is shown in Figure 4.4. This plot is typical of the ungreased pullout results. The plot has been divided into three regions to highlight the bonding behavior in each region.

Region 1 starts at the beginning of the test and ends after the adhesion bond failure, P_1. In Figure 4.4 the chemical bond failure occurs at a load, P_1, of about 10,603 lb. For a 1/2" strand, this load implies an average bond stress, U_1, of 563 psi.

The adhesion bond failure is accompanied by a sudden increase in the slip and a decrease in the applied load. This is shown by the negative slope in the beginning of region 2. In Figure 4.4, the load reduced from 10,603 lb. to 9,587 lb., which was equal to a reduction of about 90% of the chemical bond load, P_1. This reduction in load was accompanied by a slip of 0.09 in. For the

ungreased specimens the load reduction was fairly constant at approximately 10% while the accompanying slip ranged from 0.04 in. to 0.3 in.

Region 2 begins after the adhesion bond failure and extends until after the mechanical bond failure. After the adhesion bond failure the only resisting bond is caused by mechanical interlock and friction. Unlike the adhesion bond, the mechanical bond was unable to totally hold the strand slip. As load increases and the strand continues to slip, the mechanical bonding increases at approximately a linear rate. Mechanical bond failure, P_t, is noted by a severe reduction in load carrying capacity accompanied by a large increase in the strand slip. The P_t failure was often accompanied by radial cracks in the cylinder. In Figure 4.4 the P_t load was about 12,607 lb. and the slip at failure, S_t, was 0.525 in. The load was reduced to 7,791 lb. after the P_t failure.

The slip at the mechanical bond failure ranged from 0.2" to 1.7" for the ungreased tests. However, two of the three 0.6" strands did not show a similar test pattern. These specimens were unable to resist any increased load following the P_1 failure.

Region 3 begins after the mechanical bond failure and continues until the end of the test. After the P_t failure, the specimen is unable to withstand any increase in the load. Generally the concrete has some radial cracks at this point and is unable to provide adequate confinement. The specimens continued to show some resistance due to friction and mechanical interlock. In Figure 4.4 the residual strength is 5,000 lb.

4.1.2 Lightly Greased Specimens

The behavior of the lightly greased specimens generally followed the pattern of the ungreased specimens. The differences in the behavior will be discussed below. A typical plot of the load vs. the slip behavior for a lightly greased specimen, specimen 5-GCF-10-B, is shown in Figure 4.5.

Region 1 begins at the beginning of the test and continues until after the P_1 failure. For the greased specimens the adhesion bond failure was not as dramatic as the P_1 failure for the ungreased specimens. In Figure 4.5 P_1 failure occurred at a load of 3,608 lb. and a slip of 0.029".

Region 2 begins after the P_1 failure and continues until after the mechanical bond failure, P_t. The mechanical bond gains strength at a linear rate as the strand slips. P_t is noted by a sudden

increase in slip and a decrease in load. In Figure 4.5 the P_t failure occurred at a load of 12,334 lb. and a slip of 0.94".

Region 3 begins after the mechanical bond failure and continues until the end of the test. After the P_t failure, the specimen is unable to withstand any increase in load. There is, however, a fairly constant residual strength. In Figure 4.5 the residual strength is 6,000 lb.

4.1.3 Heavy Greased Specimens

The addition of heavy grease was able to eliminate the chemical bond and to reduce the friction. These tests do not have the three distinct regions defined for the other tests, because the adhesion bond has been eliminated. However, these tests do experience a mechanical bond failure. Figure 4.6 shows the load vs. slip behavior of a typical heavily greased specimen. The strand began to slip at a very low load and the P_1 bond can be assumed to be zero. As in the previous test, the P_t bond developed as the strand was pulled through the cylinder. In this case, the load at P_t failure was 4,000 lb.

4.1.4 Summary of Pullout Bond Results

The results for each test are shown in Table 4.1. Average bond strengths have been divided by the square root of the compressive strength of the concrete to create the terms U'_1 and U'_t. This was done as an attempt to account for the variation in the concrete strength and to compare the results with other studies.

$$U'_1 = \frac{U_1}{\sqrt{f'_c}} \qquad 4-2$$

$$U'_t = \frac{U_t}{\sqrt{f'_c}} \qquad 4-3$$

4.2 Transfer Length Results

The transfer length for every end of each beam was determined from the relationships of the concrete strain vs. the distance along the beam. The relationships used to determine the transfer length are shown in Figures 4.7 to 4.11. The strain was plotted for each stage of the releasing processes.

The embedded gage strain can also be used to calculate the effective prestressing force using the following relationships.

$$f_b = \frac{M}{S_b} - \frac{P_i}{A_c} - \frac{P_i\, e}{S_b} \qquad 4\text{-}4$$

$$f_b = \epsilon_c \,.\, E_c \qquad 4\text{-}5$$

$$E_c = 14500\ (3.32\ .\ \sqrt{f'_c\ .\ 6.896}\ +\ 6.9) \qquad 4\text{-}6$$

Equation 4-6 is the ACI-363 equation for the elastic modulus of high strength concrete (converted to US units).

There are currently many different equations developed to predict the modulus of elasticity of high strength concrete. Ultra-sound equipment was used to measure the modulus of elasticity of several concrete cylinders and full scale girders. It was found that equation ACI-363 (4-6) corresponded best with the ultra-sound readings.

The transfer length and the effective prestressing force can be used to calculate the average bond stress over the transfer length, U_{tl}. The average transfer bond is equal to the prestressing force divided by the diameter times π times the transfer length.

$$U_{tl} = \frac{P_e}{\pi\ .\ d_s\ .\ l_t} \qquad 4\text{-}7$$

Results of the transfer length tests are shown in Table 4.2.

4.3 Shear Strength Results

Most of the specimens failed due to a general bond slip. Figure 4.12 shows the strand slip after failure for girder 2R-12-S. In this photograph nearly all of the prestressing strands have slipped into the girder. If all of the bond is lost between the strands and the concrete, the girder will have very little resistance to flexure or shear forces. The lack of resistance to shear is explained by both the truss analogy and the strut and tie model which were discussed previously. After the bond failure, applying more pressure to the hydraulic jack would cause excessive deflection and eventually the girder would fail. Usually, failure will occur at the location of the most severe crack before the bond failure. In the test specimens, a bond failure usually caused the failure, after which one of the shear cracks caused a severe splitting of the web. Figure 4.13 shows girder 2R-12-S at failure.

The test shearing capacity for a girder that failed in bonding was taken as the maximum shear that was withstood by the girder during testing. Table 4.3 shows the results for the shear test program.

The maximum test shear was plotted along with the predicted shear strength, as determined following the codes discussed in the literature review. Figures 4.14 to 4.25 show these graphs. The test shear remained nearly constant between the support and the concentrated load because the self weight was very small in magnitude compared with the concentrated load.

4.3.1 North End Tests

Cracking patterns for the R north girders are shown in Figures 4.26 to 4.28. The R north girders had the least amount of slip of any group. The 10,000 psi girder failed in flexure - shear failure without any slippage of the strands. The 10,000 psi girder was the only girder of the twelve test girders that did not experience any strand slip. The 8,000 psi had the least amount of slip of the remaining girders.

All of the R north girders had shear cracks from the support to the load point. Web-shear cracks were prevalent from the support to a distance approximately 4 ft from the support. Flexure -

shear cracks began at this point and continued until the load point. In the 8,000 psi and 10,000 psi girders, there were no web-shear cracks that extended through the lower flange of the girder. In the 12,000 psi girder, the web-shear cracks did extend through the lower flange.

The 2R north girders all experienced flexure-shear failure after a bond failure. The cracking patterns for the 2R north girders are shown in Figures 4.29 to 4.31. After the bond failure the flexural-shear cracks widened and caused the failure of the web.

4.3.2 South End Tests

The R south girders failed in shear after a bond failure. The cracking patterns for the R south girders are shown in Figures 4.32 to 4.34. The web-shear cracks caused the concrete web failure after a general bond slip had occurred.

The 2R south girders failed in shear after a bond failure. The cracking patterns for the R north girders are shown in Figures 4.35 to 4.37. Web-shear cracks caused concrete web failure after the general bond slip had occurred.

Table 4.1 Pullout Test Results

Specimen	P1 (lb)	Pt (lb)	U1 (psi) P1/SA	Ut (psi) Pt/SA	U'1 U1/(f'c^.5)	U't Ut/(f'c^.5)
3-UC-7-A	10,725	11,858	759	839	8.70	9.62
3-UC-7-B	11,584	12,839	819	908	9.40	10.42
3-UC-11-A	11,688	16,501	827	1167	7.87	11.11
3-UC-11-B	8,218	17,255	581	1221	5.53	11.62
4-UC-7-A	11,625	12,226	705	741	8.09	8.50
4-UC-7-B	14,037	16,415	851	995	9.76	11.42
4-UC-11-A	11,986	24,627	727	1493	6.92	14.21
4-UC-11-B	12,225	24,476	741	1484	7.05	14.12
5-UC-7-A	8,658	10,101	459	536	5.27	6.15
5-UC-7-B	7,215	7,937	383	421	4.39	4.83
5-UC-8-A	6,240	8,747	331	464	3.66	5.13
5-UC-8-B	5,770	10,139	306	538	3.38	5.94
5-UC-10-A	6,901	10,029	366	532	3.68	5.34
5-UC-10-B	6,722	14,620	357	776	3.58	7.79
5-UC-11-A	7,135	16,206	379	860	3.60	8.18
5-UL-6-A	6,754	11,214	358	595	4.52	7.51
5-UL-6-B	8,406	9,220	446	489	5.63	6.17
5-UL-6-C	10,603	12,607	563	669	7.10	8.44
5-UL-6-D	7,629	8,463	405	449	5.11	5.66
5-UL-6-E	7,131	11,144	378	591	4.77	7.46
6-UC-6-A	9,615	9,615	425	425	5.36	5.36
6-UC-7-A	11,063	11,063	489	489	5.61	5.61
6-UC-11-A	14,087	20,121	623	890	5.93	8.47
3-GCW-7-A	3,905	8,924	276	632	3.17	7.25
4-GCW-7-A	6,555	15,260	398	926	4.56	10.62
4-GCW-11-A	3,686	24,627	224	1494	2.13	14.22
5-GCW-7-A	7,696	13,059	409	693	4.69	7.95
5-GCF-8-A	3,836	10,589	204	562	2.25	6.21
5-GCF-8-B	5,966	10,863	317	577	3.50	6.37
5-GCF-10-A	6,321	13,076	336	694	3.37	6.97
5-GCF-10-B	3,608	12,334	192	655	1.92	6.58
5-GLO-6-A	7,277	14,193	386	754	4.87	9.51
5-GLO-6-B	5,548	14,257	295	757	3.72	9.55
5-GLO-6-C	4,378	9,686	232	514	2.93	6.49
5-GLO-6-D	7,103	13,120	377	697	4.76	8.79
6-GCW-11-A	2,582	10,571	114	468	1.09	4.45
6-GCW-11-B	2,988	24,053	132	1064	1.26	10.13
6-GCH-6-A	0	4,000	0	177	0.00	2.23
6-GCH-6-B	0	5,222	0	231	0.00	2.92

SA = Surface area of strand

Table 4.2 Transfer Length Test Results

Girder	End	f'ci (psi)	Lt (in)	Ut (psi)	U't
R-8	North	5,450	24	665	9.00
R-8	South	5,450	24	665	9.00
2R-8	North	5,340	30	528	7.23
2R-8	South	5,340	30	528	7.23
R-10	North	6,932	18	902	10.84
R-10	South	6,932	18	902	10.84
R-12	North	8,200	21	797	8.80
R-12	South	8,200	18	930	10.27
2R-12	North	8,200	20	837	9.24
2R-12	South	8,200	18	930	10.27

Table 4.3 Summary of Shear Test Results

Girder	Failure	Distance from Support to Load (ft.)	Span (ft.)	Test Shear at Load (kips)	Test Shear at Support (kips)
R8N	bond/flexure-shear	8.5	40	270	277
R10N	flexure-shear	8.5	40	277	283
R12N	bond/flexure-shear	8.5	40	272	279
2R8N	bond/flexure-shear	8.5	40	228	235
2R10N	bond/flexure-shear	8.5	40	233	240
2R12N	bond/flexure-shear	8.5	40	273	279
R8S	bond/shear	7.08	27	296	302
R10S	bond/shear	7.08	27	293	299
R12S	bond/shear	7.08	27	270	276
2R8S	bond/shear	7.08	27	250	256
2R10S	bond/shear	7.08	27	239	245
2R12S	bond/shear	7.08	27	281	287

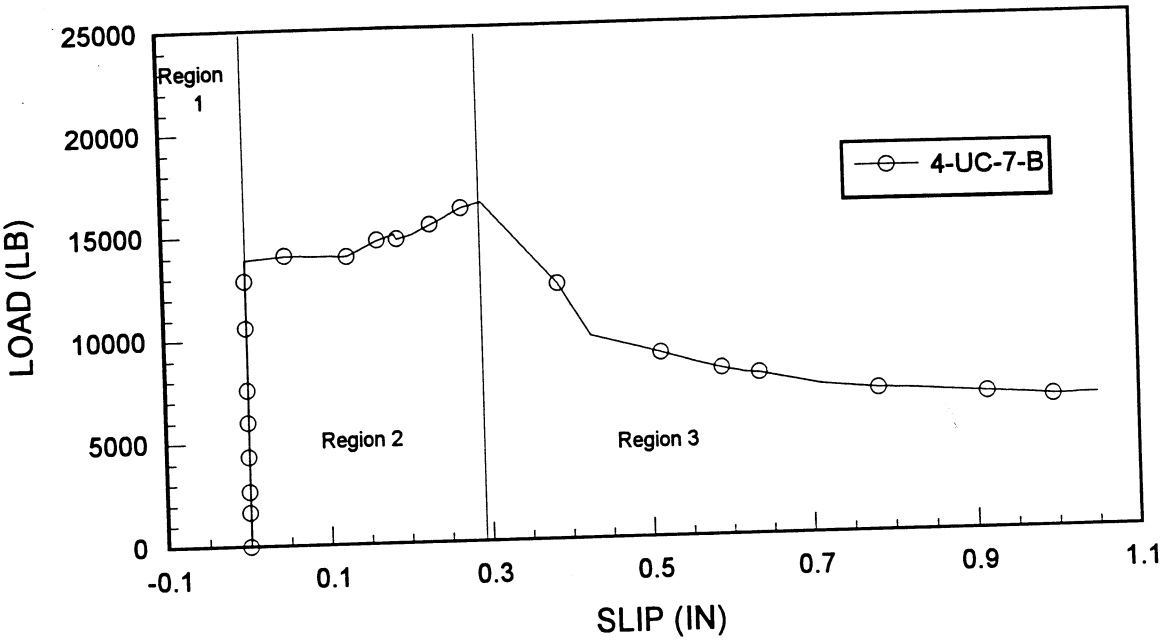

Figure 4.1 Load vs. Slip Plot or Specimen 4-UC-7-B

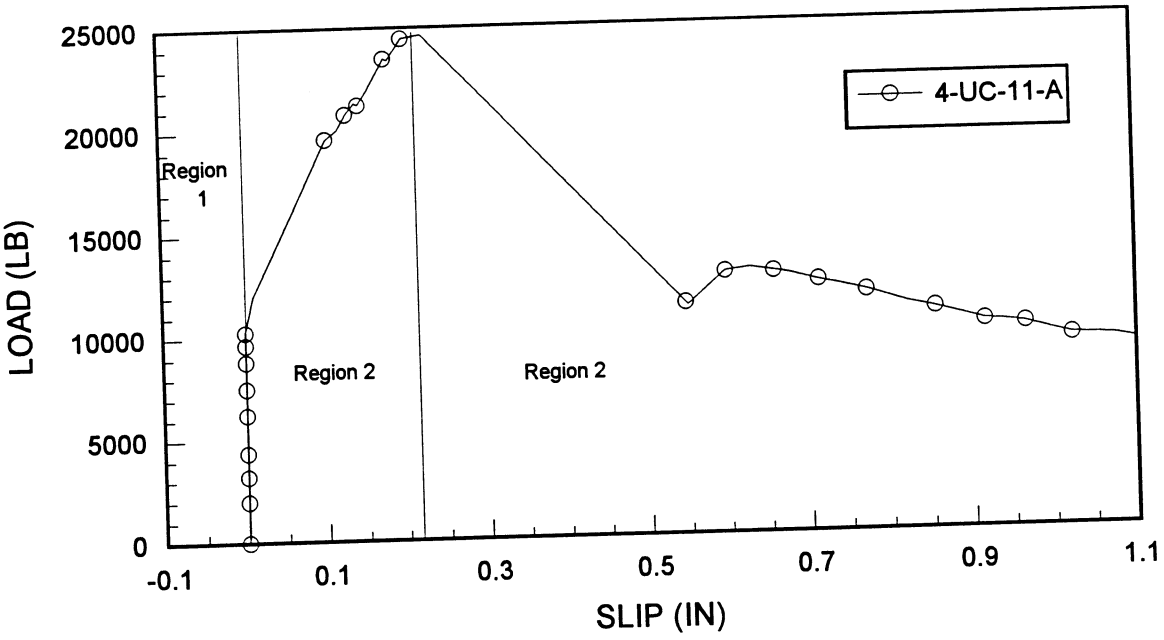

Figure 4.2 Load vs. Slip Plot or Specimen 4-UC-11-A

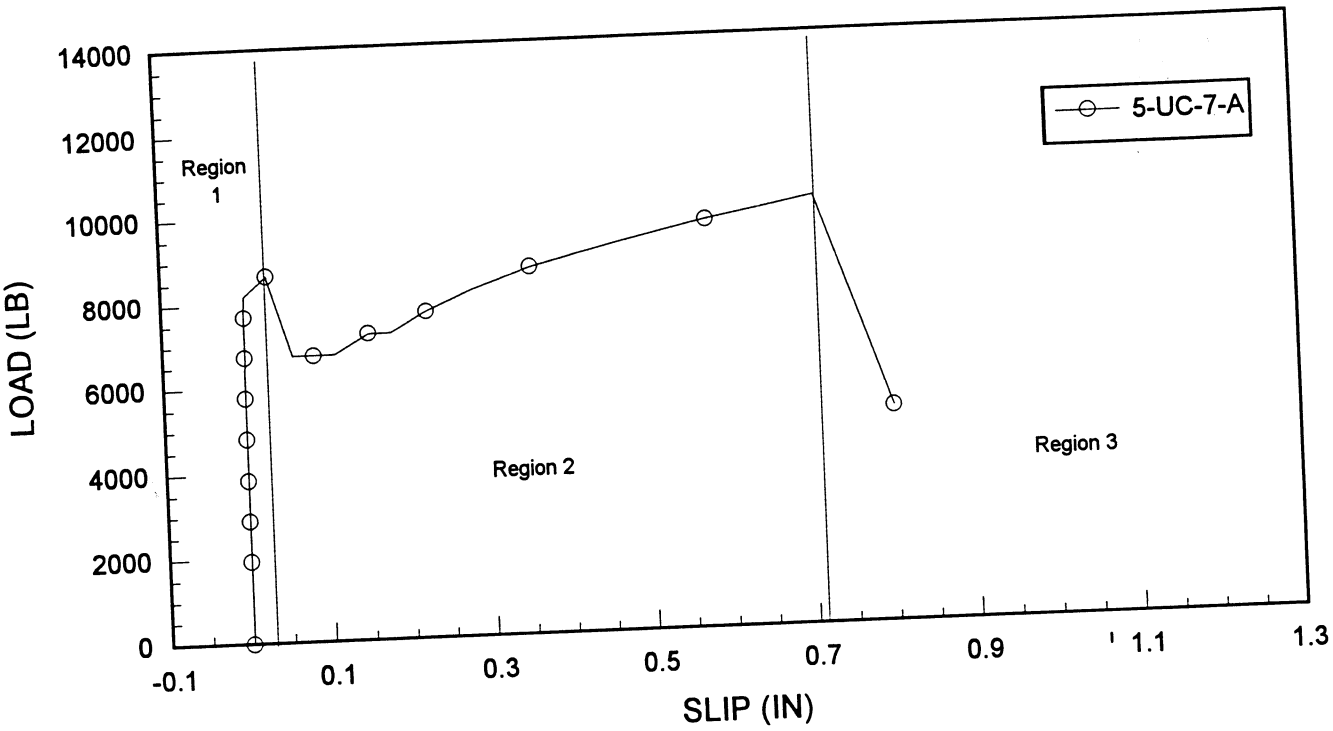

Figure 4.3 Load vs. Slip Plot for Specimen 5-UC-7-A

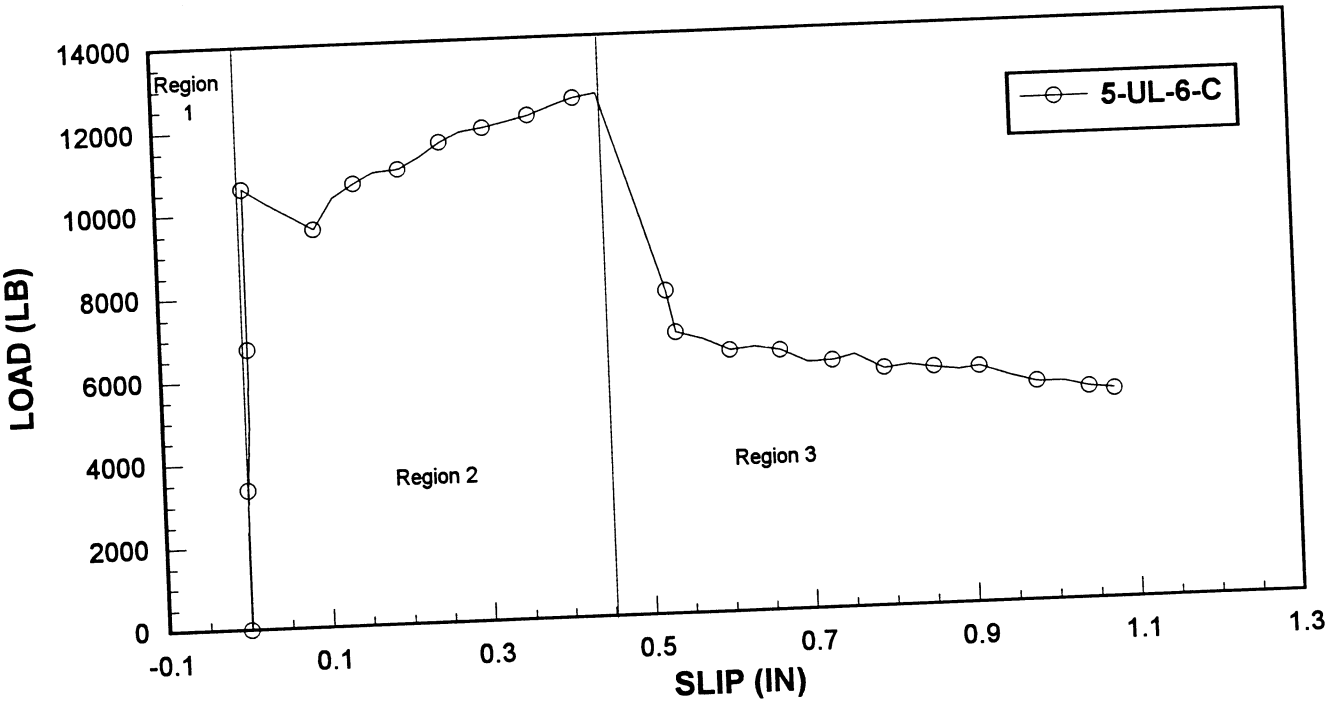

Figure 4.4 Load vs. Slip Plot for Specimen 5-UL-6-C

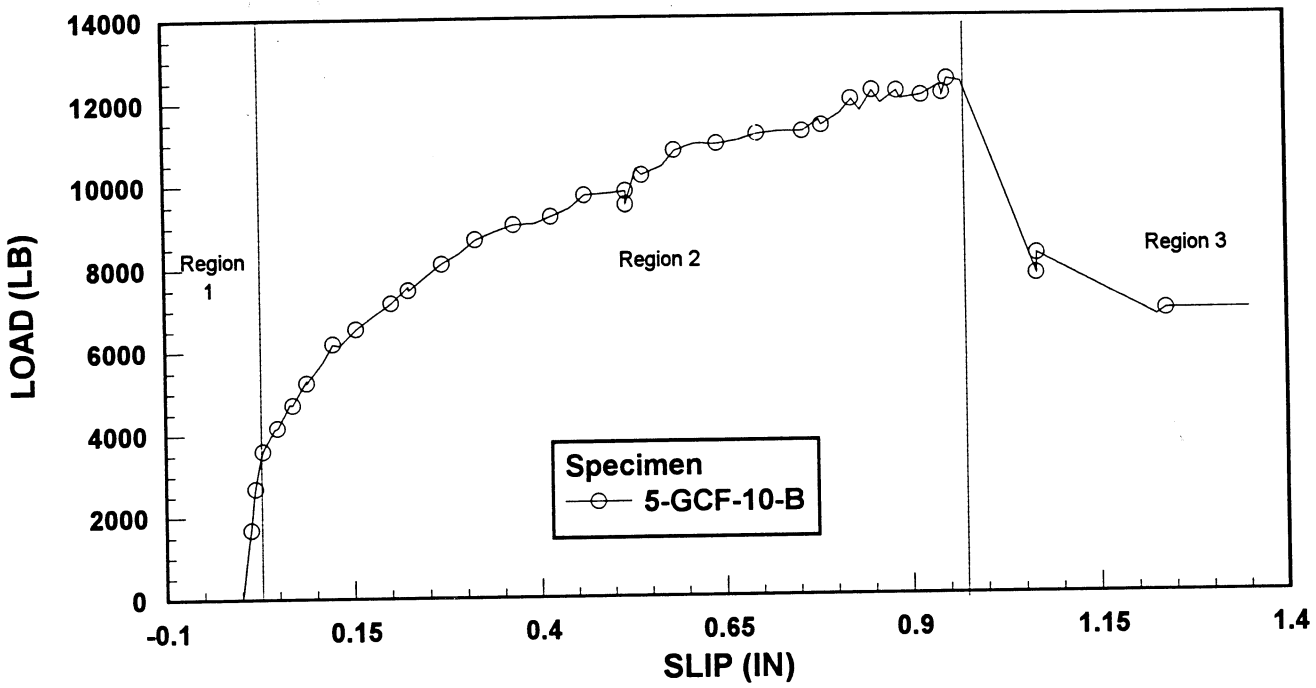

Figure 4.5 Load vs. Slip Plot for Specimen 5-GCF-10-B

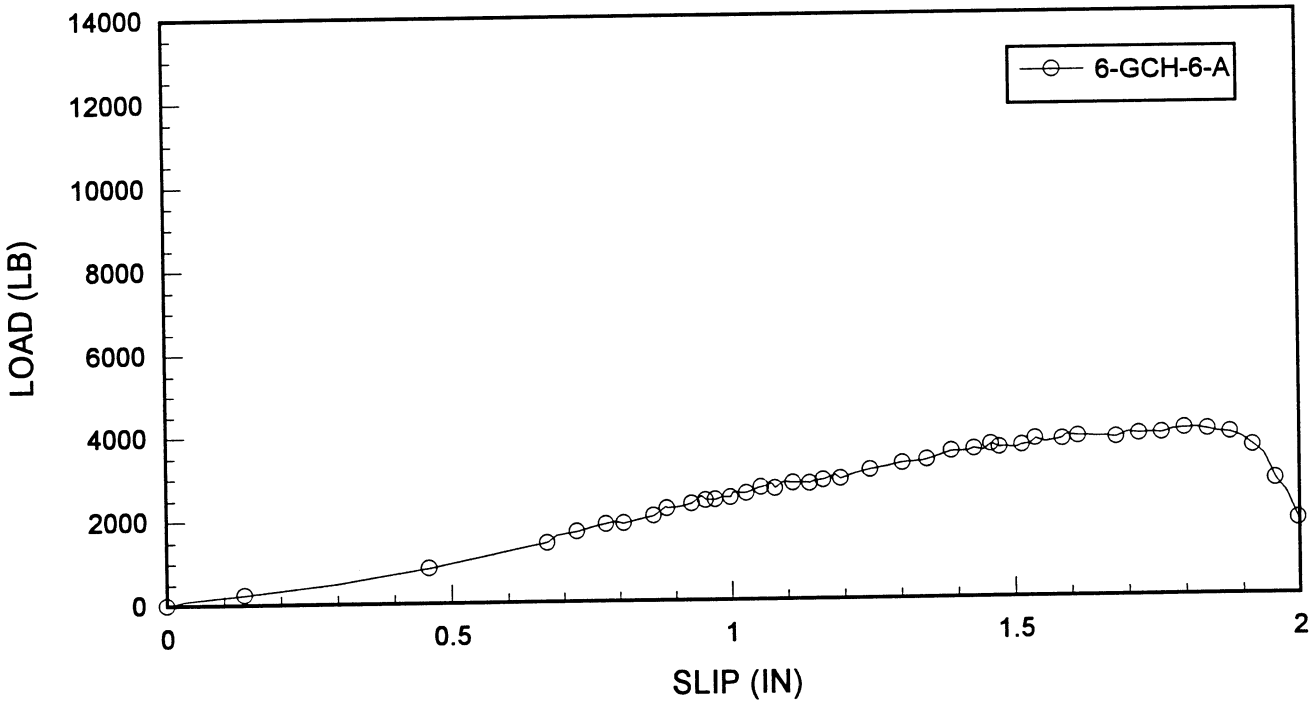

Figure 4.6 Load vs. Slip Plot for Secimen 6-GCH-6-A

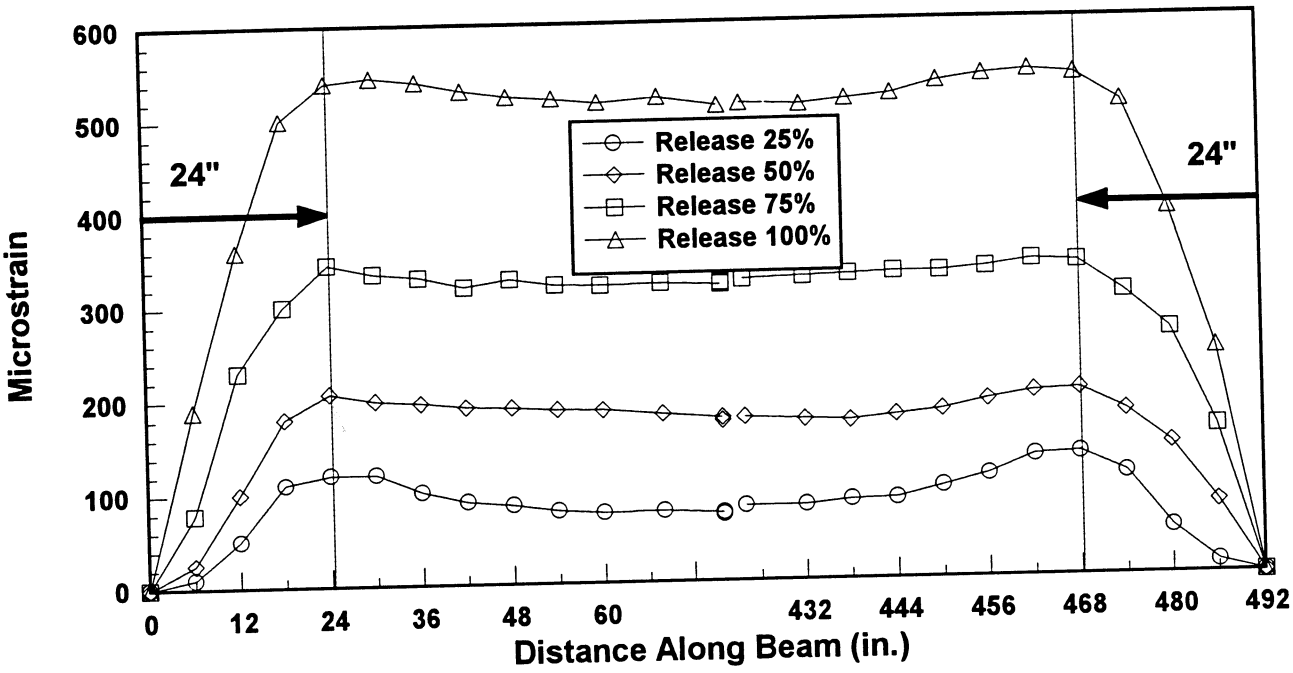

Figure 4.7 Transfer Length Plot for Girder R-8

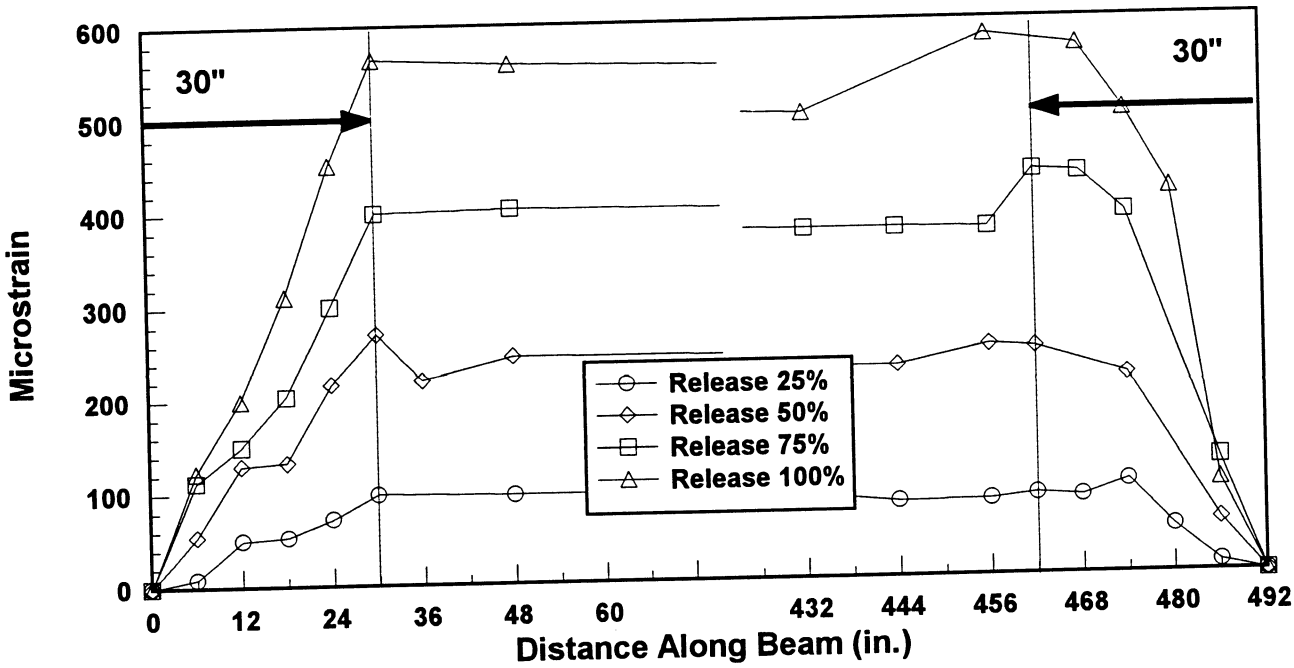

Figure 4.8 Transfer Length Plot for Girder 2R-8

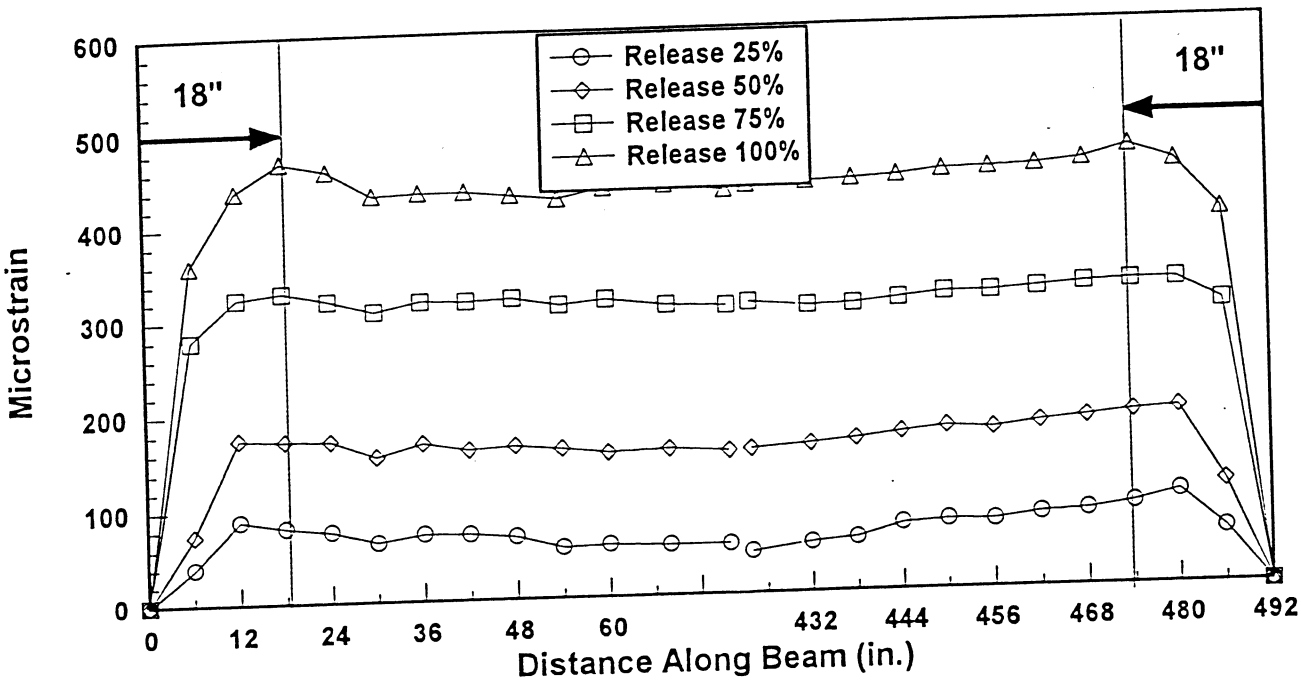

Figure 4.9 Transfer Length Plot for Girder R-10

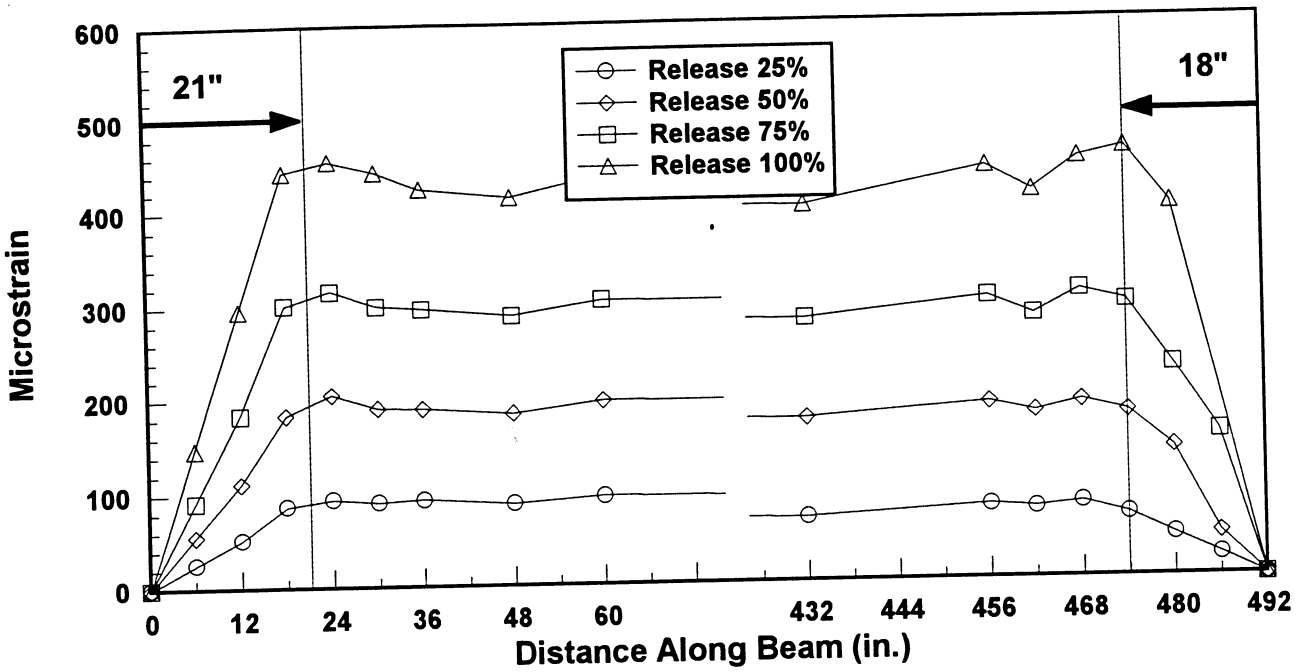

Figure 4.10 Transfer Length Plot for Girder R-12

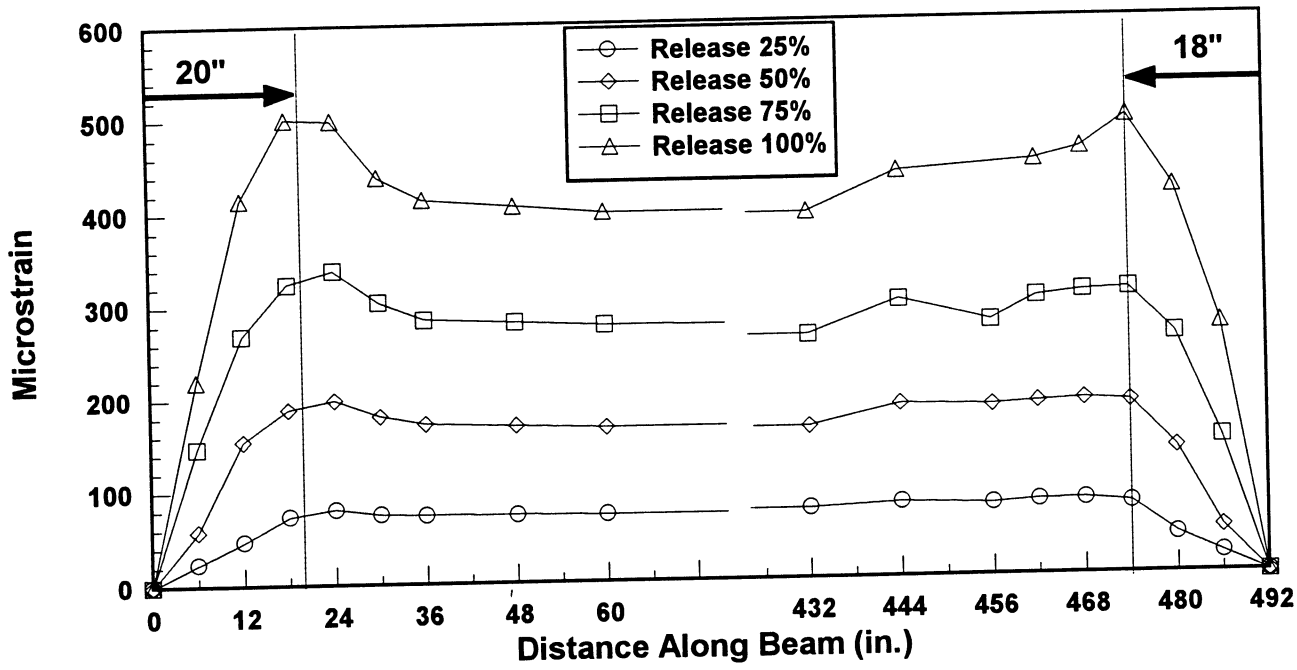

Figure 4.11 Transfer Length Plot for Girder 2R-12

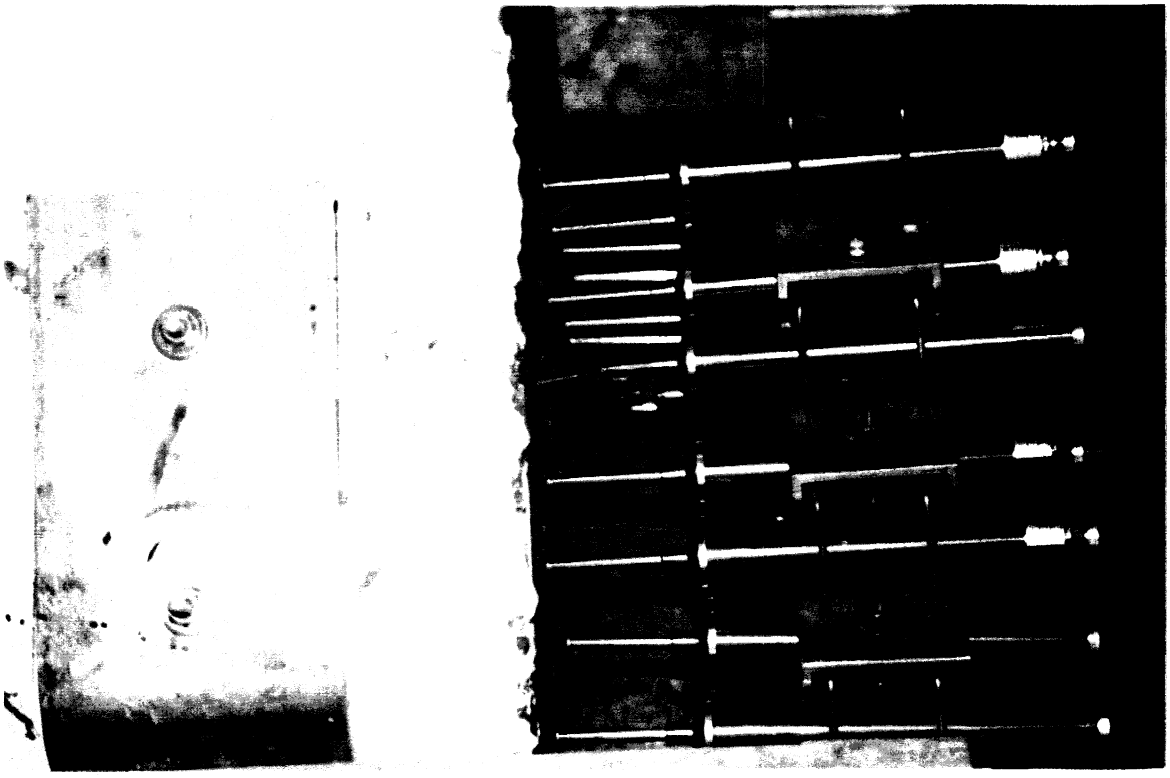

Figure 4.12 Strand Slip at Failure for Girder 2R-12-S

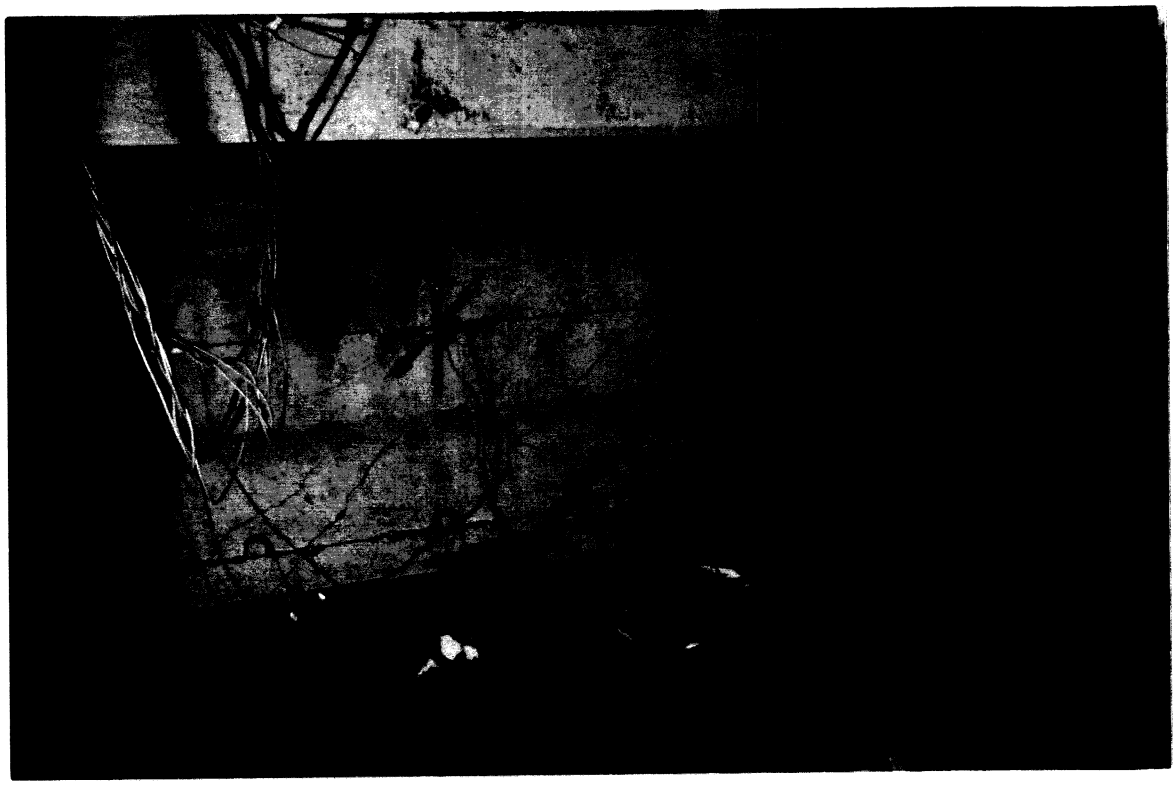

Figure 4.13 Girder 2R-12-S at Failure

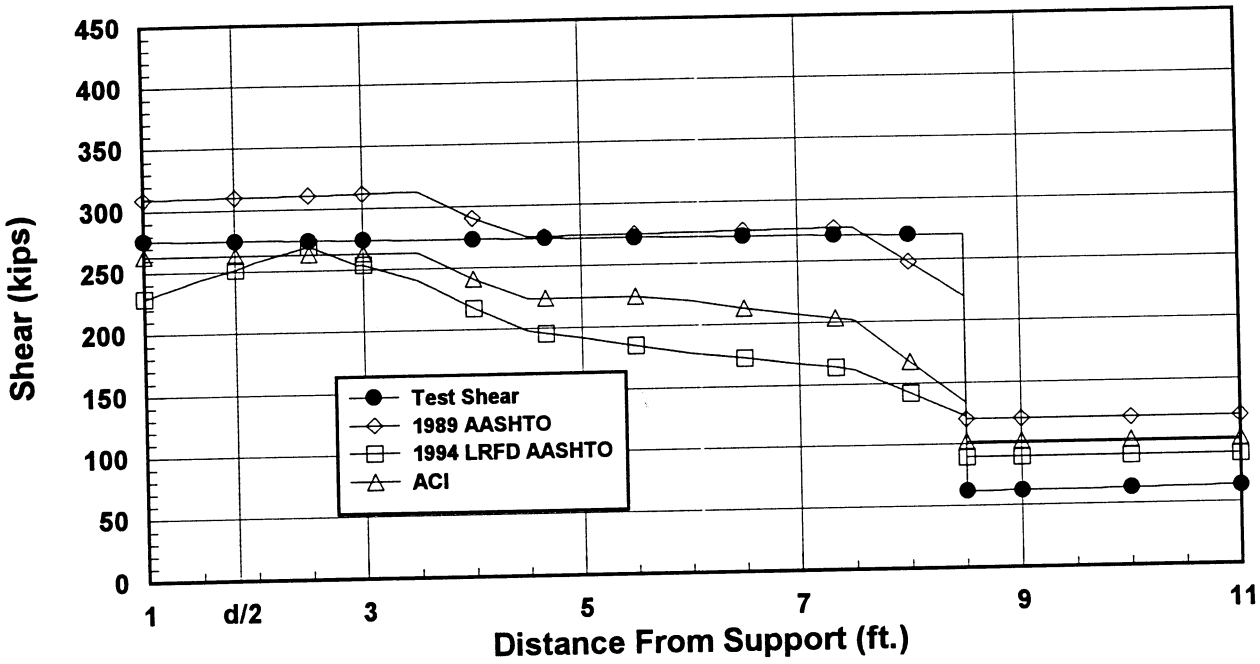

Figure 4.14 Test Shear and Predicted Shear for Girder R-8-N

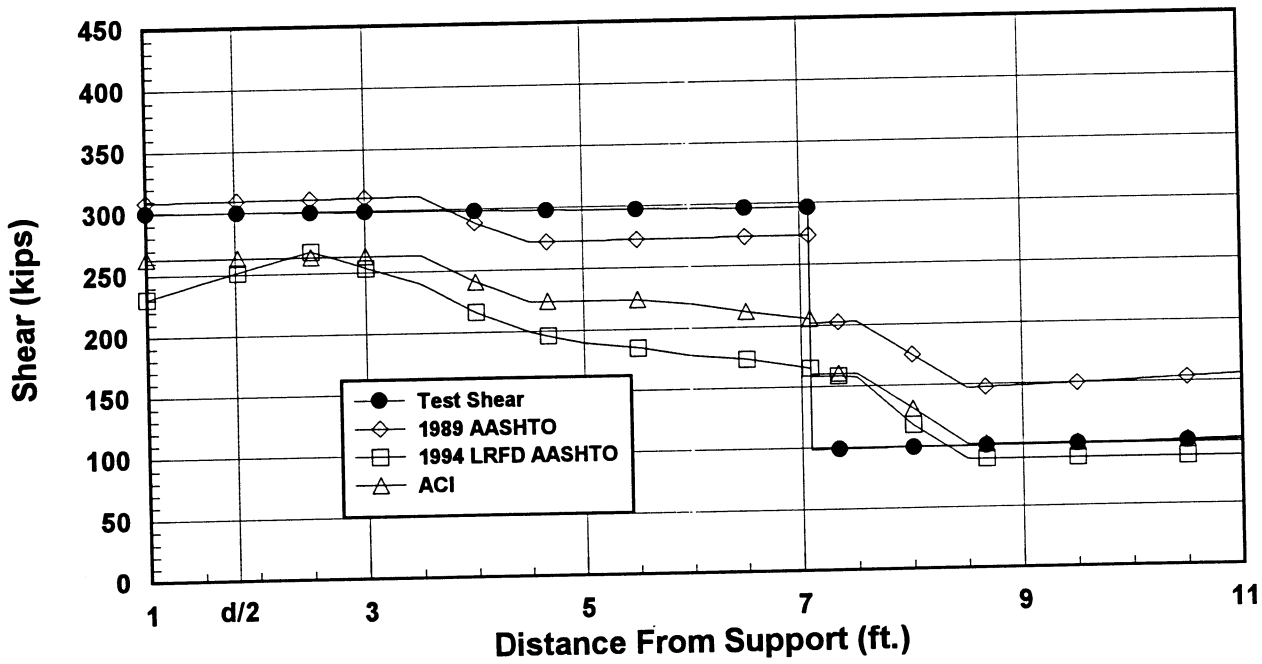

Figure 4.15 Test Shear and Predicted Shear for Girder R-8-S

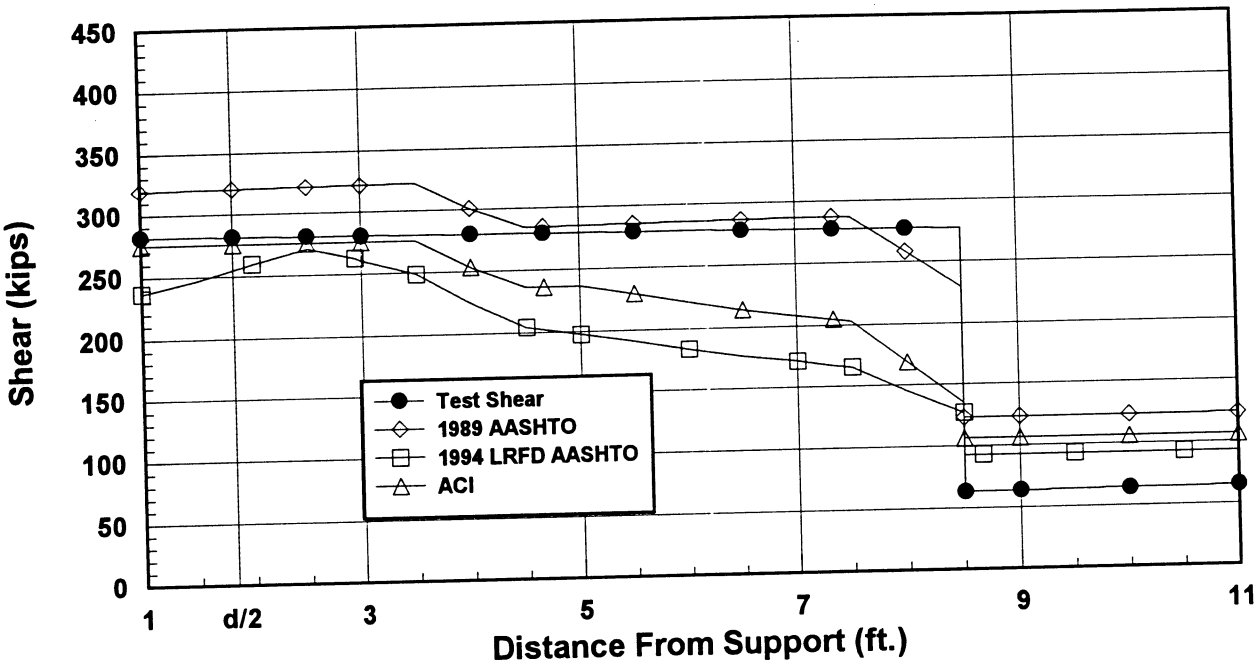

Figure 4.16 Test Shear and Predicted Shear for Girder R-10-N

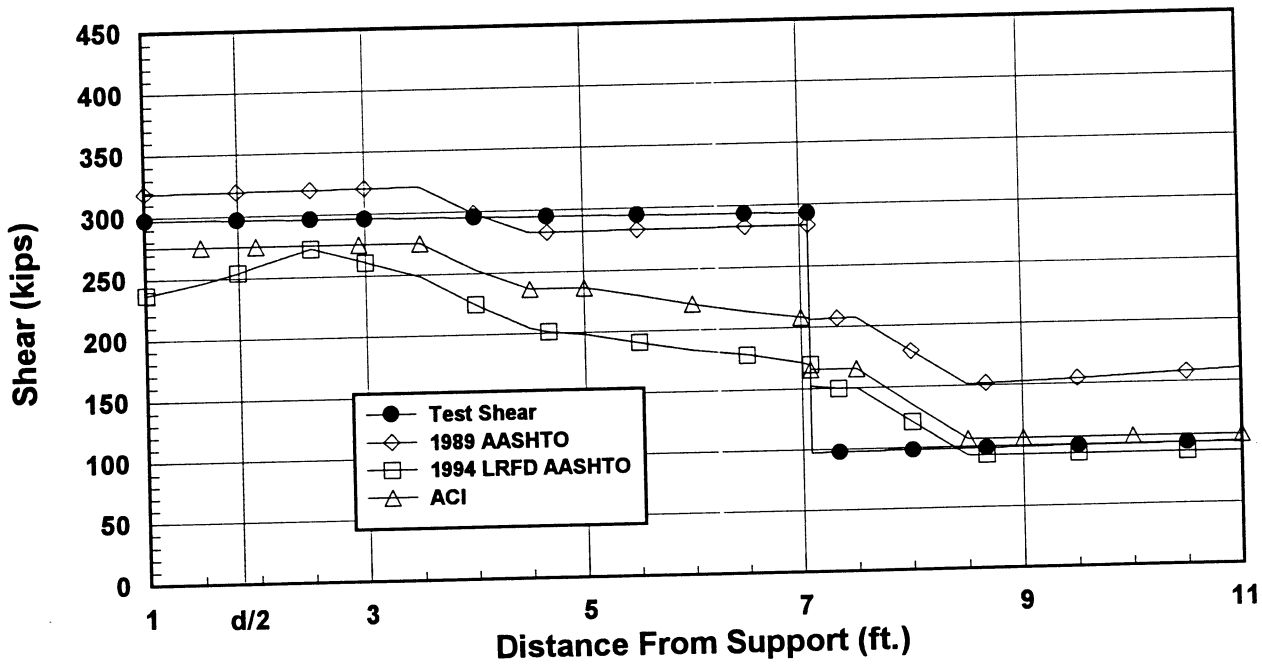

Figure 4.17 Test Shear and Predicted Shear for Girder R-10-S

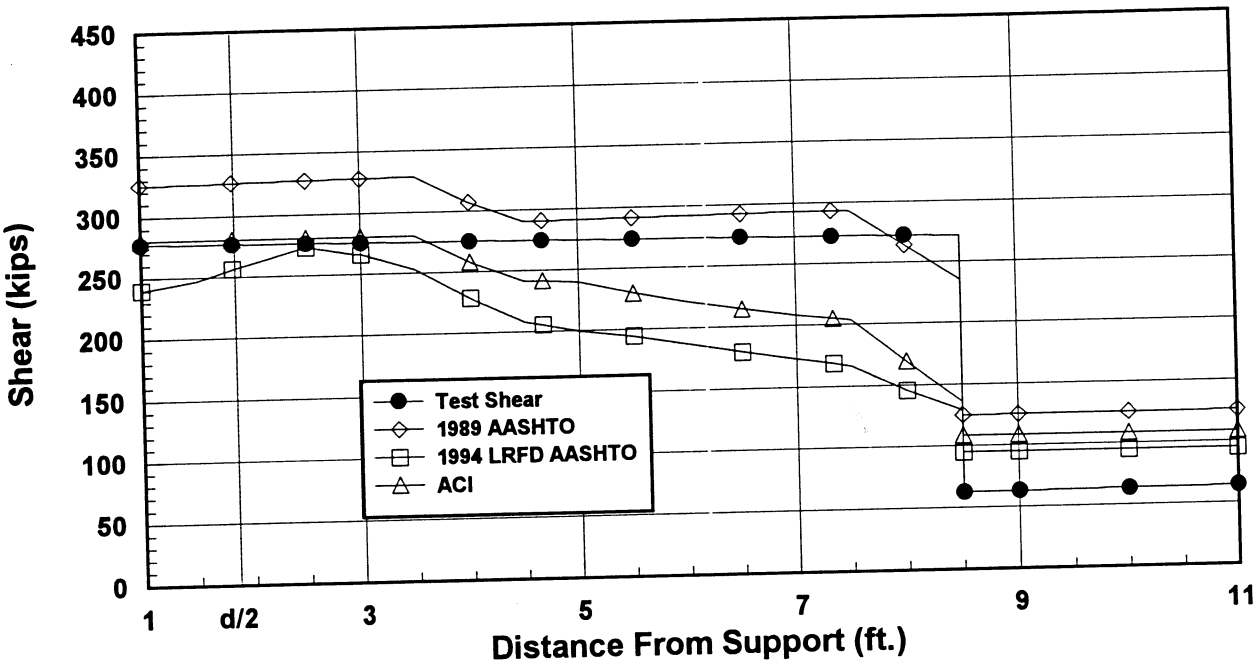

Figure 4.18 Test Shear and Predicted Shear for Girder R-12-N

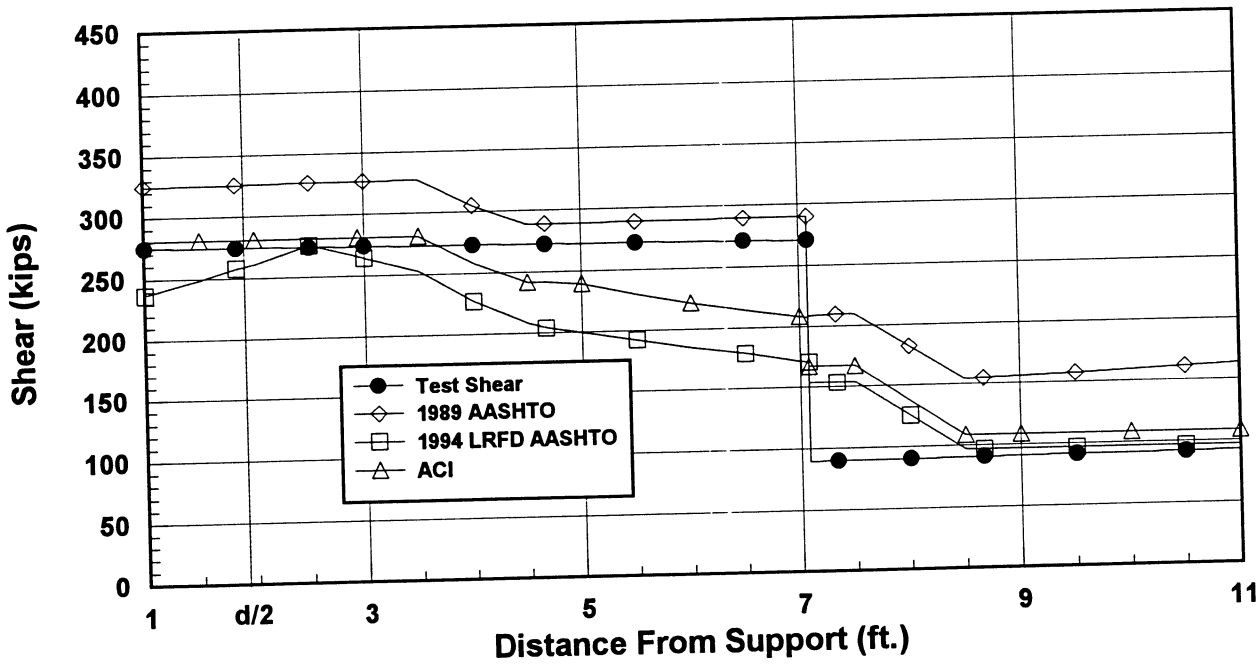

Figure 4.19 Test Shear and Predicted Shear for Girder R-12-S

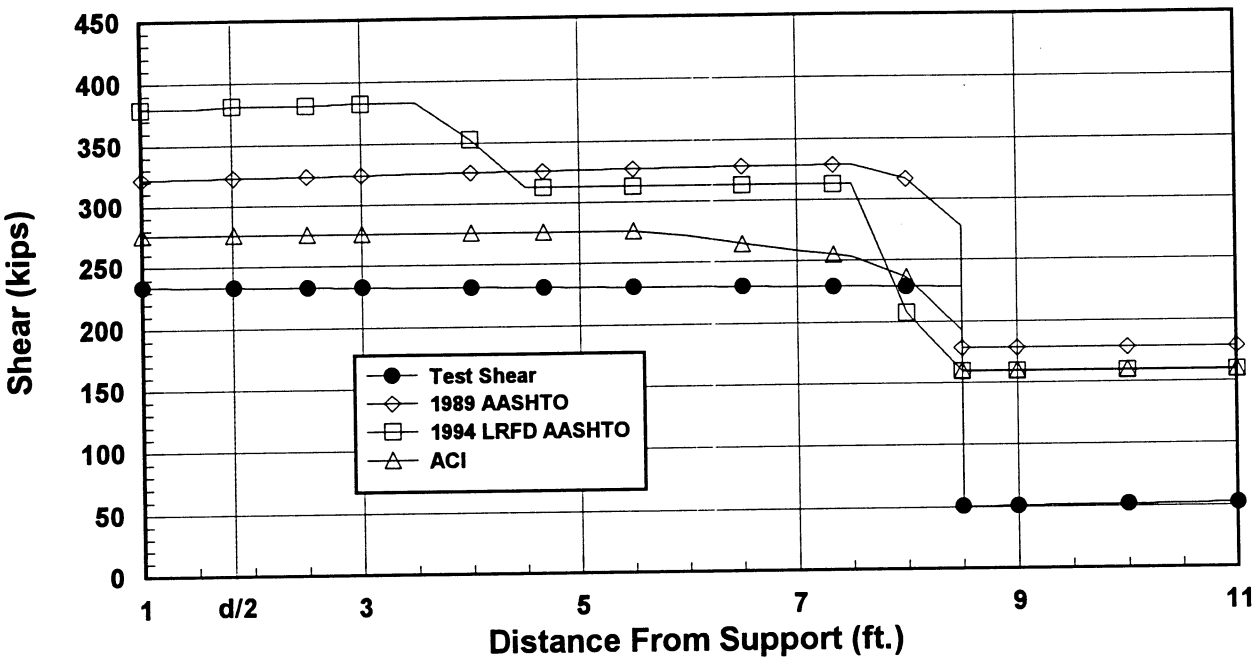

Figure 4.20 Test Shear and Predicted Shear for Girder 2R-8-N

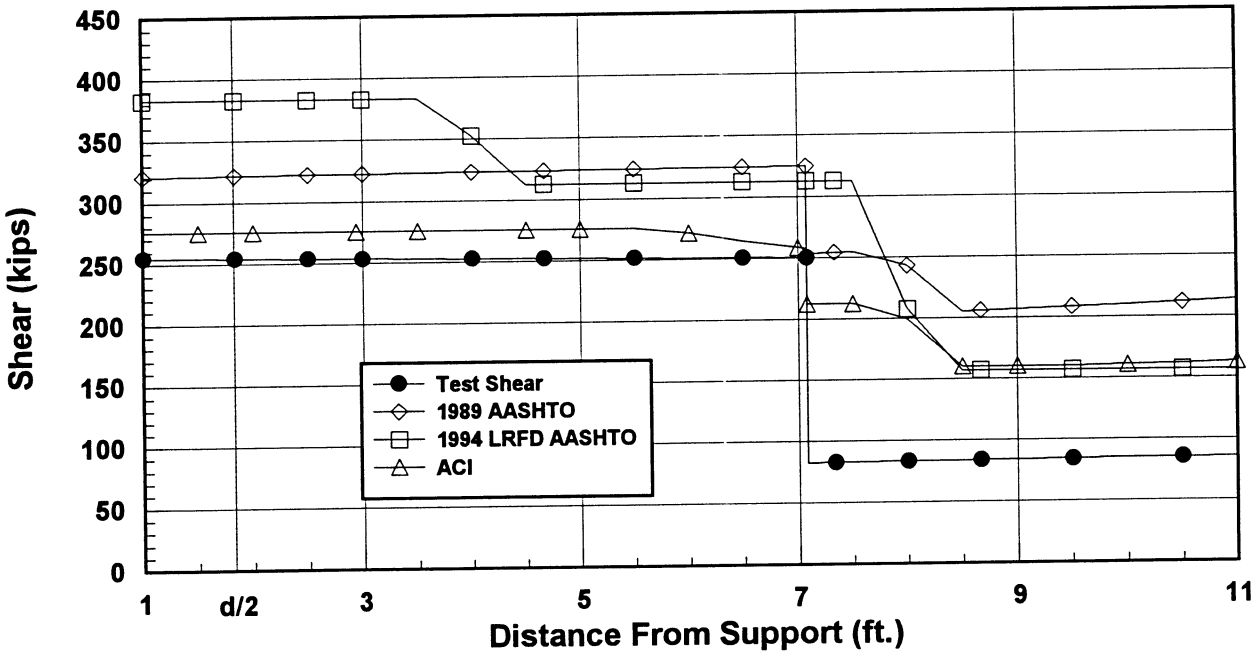

Figure 4.21 Test Shear and Predicted Shear for Girder 2R-8-S

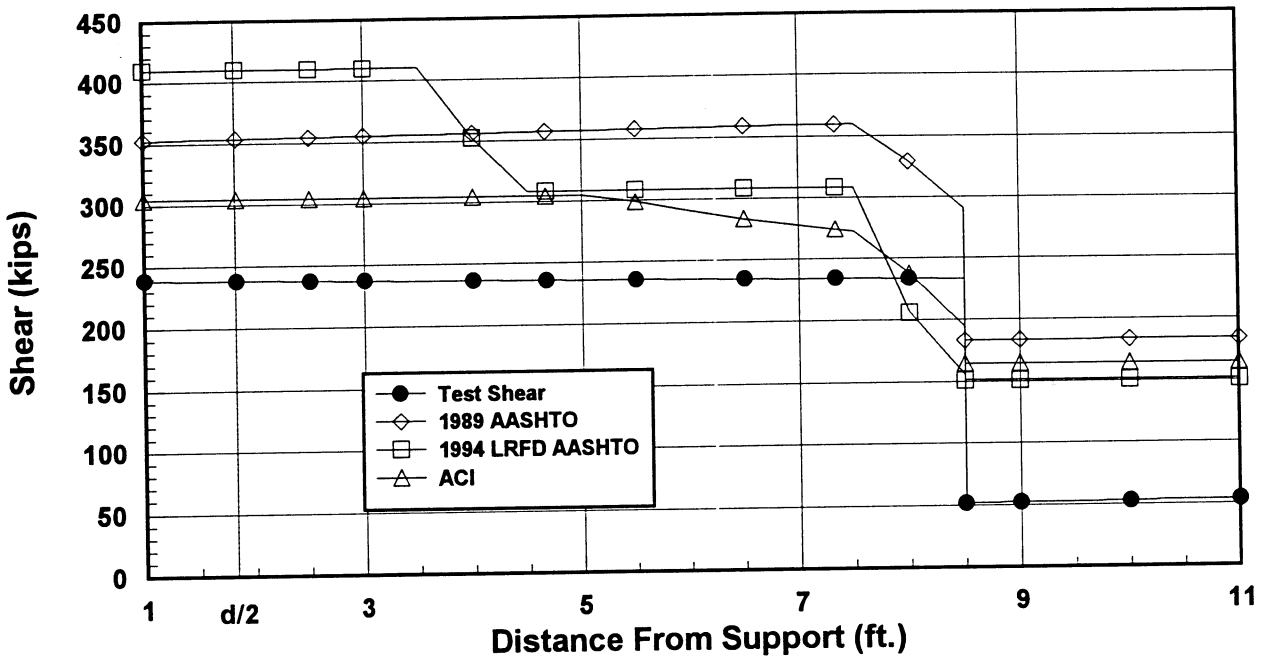

Figure 4.22 Test Shear and Predicted Shear for Girder 2R-10-N

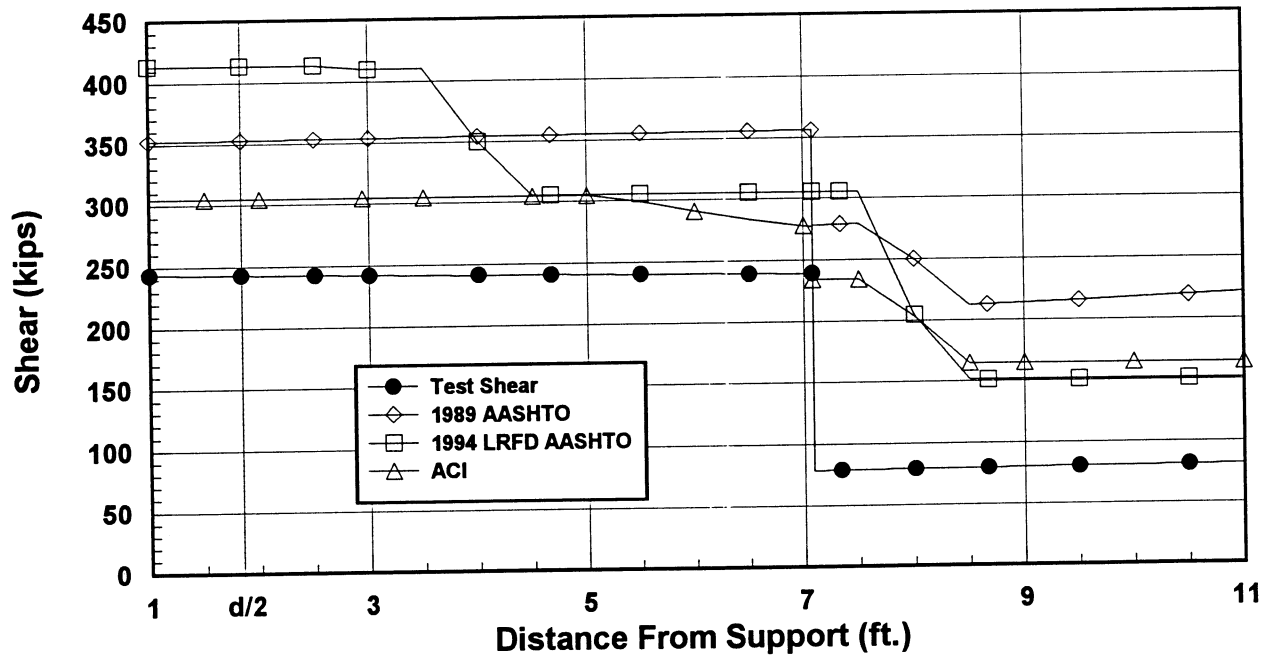

Figure 4.23 Test Shear and Predicted Shear for Girder 2R-10-S

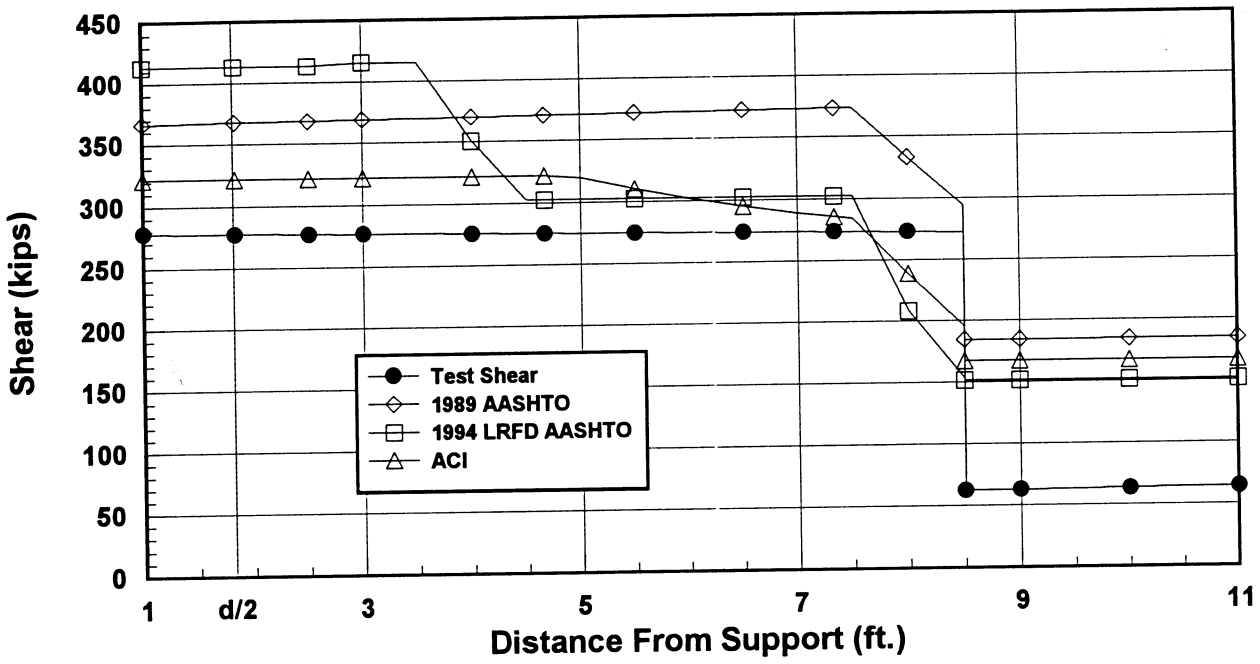

Figure 4.24 Test Shear and Predicted Shear for Girder 2R-12-N

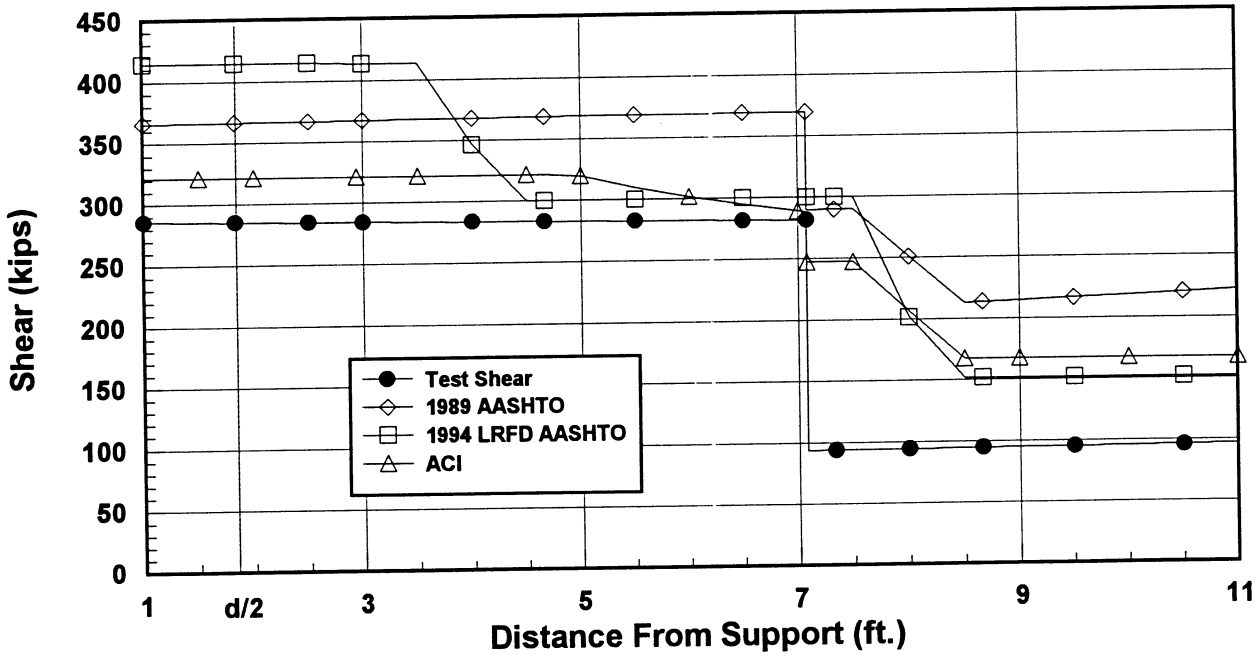

Figure 4.25 Test Shear and Predicted Shear for Girder 2R-12-S

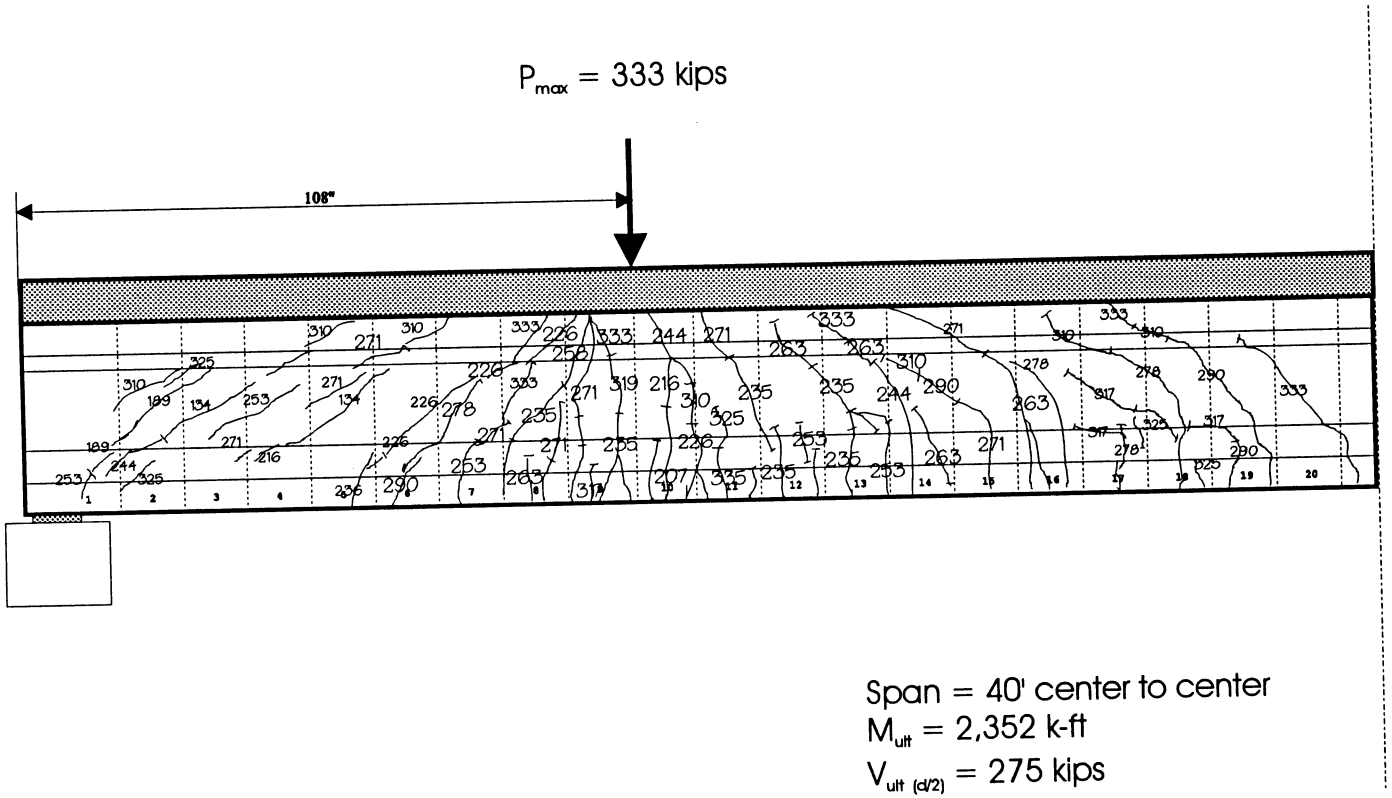

Figure 4.26 Cracking Pattern for Girder R-8-N

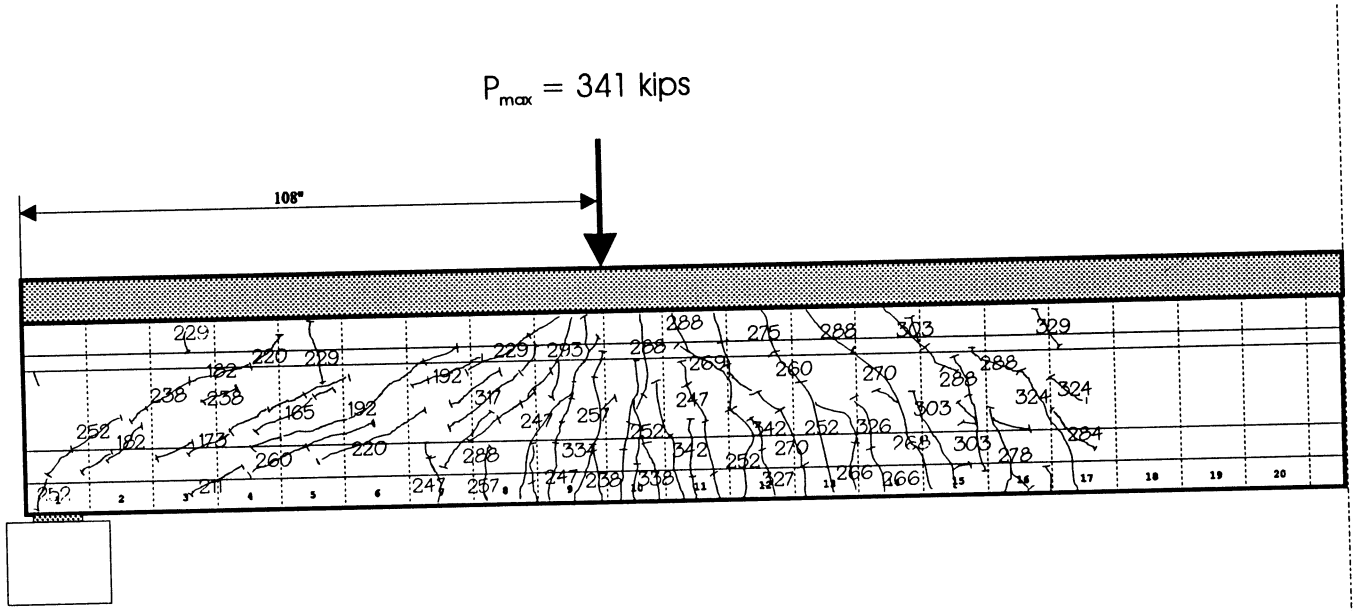

Figure 4.27 Cracking Pattern for Girder R-10-N

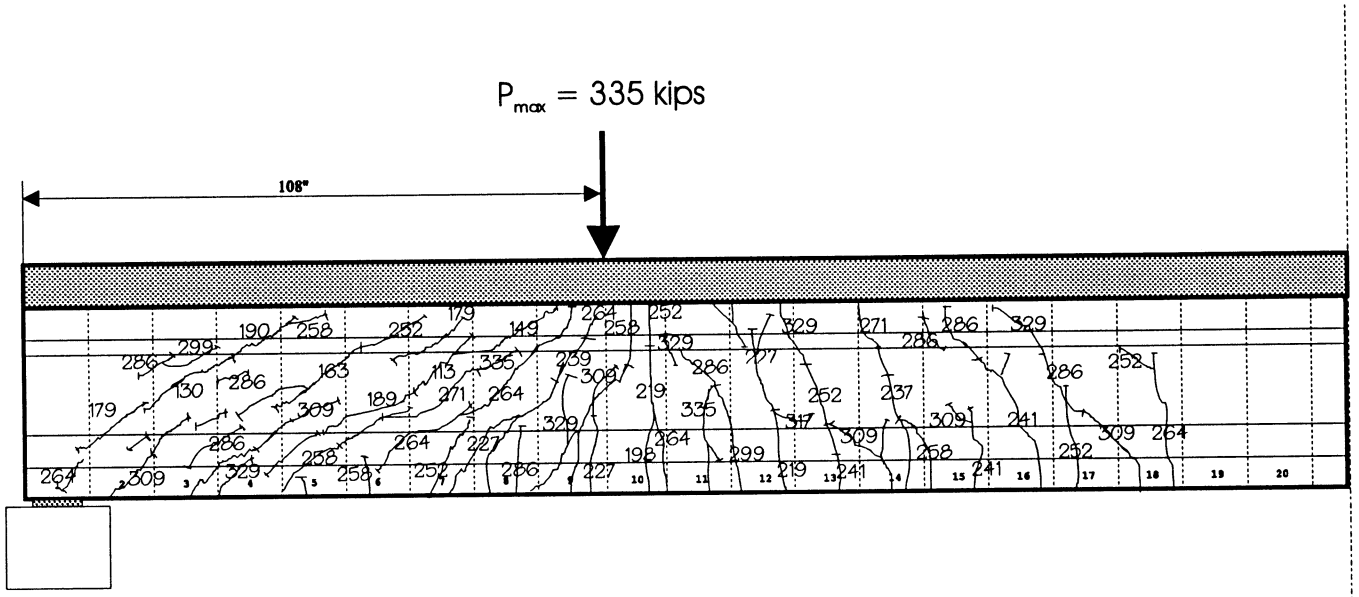

Figure 4.28 Cracking Pattern for Girder R-12-N

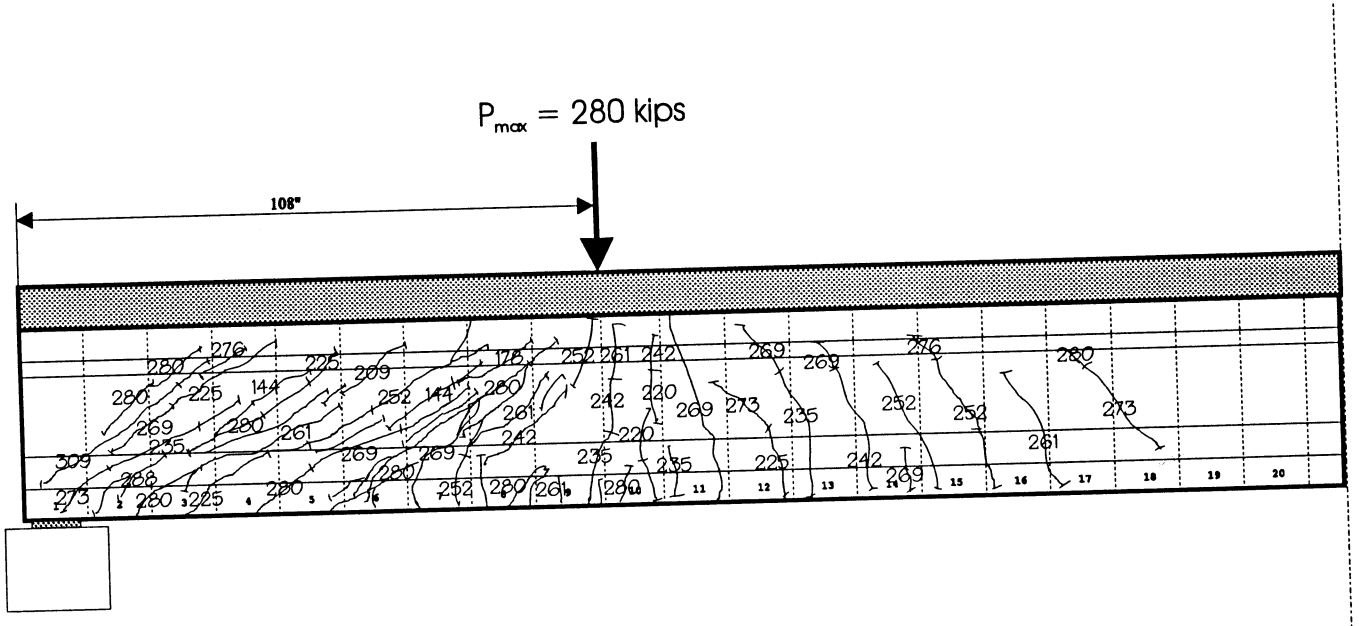

Figure 4.29 Cracking Pattern for Girder 2R-8-N

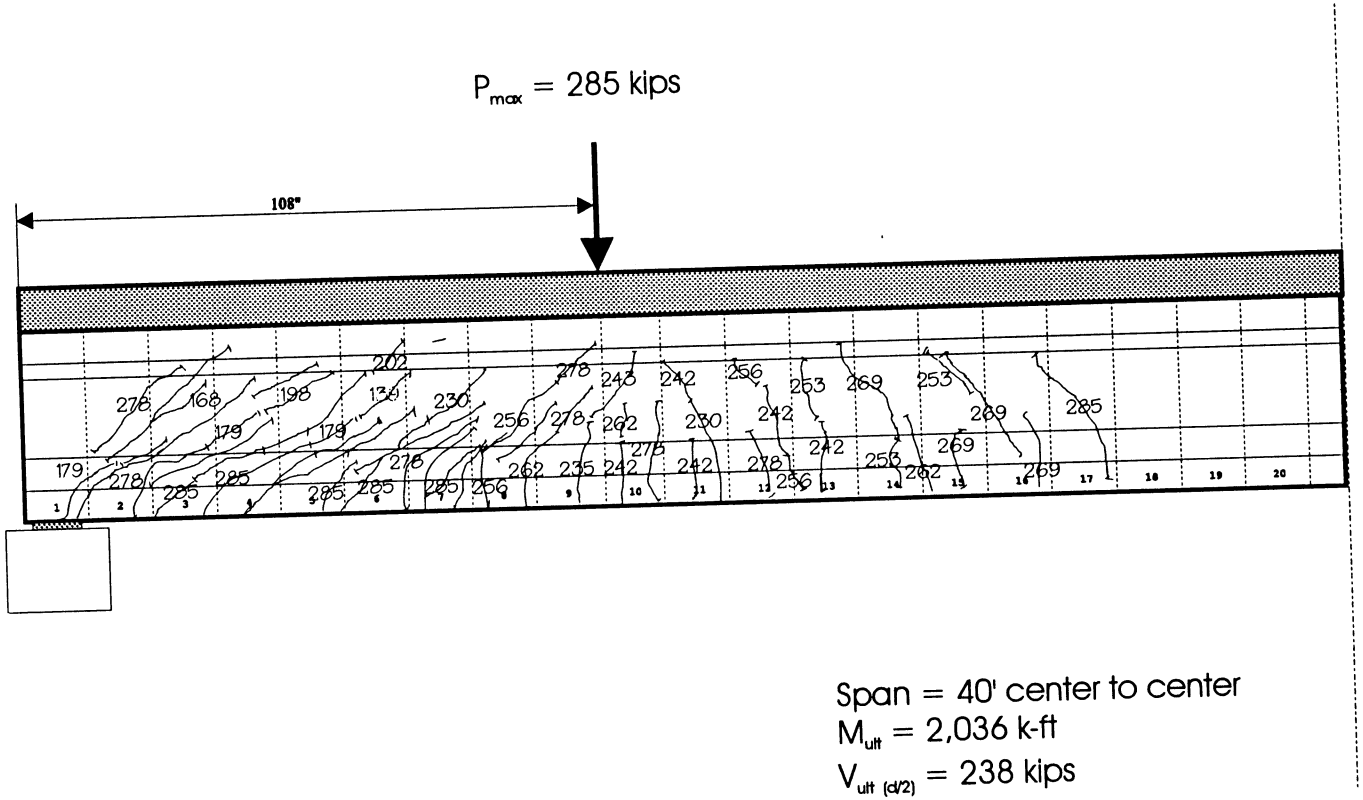

Figure 4.30 Cracking Pattern for Girder 2R-10-N

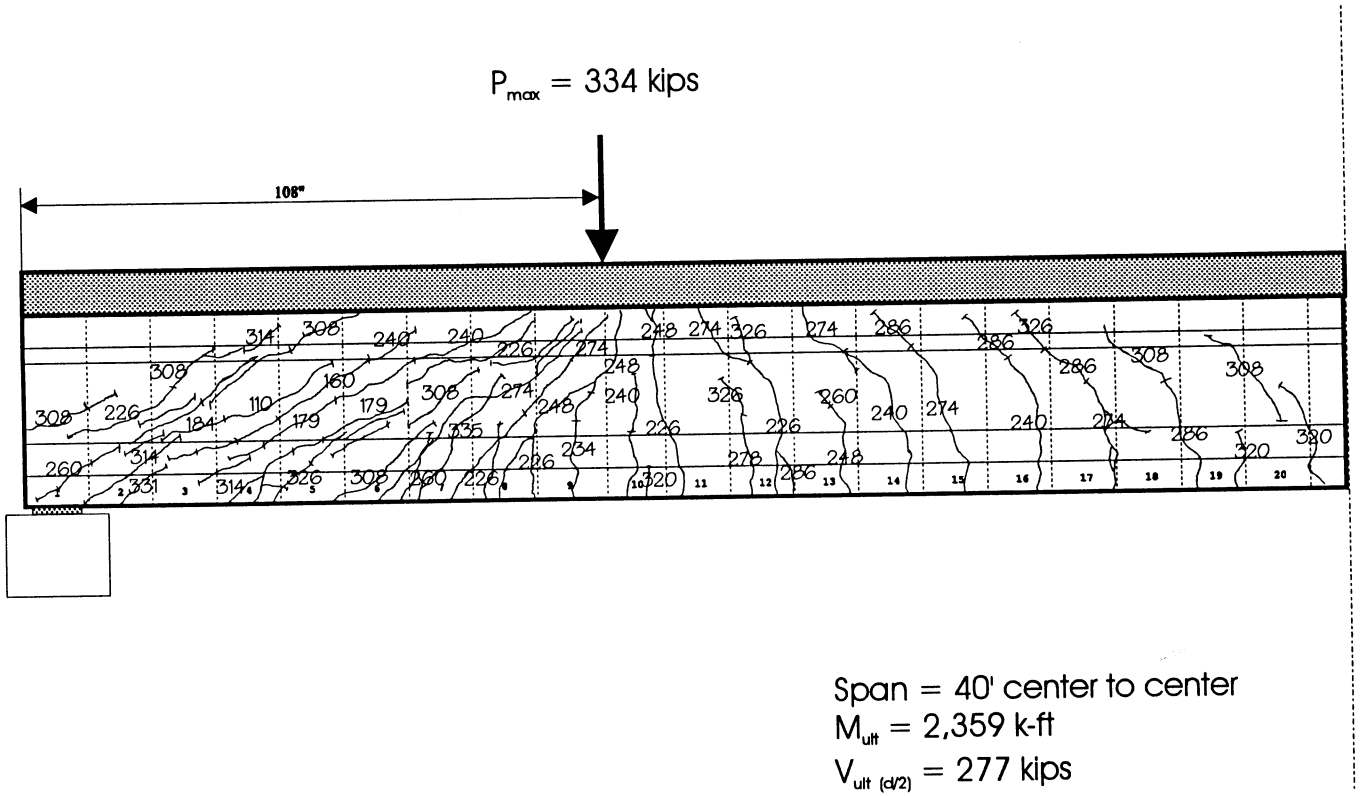

Figure 4.31 Cracking Pattern for Girder 2R-12-N

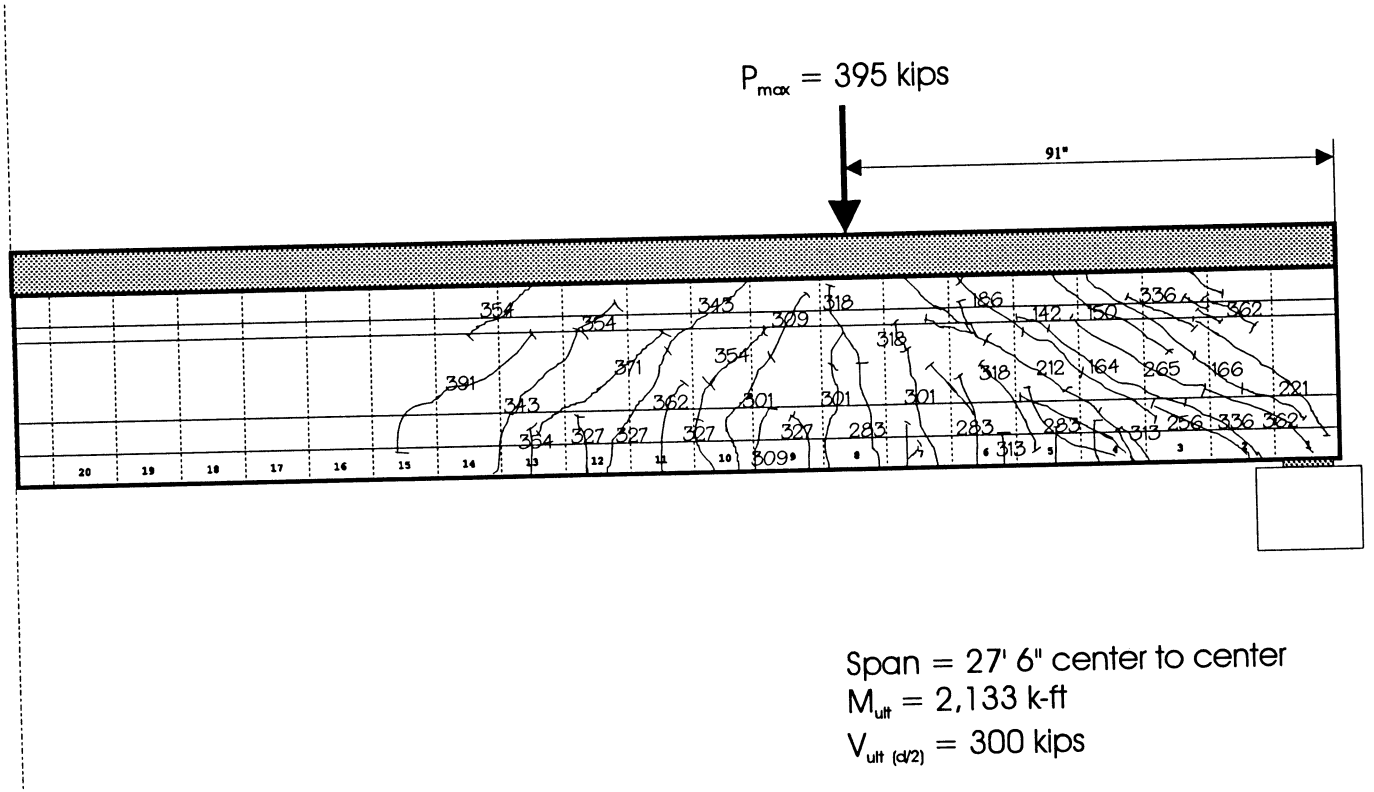

Figure 4.32 Cracking Pattern for Girder R-8-S

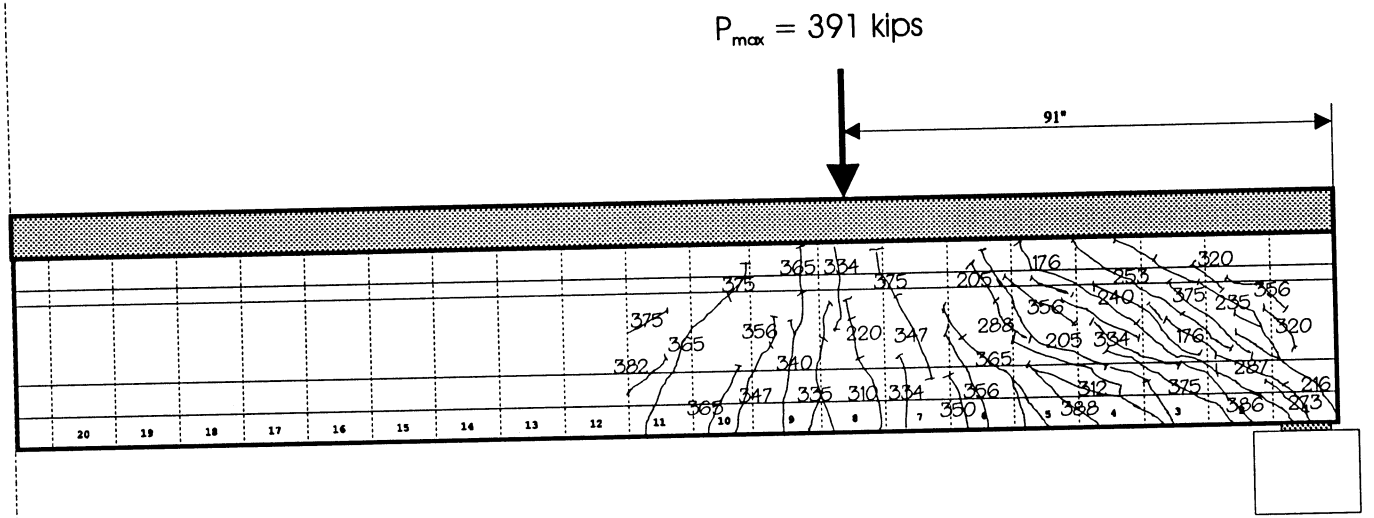

Span = 27'6" center to center
M_{ult} = 2,111 k-ft
$V_{ult\ (d/2)}$ = 297 kips

Figure 4.33 Cracking Pattern for Girder R-10-S

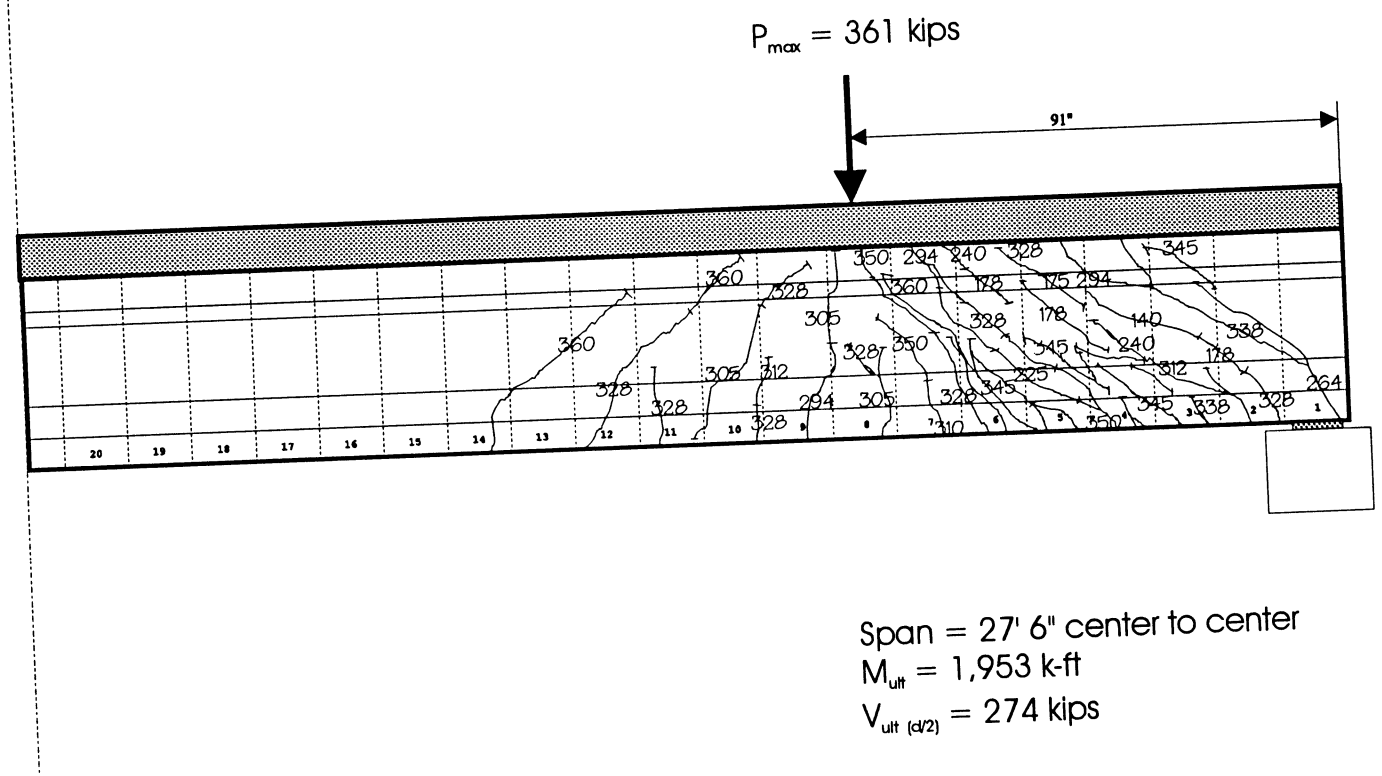

Figure 4.34 Cracking Pattern for Girder R-12-S

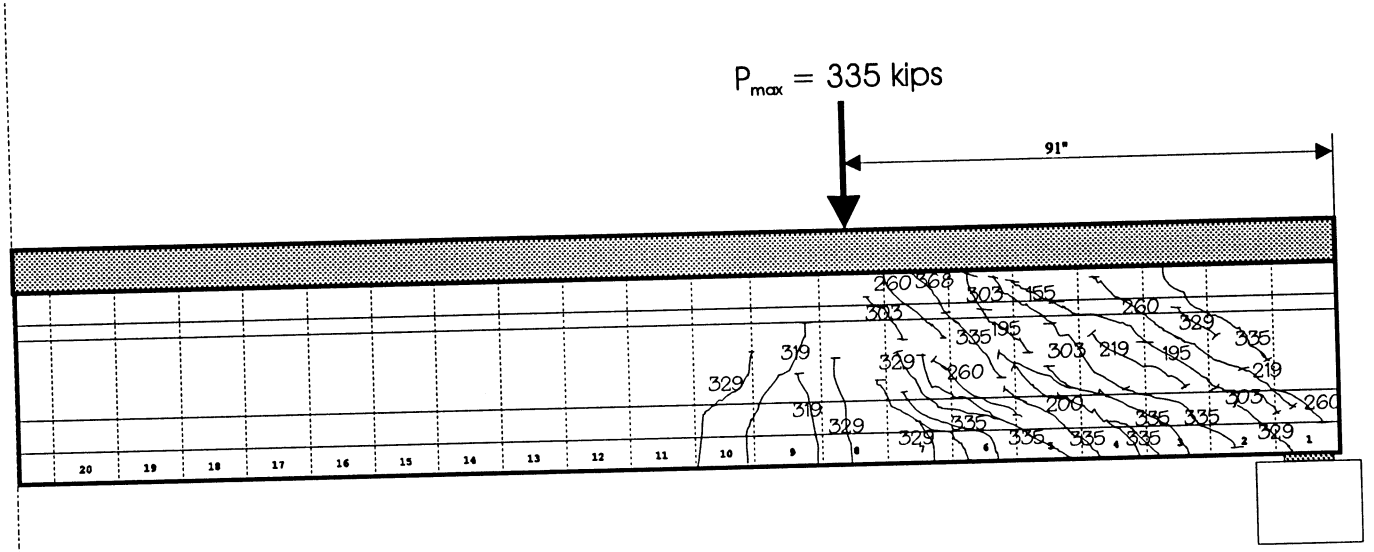

Span = 27' 6" center to center
M_{ult} = 1,809 k-ft
$V_{ult\ (d/2)}$ = 254 kips

Figure 4.35 Cracking Pattern for Girder 2R-8-S

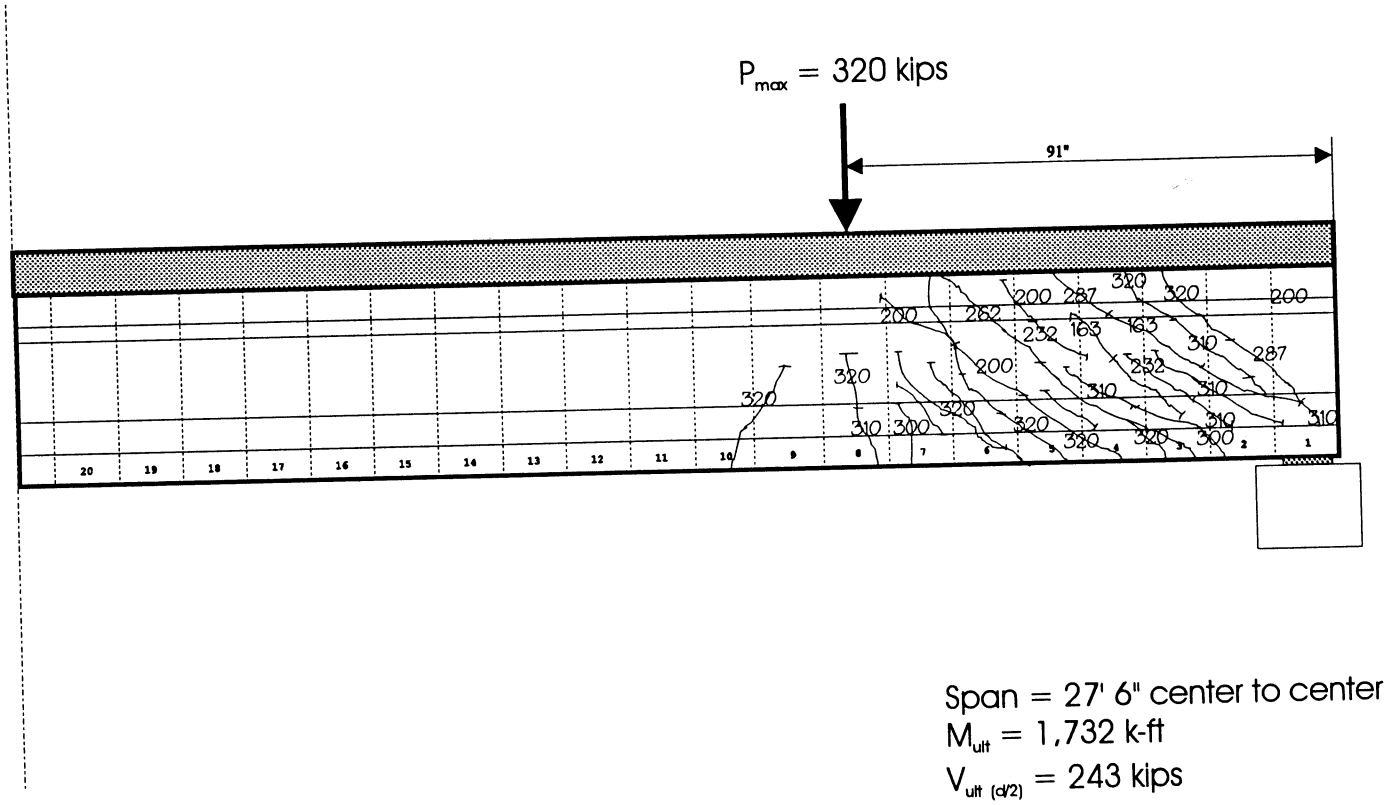

Figure 4.36 Cracking Pattern for Girder 2R-10-S

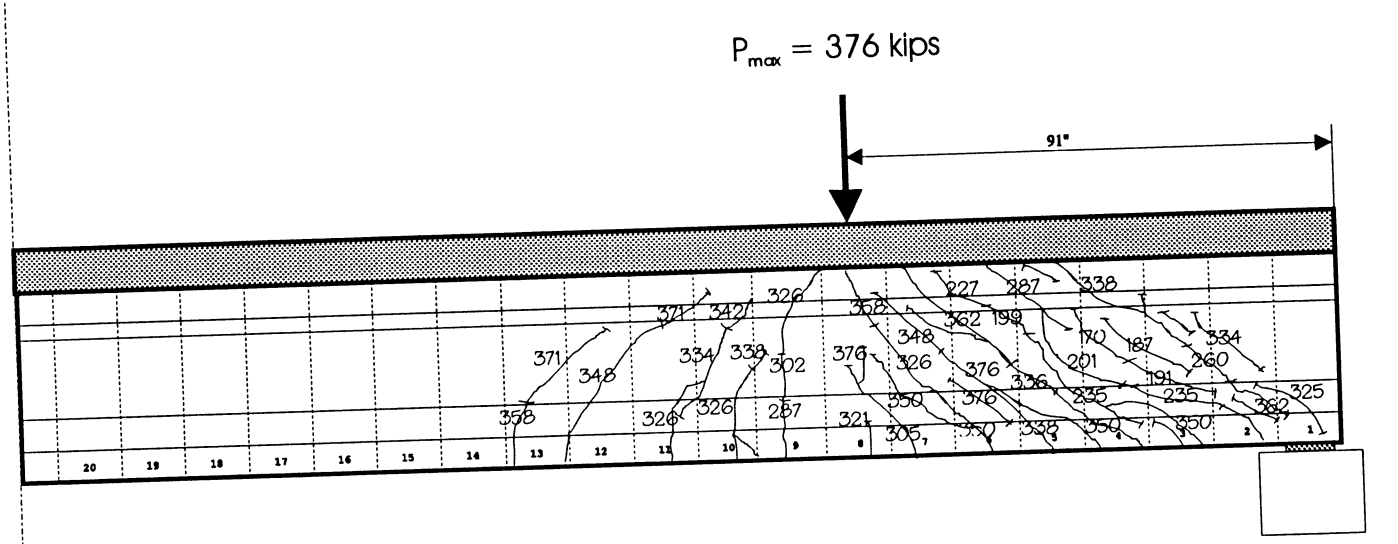

Span = 27' 6" center to center
M_{ult} = 2,026 k-ft
$V_{ult\ (d/2)}$ = 285 kips

Figure 4.37 Cracking Pattern for Girder 2R-12-S

CHAPTER 5
DISCUSSION OF RESULTS

5.1 Pullout Bond Tests

Most of the 3/8", 7/16" and 1/2" pullout specimens followed the same failure pattern. The adhesion bond prevented any slip of the strand relative to the concrete until a load P_1 was reached. At this load, the strand began to slip. After the initial slip the specimen can withstand increasing loads beyond the P_1 load. The applied load increased until P_t was reached. Some specimens with 0.6" diameter strands had concrete splitting failures at the P_1 failure and were not able to resist higher loads.

5.1.1 Adhesion Bond Performance

Adhesion bond failed upon slippage of the strand. The size of the strand and the surface condition were the most important factors that affected the bond strength. The varying strength of the concrete was accounted for by dividing the bond stresses by the root of the compressive strength. The U'_1 pullout test results presented in Table 4.1 have been simplified and are presented in Table 5.1. Table 5.1 shows the pullout results where the results from duplicate specimens have been averaged.

The average U'_1 bond strength varies greatly between the different strand diameters. The 3/8" and 7/16" strands have approximately twice the adjusted adhesion bond strength as the 1/2" strand. The 3/8" and 7/16" strand also have a significantly higher adjusted adhesion bond strength than the 0.6" strand. The two smaller strand sizes have significantly higher adhesion bond stresses than the two larger strand sizes. Therefore, there may be a trend of higher adjusted adhesion bond strength as strand diameter decreases. However, the trend does not exist between the 3/8" strand and the 7/16" strand, nor does the trend exist between the 1/2" strand and the 0.6" strand. These findings are inconclusive with the findings of other researchers who have investigated the effects of strand size on bonding.

The amount of rust also had an effect on the initial bonding of the strand. From Table 5.1 it can be seen that the 1/2" diameter lightly rusted strand had an average U'_1 bond stress 38% higher than the clean 1/2" strand. Therefore, the amount of rust significantly affects the initial bonding.

These findings agree with the findings of other studies who have investigated the effect of weathering on strand bonding.

The lubricated strands had less adhesion than the ungreased strands. For a given diameter, the average U'_1 results of greased strand were always less than the average U' results of the ungreased strand. Apparently, any type of lubricant reduces the adhesion bond. However, the amount of the adhesion bond reduction due to lubricant is more severe for the smaller strands than for the larger strands.

5.1.2 Mechanical Bond Performance

The mechanical bond strength is dependant on the diameter of the strand, the condition of the strand and the strength of the concrete. The effect of the concrete is not fully accounted for by dividing the bond stress by the root of the compressive strength. Therefore, the U_t results, as opposed to U'_t, will be used for comparison in this section. The $_tU$ and $_tU'$ pullout test results presented in Table 4.1 have been simplified and are presented in Table 5.2. Table 5.2 shows the pullout results where the results from duplicate specimens have been averaged.

Perhaps the most significant results for the pullout study involve the relationship between the mechanical bond strength and the compressive strength of the concrete. For each of the strand diameters tested, there is an increase in the average U'_t bond strength with an increased concrete strength. A linear regression analysis were performed on the 1/2" ungreased specimens to quantify the effects of the concrete strength.

The regression using the average of the data points resulted in the following expression:

$$U_t = 0.0687 \cdot f'_c \qquad 5\text{-}1$$

Other researchers have found U' values to be constant for a given size and condition of strand. Results can also be presented in terms of a constant C where:

$$C = \frac{U}{\sqrt{f'_c}} \qquad 5\text{-}2$$

C is a constant for a given strand diameter and condition.

This study used a much wider range in concrete strengths than previous studies and found that the U'_t values were not constant for the wide range of concrete strengths. The results from this study show that the U_t bond strength may vary linearly with the compressive strength of the concrete.

The diameter of the strand also had an effect on the mechanical bond strength similar to the effect the diameter had on the U'_1 results. U_t bond strengths for the 3/8" and 7/16" strands were higher than the U_t results for the 1/2" and 0.6" strand. However, the results comparing the 3/8" with the 7/16" strand, and the results comparing the 1/2" strand with the 0.6" strand are inconclusive.

Lubrication of the strand affects the mechanical bond strength. It is unclear if the type of lubricant is significant. The averaged results in Table 5.2 show a slight increase in mechanical bond strength with the lubricated strand.

5.1.3 Comparison of Pullout Bond Results with Other Studies

The average values for U'_1 and U'_t and their standard deviations are presented in Tables 5.3 and 5.4 along with values from other researchers. Although the results from this study indicate that the bond strength varies linearly with the concrete compressive strength, U' results will be used for comparison to be consistent with previous studies.

Averaging the U' results will result in a larger standard deviation for the current results. The U'_1 values obtained in this study correlate well from the values obtained by other researchers using a direct tension pullout test. The U'_t values are greater than the U' values obtained from direct tension pullout tests. However, the U'_t results are less than the U' values obtained from test using prestressed strands incorporating the Hoyer effect.

5.2 Transfer Length Results

The results from the 22 transfer length tests shown in Table 4.2 were used to develop an equation that predicts the transfer length. Variables in the transfer length test were the compressive strength of the concrete and the effective prestressing force. The pullout test show that the diameter affects the bonding and it is therefore reasonable to assume the diameter will significantly affect the transfer length. However, the diameter was held constant at 1/2" in the transfer length tests. A relationship will first be developed that predicts the transfer length based on the compressive strength and the effective prestress. The equation will then be modified to include the effects of different diameters.

Pullout test results show that the mechanical bond stress is directly proportional to the compressive strength of the concrete. The literature review suggests the mechanical bond strength is the appropriate strength to compare with the transfer length bond stress because there is slip over the transfer length. Therefore as the compressive strength of the concrete increases, the bond strength will increase and the transfer length will decrease. Because the bond strength should be constant for the small ranges of effective prestressing force, the transfer length should increase as the effective prestressing force increases. Thus, the transfer length expression should resemble the following form:

$$l_t = \frac{C \cdot f_{se}}{f'_{ci}} \qquad 5\text{-}3$$

Several regression analyses were preformed using different transforms on both f_{se} and f'_{ci}. The best model was the above model with all of the variables in their natural form. The resulting expression is shown below in equation 5-4.

$$l_t = \frac{0.89 \cdot f_{se}}{f'_{ci}} \qquad 5\text{-}4$$

Where f_{se} and f'_{ci} are in the same units psi or ksi.

The above equation was then modified to reflect the influence of the strand diameter. The modification should reflect the fact that small strands have been found to have significantly higher bond strengths which implies smaller transfer lengths. The modification should be conservative because of the fact that no full scale girders with small strands were tested. The diameter was

$$l_t = \frac{1.78 \cdot f_{se} \cdot d_s}{f'_{ci}} \qquad 5\text{-}5$$

included in the numerator of the initial equation without any transformation. The equation becomes: and is dimensionally homogeneous. A scatter plot of the data points and the above expression is shown in Figure 5.1.

In the transfer beams tested the effective prestressing force remained relatively constant. The prestressing force increased from 160 ksi for the 6,000 psi girder to 177 ksi for the 12,000 psi girder. The lower strength girders had a greater transfer length, more slip and elastic shortening, resulting in a lower effective prestressing force. Assuming all of the girders had the same initial prestress, there is strong evidence that the reduction in the prestressing force caused by elastic shortening is dependant on the compressive strength of the concrete. Thus, a regression analysis containing both f_{se} and f'_{ci} may be collinear. The f_{se} term can replaced by f_{si} which was constant for all of the tested girders. The expression now becomes:

$$l_t = \frac{1.61 \cdot f_{si} \cdot d_s}{f'_{ci}} \qquad 5\text{-}6$$

A scatter plot of the data points and the above expression is shown in Figure 5.2.

5.3 Relationship Between Pullout Bond and Transfer Length Bond

The pullout test results show that the strand condition significantly affects the bond strength. Equations 5.5 and 5.6 should accurately predict the transfer length of most prestressed members encountered in practice. However, no general equation can accurately predict the transfer length for prestressed members with unusual strand conditions. Other researchers have observed that different grit conditions of epoxy coated strands will significantly affect the bonding and transfer length.

Equations could be developed that reflect the grit condition or rust condition of prestressing strands. However, the quality control necessary to quantify varying strand conditions would be impractical in actual manufacturing conditions.

It is desirable to establish a relationship between the pullout test and the transfer length. If an accurate relationship is established pullout specimens could be easily prepared and tested in the field. Equations 5-5 and 5-1 can be used to develop an equation that will predict the transfer transfer length given the results from a direct tension pullout test.

The pullout bond strength for a 1/2" clean strand was found to be:

$$U_t = 0.0687 \cdot f'_c \qquad 5\text{-}1$$

The equation developed for the transfer length in section 5.2 was:

$$l_t = \frac{1.78 \cdot f_{se} \cdot d_s}{f'_{ci}} \qquad 5\text{-}5$$

At the time of transfer, the concrete strength, f'_c, in equation 5-1 will be equal to the concrete strength at transfer, f'_{ci} in equation 5-5. Therefore the transfer length is related to the pullout bond strength by the following relationship:

$$l_t = \frac{0.122 \cdot f_{se} \cdot d_s}{U_t} \qquad 5\text{-}7$$

5.4 Shear Strength Tests

5.4.1 Effect of Concrete Strength

Table 5.5 shows the shear at the initial slip, shear when all strands have slipped and the maximum shear. The six tests with 2R girders show an increase in shear strength with an increase in concrete compressive strength. Six tests with R girders show a constant shear strength for the 8,000 psi and 10,000 psi girders and a decreasing shear strength for the 12,000 psi girder. The total increase in shear strength, for all of the tests, between the 10,000 psi girders and the 8,000 psi girders was 0.003%. The increase in shear strength, for all of the tests, between the 12,000 psi girders and

the 8,000 psi girders was 4.7%. Thus the compressive strength of the concrete had little effect on the shear strength of the girders when tested inside the development length.

It was theorized in the pullout analysis that as the slip increased, the helical strand shape caused increased bond stresses. Thus, as slip increases, bond stresses increase until the bond fails. So after slip has begun the shear resistance can be expected to increase until the bond fails. The pullout tests also demonstrated that increased concrete strength increases the U_t bond strength. In table 5.4 the difference between the shear at which all of the strands have slipped and the shear at failure was calculated. As the strength of the concrete increases, the additional amount of shear strength after adhesion bond failure increases.

Summarizing the primary observations discussed in this section:

1) After a general bond slip, where all of the strands have slipped, the girder will resist additional loads.

2) The load that causes the initial bond slip does not appear to be greatly effected by the concrete compressive strength.

3) Applying increased loads after a bond failure causes increased slip that will eventually fail the mechanical bond.

4) Higher concrete strength can resist higher mechanical bond stresses. Therefore, girders manufactured with high strength concrete can resist higher additional loads after the initial bond failure.

Therefore, if the shear that causes the general bond slip can be predicted, the ultimate shear strength can be determined. A study of the loads that cause bond failure is essentially a study of the development length. As mentioned previously, a study of the development length requires a large number of specimens and was beyond the scope of this project. However, the recent studies on the development length discussed in the literature review suggest that the condition of the strand is the most significant factor that affects the development length.

5.4.2 Effect of Increased Shear Reinforcement

It appears that the amount of steel resisting the shear forces is not critical to the strength of the beams studied in this project. It has been shown that the bond between the prestressing steel and

the concrete is the critical factor affecting the strength of the girders tested in this project. The truss analogy can be used to explain the lack of strength gain in the specimens tested. In the truss analogy the prestressing strand, inclined compression strut and the web reinforcement in tension act as a truss in resisting the applied shear. Prior to bond failure, the strand can withstand additional loads, and the forces in the stirrups and inclined concrete compressive strut are increased. At failure the additional forces carried by the prestressing strands were not able to be resisted by the bond between the prestressing steel and the concrete. Thus in most of the tests the longitudinal tension member, in particular the bond between the tendons and concrete, is the critical member of the truss.

Experimental observations prove that the bond failure is critical for most of the tests. For the test setup used in this project the bond failure becomes critical before the web shear strength in all cases except the R-10-N test. If the bond stresses are critical for the R girders then it is likely that the bond stresses will be critical for the 2R girders. If more of the R tests had not failed because of the bond failure, it is possible that the additional shear reinforcement in the 2R girders would have given the girders additional shear strength.

There is a possible explanation for the small reduction in shear strength of the 2R girders. Because all of the stirrups are tied to the prestress reinforcement, increasing the number of stirrups will decrease the surface area of the strands that is bonded to the concrete. The decreased bonding area may cause the bond to fail in the 2R girders before the bond fails in the R girders.

5.4.3 Code Prediction Results

Figures 4.11 to 4.22 show that while the test shear remains constant from the support to the concentrated load, the predicted shear changes considerably over the same region. This is due to the changing steel spacing and the increased moment as section under inspection moves from the support to the concentrated load.

Section 9.20.1.4 of the 1989 AASHTO code states that sections located at a distance less than h/2 from the face of the support may be designed for the same shear V_u as that computed at a distance h/2. Section 5.8.3.2 of the AASHTO LRFD code states that the location of the critical section for shear shall be taken as the larger of $0.5\, d_v \cot\theta$ *or* d_v from the internal face of the support. The value of d_v is larger than $0.5\, d_v \cot\theta$ for the girders studied in this project. Table 5.6 shows the test shear

and predicted shear values at a distance of h/2 from the support. Table 5.7 shows the test shear and predicted shear values at a distance of d_v from the support.

All of the codes predict increasing shear strength when the web reinforcement is increased from R to 2R. While the 1989 AASHTO code and ACI code both limit the amount of shear carried by the steel, the AASHTO LRFD code only limits the total shear carried by the sum of the concrete and steel contributions. Because the test girders did not experience any strength gain when the reinforcement was increased from R to 2R, each code over predicts the shear strength of the 2R girders. The ACI code best predicted the strength of the 2R girders.

Each of the codes closely predicted the shear strength of the R girders. The AASHTO LRFD code underestimated the shear strength at section d_v by an average of 5%. The ACI code underestimated the shear strength by 4% at the section h/2. The 1989 AASHTO code overestimated the shear strength by 13% at the section h/2.

5.4.4 Strut and Tie Models

As discussed in section 2.3.4, a strut and tie model may be an appropriate model to predict the strength of the test girders because of the short shear span. In the testing program the length between the end of the girder and the inner face of the nodal zone was ten inches for each test. This length is less than the required anchorage length specified in the AASHTO code. The measured transfer length is greater than twice the distance from the end of the girder to the nodal zone. The development length, although not measured in this project, will be greater than the transfer length. Thus, the premise of strut and tie models, that the girder will resist external loads through a truss action between the tension tie and the concrete compressive strut, has been violated. Because of the insufficient anchorage length, the truss action predicted by the model will not fully develop.

Given the inadequate embedded length, a strut and tie analogy would indicate that the nodal zone over the support would likely fail and cause the girder to fail prior to the failure of the concrete compressive strut or the tension tie. A strut and tie model for the test girders agrees with the test results, a bond failure usually causes failure and that there is no additional shear strength between the R and 2R girders.

Because of the agreement with the test results and the inclusion of the strut and tie model in the 1994 LRFD AASHTO code, the strength of the concrete compressive strut and tension tie were computed using a strut and tie model. The strut and tie models presented in the 1994 LRFD AASHTO code and the text by Collins do not suggest a method to calculate the limiting strength of the nodal zone for the test girders. Therefore, it should be reemphasized that the strut and tie models used for the test girders do not reflect the limiting strength of the nodal zone. The strut and tie models used in this project do not meet the anchorage requirements of the 1994 LRFD AASHTO code.

Table 5.8 shows the test results compared with the results predicted by the strut and tie models. Strut and tie models show that the concrete compressive strut will fail before the tension tie. The predicted strengths correctly predict increased strength for the south end loading configuration and a lack of increased strength for increased reinforcement beyond R. However, because the girders failed in bond, and the bond strength is not quantified by the code, the strut and tie models may be conservative if the required embedded lengths were provided.

5.4.5 Development Length

The development length is the distance from the end of a prestressed member where the critical section will fail without a bond failure. The method used by Cousins and Over to measure the development length was to move the concentrated load, and thus the critical section, between various tests. If a bond failure occurred at a given critical section, the distance between the critical section and the support would be incrementally increased until a flexural failure occurred without a bond failure. The limited number of samples tested in the current study did not allow the development length to be measured.

Four of the six north end tests had a bond failure that led to shear failure. The R-10-N girder had no slip and thus the development length for this girder was less than 108 in. The R-8-N girder did have some slip before the shear failure. However, the amount of slip was very small in comparison with the other girders. In addition the range of the slip at failure was in the range where the beam can withstand increased loads in other test. It is reasonable to assume that the development length for this girder was approximately equal to 108 in. Because the remaining girders had a

substantial bond slip, the development length for these girders is greater than 108 in. Because all of the south end tests had a general bond failure, it can be concluded that all of the development lengths are greater than 91 in., which is supported by the north end test results.

5.4.6 Test Girder Behavior

The sixty-four gages monitored during testing can be used to examine the girders performance under the applied load. Generally, the gages performed well during testing. However, after considerable cracking, some gages begun to give erratic readings.

5.4.6.1 Total Moment vs. Deflection

Relationships of the total moment vs. the deflection for each girder are shown in Figures 5.3 to 5.14. The total moment is the moment at the applied load due to the dead load and applied loads. The deflection is measured at both the applied load and the center of the girder. The moment vs. deflection line appears linear until a moment of approximately 1,500 k-ft, at this point significant cracking and strand slip begins to occur and the slope of the line decreases. The slope of the moment vs. deflection line can be used to determine if there are any significant differences between the girders in the test program. Two different slopes for each plot were measured. The first slope was measured as the moment increased from 100 k-ft to 1,500 k-ft. The second measurement was taken when the moment increased from 1,500 k-ft to 2,000 k-ft. The results are shown in Table 5.9.

Several observations can be made concerning the initial slope of the moment vs. deflection plots for the test girders. The effect of the strength of the concrete can be examined by considering the slope within a particular group. Each of the four groups show a trend of increasing slope as the strength of the concrete increases. The trend is more pronounced in the south tests than the north tests. The increased slope indicates that a girder with higher concrete strength will deflect less under a given moment. This results can be attributed to the higher elastic modulus of the high strength concrete. The effects of the increased shear reinforcement on the initial slope can also be examined. For the north tests, increasing the web reinforcement for a given girder decreased the slope in all three cases. For the south end tests the slope increased in all three cases. The major difference between the north and south tests was the moment: shear ratio. The south tests had a greater shear for a given

moment, compared with the north tests. Providing additional web reinforcement will help control deflection in areas of high shear and low moment, but the additional reinforcement will decrease the deflection resistance of a girder in areas of high moment and low shear.

Several observations can also be made about the second slope of the moment vs. deflection curve. No definite trend can be established concerning the concrete strength and the secondary slope. It appears that increasing the concrete strength may increase the slope of the moment vs. deflection plot after significant cracking and slip has occurred. The effect of the increased web reinforcement has little effect on the secondary slope of the north tests. However, the increased reinforcement results in a greater secondary slope in the south end tests. In areas of high shear, after significant cracking and slip have occurred, additional web reinforcement reduces the deflection of the test girders.

5.4.6.2 Total Moment vs. Strand Slip

The effect of the strand bonding was extensively discussed in earlier sections of this chapter. Different slip patterns for individual strands will be discussed in this section. In this section plots showing the slip of the individual strands will be presented. Three plots are required to show the moment vs. strand slip plot for each test. These plots are shown in Figures 5.15 to 5.50. The first plot, strands 1 through 4, contains the first two rows of strands. The second plot, strands 5 through 9, contains the third row of strands. The third plot contains the fourth and final row of strands. The south end tests had the largest amounts of slip and are useful in determining any relationship between the strand's location and the amount of slip that occurred during testing.

Two general relationships can be found through examination of the three plots for any test. It appears that the top rows of strands will generally slip before the lower rows. After the bond failure, the lower rows will have more slip than the upper rows. In summary the top rows of strands will slip first but the lower rows will slip more.

Examination of the R-8-S test will illustrate these observations. Figure 5.24 shows that the top strand slipped at a moment of approximately 1,300 k-ft, while most of the second row of strands slipped at a moment of 1,650 k-ft. Also, Figure 5.25 shows that most of the second row of strands has slipped at a moment of 1,900 k-ft. In Figure 5.26, most of the third row of strands has slipped

at a moment of 2,000 k-ft. After testing, Figure 5.24 shows that the first two rows slipped an average of approximately 0.95", and Figure 5.26 shows that the bottom row slipped approximately 1.1". Therefore, the lower rows slipped more that the upper rows.

5.4.6.3 Moment and Slip vs. Deflection

A coupled plot of the total moment and slip was plotted against the deflection and was used to examine the relationship between the moment, slip and deflection for a particular girder. A plot of moment and slip vs. deflection for each test is shown in Figures 5.51 to 5.62. In section 5.4.6.1, the total moment vs. slip relationship was divided into two regions of different slopes. The slope was generally found to decrease at a moment of approximately 1,500 k-ft. The relationships of moment and slip vs. deflection show that the change of slope is accompanied or perhaps caused by slippage of the strands. These relationships also show that the girder failure, noted by a decrease in the total moment, is accompanied by a dramatic increase in strand slip.

Examination of Figure 5.52, the moment and slip vs. deflection relationship for girder R-8-S illustrates the above observations. The slope of the moment vs. deflection line begins to decrease at a moment of approximately 1,550 k-ft. At this moment strands 1 through 4 begin slipping. This slipping is noticed by the slip vs. deflection lines being above the x axis. In the region where the moment vs. deflection line is considered to be in the second slope area, from a moment of 1,550 k-ft to a moment of 2,100 k-ft, the slip of the strands is also increasing at approximately linear rate. At failure, 2,100 k-ft, the amount of slip increases dramatically as the moment capacity of the girder decreases significantly.

5.4.6.4 Total Moment vs. Confining Bar Strain

Each girder had three instrumented confining bars at each end of the girder. These bars were in the same location for all of the test girders. Each of these bars was instrumented with a strain gage to record the strains in the bars that develop during testing. Figures 5.69 to 5.80 show the plots of the total moment vs. the confining bar strain The first confining bar was located 1/2 inch from the centerline of the support and experienced very little strain in all of the tests. The other instrumented bars were located approximately two and three feet from the end of the girder were strained in the

tests.

The confining bars have little strain until the strands begin to slip. This relationship can be seen by comparing the moment vs. slip plot with the moment vs. confining bar strain plot for any test girder. In many of the plots the confining bars become highly strained when the total moment reaches approximately 1,500 k-ft. This is when the strands begin to slip and the slope of the moment vs. deflection plot decreases. In the pullout test it was observed that the radial cracks developed in the concrete after the strand had begun to slip. These cracks caused the concrete cylinder to loose the confinement of the strand, and the force required to extract the strand decreased. In the test girders the confining bars act to keep the concrete cover intact around the strands.

While the number and spacing of the confining bars were not variables in this testing program, the effects of the confinement can be extrapolated from the results. The test results presented so far can be generalized as follows: Most of the test girders failed in bond, and, after a bond failure the girder may support additional loads until the strands slip dramatically. Increasing the confinement of the strands will not affect the initial slip of the strands, which is primarily dependant on the strand condition. Increasing the confinement of the strands will likely increase the additional loads that can be supported after the first slip of the strands. After the strands begin to slip confinement stresses increase until the concrete cover surrounding the strands fails and the strands slip dramatically. Thus increased confining strength can delay the failure as additional loads are applied. The means for providing increased confining strength was not examined in this project.

Table 5.1 Pullout Test Results Showing Average U'1 Results

Specimen	Diameter	Greased or Ungreased	P1 (lb)	U1 (psi)	U'1	U'1 (avg)	S.D.
3-UC-7-A	3/8"	U	10,725	759	8.70	7.88	1.46
3-UC-7-B	3/8"	U	11,584	819	9.40		
3-UC-11-A	3/8"	U	11,688	827	7.87		
3-UC-11-B	3/8"	U	8,218	581	5.53		
4-UC-7-A	7/16"	U	11,625	705	8.09	7.96	1.14
4-UC-7-B	7/16"	U	14,037	851	9.76		
4-UC-11-A	7/16"	U	11,986	727	6.92		
4-UC-11-B	7/16"	U	12,225	741	7.05		
5-UC-7-A	1/2"	U	8,658	459	5.27	3.94	0.62
5-UC-7-B	1/2"	U	7,215	383	4.39		
5-UC-8-A	1/2"	U	6,240	331	3.66		
5-UC-8-B	1/2"	U	5,770	306	3.38		
5-UC-10-A	1/2"	U	6,901	366	3.68		
5-UC-10-B	1/2"	U	6,722	357	3.58		
5-UC-11-A	1/2"	U	7,135	379	3.60		
5-UL-6-A	1/2"	U	6,754	358	4.52	5.42	0.91
5-UL-6-B	1/2"	U	8,406	446	5.63		
5-UL-6-C	1/2"	U	10,603	563	7.10		
5-UL-6-D	1/2"	U	7,629	405	5.11		
5-UL-6-E	1/2"	U	7,131	378	4.77		
6-UC-6-A	0.6"	U	9,615	425	5.36	5.63	0.23
6-UC-7-A	0.6"	U	11,063	489	5.61		
6-UC-11-A	0.6"	U	14,087	623	5.93		
3-GCW-7-A	3/8"	G	3,905	276	3.17	3.17	0.00
4-GCW-7-A	7/16"	G	6,555	398	4.56	3.35	1.22
4-GCW-11-A	7/16"	G	3,686	224	2.13		
5-GCW-7-A	1/2"	G	7,696	409	4.69	3.15	0.98
5-GCF-8-A	1/2"	G	3,836	204	2.25		
5-GCF-8-B	1/2"	G	5,966	317	3.50		
5-GCF-10-A	1/2"	G	6,321	336	3.37		
5-GCF-10-B	1/2"	G	3,608	192	1.92		
5-GLO-6-A	1/2"	G	7,277	386	4.87	3.56	0.80
5-GLO-6-B	1/2"	G	5,548	295	3.72		
5-GLO-6-C	1/2"	G	4,378	232	2.93		
5-GLO-6-D	1/2"	G	7,103	377	4.76		
6-GCW-11-A	0.6"	G	2,582	114	1.09	1.17	0.09
6-GCW-11-B	0.6"	G	2,988	132	1.26		
6-GCH-6-A	0.6"	G	0	0	0.00	0.00	0.00
6-GCH-6-B	0.6"	G	0	0	0.00		

Table 5.2 Pullout Test Results Showing Average Ut Results

Specimen	Diameter	Greased or Ungreased	Pt (lb)	Ut (psi)	Ut Avg (psi)	S.D.
3-UC-7-A	3/8"	U	11858	839	873	35
3-UC-7-B	3/8"	U	12839	908		
3-UC-11-A	3/8"	U	16501	1167	1194	27
3-UC-11-B	3/8"	U	17255	1221		
4-UC-7-A	7/16"	U	12226	741	868	127
4-UC-7-B	7/16"	U	16415	995		
4-UC-11-A	7/16"	U	24627	1493	1489	5
4-UC-11-B	7/16"	U	24476	1484		
5-UC-7-A	1/2"	U	10101	536	478	57
5-UC-7-B	1/2"	U	7937	421		
5-UC-8-A	1/2"	U	8747	464	501	37
5-UC-8-B	1/2"	U	10139	538		
5-UC-10-A	1/2"	U	10029	532	654	122
5-UC-10-B	1/2"	U	14620	776		
5-UC-11-A	1/2"	U	16206	860	860	0
5-UL-6-A	1/2"	U	11214	595	559	79
5-UL-6-B	1/2"	U	9220	489		
5-UL-6-C	1/2"	U	12607	669		
5-UL-6-D	1/2"	U	8463	449		
5-UL-6-E	1/2"	U	11144	591		
6-UC-6-A	0.6"	U	9615	425	425	0
6-UC-7-A	0.6"	U	11063	489	489	0
6-UC-11-A	0.6"	U	20121	890	890	0
3-GCW-7-A	3/8"	G	8924	632	632	0
4-GCW-7-A	7/16"	G	15260	926	926	0
4-GCW-11-A	7/16"	G	24627	1494	1494	0
5-GCW-7-A	1/2"	G	13059	693	693	0
5-GCF-8-A	1/2"	G	10589	562	569	7
5-GCF-8-B	1/2"	G	10863	577		
5-GCF-10-A	1/2"	G	13076	694	675	20
5-GCF-10-B	1/2"	G	12334	655		
5-GLO-6-A	1/2"	G	14193	754	680	99
5-GLO-6-B	1/2"	G	14257	757		
5-GLO-6-C	1/2"	G	9686	514		
5-GLO-6-D	1/2"	G	13120	697		
6-GCW-11-A	0.6"	G	10571	468	766	298
6-GCW-11-B	0.6"	G	24053	1064		
6-GCH-6-A	0.6"	G	4000	177	204	27
6-GCH-6-B	0.6"	G	5222	231		

Table 5.3 Bond Test Results from Direct Tension Pullout Tests

Diameter	U'_1 ± S.D. Current	U'_p ± S.D. Brearly	U'_m ± S.D. Brearly	U' ± S.D. Deatherage
3/8"	7.88 ± 1.46	6.58 ± 0.83	7.47 ± 1.64	
7/16"	7.98 ± 1.14			
1/2"	3.94 ± 0.62	3.67 ± 0.55	3.81 ± 0.76	3.32 ± 0.28
0.5224"				3.91 ± 0.92
0.6"	5.63 ± 0.23	3.29 ± 0.30	3.33 ± 0.31	5.40 ± 0.41

Table 5.4 Bond Test Results Compared With Pretensioned Bond Tests

Diameter	U'_t ± S.D. Current	U'_s ± S.D. Cousins	U' ± S.D. Yu
3/8"	10.69 ± 0.75	16.68 ± 1.78	
7/16"	12.06 ± 2.34		
1/2"	6.19 ± 1.21	7.00 ± 1.04	6.18 ± 0.13
0.6"	6.48 ± 1.41	9.69 ± 0.65	

Table 5.5 Summary of Slip Results for Shear Tests (all shear values at h/2)

Girder	Shear when First Strand Slipped (kips) (1)	Shear at All Strands Slipped (kips) (2)	Shear at Failure (kips) (3)
R-8-N	197	263	275
R-10-N	251	-2	281
R-12-N	213	249	277
2R-8-N	208	226	233
2R-10-N	183	217	238
2R-12-N	198	256	277
R-8-S	233	280	300
R-10-S	213	276	297
R-12-S	225	225	274
2R-8-S	233	247	254
2R-10-S	203	243	243
2R-12-S	228	259	285

Table 5.6 Test Shear and PredictedShear Values
(all shear values taken at h/2 as specified by 1989 AASHTO)

Girder	Support to Load (ft.)	Span (ft.)	Test Shear (kips)	Predicted Values: 1989 AASHTO (kips)	Predicted Values: ACI (kips)	Predicted Values: 1994 LRFD AASHTO (kips)	Predicted Shear / Test Shear: 1989 AASHTO	Predicted Shear / Test Shear: ACI	Predicted Shear / Test Shear: 1994 LRFD AASHTO
R-8-N	8.5	40	275	311	263	252	1.13	0.96	0.92
R-10-N	8.5	40	281	320	276	256	1.14	0.98	0.91
R-12-N	8.5	40	277	327	281	257	1.18	1.01	0.93
R-8-S	7.08	27.5	300	310	263	252	1.03	0.88	0.84
R-10-S	7.08	27.5	297	320	276	254	1.08	0.93	0.86
R-12-S	7.08	27.5	274	326	281	256	1.19	1.03	0.93
						Average	1.13	0.96	0.90

Girder	Support to Load (ft.)	Span (ft.)	Test Shear (kips)	Predicted Values: 1989 AASHTO (kips)	Predicted Values: ACI (kips)	Predicted Values: 1994 LRFD AASHTO (kips)	Predicted Shear / Test Shear: 1989 AASHTO	Predicted Shear / Test Shear: ACI	Predicted Shear / Test Shear: 1994 LRFD AASHTO
2R-8-N	8.5	40	233	323	276	381	1.39	1.18	1.64
2R-10-N	8.5	40	238	354	305	410	1.49	1.28	1.72
2R-12-N	8.5	40	277	367	322	413	1.32	1.16	1.49
2R-8-S	7.08	27.5	254	322	276	383	1.27	1.09	1.51
2R-10-S	7.08	27.5	243	353	305	414	1.45	1.26	1.70
2R-12-S	7.08	27.5	285	367	322	415	1.29	1.13	1.46
						Average	1.37	1.18	1.59

Table 5.7 Test Shear and PredictedShear Values
(all shear values taken at dv as specified by 1994 LRFD AASHTO)

Girder	Support to Load (ft.)	Span (ft.)	Test Shear (kips)	Predicted Values 1989 AASHTO (kips)	ACI (kips)	1994 LRFD AASHTO (kips)	Predicted Shear / Test Shear 1989 AASHTO	ACI	1994 LRFD AASHTO
R-8-N	8.5	40	275	311	263	254	1.13	0.96	0.92
R-10-N	8.5	40	281	322	276	263	1.15	0.98	0.94
R-12-N	8.5	40	276	327	281	280	1.18	1.02	1.01
R-8-S	7.08	27.5	300	310	263	268	1.03	0.88	0.89
R-10-S	7.08	27.5	297	320	276	275	1.08	0.93	0.93
R-12-S	7.08	27.5	273	326	281	280	1.19	1.03	1.03
						Average	1.13	0.97	0.95

Girder	Support to Load (ft.)	Span (ft.)	Test Shear (kips)	Predicted Values 1989 AASHTO (kips)	ACI (kips)	1994 LRFD AASHTO (kips)	Predicted Shear / Test Shear 1989 AASHTO	ACI	1994 LRFD AASHTO
2R-8-N	8.5	40	233	324	276	383	1.39	1.18	1.64
2R-10-N	8.5	40	237	355	305	410	1.50	1.29	1.73
2R-12-N	8.5	40	277	369	322	413	1.33	1.16	1.49
2R-8-S	7.08	27.5	253	323	276	383	1.28	1.09	1.51
2R-10-S	7.08	27.5	242	354	305	410	1.46	1.26	1.69
2R-12-S	7.08	27.5	284	367	322	416	1.29	1.13	1.46
						Average	1.38	1.19	1.59

Table 5.8 Test Shear and Strut and Tie Predicted Shear

Girder	F'c (psi)	Support to Load (ft.)	Span (ft.)	Test Shear at Load (kips)	Predicted Shear (kips)	Predicted / Test
R-8-N	8150	8.5	40	270	181.3	0.67
R-10-N	10130	8.5	40	277	225.4	0.81
R-12-N	11040	8.5	40	272	245.6	0.90
2R-8-N	8120	8.5	40	228	180.6	0.79
2R-10-N	9910	8.5	40	233	220.5	0.95
2R-12-N	11040	8.5	40	273	245.6	0.90
R-8-S	8150	7.08	27	296	214.0	0.72
R-10-S	10130	7.08	27	293	265.9	0.91
R-12-S	11040	7.08	27	270	289.8	1.07
2R-8-S	8120	7.08	27	250	213.2	0.85
2R-10-S	9910	7.08	27	239	260.2	1.09
2R-12-S	11040	7.08	27	281	289.8	1.03
					Average	0.89

Table 5.9 Slope of Moment VS Deflection Plots

Girder	Slope 1 (k-ft/in)	Slope 2 (k-ft/in)
R-8-N	2979	627
R-10-N	3500	696
R-12-N	3415	660
2R-8-N	2917	743
2R-10-N	3111	680
2R-12-N	3111	628
R-8-S	4000	800
R-10-S	4516	1050
R-12-S	4828	857
2R-8-S	4590	1484
2R-10-S	4667	1573
2R-12-S	5283	1167

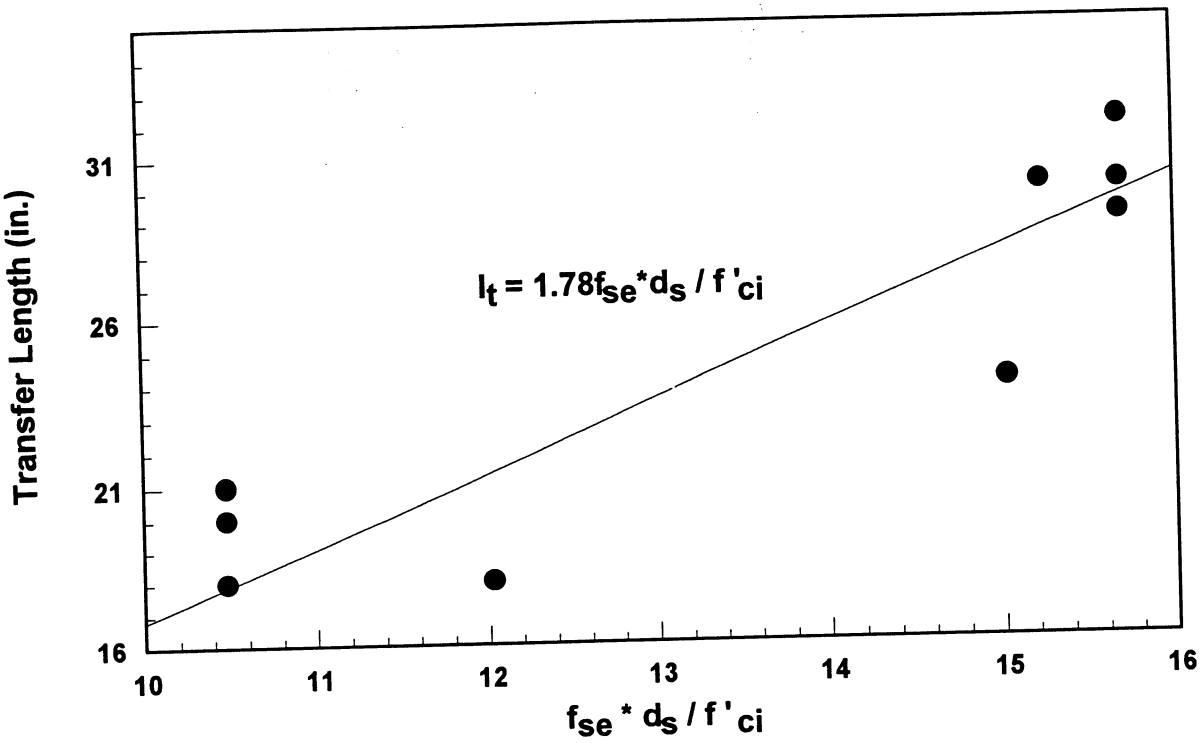

Figure 5.1 Transfer Length Regression Results

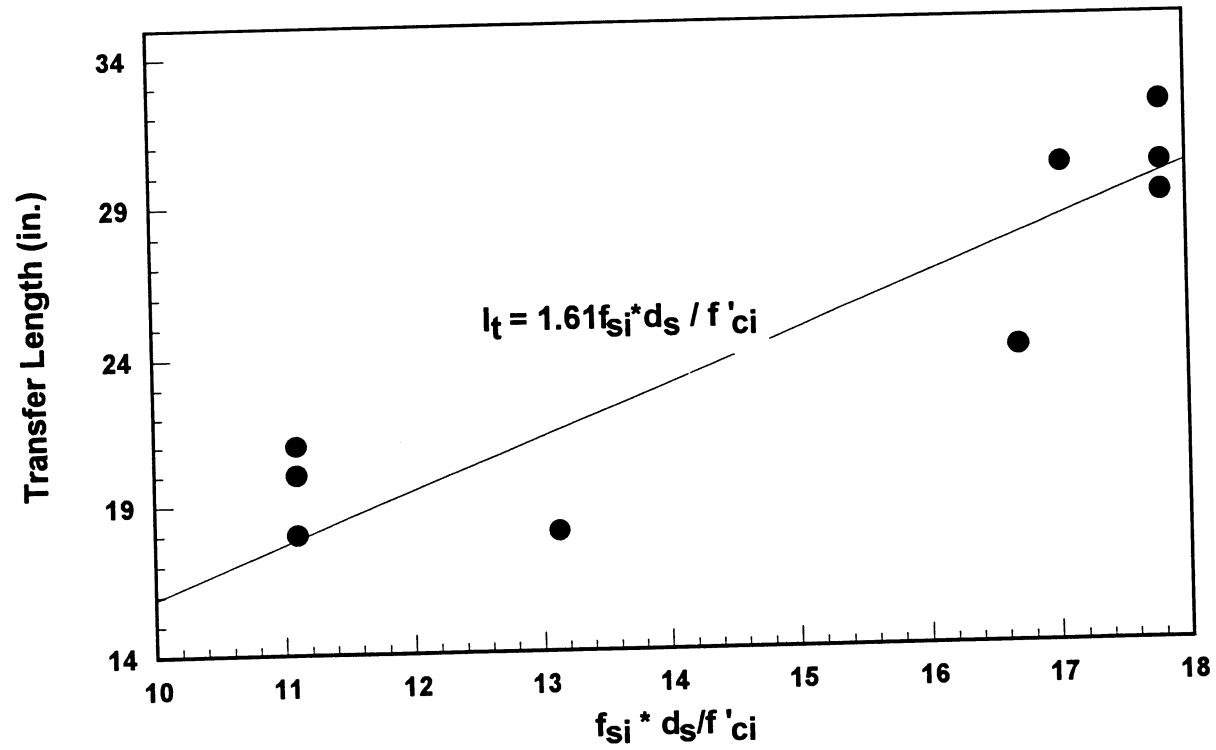

Figure 5.2 Transfer Length Regression Results

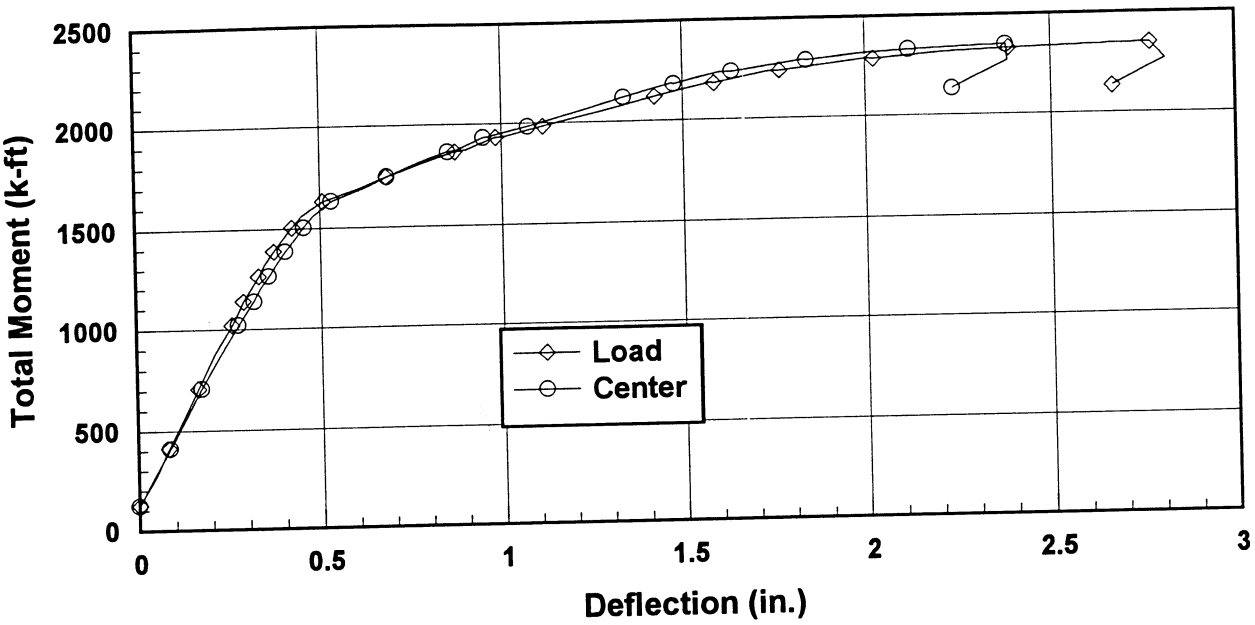

Figure 5.3 Total Moment vs. Deflection for Girder R-8-N

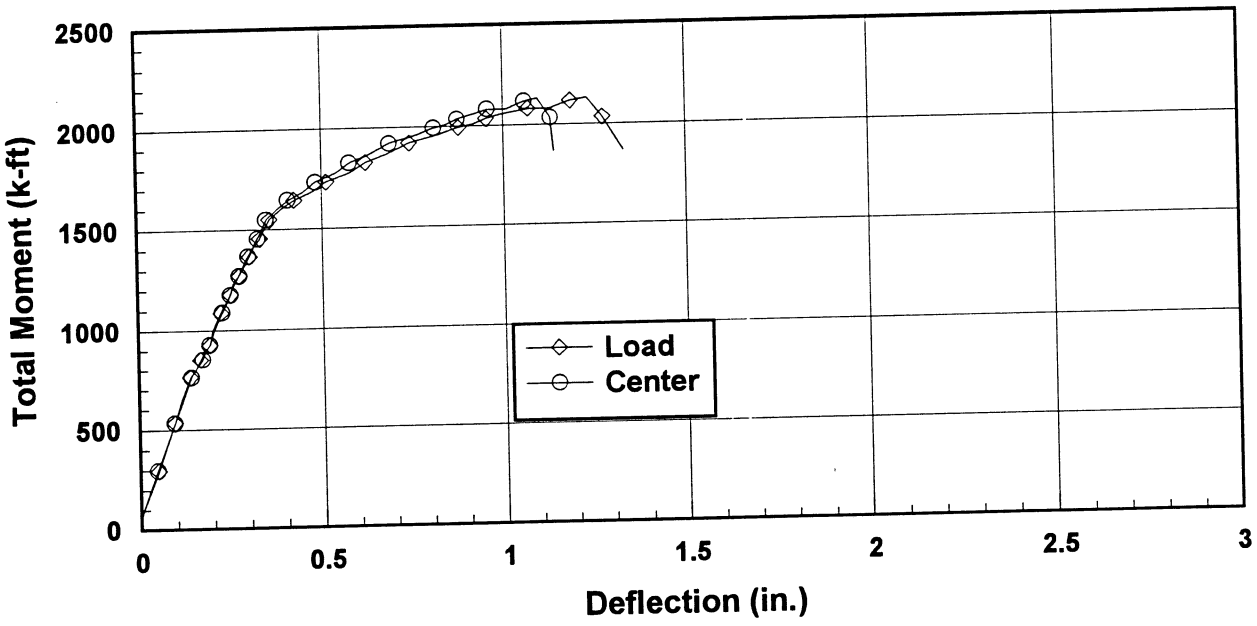

Figure 5.4 Total Moment vs. Deflection for Girder R-8-S

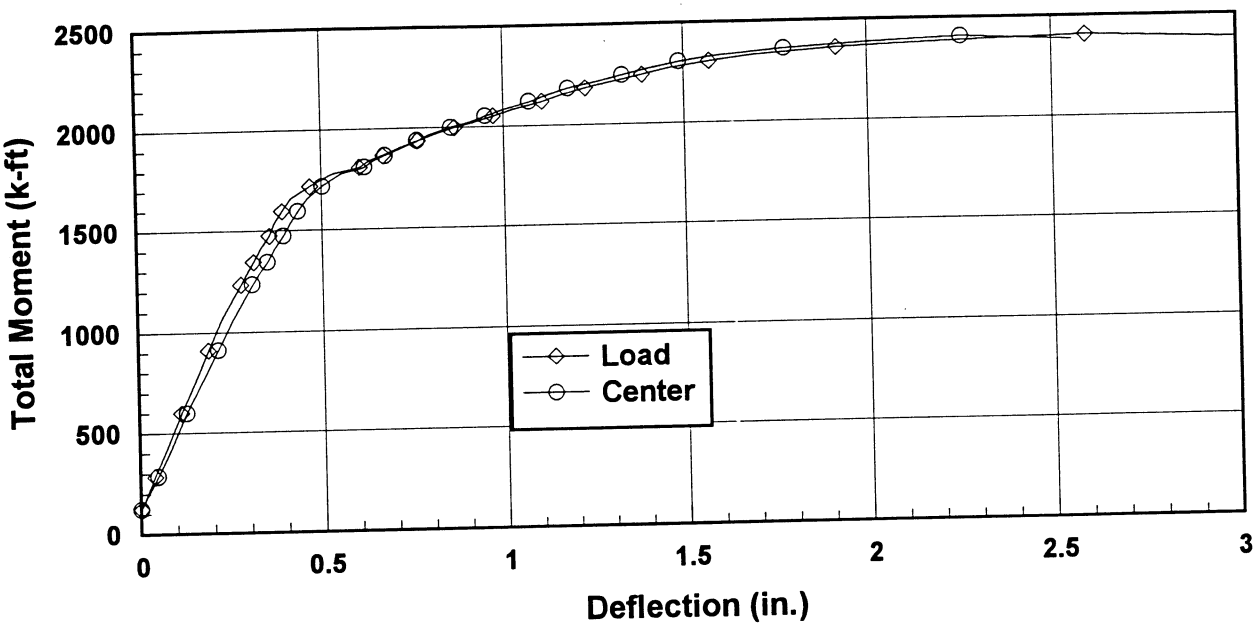

Figure 5.5 Total Moment vs. Deflection for Girder R-10-N

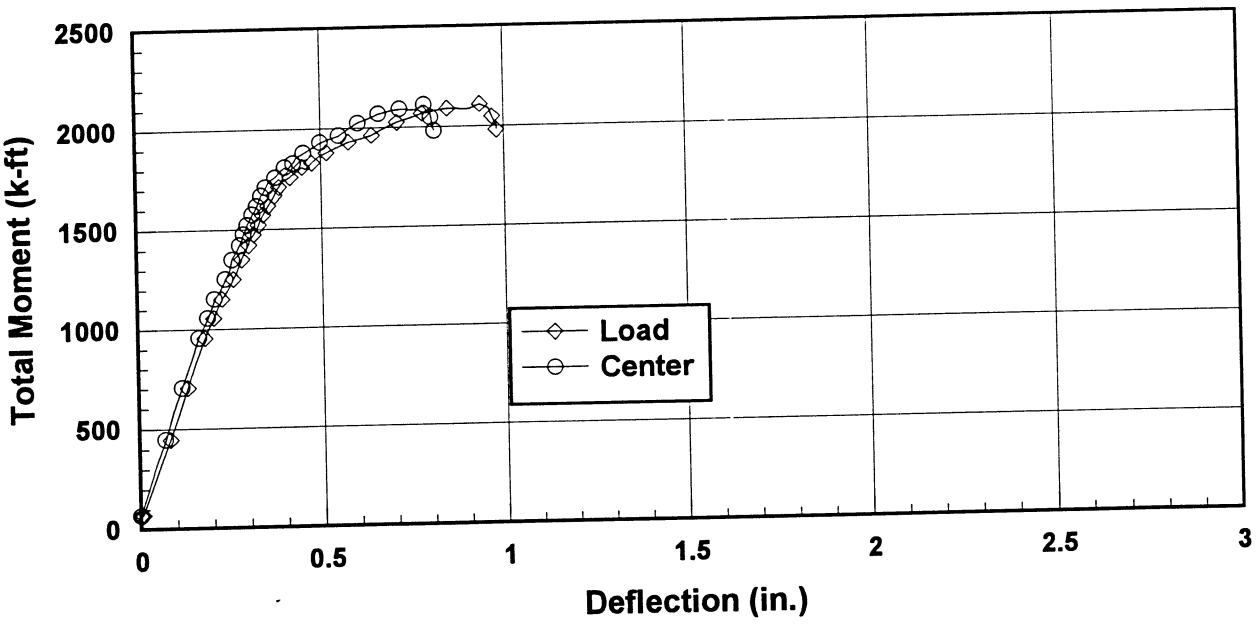

Figure 5.6 Total Moment vs. Deflection for Girder R-10-S

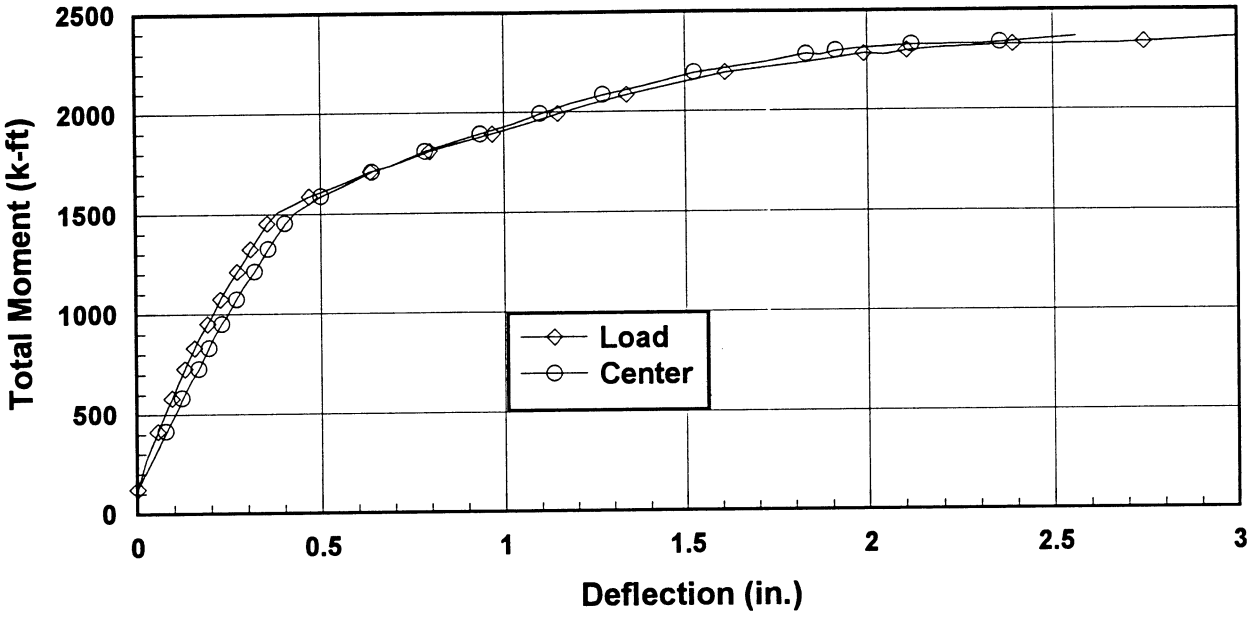

Figure 5.7 Total Moment vs. Deflection for Girder R-12-N

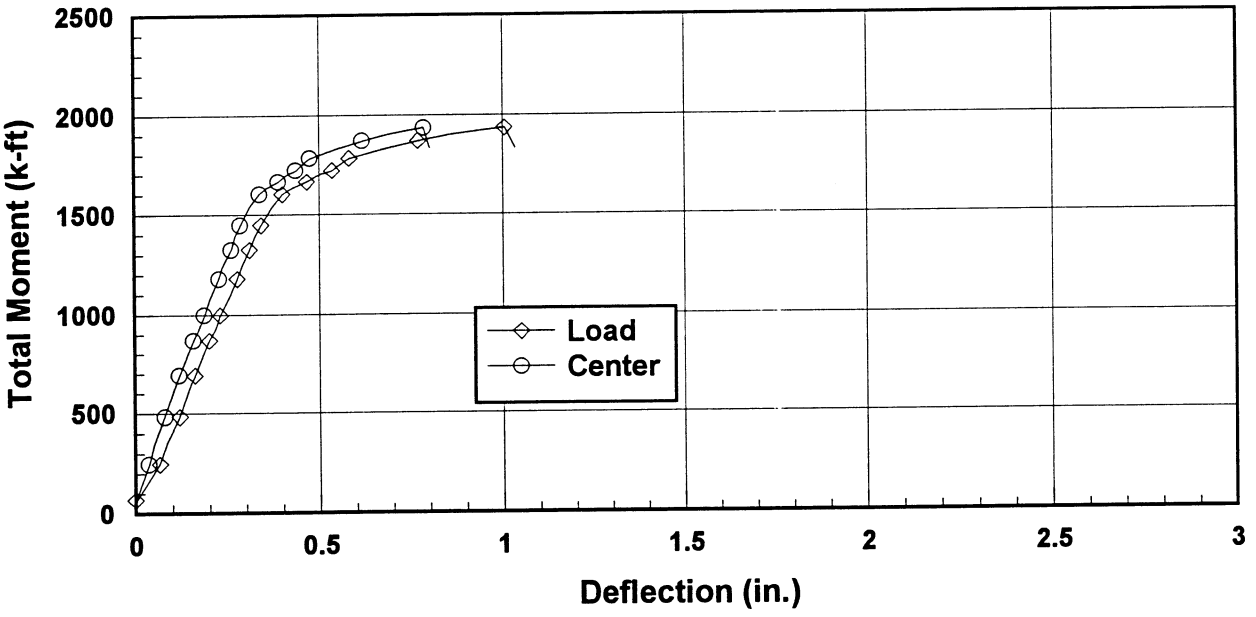

Figure 5.8 Total Moment vs. Deflection for Girder R-12-S

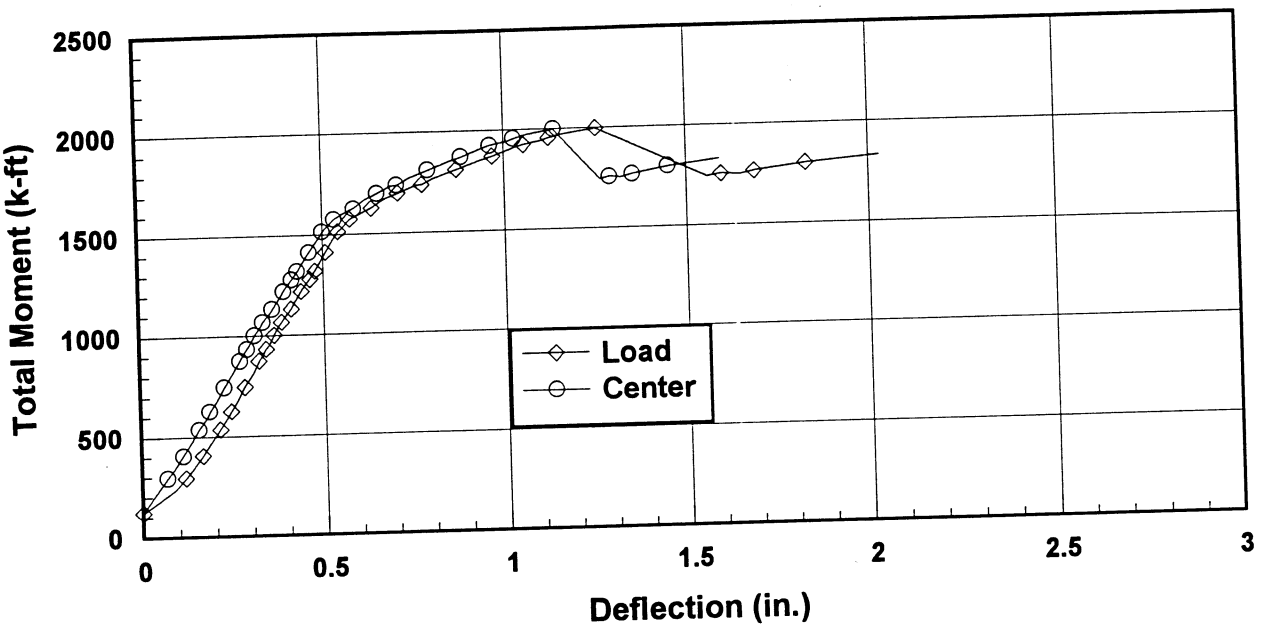

Figure 5.9 Total Moment vs. Deflection for Girder 2R-8-N

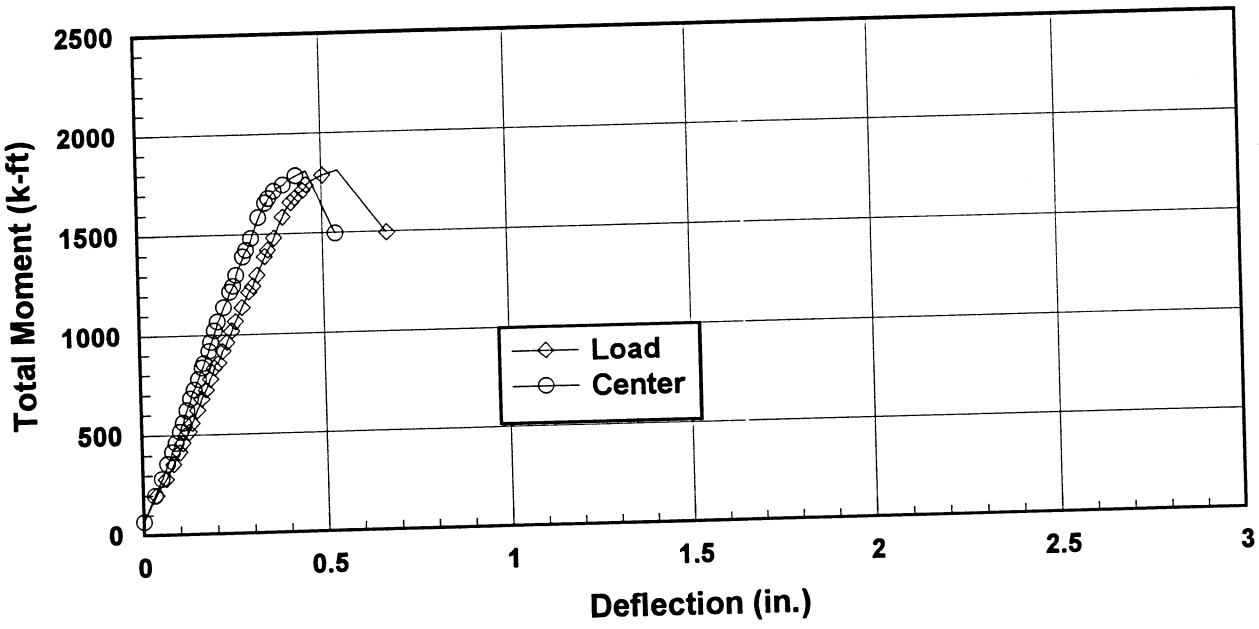

Figure 5.10 Total Moment vs. Deflection for Girder 2R-8-S

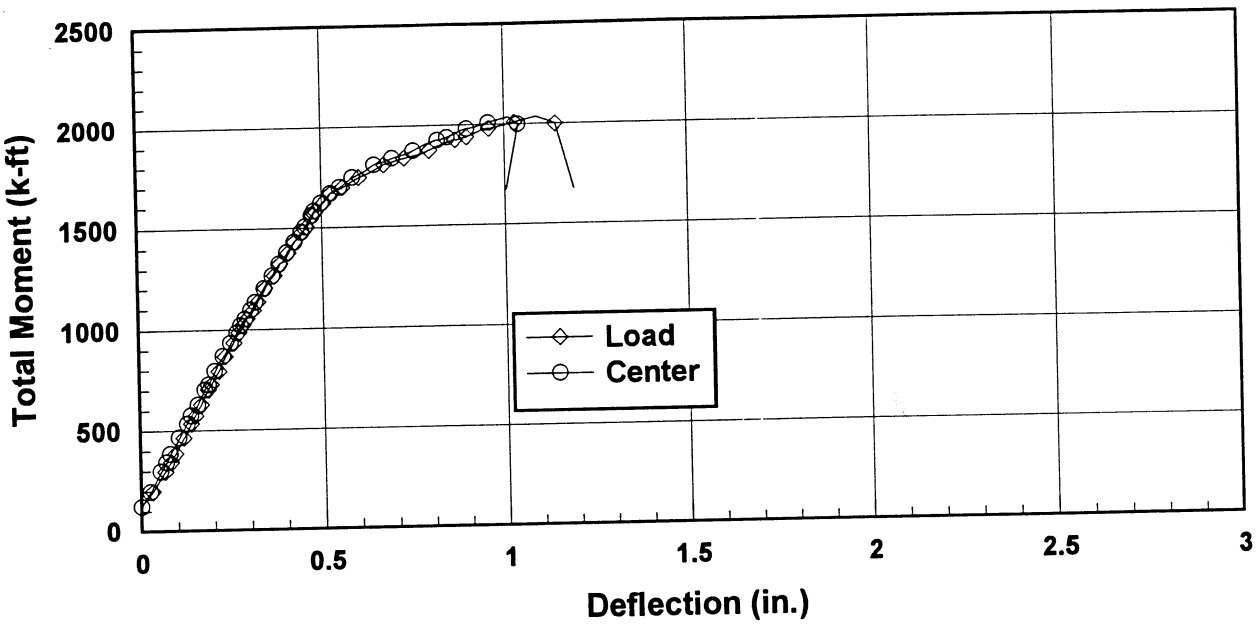

Figure 5.11 Total Moment vs. Deflection for Girder 2R-10-N

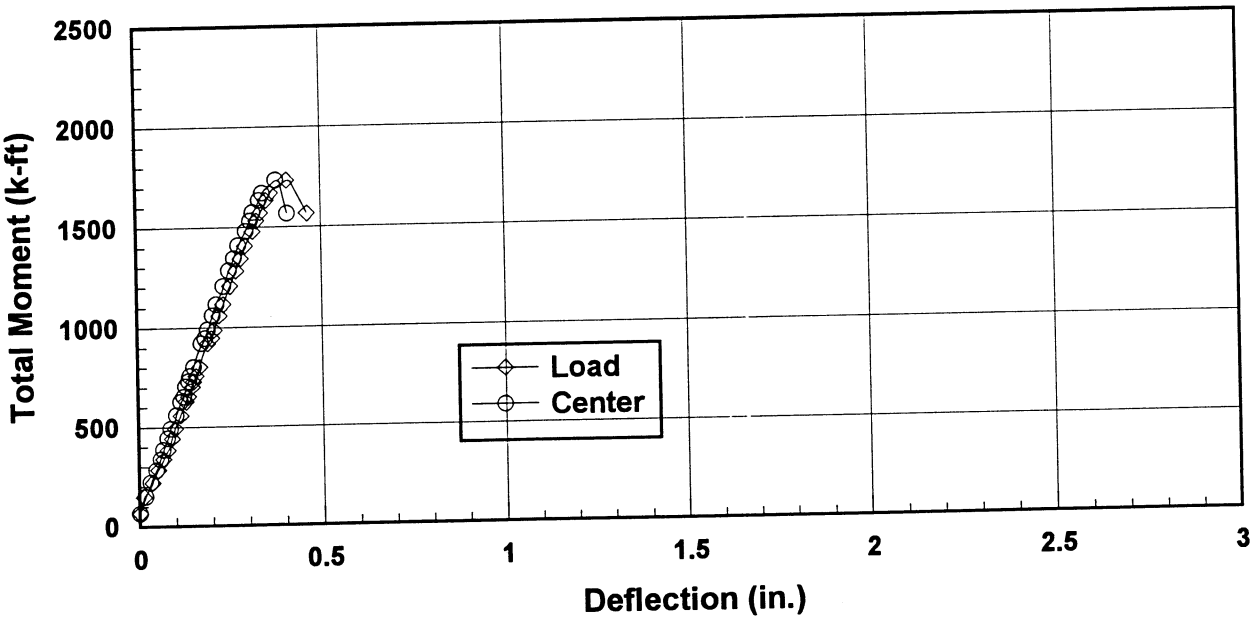

Figure 5.12 Total Moment vs. Deflection for Girder 2R-10-S

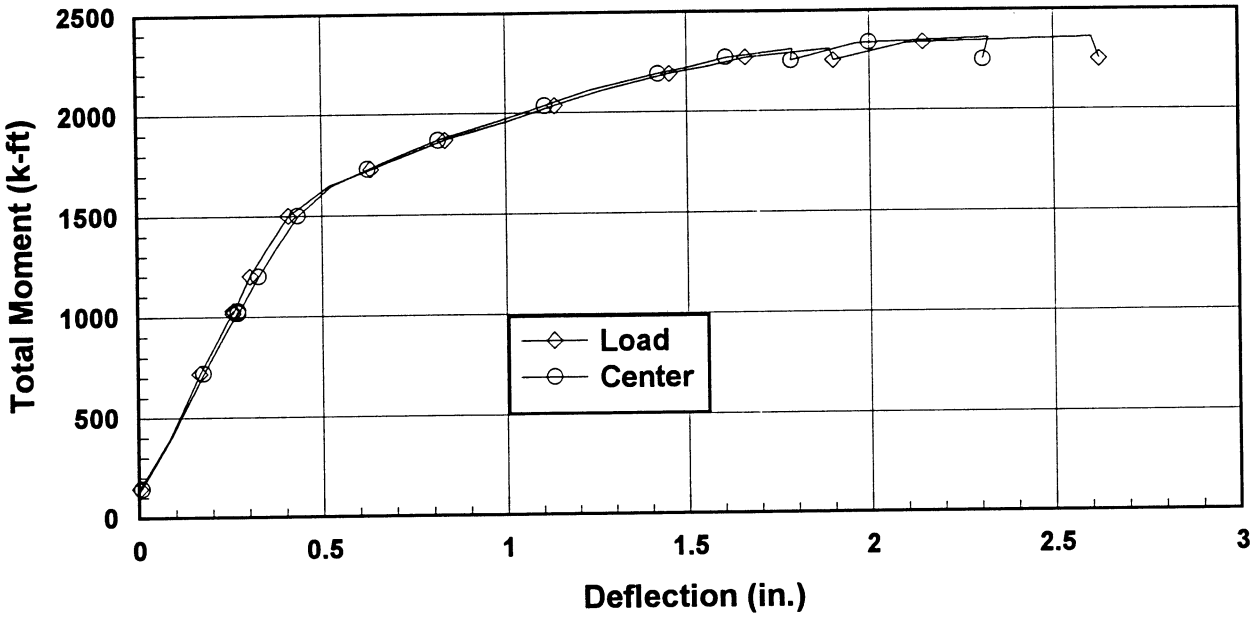

Figure 5.13 Total Moment vs. Deflection for Girder 2R-12-N

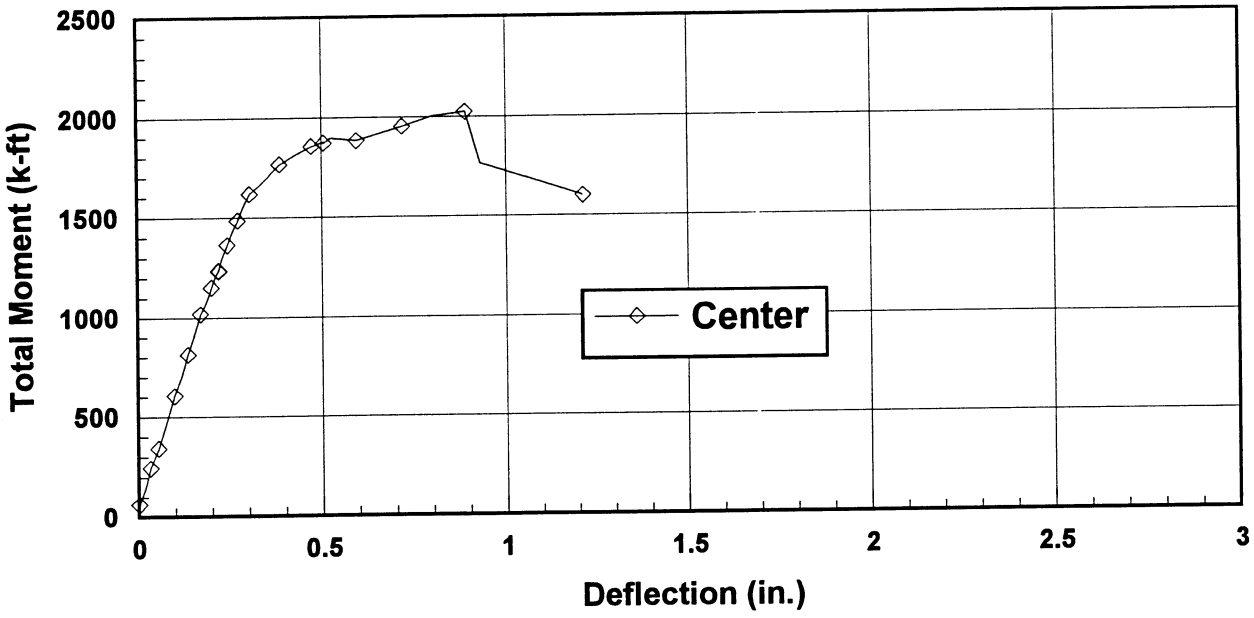

Figure 5.14 Total Moment vs. Deflection for Girder 2R-12-S

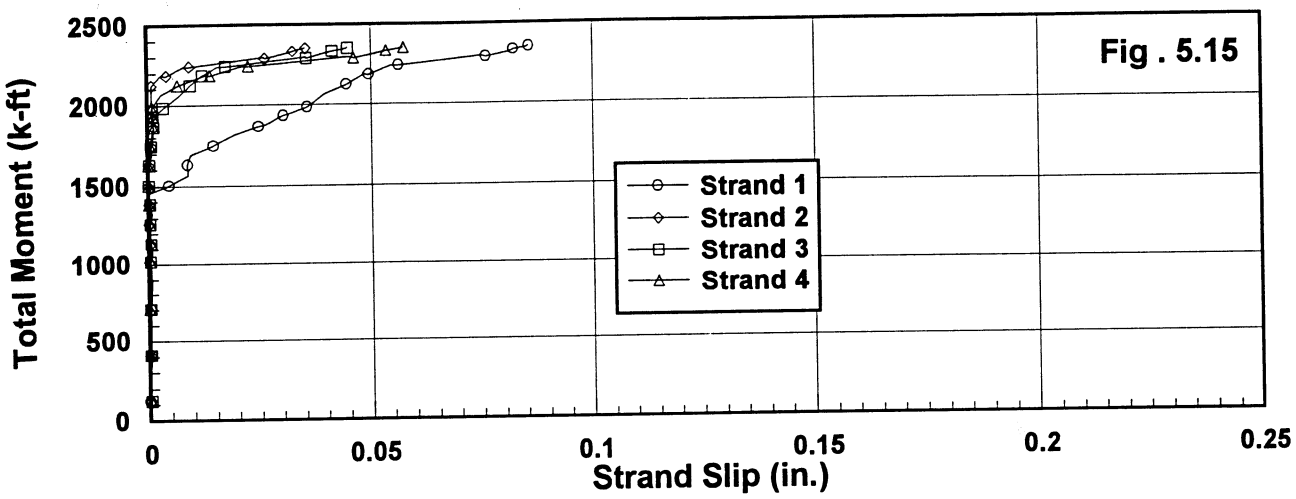

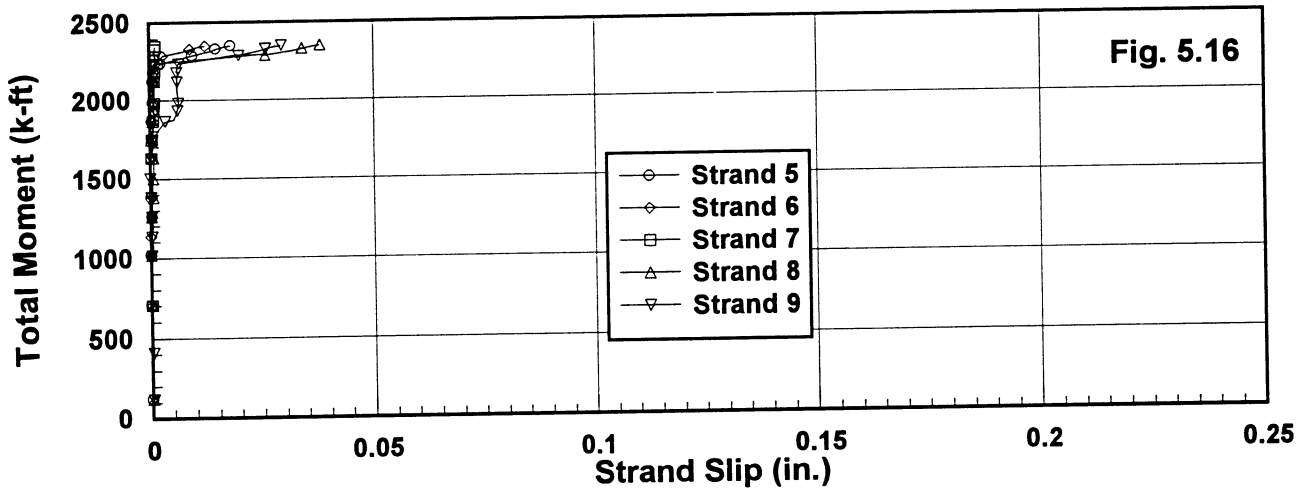

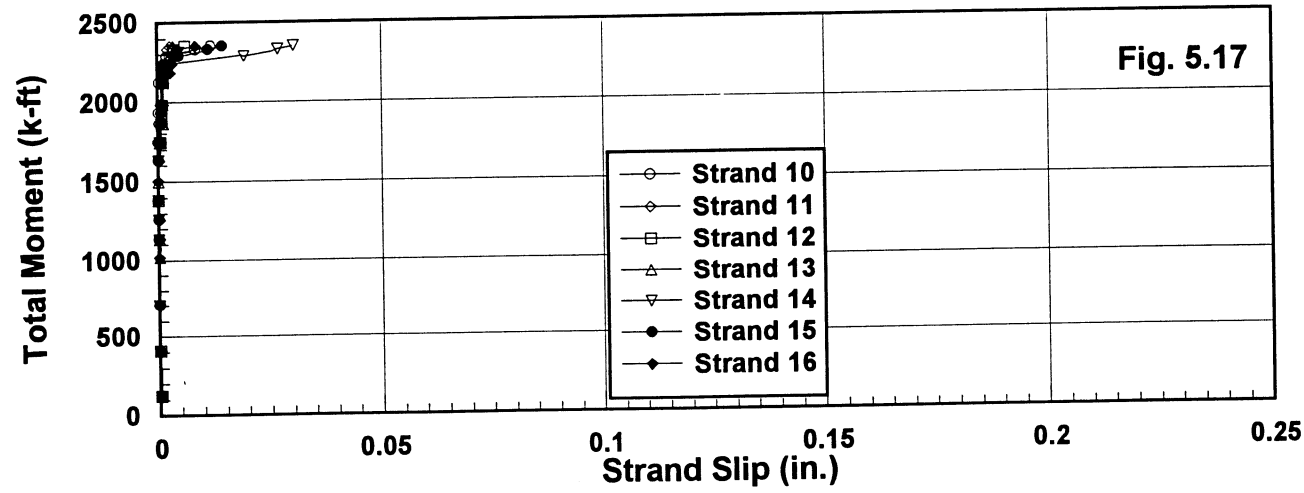

Figures 5.15 to 5.17 Total Moment vs Slip for Girder R-8-N

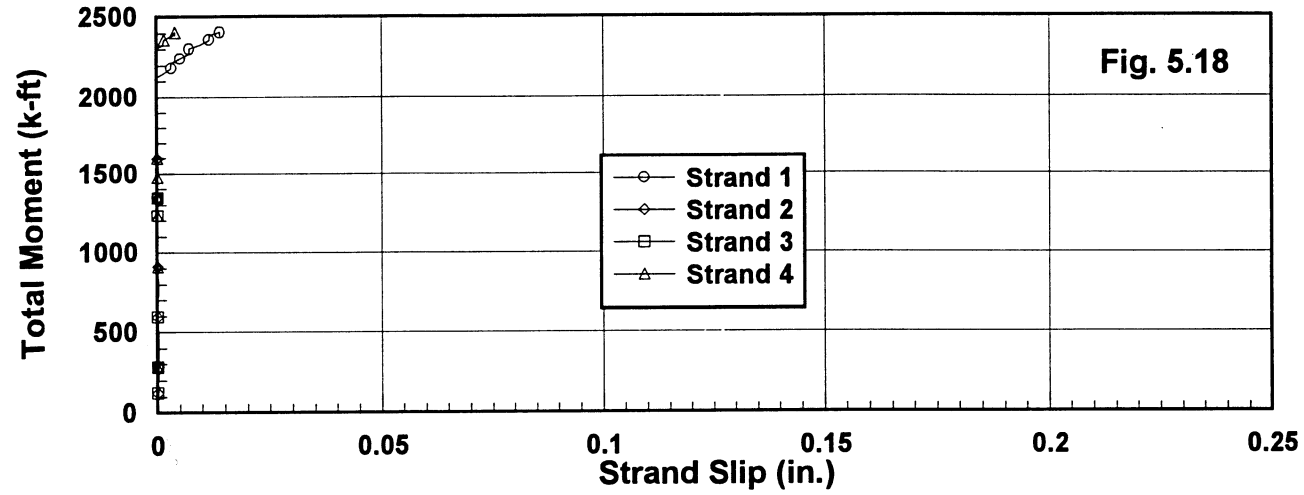

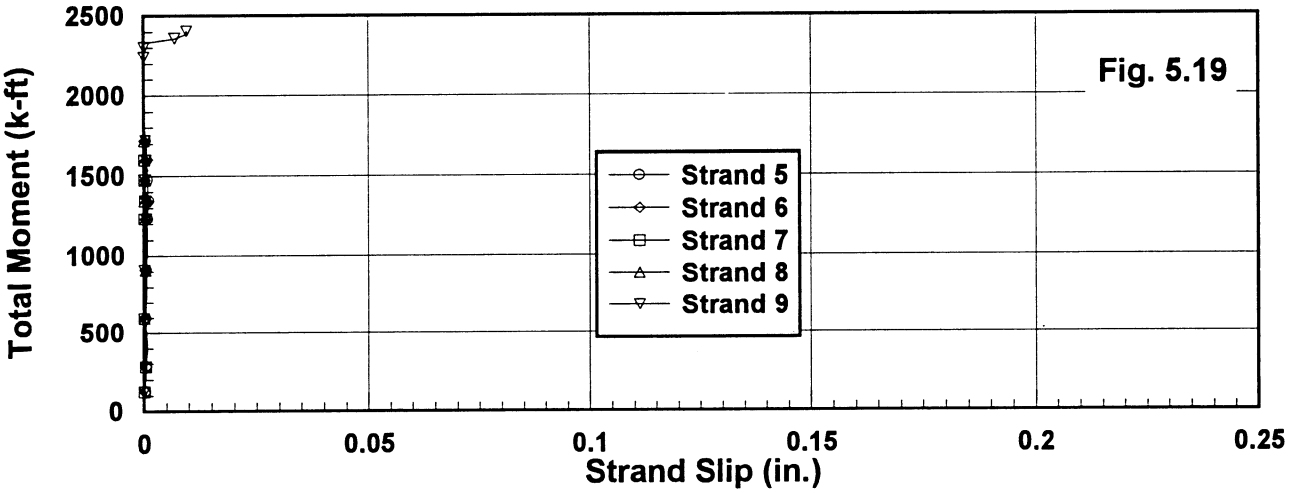

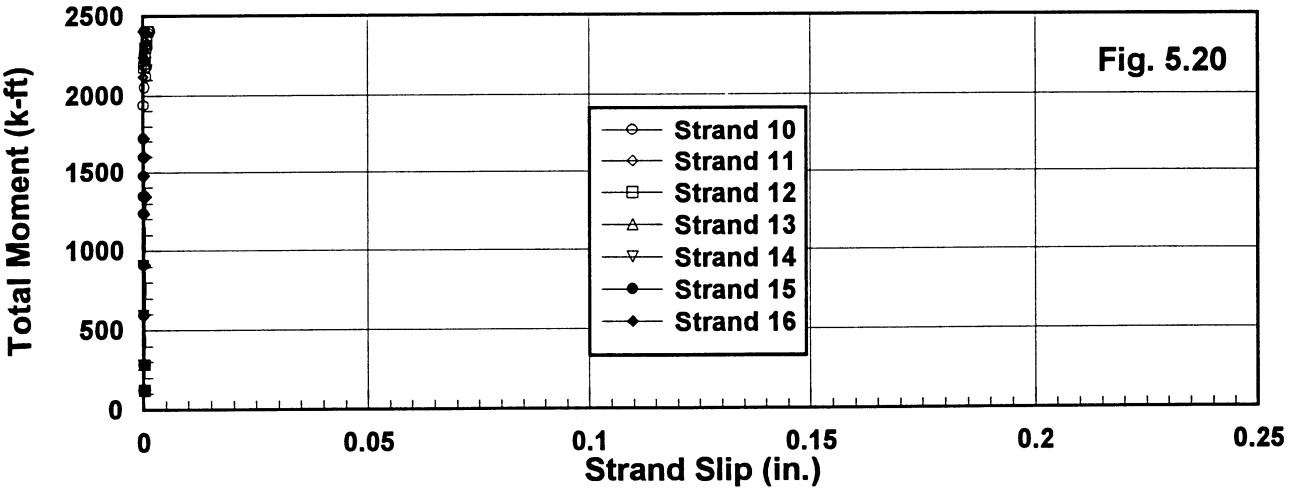

Figures 5.18 to 5.20 Total Moment vs Slip for Girder R-10-N

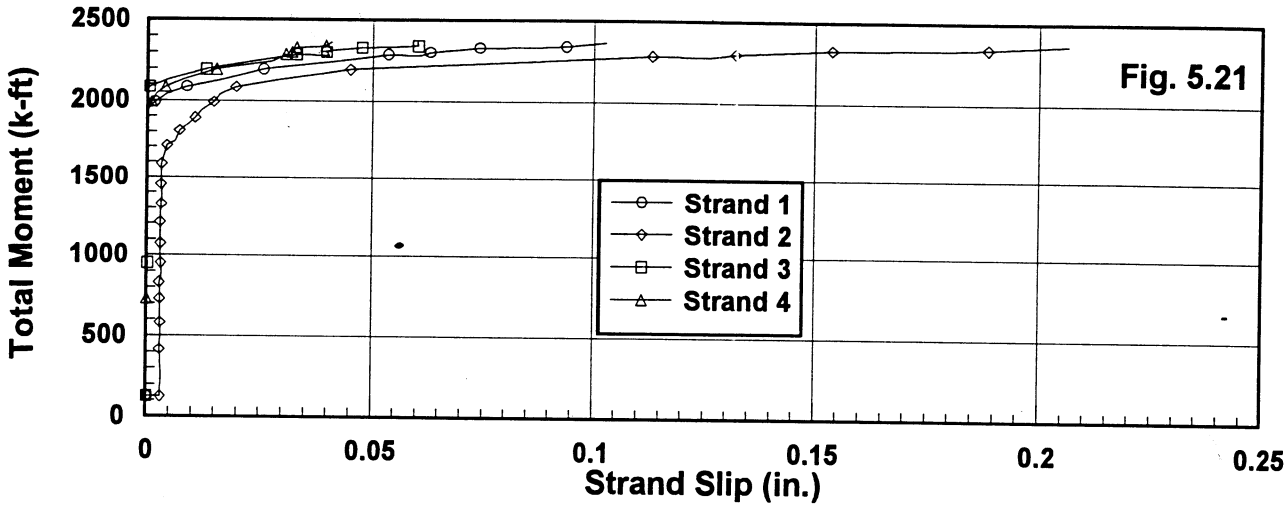

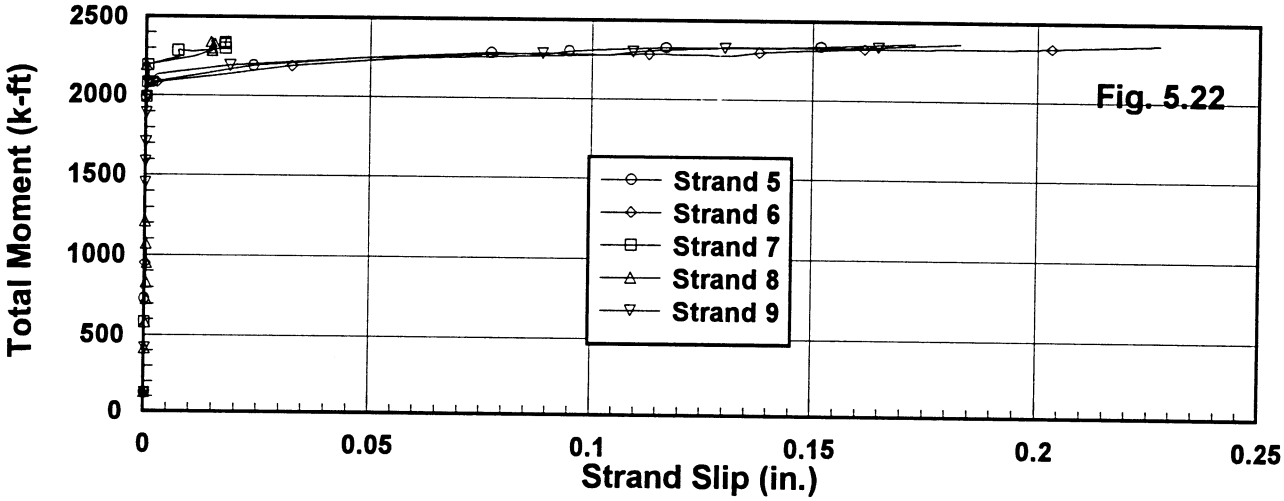

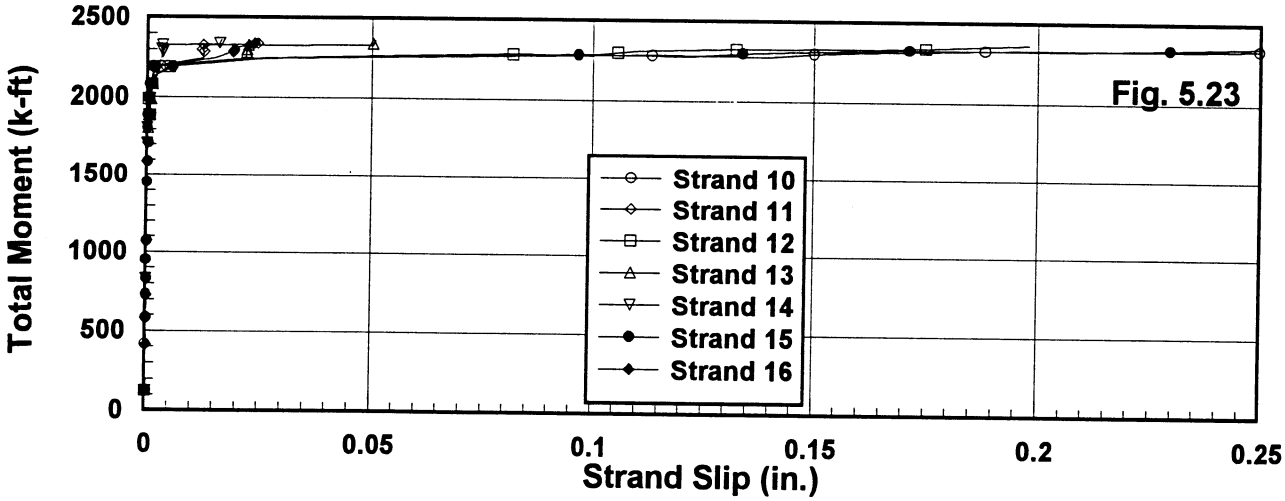

Figures 5.21 to 5.23 Total Moment vs Slip for Girder R-12-N

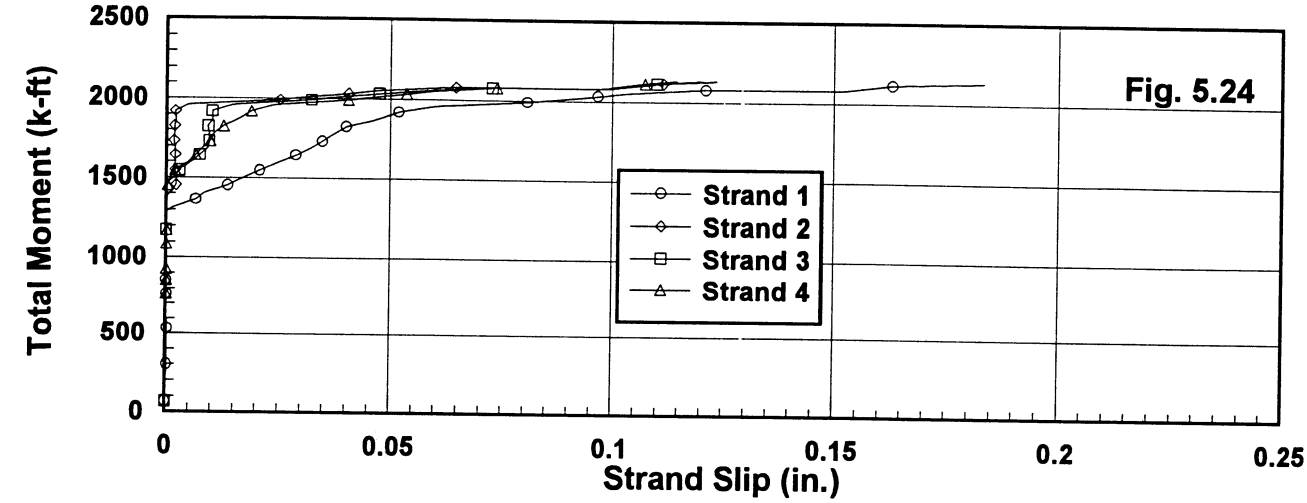

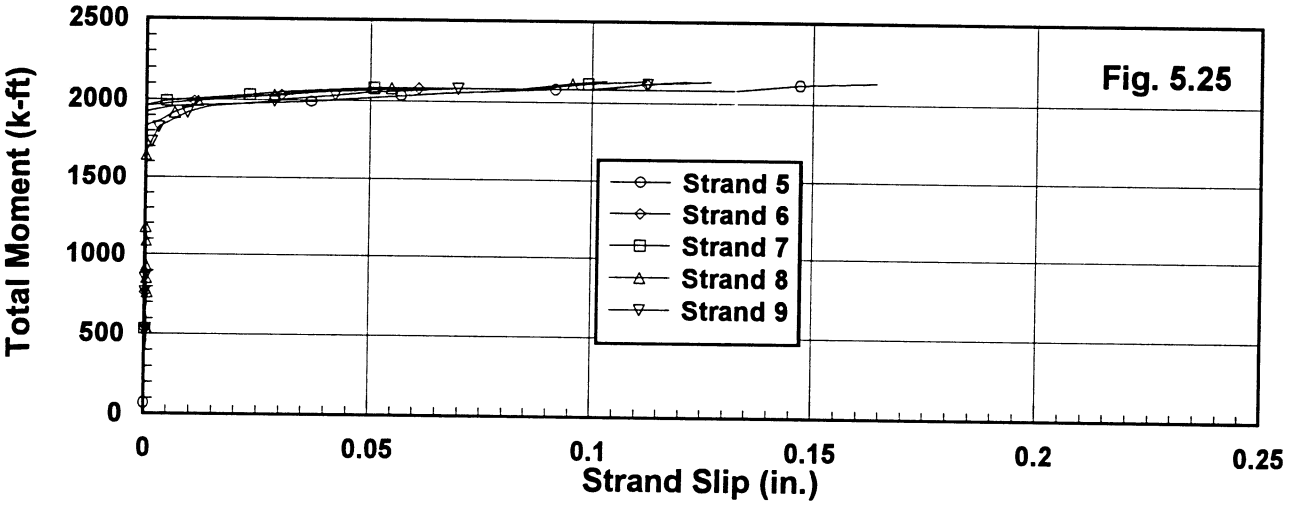

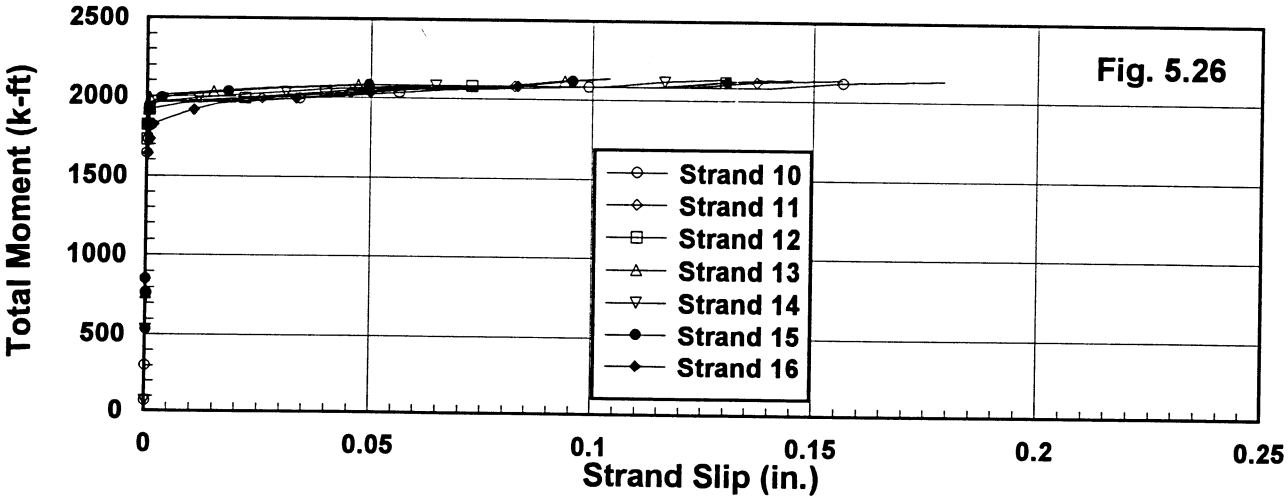

Figures 5.24 to 5.26 Total Moment vs Slip for Girder R-8-S

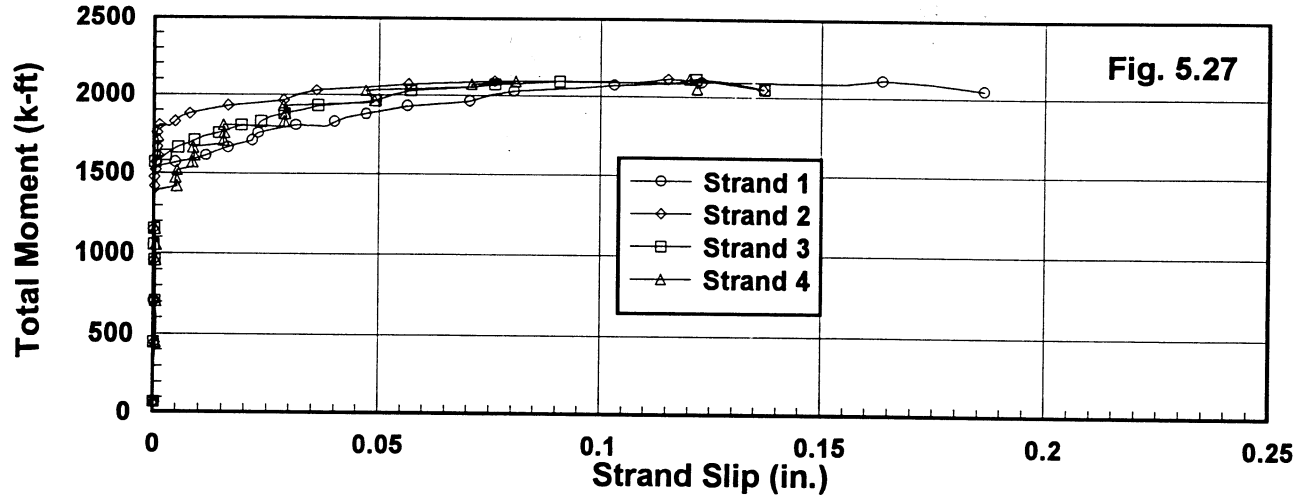

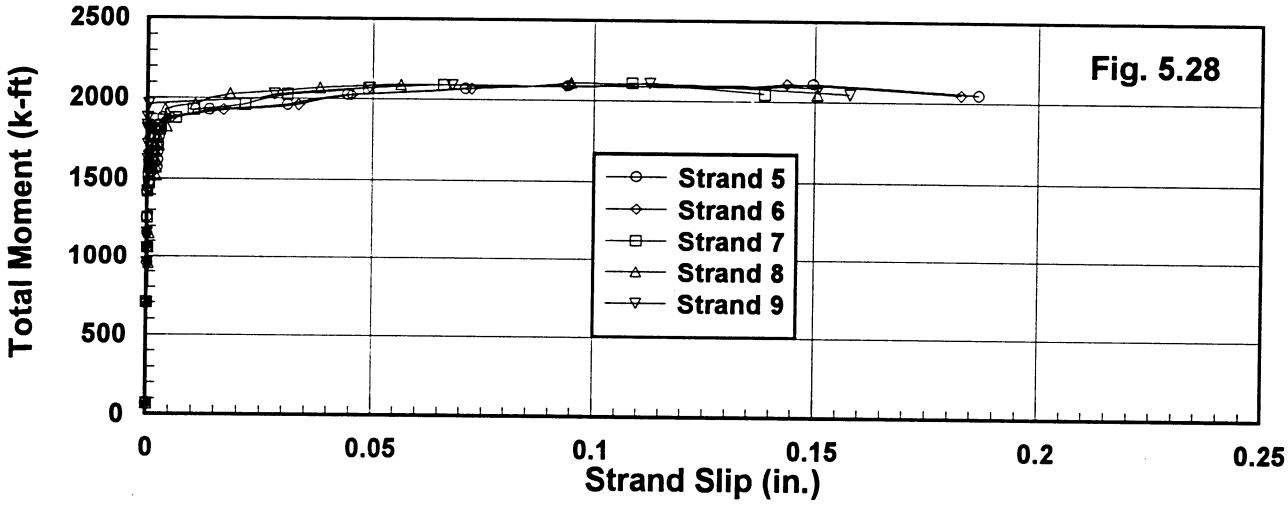

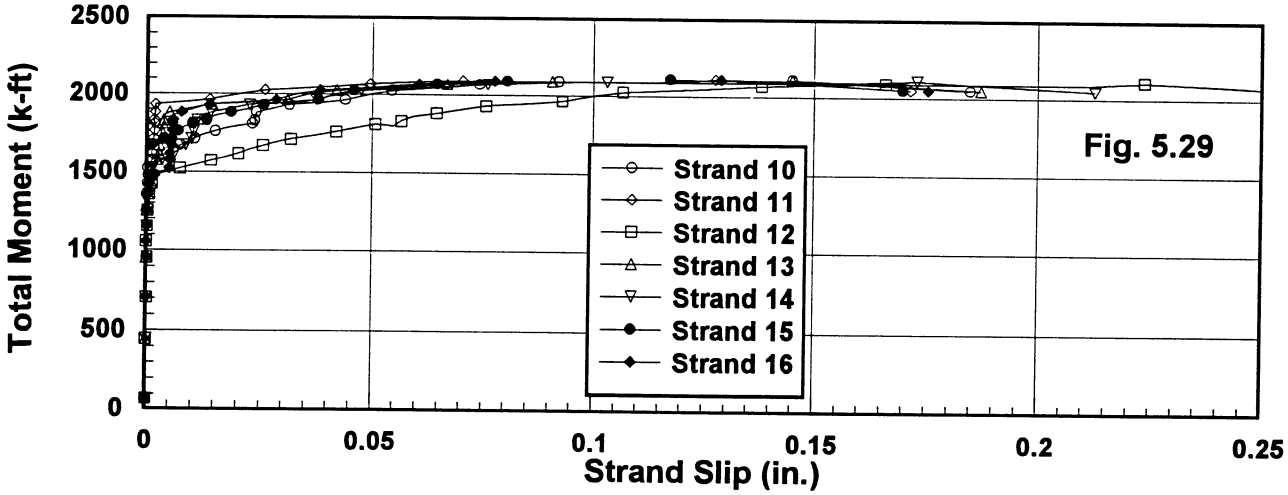

Figures 5.27 to 5.29 Total Moment vs Slip for Girder R-10-S

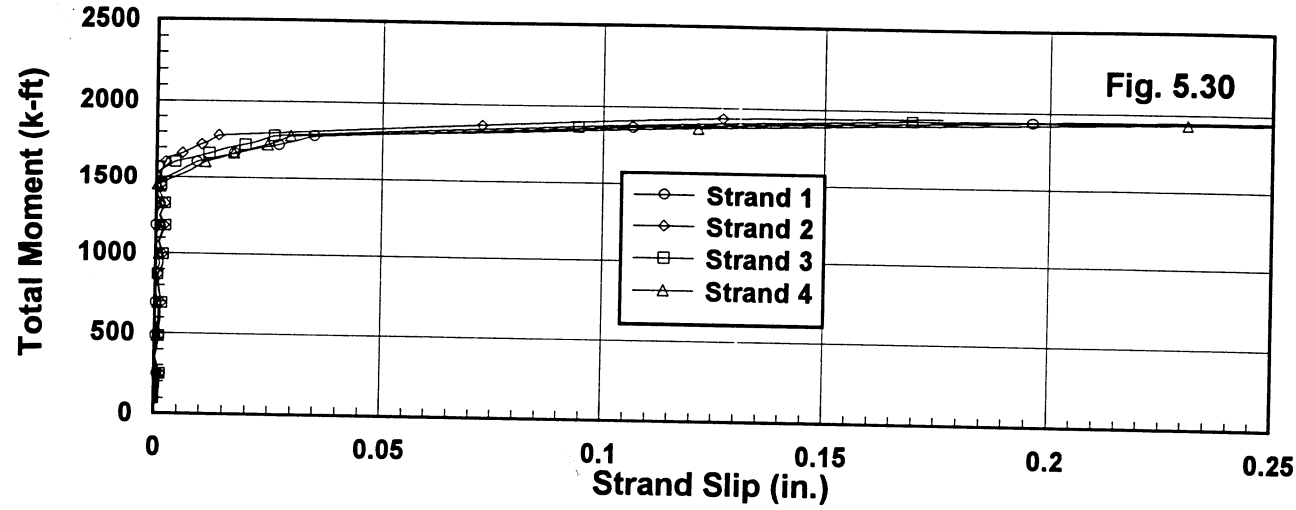

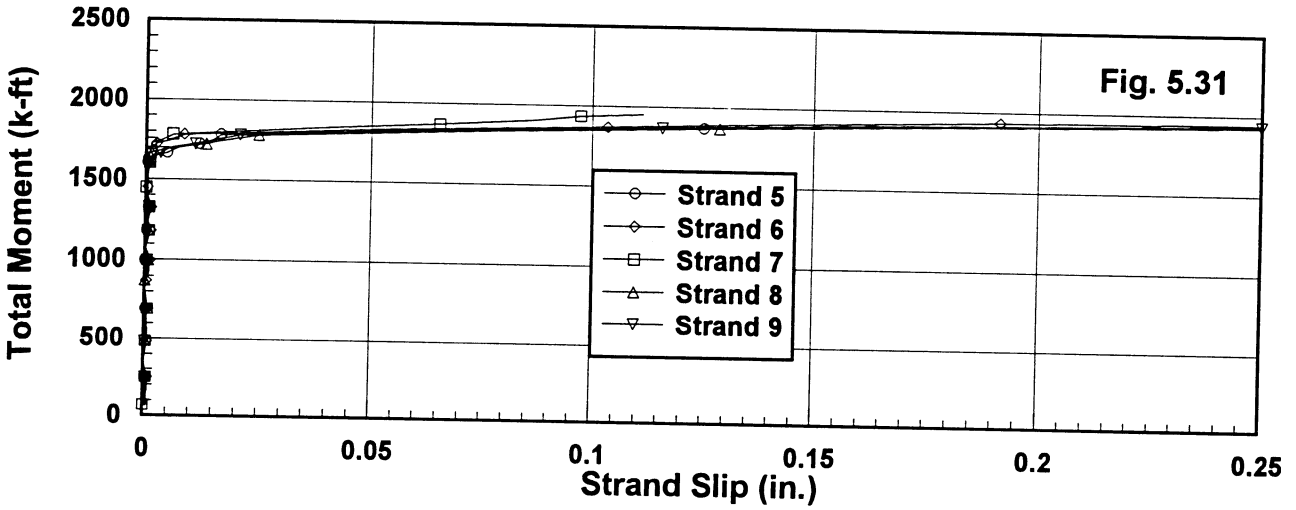

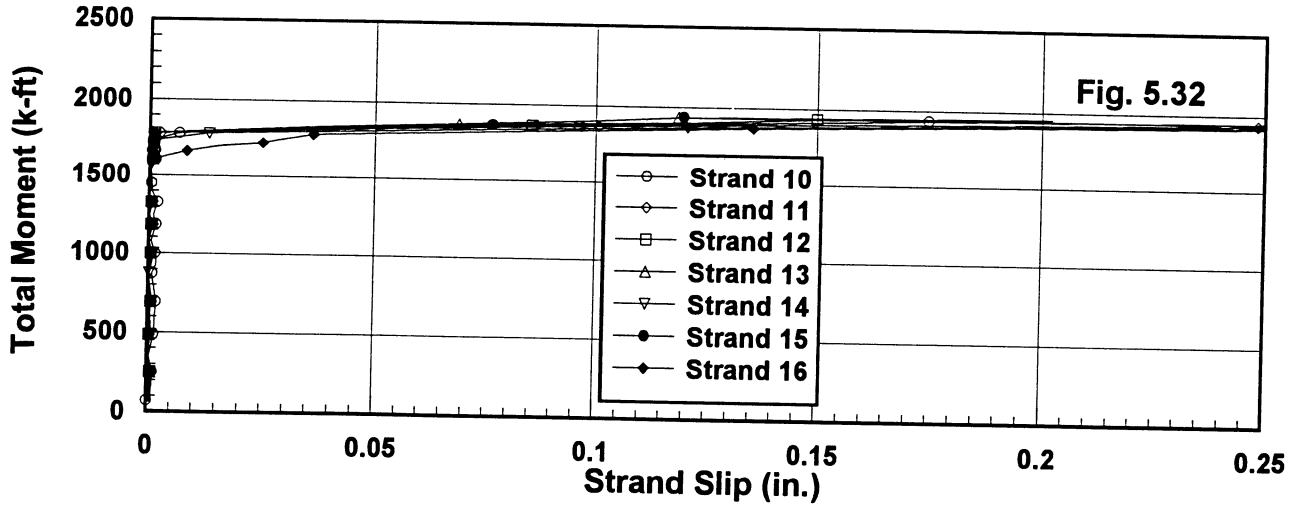

Figures 5.30 to 5.32 Total Moment vs Slip for Girder R-12-S

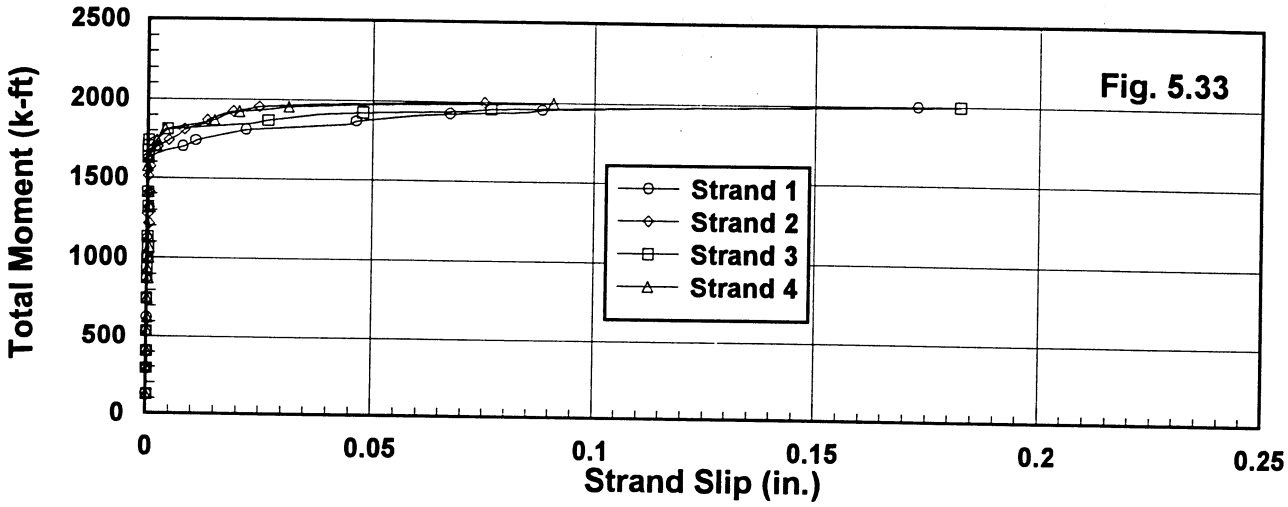

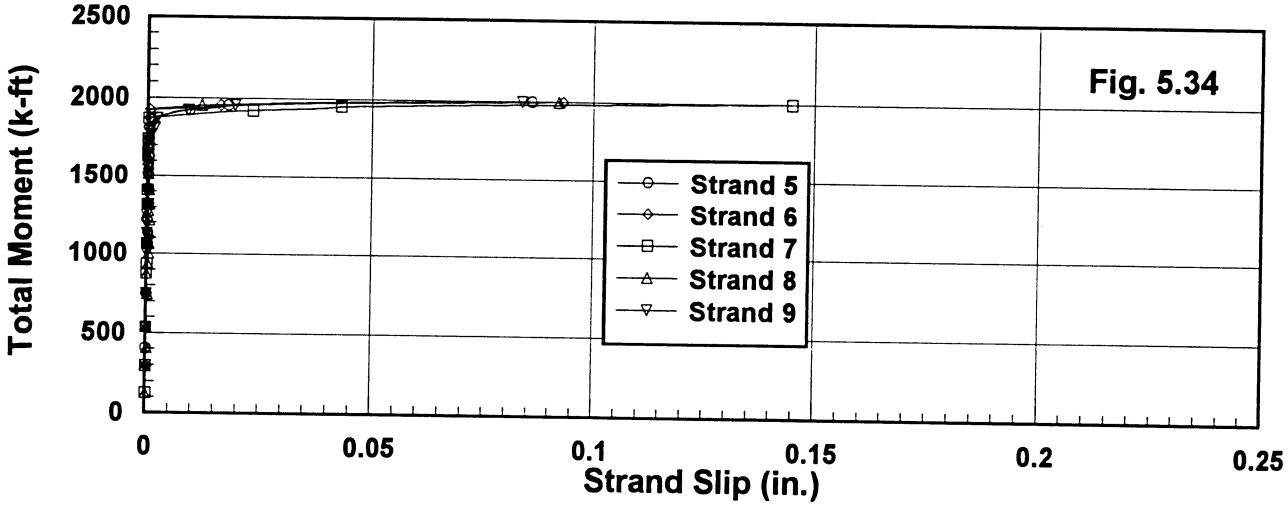

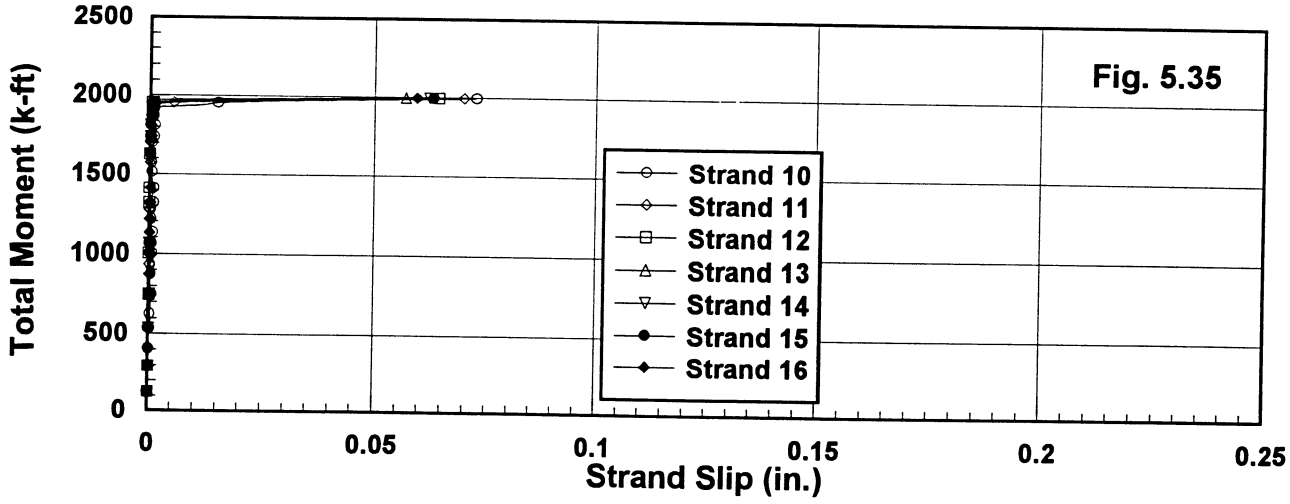

Figures 5.33 to 5.35 Total Moment vs Slip for Girder 2R-8-N

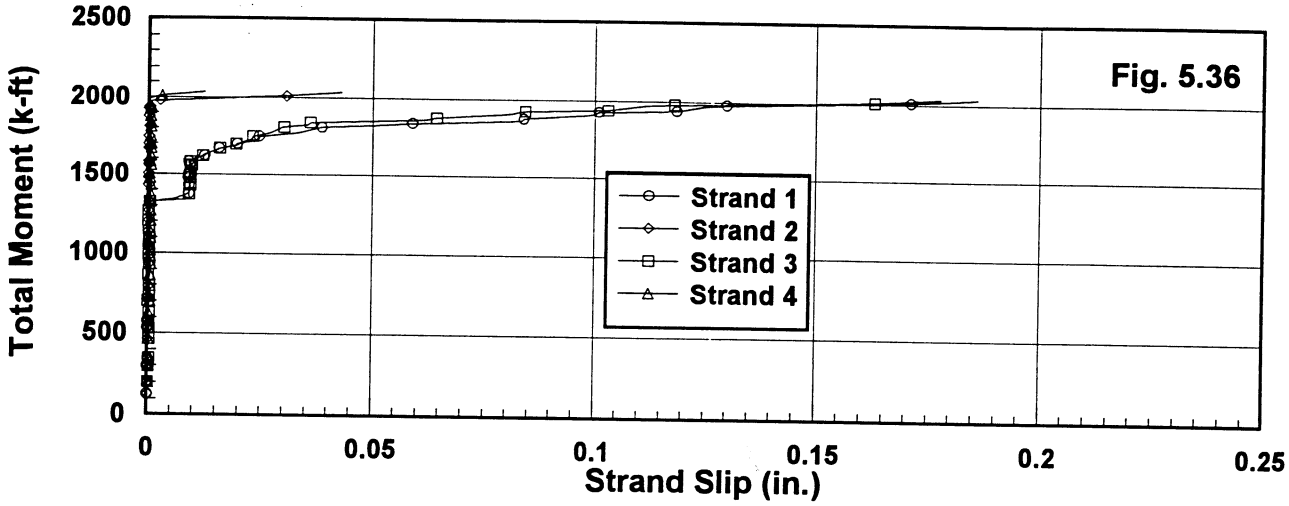

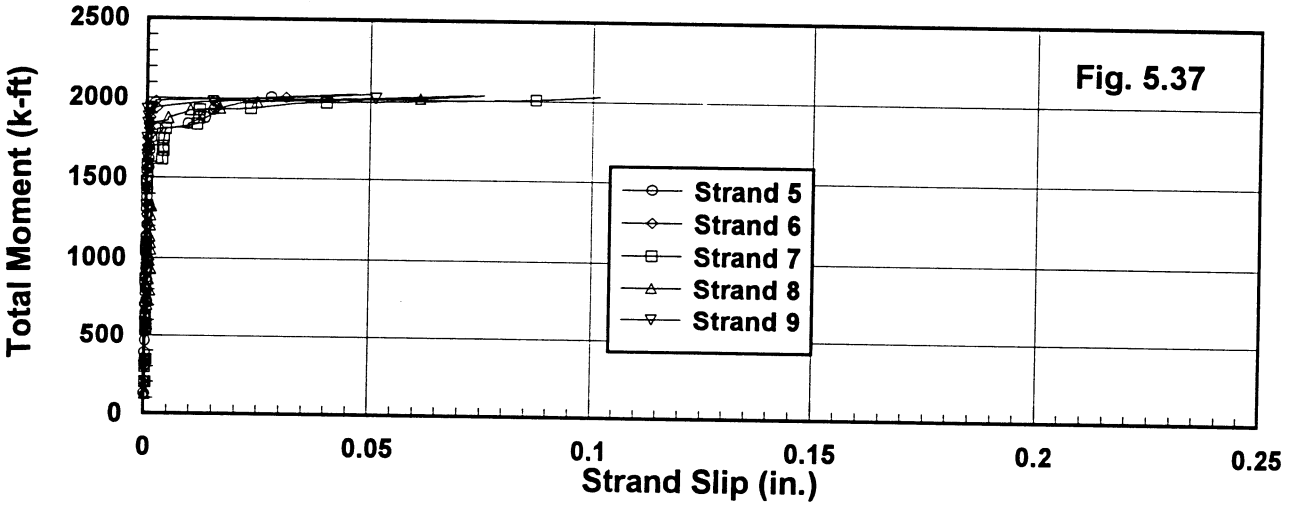

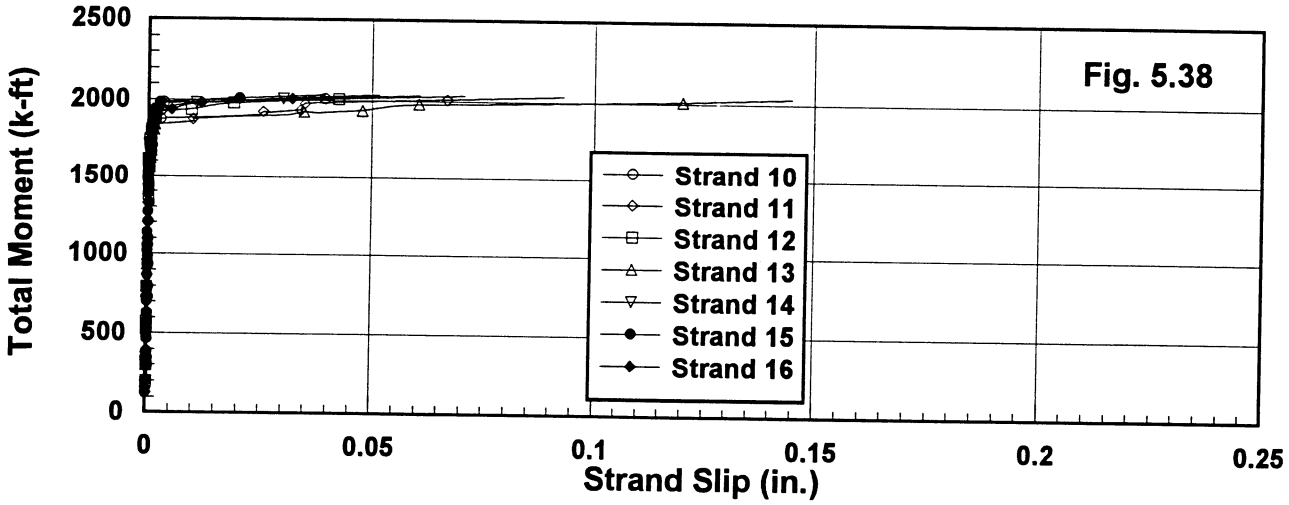

Figures 5.36 to 5.38 Total Moment vs Slip for Girder 2R-10-N

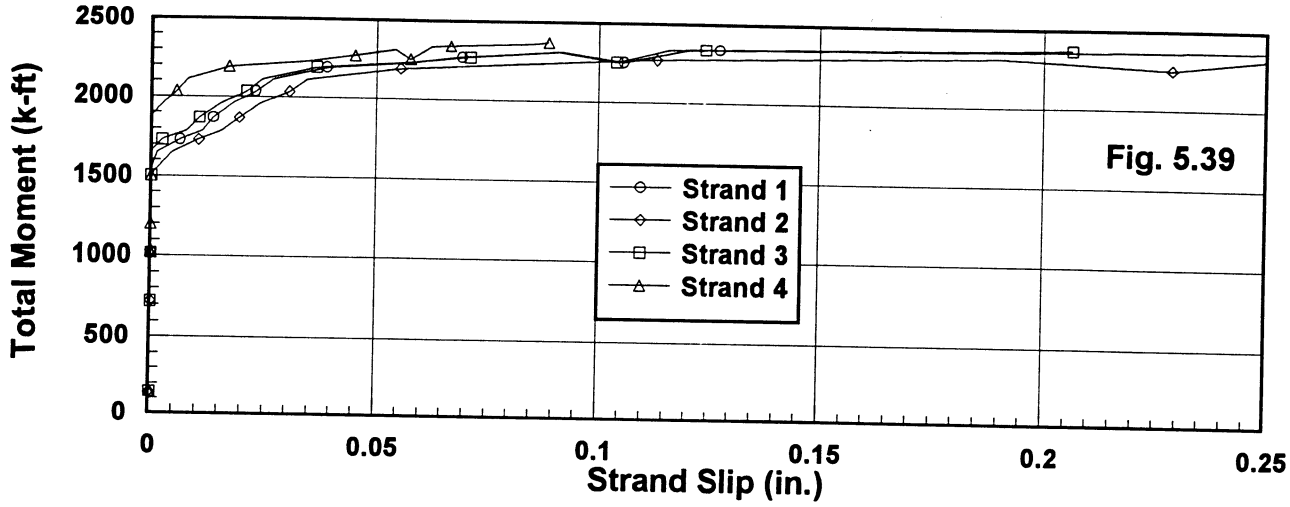

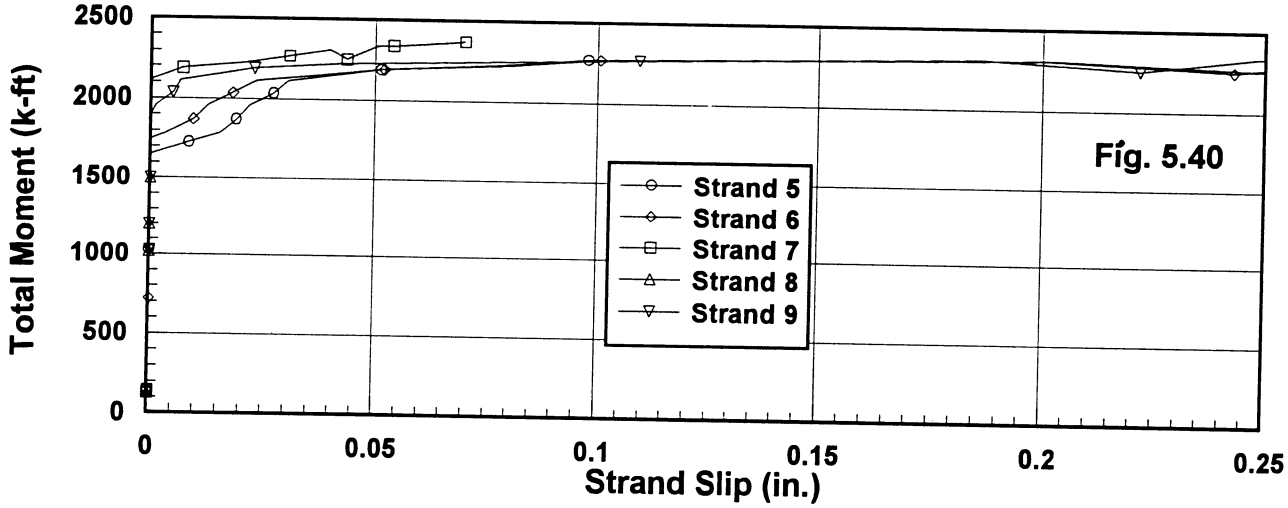

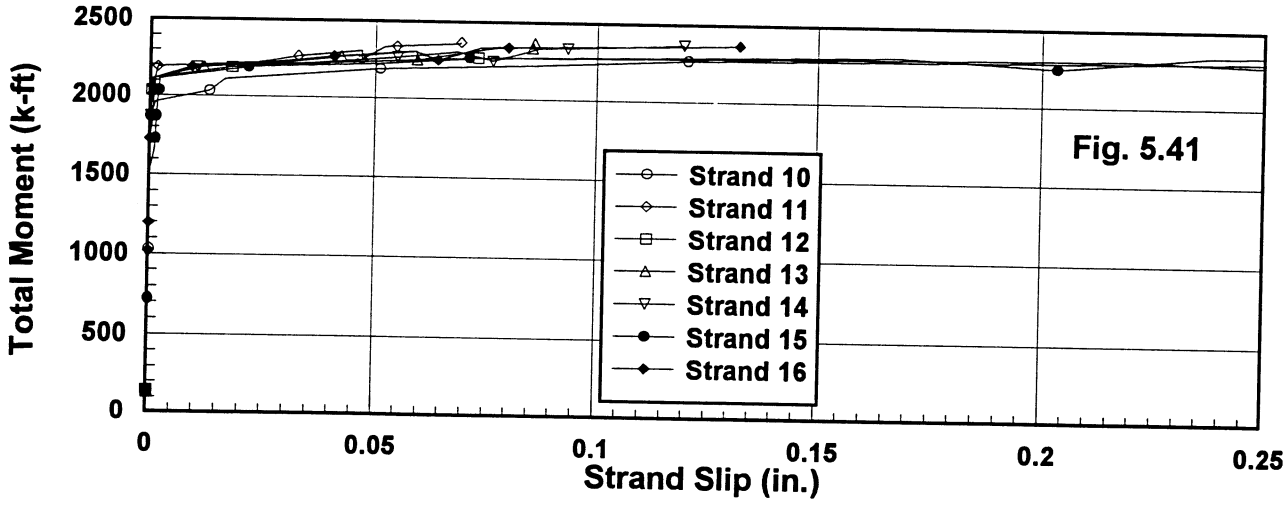

Figures 5.39 to 5.41 Total Moment vs Slip for Girder 2R-12-N

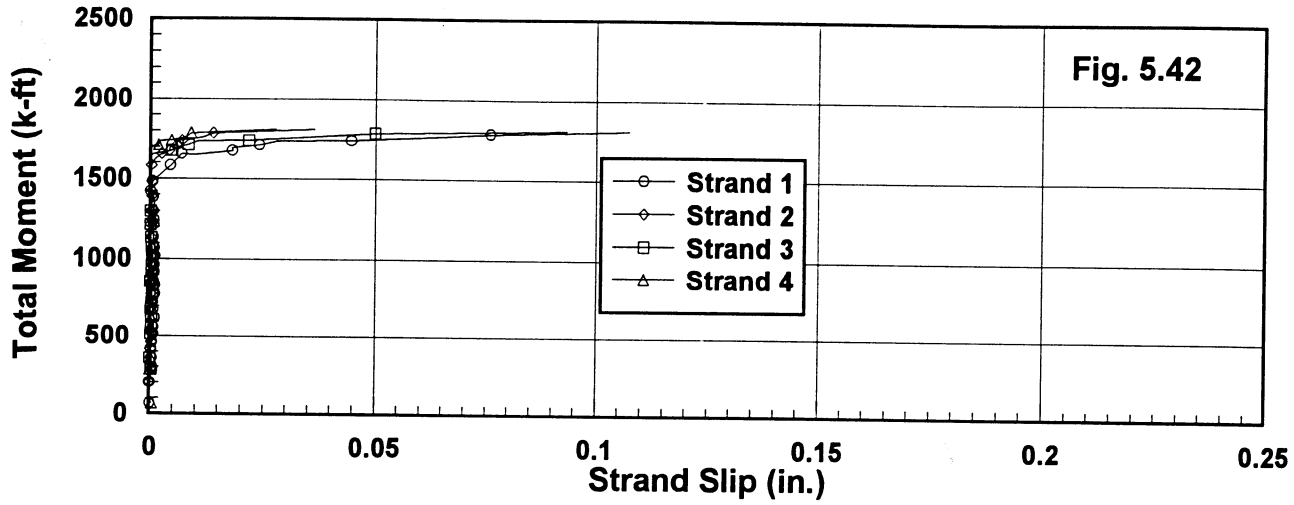

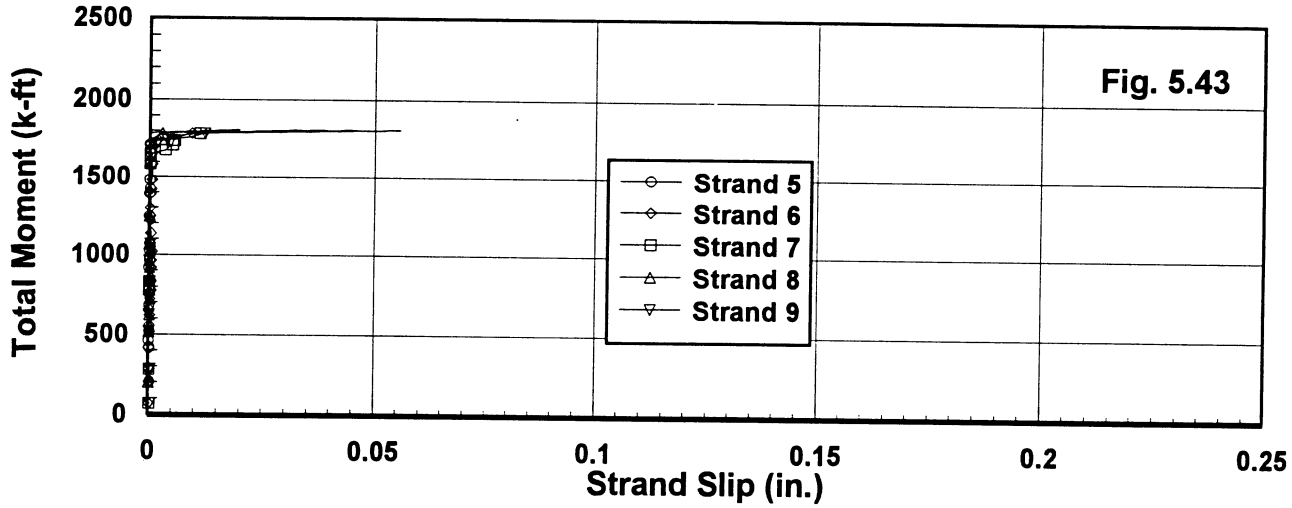

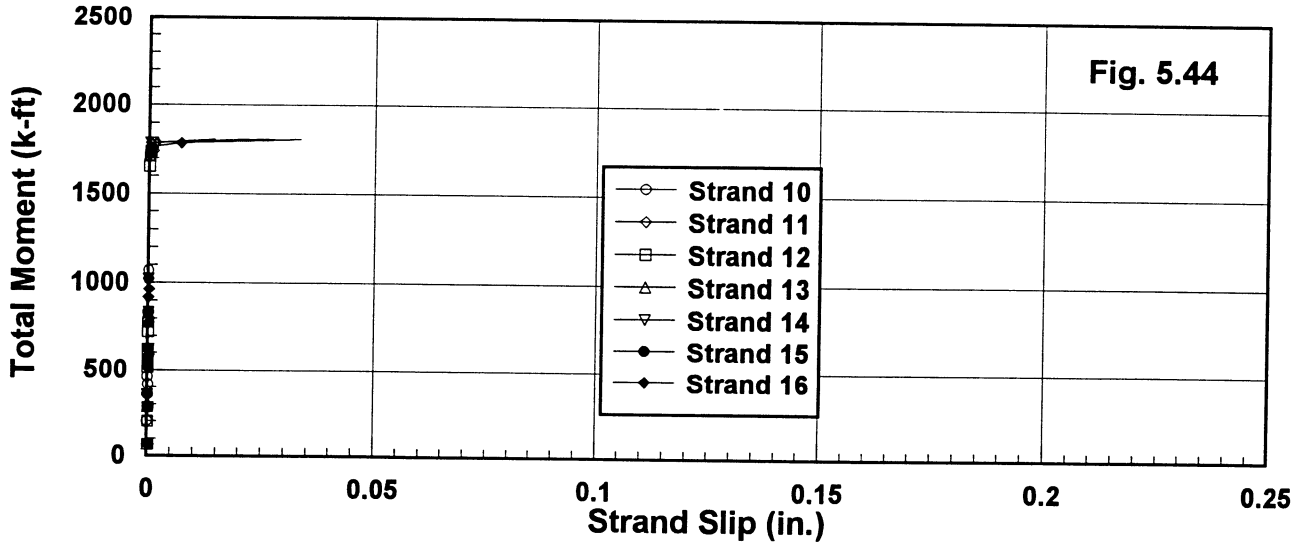

Figures 5.42 to 5.44 Total Moment vs Slip for Girder 2R-8-S

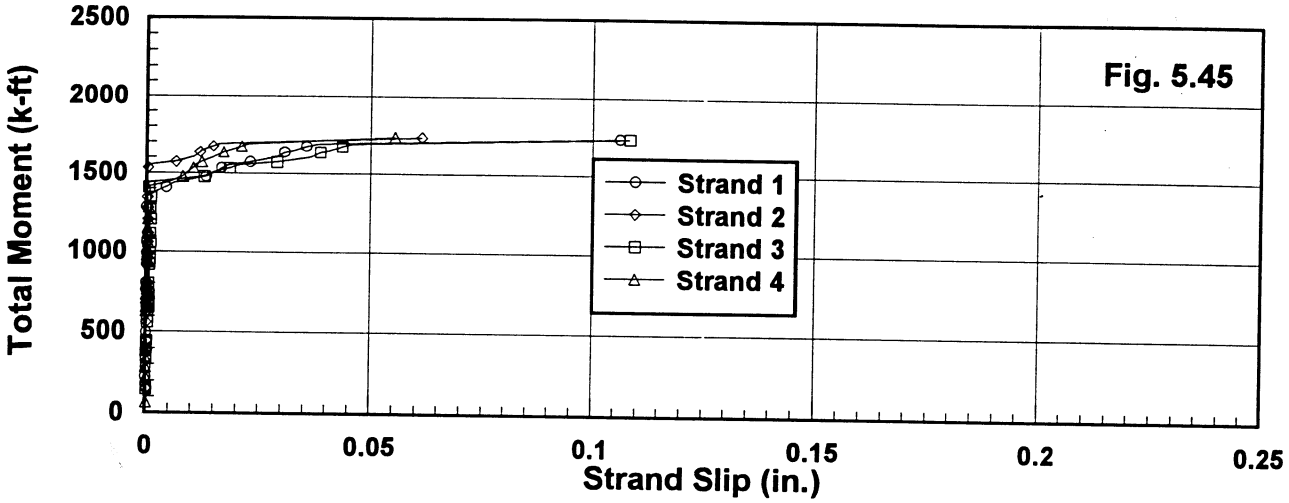

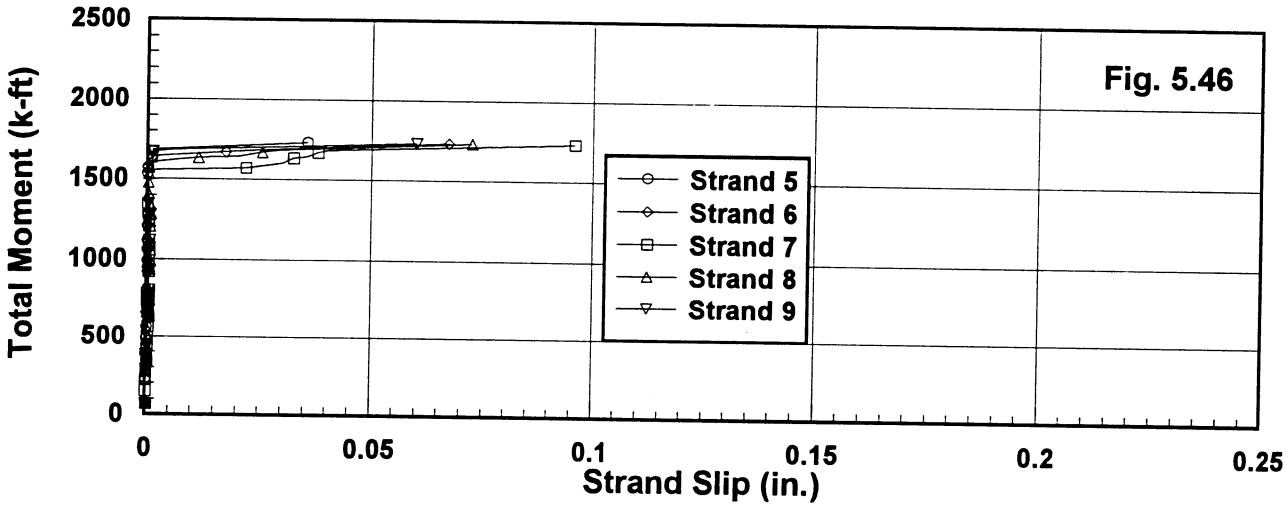

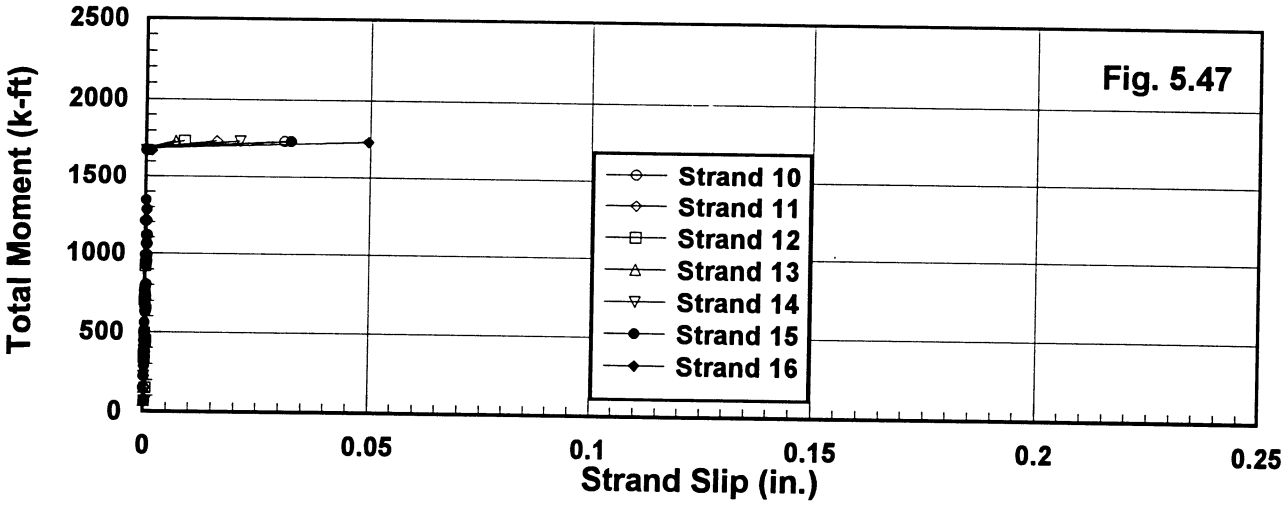

Figures 5.45 to 5.47 Total Moment vs Slip for Girder 2R-10-S

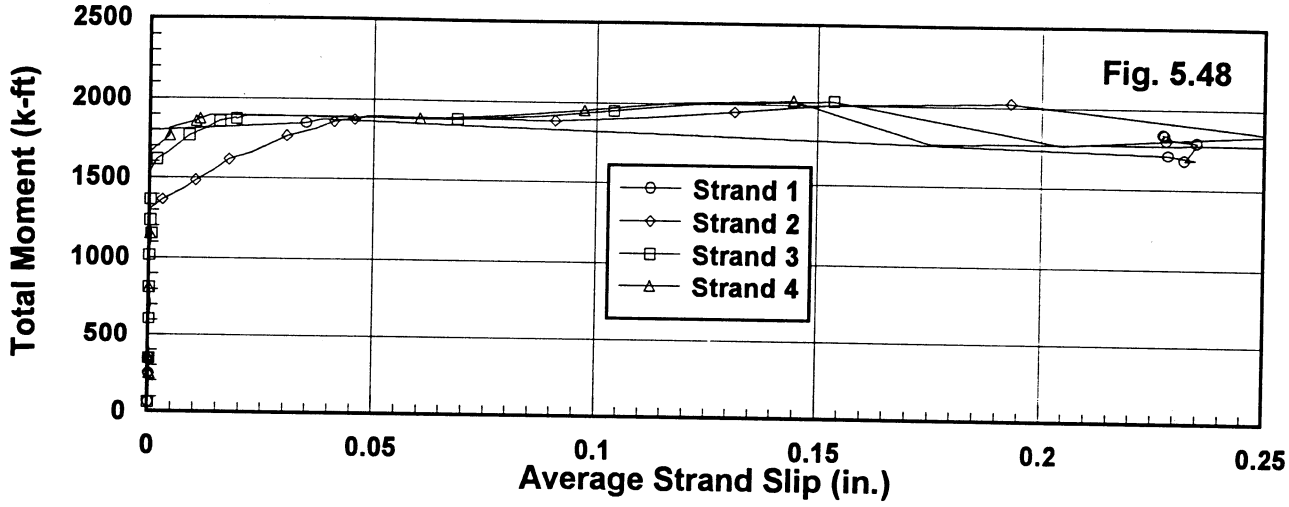

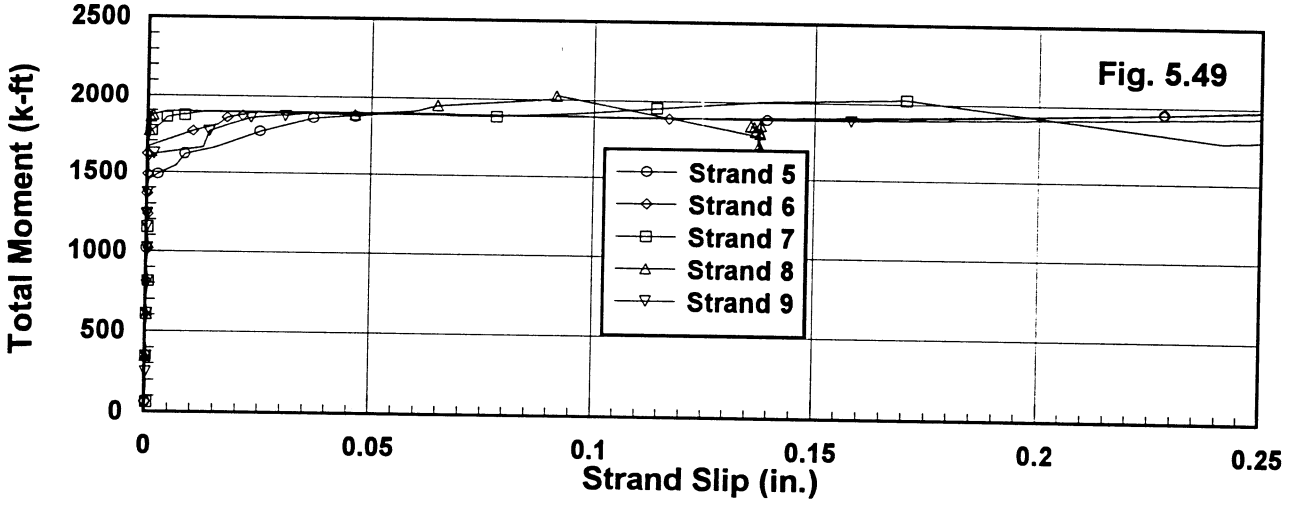

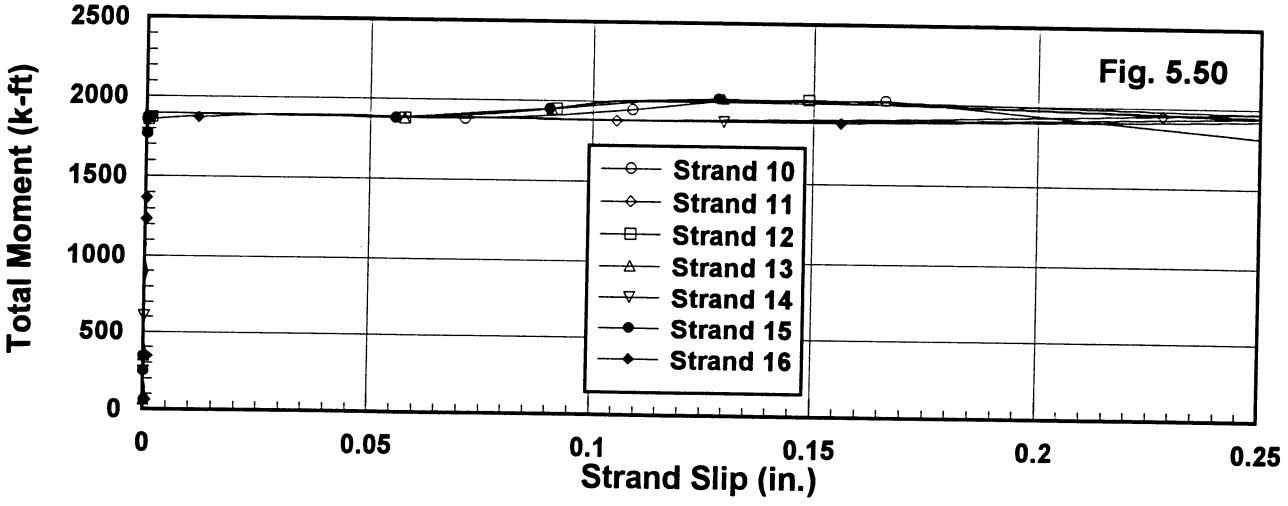

Figures 5.48 to 5.50 Total Moment vs Slip for Girder 2R-12-S

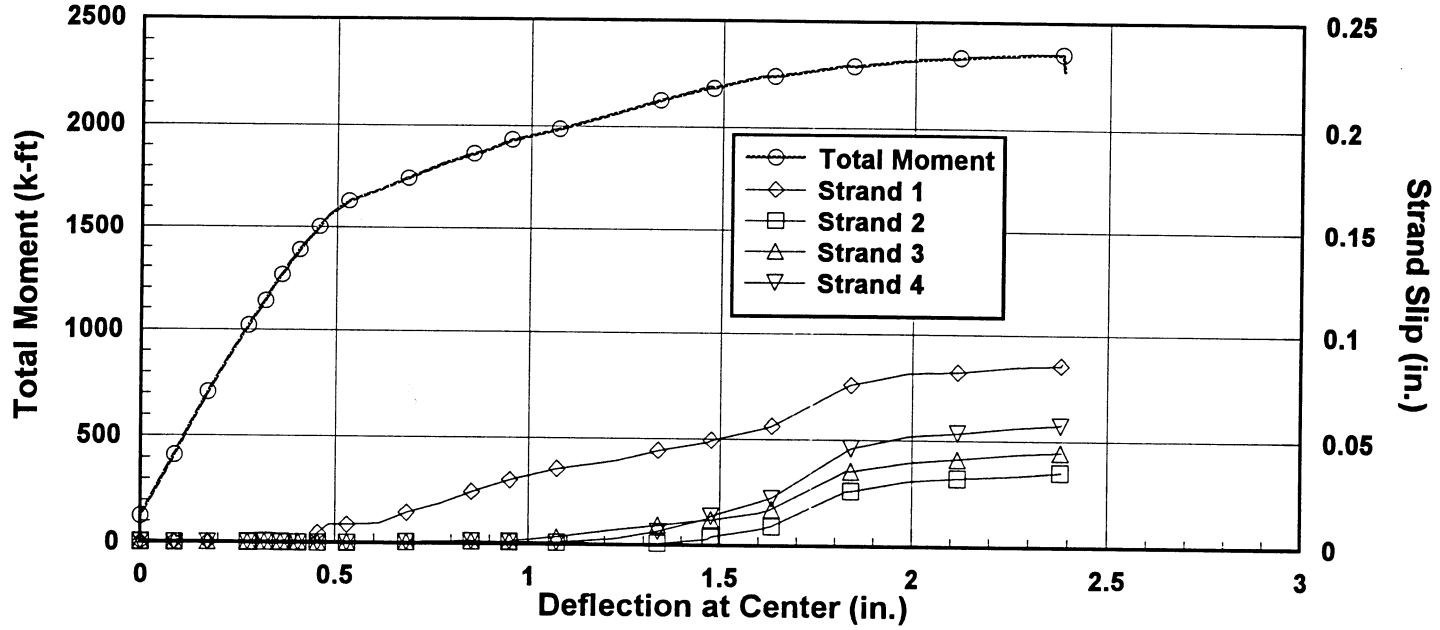

Figure 5.51 Moment and Slip vs. Deflection for Girder R-8-N

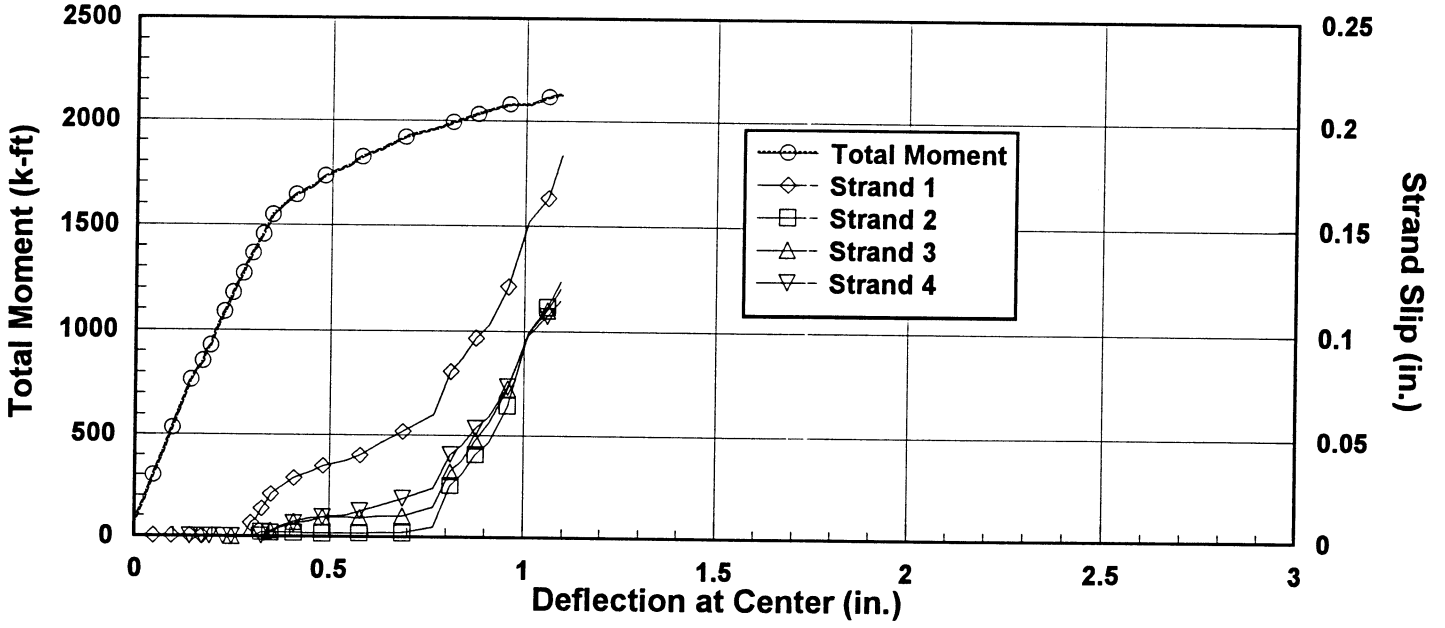

Figure 5.52 Moment and Slip vs. Deflection for Girder R-8-S

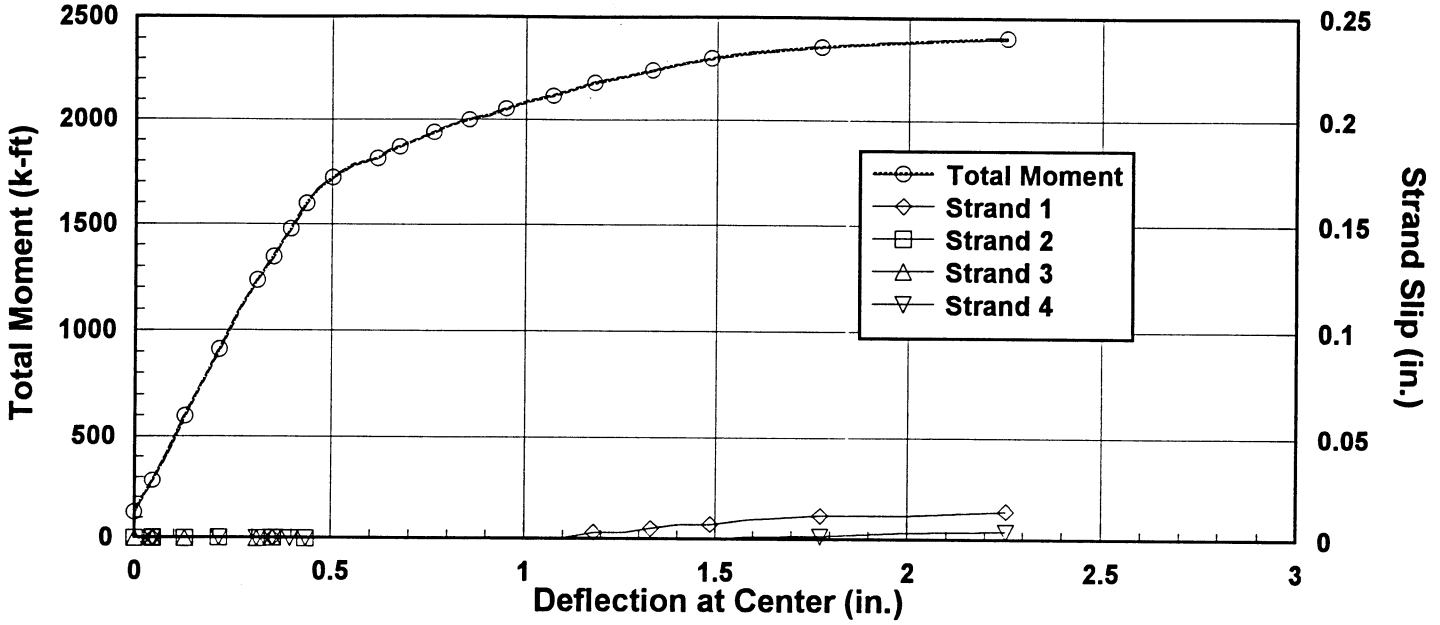

Figure 5.53 Moment and Slip vs. Deflection for Girder R-10-N

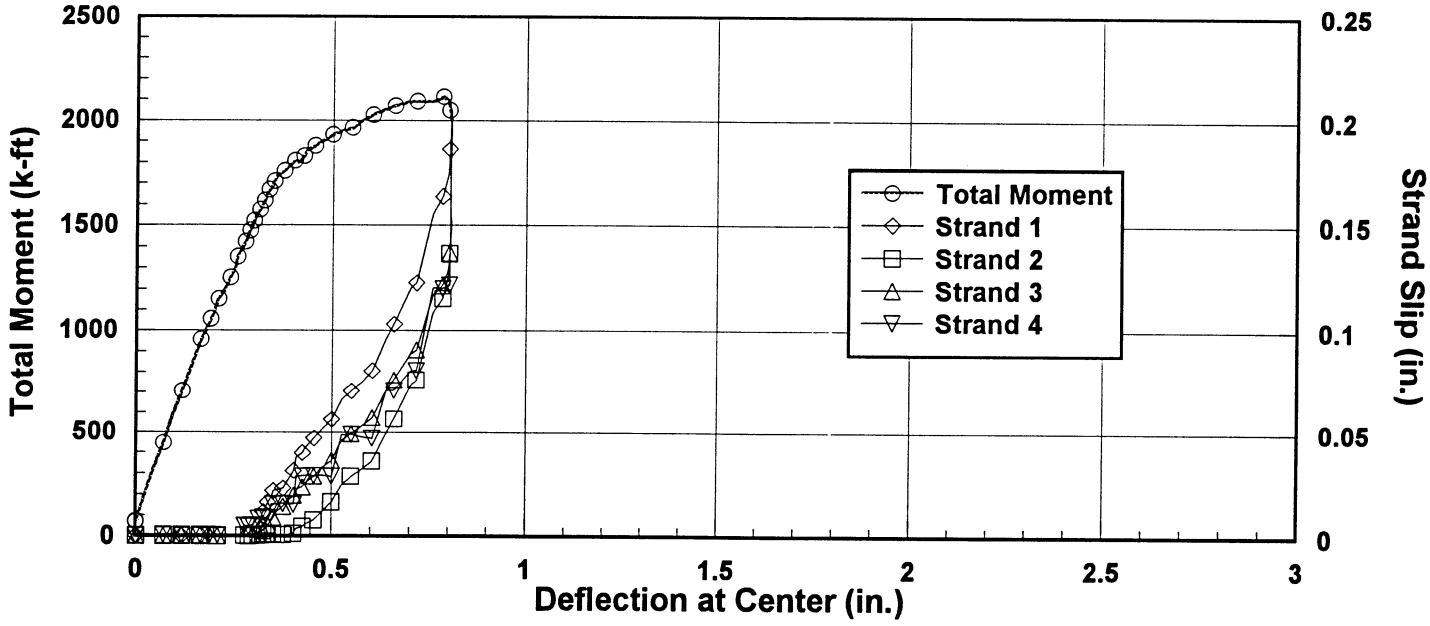

Figure 5.54 Moment and Slip vs. Deflection for Girder R-10-S

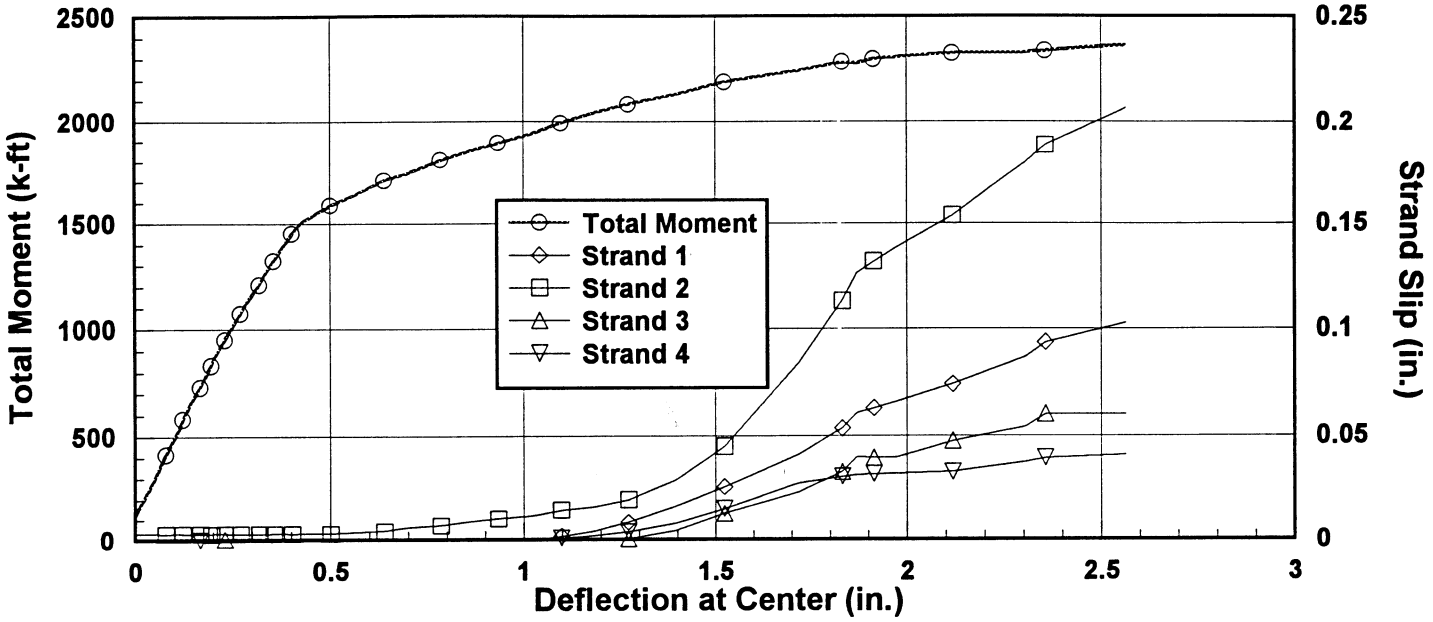

Figure 5.55 Moment and Slip vs. Deflection for Girder R-12-N

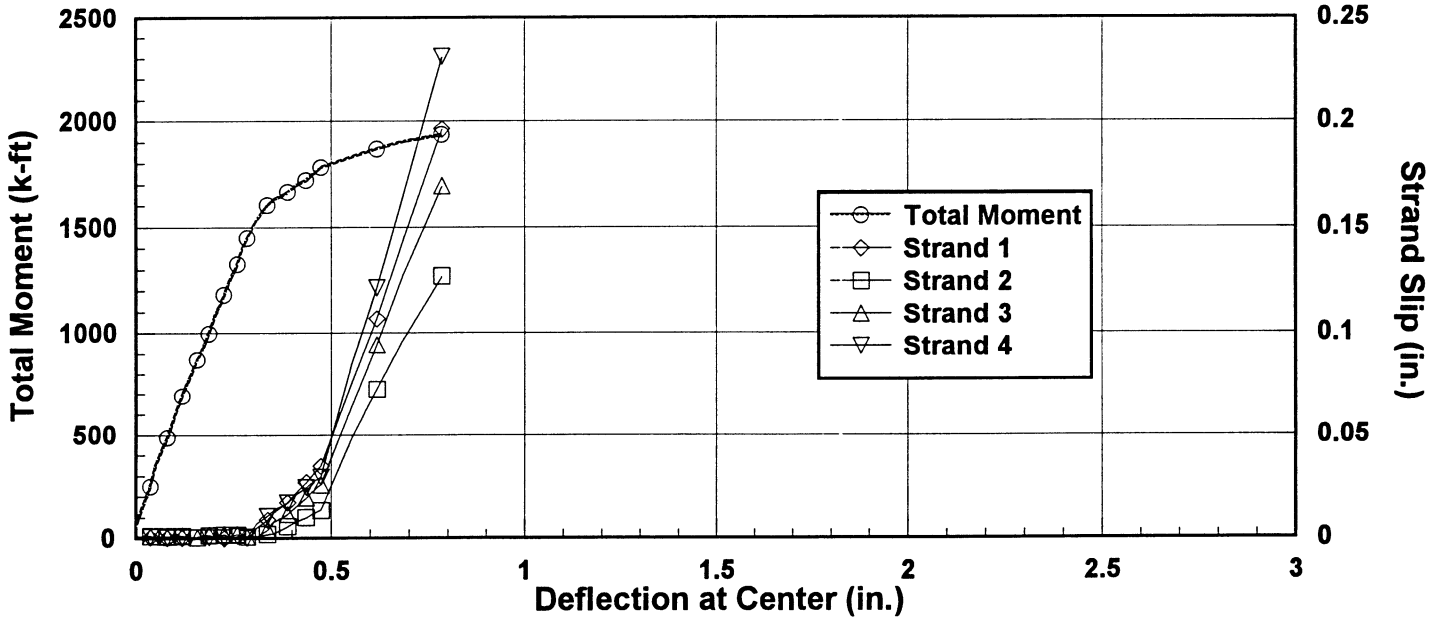

Figure 5.56 Moment and Slip vs. Deflection for Girder R-12-S

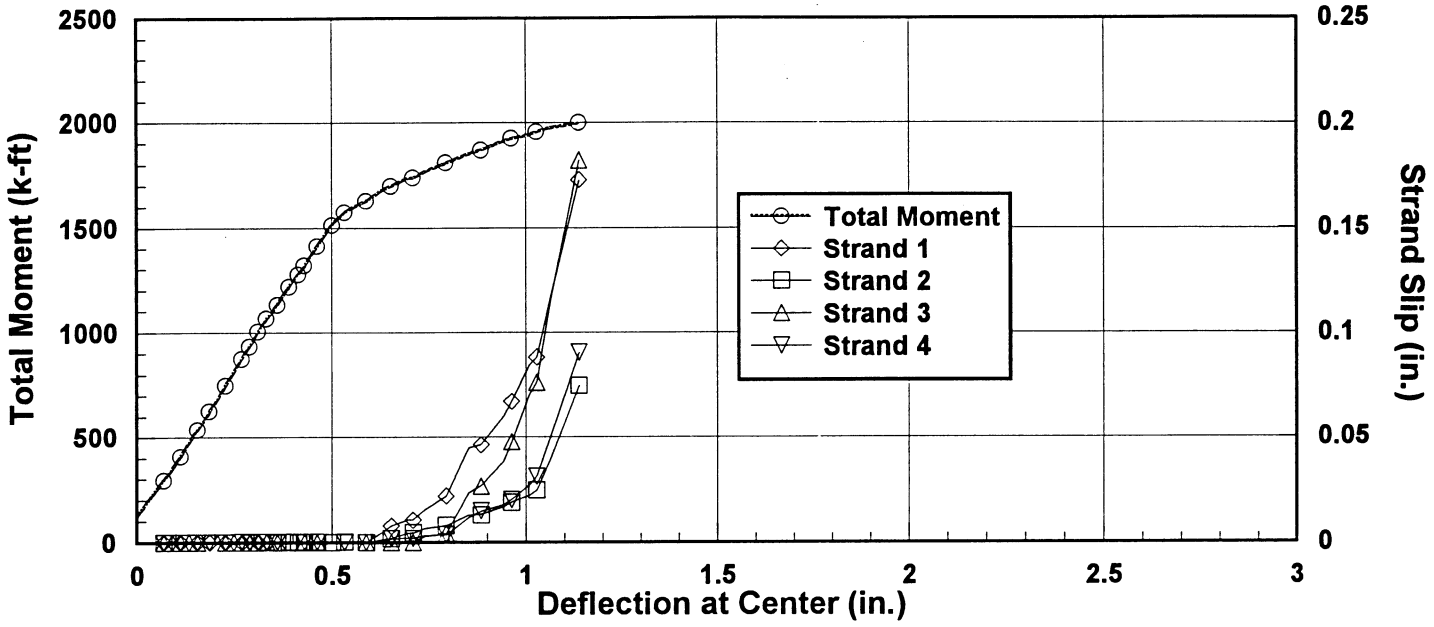

Figure 5.57 Moment and Slip vs. Deflection for Girder 2R-8-N

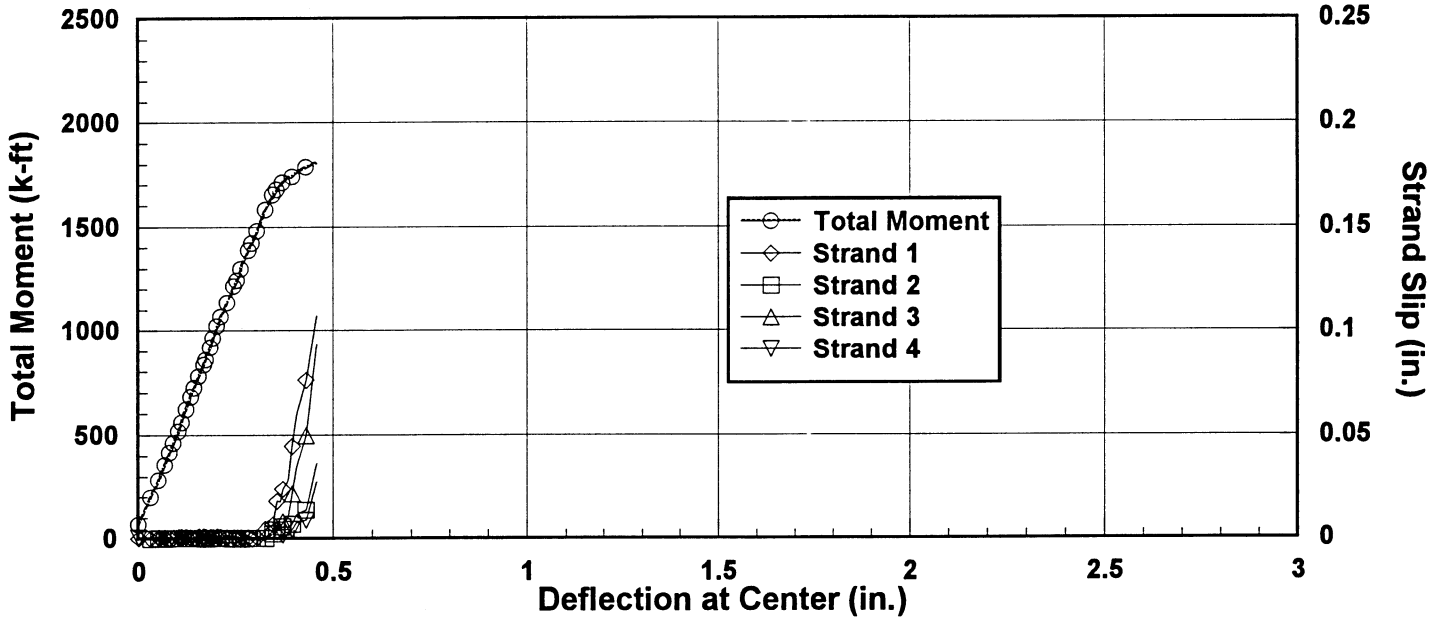

Figure 5.58 Moment and Slip vs. Deflection for Girder 2R-8-S

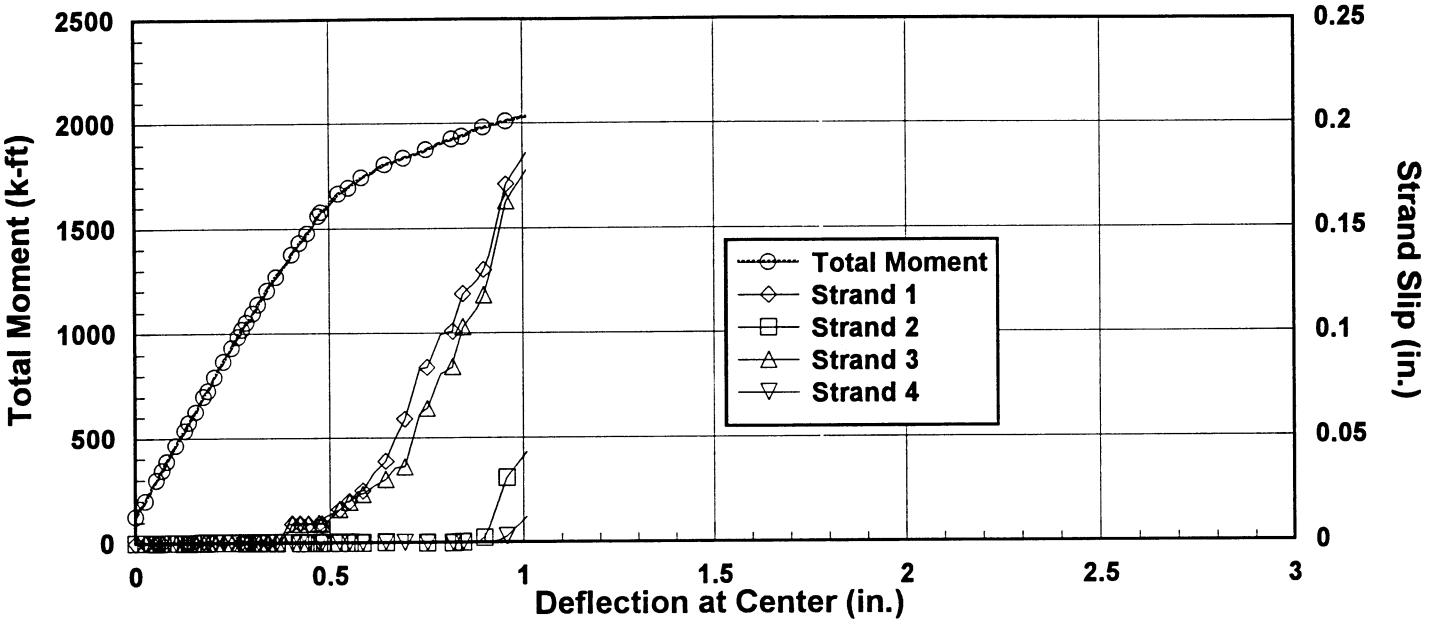

Figure 5.59 Moment and Slip vs. Deflection for Girder 2R-10-N

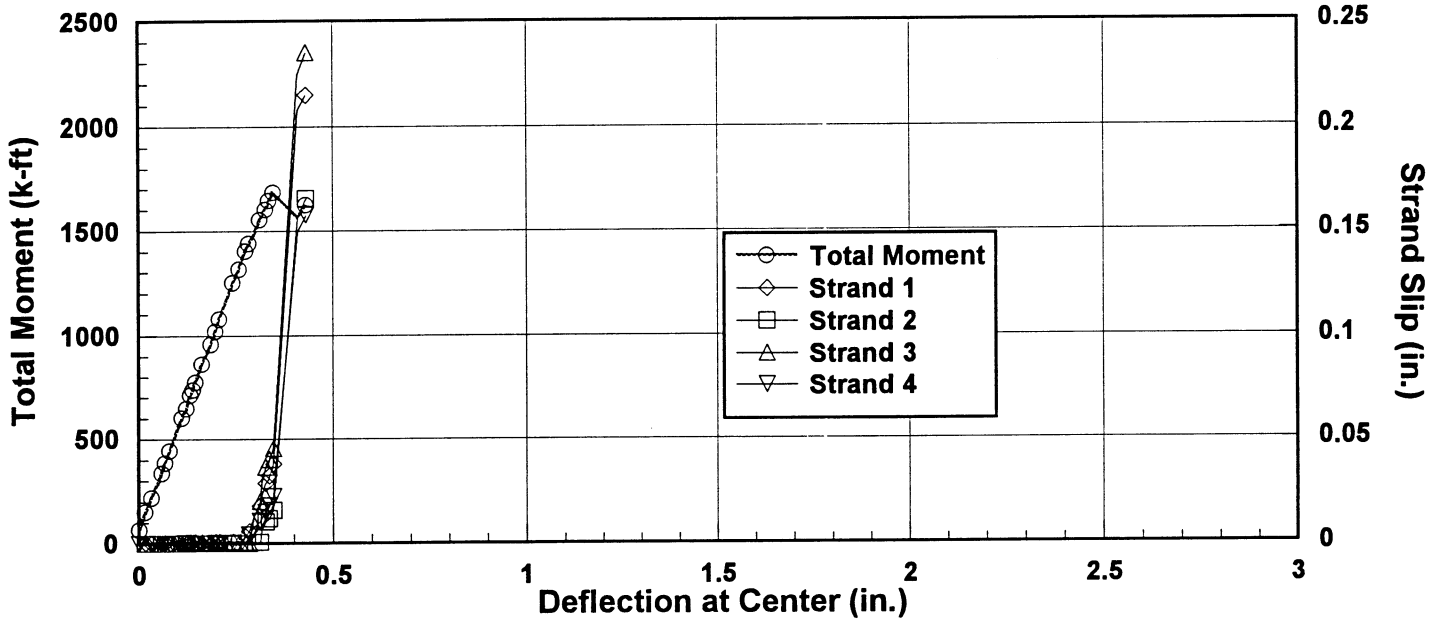

Figure 5.60 Moment and Slip vs. Deflection for Girder 2R-10-S

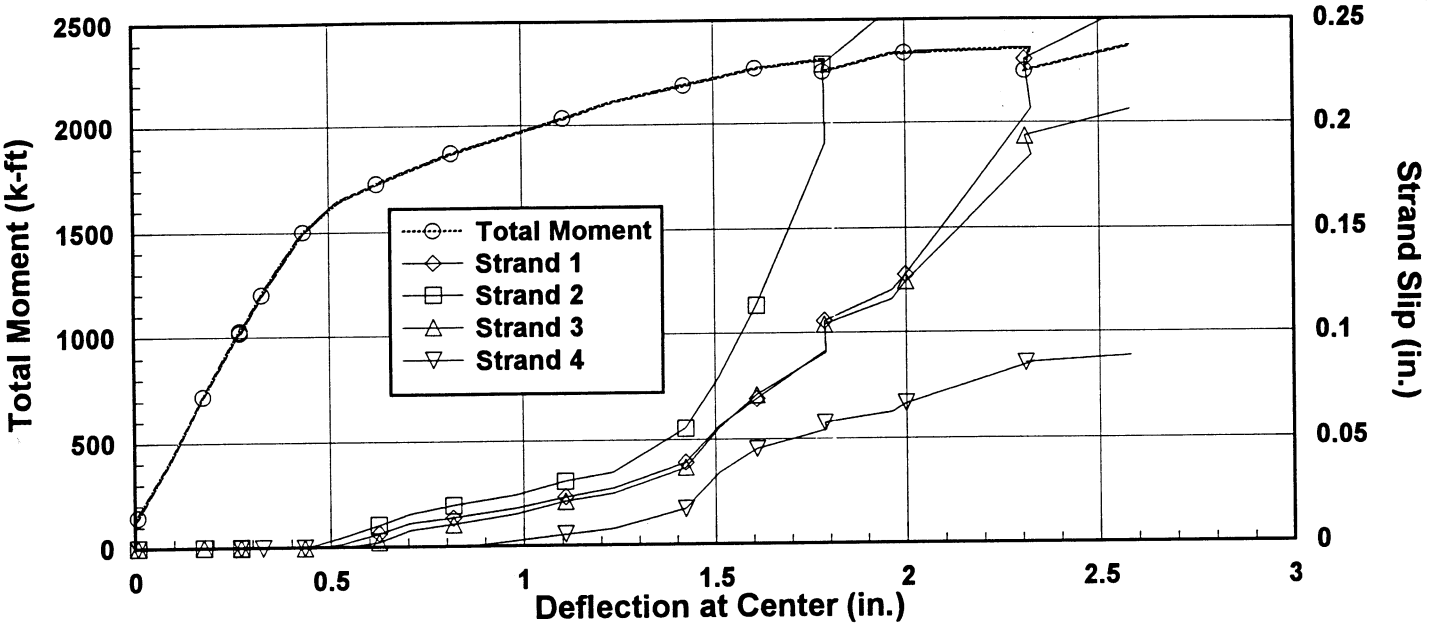

Figure 5.61 Moment and Slip vs. Deflection for Girder 2R-12-N

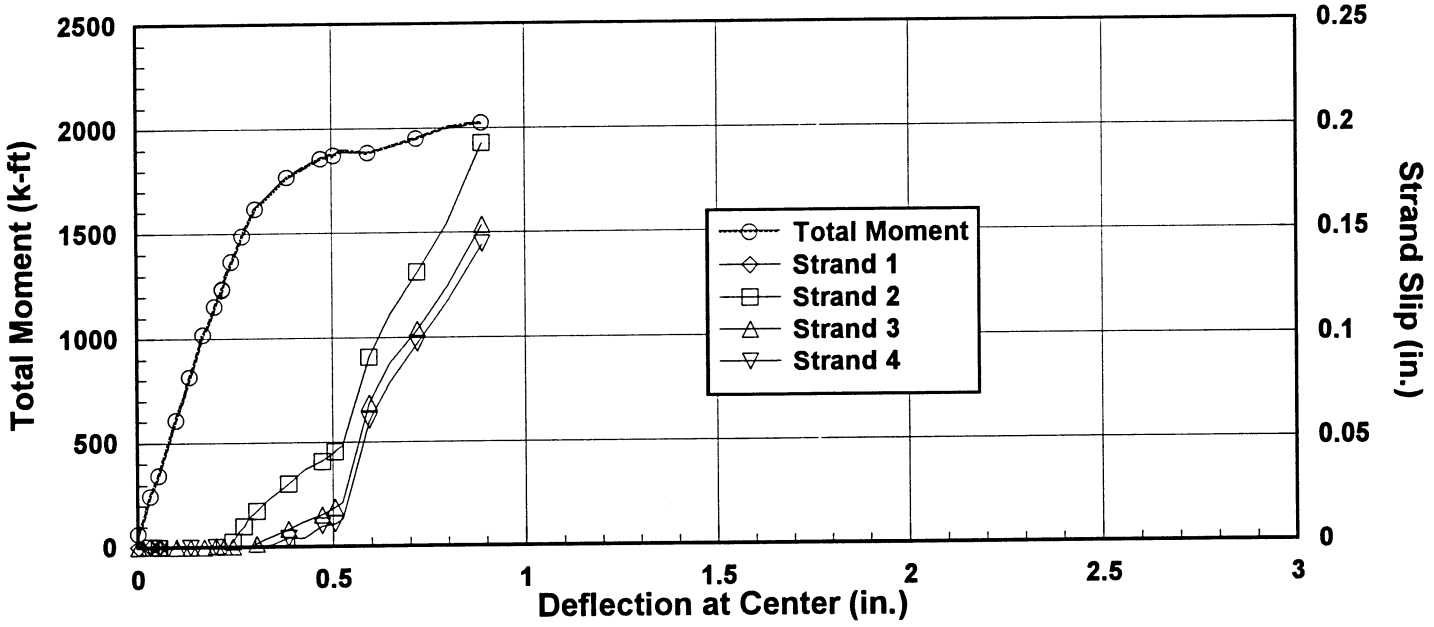

Figure 5.62 Moment and Slip vs. Deflection for Girder 2R-12-S

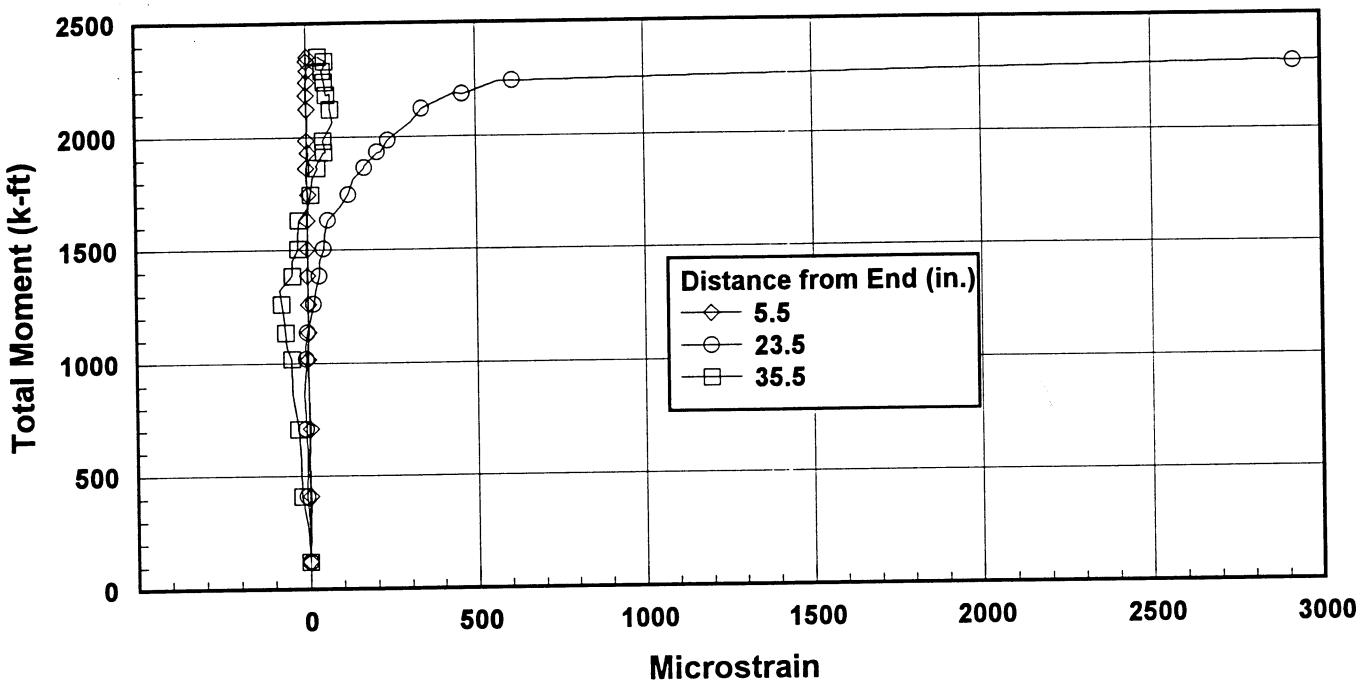

Figure 5.63 Total Moment vs. Confining Bar Strain for Girder R-8-N

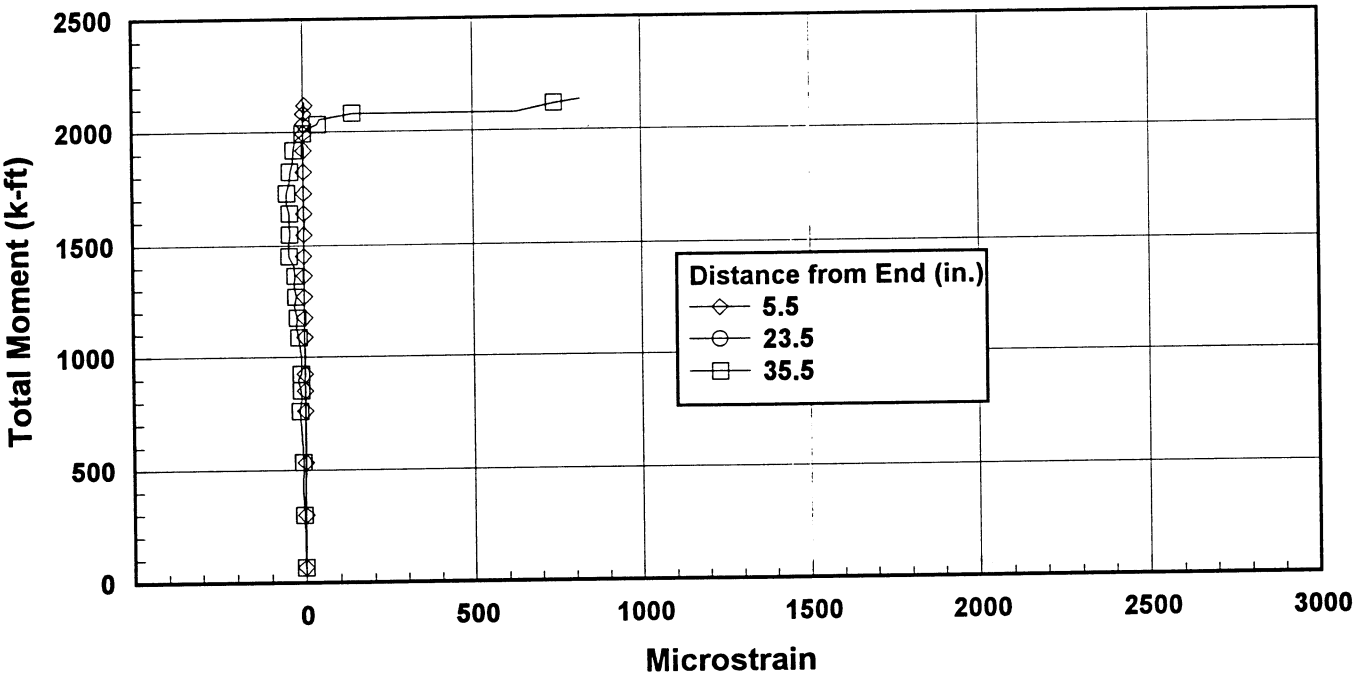

Figure 5.64 Total Moment vs. Confining Bar Strain for Girder R-8-S

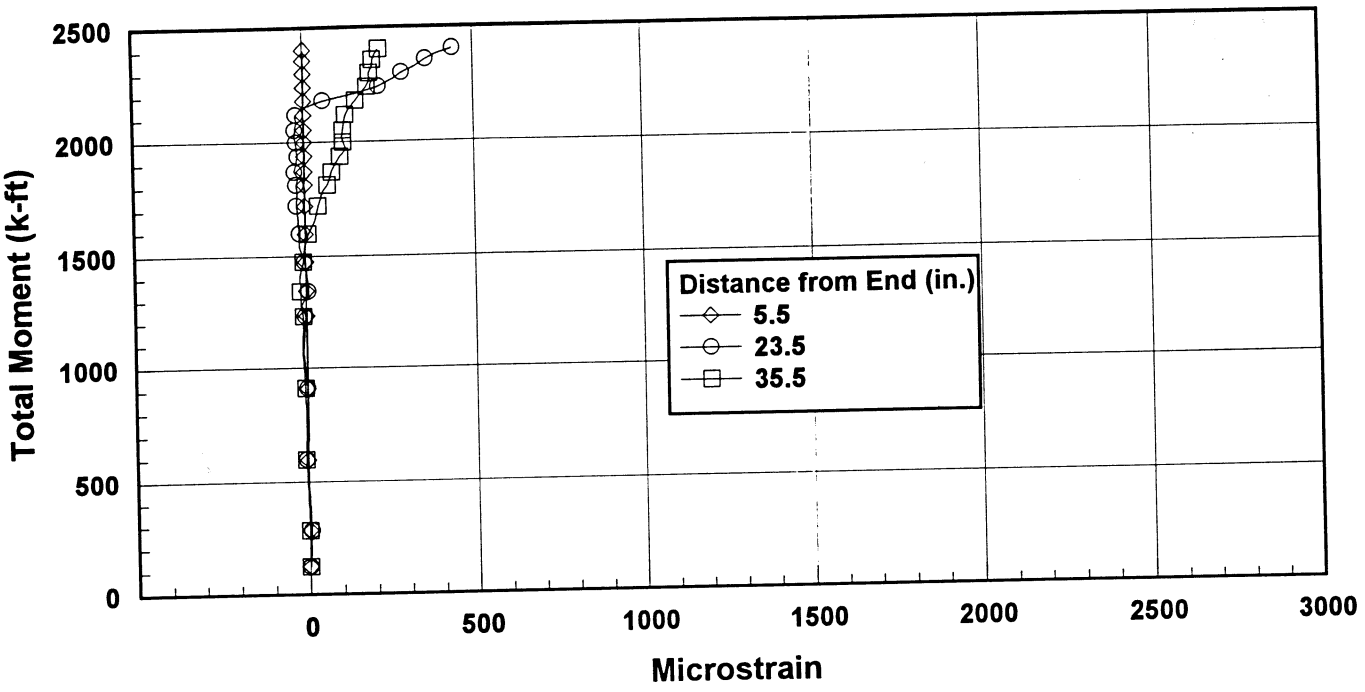

Figure 5.65 Total Moment vs. Confining Bar Strain for Girder R-10-N

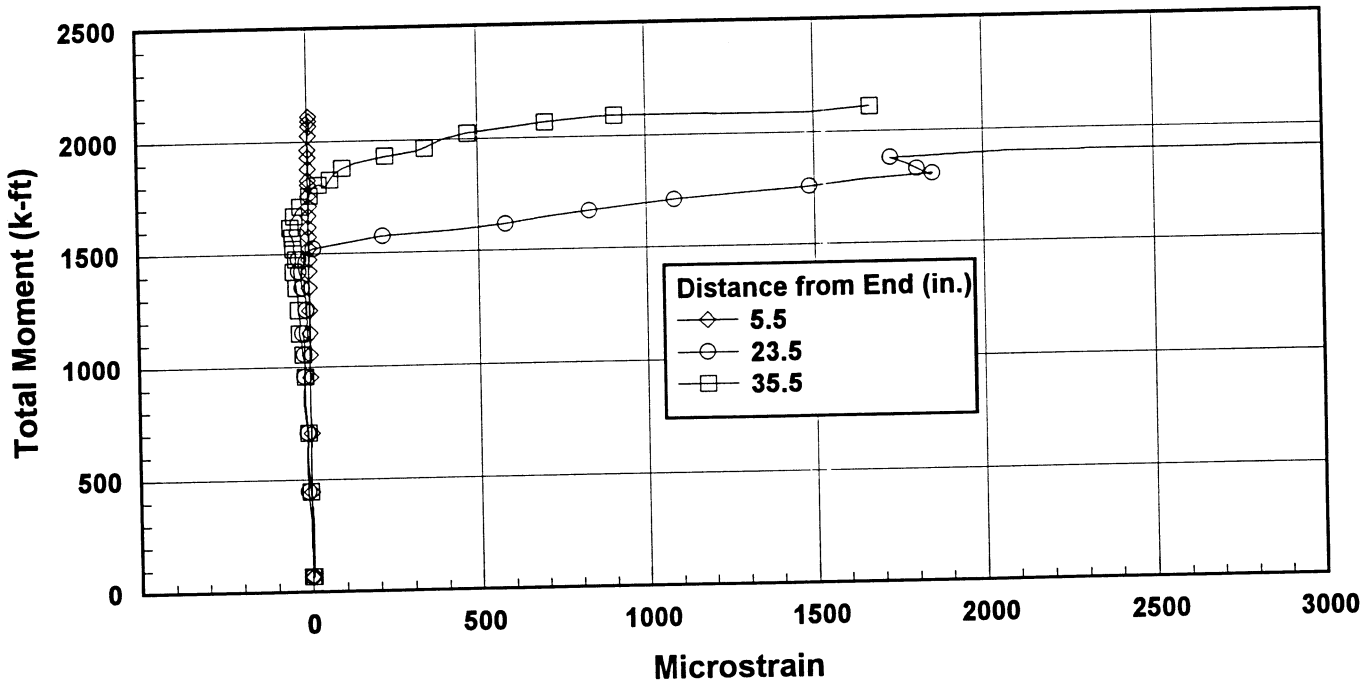

Figure 5.66 Total Moment vs. Confining Bar Strain for Girder R-10-S

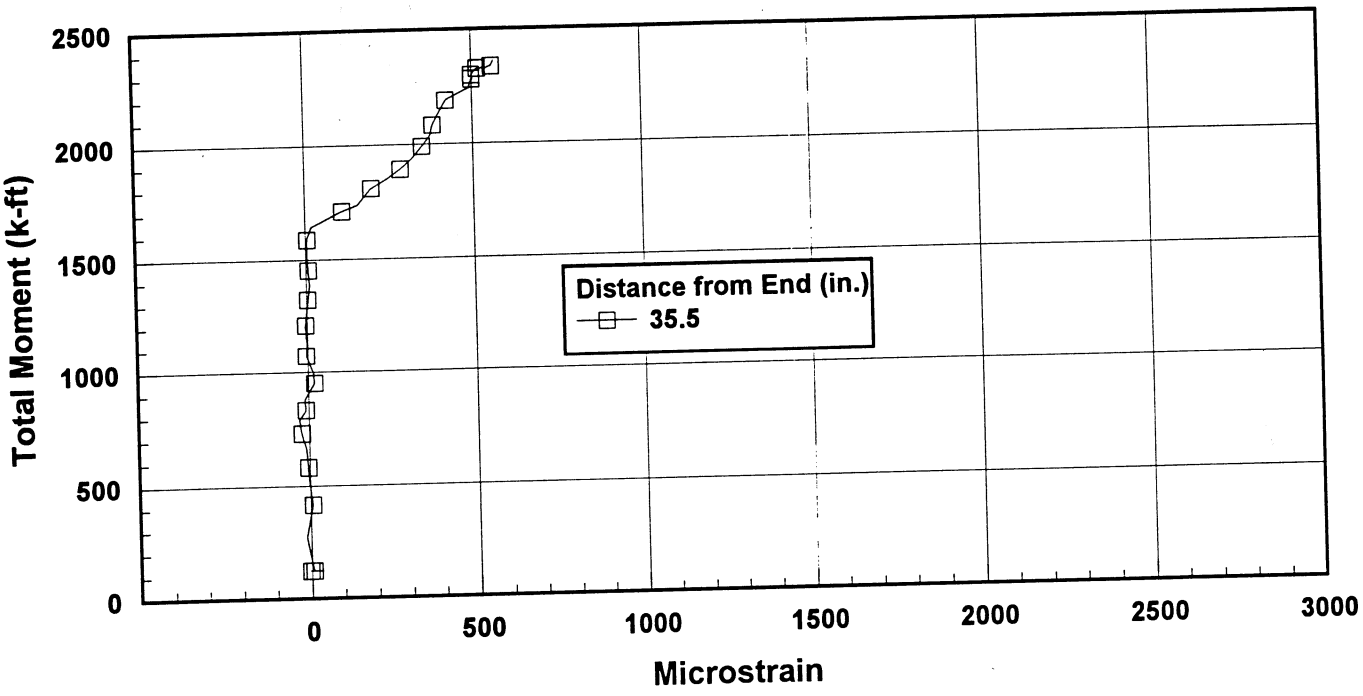

Figure 5.67 Total Moment vs. Confining Bar Strain for Girder R-12-N

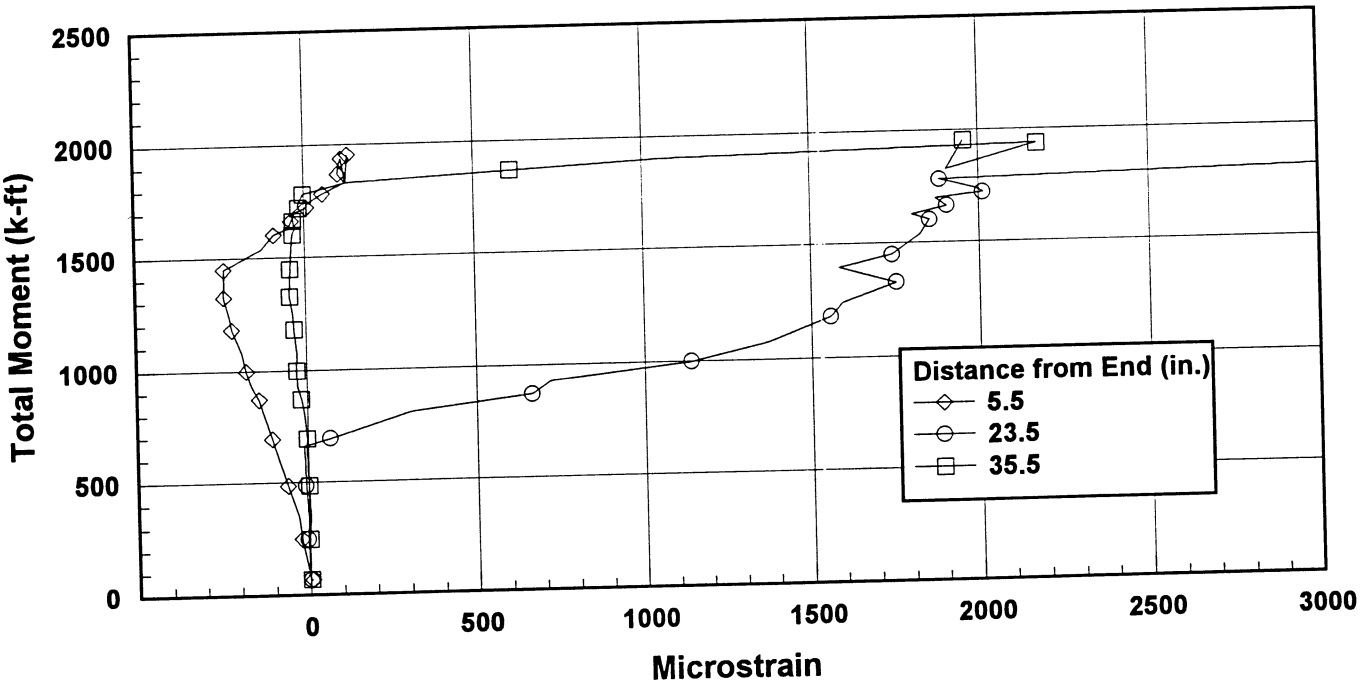

Figure 5.68 Total Moment vs. Confining Bar Strain for Girder R-12-S

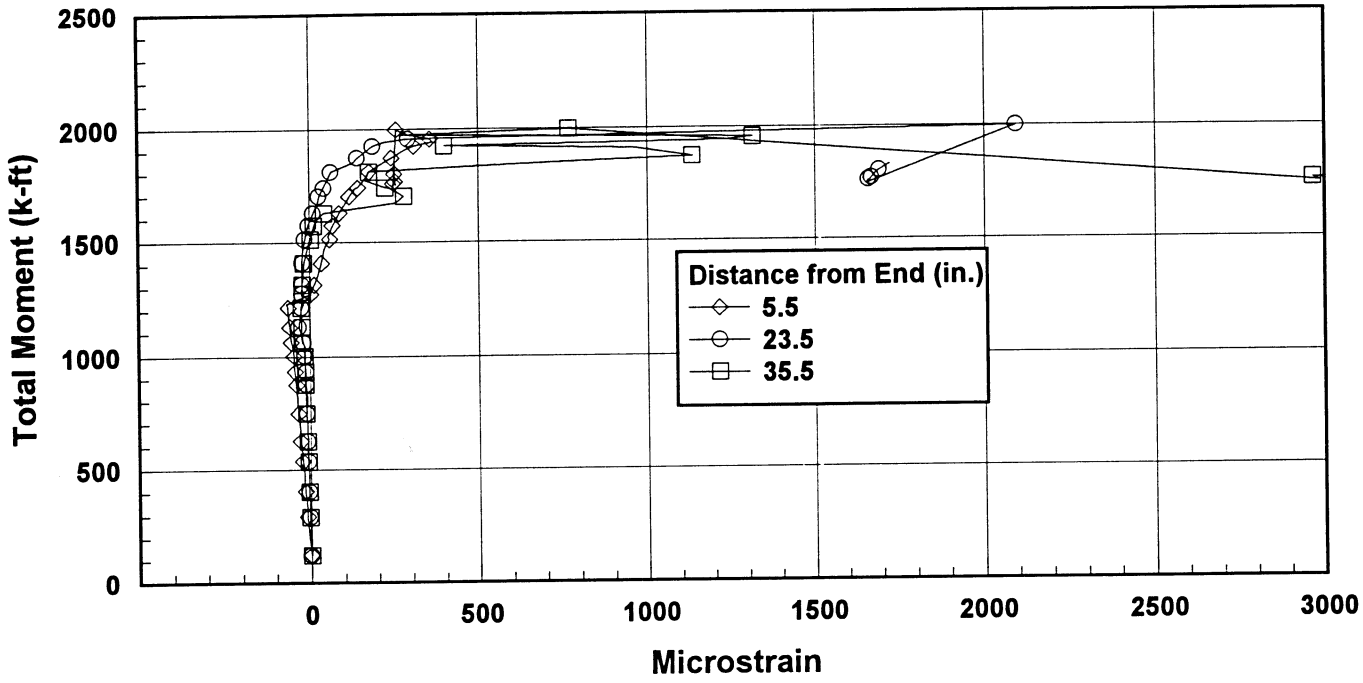

Figure 5.69 Total Moment vs. Confining Bar Strain for Girder 2R-8-N

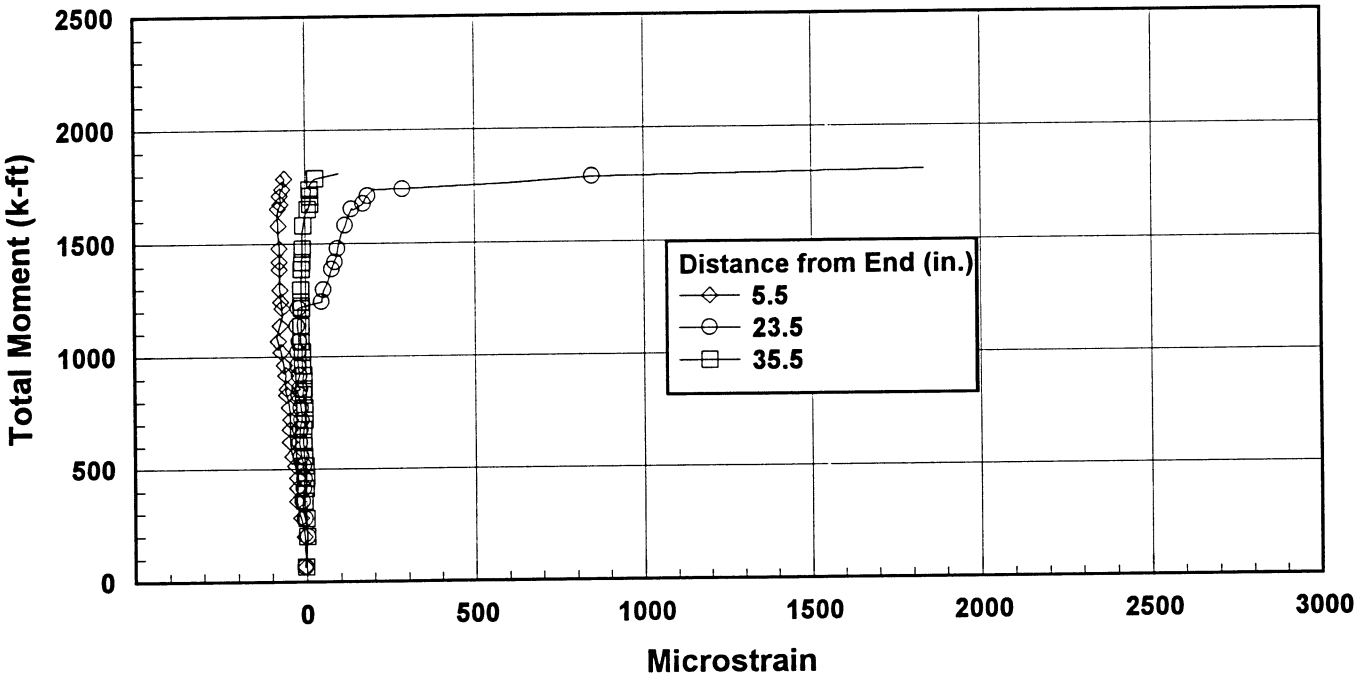

Figure 5.70 Total Moment vs. Confining Bar Strain for Girder 2R-8-S

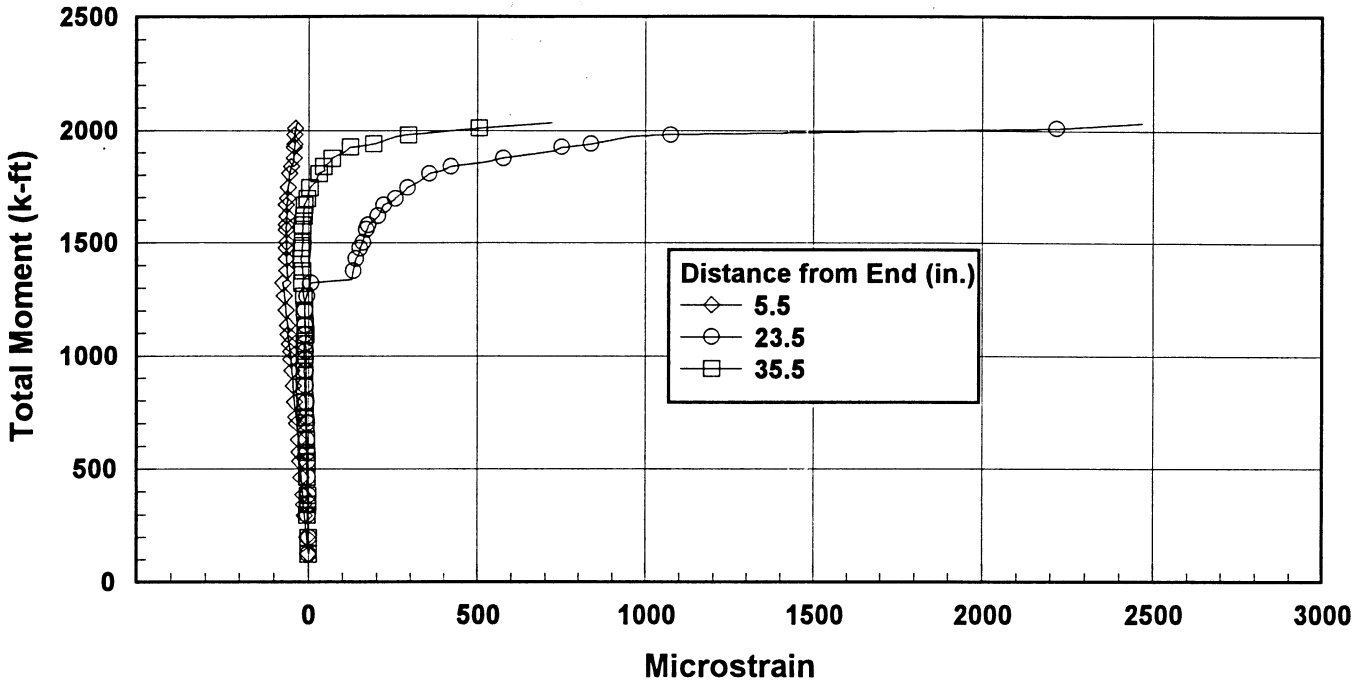

Figure 5.71 Total Moment vs. Confining Bar Strain for Girder 2R-10-N

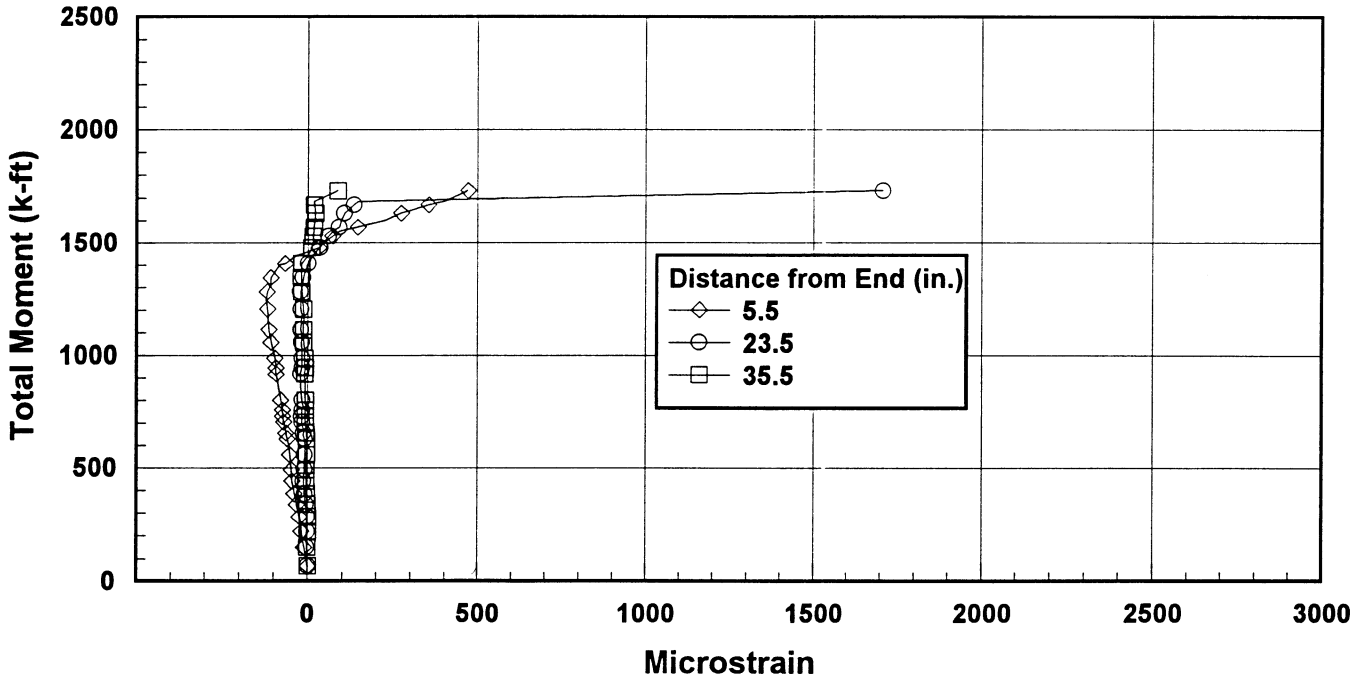

Figure 5.72 Total Moment vs. Confining Bar Strain for Girder 2R-10-S

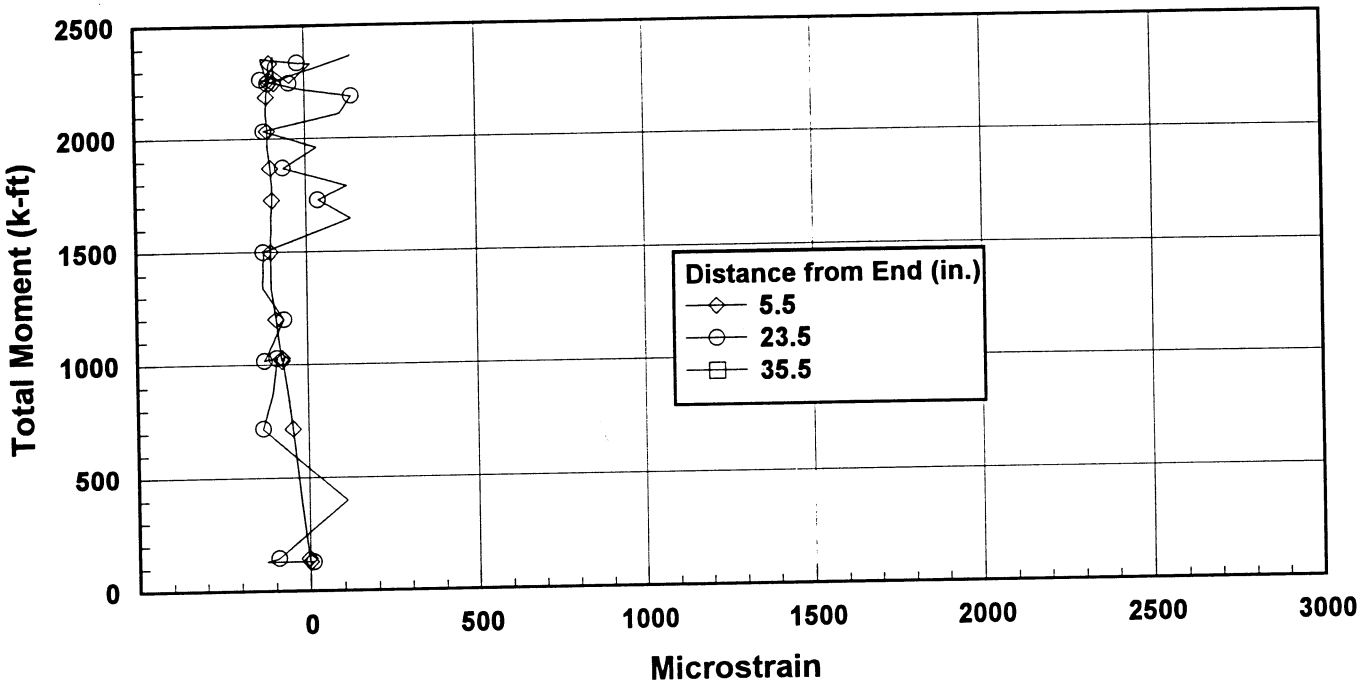

Figure 5.73 Total Moment vs. Confining Bar Strain for Girder 2R-12-N

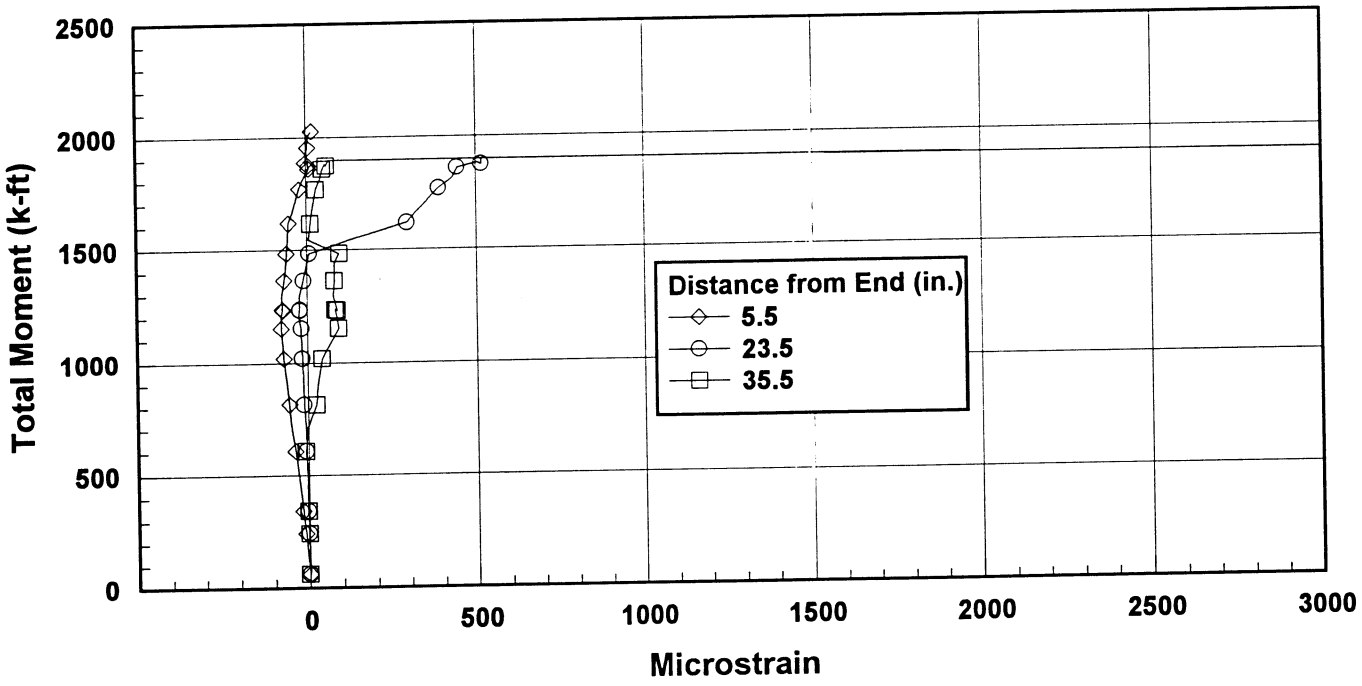

Figure 5.74 Total Moment vs. Confining Bar Strain for Girder 2R-12-S

CHAPTER 6
CONCLUSIONS

1) The bond between the prestressing strand and concrete determines the transfer length and development length of prestressed girders. The bond may also limit the ultimate strength of prestressed girders, depending on the loading condition.

2) Forty direct tension pullout tests were performed to examine the bond between the prestressing strand and concrete. There are two distinct independent bond mechanisms that characterize the bond performance. The two bond mechanisms were termed the adhesion bond and the mechanical bond U_1 and U_t, respectively.

3) The adhesion bond is the initial bond that resists bond stresses. Before the adhesion bond failure there is no movement of the strand relative to the concrete. It was found that the adhesion bond is most affected by the surface condition of the strand. The adhesion bond strength increases with a courser strand condition.

4) After the adhesion bond fails, the helical shape of the strand and friction causes a mechanical interlock between the strand and concrete. The mechanical bond is developed as loads are applied and the strand is displaced relative to the concrete. As the strand slips, hoop stresses in the concrete are developed due to the helical shape of the strand. Frequently the mechanical bond strength is greater than the adhesion bond strength. Mechanical bond failure was often noted by splitting of the concrete. The mechanical bond is most affected by the strand diameter and strength of the concrete. The mechanical bond increases with smaller strand diameters. The mechanical bond also increases with higher concrete strength. A regression analysis resulted in the following equation that predicts the mechanical bond strength for a 1/2" clean strand:

$$U_t = 0.0687 \cdot f'_c \qquad 5\text{-}1$$

5) The transfer length for six full-scale AASHTO Type II prestressed girders was measured to determine the effect of the concrete strength on the transfer length. Three different compressive strengths of concrete were used; 8,000 psi, 10,000 psi and 12,000 psi. In addition, published results from FDOT transfer length tests with similar girders made with 6,000 psi concrete were used in the analysis. When the strands are released there is movement of the strands relative to the concrete. A mechanical bond resists the prestressing force over most of the transfer length and a adhesion bond resists the prestressing force over a small amount of the transfer length.

6) Girders with higher concrete strengths had a shorter transfer length and thus a higher bond stress. High strength concrete is more able to resist the hoop stresses and strains that develop because of the mechanical nature of the bond. The following empirical relationships were developed to predict the transfer length based on the test results:

$$l_t = \frac{1.78 \cdot f_{se} \cdot d_s}{f'_{ci}} \qquad 5\text{-}5$$

or

$$l_t = \frac{1.67 \cdot f_{si} \cdot d_s}{f'_{ci}} \qquad 5\text{-}6$$

7) The current AASHTO equation used to predict the transfer length does not reflect the observed effect of the concrete strength on the transfer length. Recently, after several full-scale tests, the authors of reference 12 suggested the following equation for transfer length:

$$l_t = \frac{f_{si} \cdot D}{3}$$

The difference between the equation developed in this study and the equation proposed by Shahawy et al. 1992 is the term $1.67/f'_{ci}$. The girders in Shahawy et al. study had a f'_{ci} of about 5.11 ksi, so the term $1.67/f'_{ci}$ for the girders is 0.33. Therefore, the results from the that study fit well within the current results.

8) The relationship between the pullout bond strength, U_b and the transfer length was examined. The major similarity between the two tests was the mechanical nature of the bond. The only difference between the two tests was in simulating the Hoyer effect in the laboratory. However, it appears that a pullout test specimen, made with the same materials as of the transfer length beams, can be used to predict the bond strength and, thus, the transfer length.

9) Each end of the six full-scale girders were tested in a manner that was intended to produce a shear failure. The girders had concrete strengths of 8,000 psi, 10,000 psi and 12,000 psi and varying amounts of shear reinforcement. Most of the girders failed due to a bond failure of the prestressing strand and concrete.

10) The bond between the prestressing strand and the concrete in the full scale girders behaved in a similar manner as the pullout tests. Initially, as external loads were applied there was no slippage of the strand and the girder was able to withstand increasing loads. Eventually, as the external loads increased, the adhesion bond failed and the strands began to slip. After the adhesion bond failure, the mechanical bond sustained increased external loads. As increased external loads were applied, the mechanical bond stresses increased and the strands slipped excessively. The failure of the girder was noted by a sudden increase in the amount of slip and a decrease in the girders ability to withstand external loads.

11) Increased concrete strength did not significantly affect the shear strength of the test girders. However, increased concrete strength did improve several aspects of the girders performance. High concrete strength reduced the deflection of the girders due to the higher modulus of elasticity. Also, higher concrete strength increased the additional loads that could be

of elasticity. Also, higher concrete strength increased the additional loads that could be carried by the mechanical interlock after the adhesion bond failure.

12) For the two amounts of shear reinforcement studied in this project, increasing the amount of reinforcement did not increase the ultimate shear capacity of the test girders.

REFERENCES

1. Hoyer, E. and Fredrich, E., "Bietrag zür Frag der Nalftspannug in Eigen-beton-bauteinten," Beton ünd Eisen, V. 38, 1939.

2. Brearly, L., Johnston, D., "Pull-Out Bond Tests of Epoxy-Coated Prestressing Strand," Journal of Structural Engineering, ASCE, V. 116, No. 8, August 1990, pp. 2236-2252.

3. Deatherage, J., Burdette, E., "Development Length and Lateral Spacing Requirements of Prestressing Strand for Prestressed Concrete Bridge Products," A Final Report Submitted to Precast/Prestressed Concrete Institute, September 1991.

4. Cousins, T., Badeaux, M., Moustafa, S., "Proposed Test for Determining Bond Characteristics of Prestressing Strand," PCI Journal, V. 37, No. 1, January/February 1992, pp. 66-73.

5. Yu, S., "Transfer Bond Performance of Prestressing Strands," Unpublished Report.

6. Hognestad, E., Janney, J., "The Ultimate Strength of Pre-Tensioned Prestressed Concrete Failing in Bond," Magazine of Concrete Research, V. 6, No. 16, June 1954, 11-16.

7. Janney, J., "Nature of Bond in Pre-Tensioned Prestressed Concrete," ACI Journal, V. 25, No. 9, May 1954, pp.717-736.

8. Hanson, N., Kaar, K., "Flexural Bond Tests of Pretensioned Prestressed Beams," ACI Journal, V. 30, No. 7, January 1959, pp.783-802.

9. Over, S., Au, T., "Prestress Transfer Bond of Pretensioned Strands in Concrete," ACI Journal, V. 62, No. 11, November 1965, pp.1451-1460.

10. Cousins, T., Johnston, J., Zia, P., "Transfer and Development Length of Epoxy Coated and Uncoated Prestressing Strand," PCI Journal, V. 35, No. 4, July/August 1990, pp.92-103.

11. Cousins, T., Johnston, J., Zia, P., "Bond of Epoxy Coated Prestressing Strand," Final Report for the North Carolina Department of Transportation, December 1990.

12. Shahawy, M., Issa, M., Batchelor, B., "Strand Transfer Lengths in Full Scale AASHTO Prestressed Concrete Girders," PCI Journal, June 1992, pp. 84-96.